Cooperative Reactivity of Boron-Containing Molecules and Lewis Bases for Metal Free Catalysis

Thèse

Marc-André Légaré

Doctorat en Chimie
Philosophiæ Doctor (Ph. D.)

Québec, Canada

Résumé

La catalyse par métaux de transition est omniprésente de nos jours dans tous les secteurs de l'industrie chimique. Les réactions activées de cette façon permettent la production d'un grand nombre de produits utiles de grande importance commerciale. Considérant uniquement le domaine de la synthèse organique, le développement de réactions catalytiques a été récompensé par plusieurs prix Nobel au cours du 20^{e} siècle, ce qui témoigne de l'importance de ces contributions.

L'utilisation de métaux de transition, et surtout des métaux précieux, en catalyse comprend cependant des inconvénients qui proviennent de leur coût élevé, de leur rareté, ainsi que de leur toxicité potentielle et de l'impact environnemental que leurs déchets peuvent avoir. De fait, plusieurs agences nationales et internationales régulent de nos jours la teneur en métaux à l'état de traces qui peuvent être présents dans beaucoup de produits. Pour cette raison, il est de grand intérêt de découvrir des systèmes catalytiques alternatifs composés d'éléments abondants, non-toxiques et peu coûteux.

Le bore, en tant qu'élément léger du groupe principal, répond à ces critères. Cependant, la réactivité des composés organoborés est très différente de celle des métaux de transition et peu adaptée aux réactions catalytiques existant de nos jours. Pour cette raison, de nouveaux concepts et de nouvelles réactions doivent être inventés et développés afin d'introduire le bore au domaine de la catalyse.

Dans le but de développer de tels concepts, et dans le but de concevoir de nouveaux catalyseurs à base de bore, nous avons investigué plusieurs cas où la présence de bases de Lewis influence la réactivité de composés borés. Notre hypothèse était que la combinaison d'un organoboré et d'une base de Lewis pourrait agir dans des réactions qui seraient impossibles pour chacun individuellement.

Dans une première étude de cas, nous avons étudié en profondeur la réactivité d'adduits neutres de borabenzène vis-à-vis de bases de Lewis. Nous avons ainsi trouvé que, contrairement au formalisme courant, le borabenzène coordonné à une base réagit comme un nucléophile plutôt qu'un électrophile. Les propriétés et la réactivité de nombreux composés à base de borabenzène ont été étudiées par des méthodes computationnelles et expérimentales en une recherche qui est présentée dans cette thèse.

Par la suite, nous nous sommes penchés sur le problème de la réduction du dioxyde de carbone catalysée par des composés organoborés ambiphiles. À l'issu de ce travail, nous décrivons de nouveaux modes d'interaction entre le bore et des bases de Lewis inusités et les applications de ces concepts à la réduction du CO_2 en dérivés de méthanol.

Finalement, nos travaux de recherche culminent avec le développement d'un catalyseur ambiphile sans métal pour l'activation et la borylation des liens C-H d'hétéroarènes. Dans cette thèse, nous décrivons le processus de réflexion qui a mené à la conception rationnelle de cette réaction, ainsi que les propriétés uniques de ce système.

Abstract

Transition metal catalysis is currently ubiquitous in all sectors of the chemical industry. The reactions it enables allow the production of countless useful chemicals. In the field of organic synthesis alone, the impact and development of catalytic reactions have been recognized several times by the award of Nobel prizes.

The use of transition metals for catalysis, however, suffers from several drawbacks that include their high cost, their rarity and their potential toxicity and environmental impact. National and international agencies, as a matter of fact, regulate the trace amounts of residual metal that can be present in many end products. For this reason, there is great interest in discovering alternative catalysts produced from earth-abundant, nontoxic and inexpensive elements.

Boron, as a light element of the main group, follows these criteria. The reactivity of organoboron compounds, however, is very different from that of organometallic complexes, and less adapted to typical catalytic process. For this reason, new concepts and new reactions have to be developed in order to introduce boron to the world of catalysis.

In order to discover and develop novel ideas towards the design of boron catalysts, we have studied different instances in which Lewis bases influence the reactivity of boron compounds. We hypothesized that the combination of an organoborane and a Lewis base could achieve reactions that would be impossible for the separate units to accomplish.

In a first case study, we have investigated in depth the reactivity of neutral adducts of borabenzene towards Lewis bases. We have found that, contrary to usual formulations, borabenzene, under the influence of a Lewis base, reacts as a nucleophile rather than an electrophile. The properties and reactivity of a great number of borabenzene compounds have been studied computationally and experimentally in a work that will be presented in this dissertation.

Next, we have studied the reduction of carbon dioxide catalyzed by ambiphilic organoboron compounds. We describe new modes of coordination for boranes with Lewis bases and the application of these interactions to the reduction of CO_2 to methanol derivatives.

Finally, the culmination of our research efforts is shown as the rational development of a metal-free ambiphilic catalyst for the C-H bond activation and borylation of heteroarenes. In this dissertation, we describe the process by which we designed and implemented this catalytic reaction, as well as the specifics of the system.

Table of Contents

List of Tables

List of Equations

List of Figures

List of Abbreviations

3d	Three-dimensional
9-BBN	9-Borabicyclo[3.3.1]nonane
Ar	Aryl
ArF	Perfluoroaryl
DFT	Density Functional Theory
ca.	Circa
cat	Catechol (1,2-dihydroxybenzene)
cat.	Catalyst
CBS	Corey-Bakshi-Shibata
CCD	Charge Coupled Device
COE	Cyclooctene
COSY	Correlation Spectroscopy
Cy	Cyclohexyl
ΔH	Enthalpy variation
ΔG	Gibbs free energy variation
DMSO	Dimethylsulfoxide
Et	Ethyl
FLP	Frustrated Lewis Pair
Fpin	Perfluoropinacol (tetrakis(trifluoromethyl)ethylene glycol)

HMB	Hexamethylbenzene
HOMO	Highest Occupied Molecular Orbital
HSQC	Heteronuclear Single Quantum Coherence
IMe	Dimethylimidazolylidene
IMes	Dimesitylimidazolylidene
iPr	Isopropyl
KIE	Kinetic Isotope Effect
L	Lewis base, ligand
Lu	2,6-Lutidine
LUMO	Lowest Unoccupied Molecular Orbital
Me	Methyl
Mes	Mesityl
mol. %	Molar percent
NHC	N-Heterocyclic carbene
NMR	Nuclear Magnetic Resonance
ox	oxalate
Ph	Phenyl
Pin	Pinacol (tetramethylethylene glycol)
ppm	Parts per million
PS	Proton Sponge
Py	Pyridine

Scat	Thiocatechol (1,2-dithioxybenzene)
SCF	Self-Consistent Field
tBu	Tert-butyl
THF	Tetrahydrofuran
thio	2-Thienyl
TIPS	Tri(isopropyl)silyl
TMS	Trimethylsilyl
TMP	2,2,6,6-Tetramethylpiperidine
TOF	Turn-Over Frequency
TON	Turn-Over Number
TS	Transition State
XRD	X-ray Diffraction
Z	Lewis acid

NMR multiplicity:

s: singlet, d: doublet, t: triplet, q: quadruplet, qt: quintuplet, sept: septuplet, n: nonuplet, br: broad signal.

Computationally optimized structures for intermediates and transition states are numbered independently in each chapter.

Elle a vécu chacune de ces pages,
Elle les comprend mieux que quiconque,
Sans elle rien n'aurait été fait.
À ma précieuse épouse, ma muse et ma joie,

Dédié à Jacquelyn Légaré

S. D. G.

Remerciements

J’aimerais profiter de cette occasion pour remercier plusieurs personnes qui ont grandement contribué à mon cheminement et que je suis incroyablement reconnaissant d’avoir eu la chance de rencontrer.

Premièrement, je remercie profondément et sincèrement le professeur Frédéric-Georges Fontaine pour ces années passées sous sa direction. Ces années représentent pour moi une véritable tranche de vie, alors que mon entrée dans le groupe Fontaine – en tant que stagiaire – date du 5 mai 2008. Je te remercie donc, Fred, pour l’occasion d’avoir vécu ces dernières années de cette façon, pour la recherche stimulante que nous avons faite, pour tes conseils, pour l’inspiration et pour les personnes de qui tu t’es entouré et qui sont devenus aussi mes compagnons.

J’aimerais aussi remercier ces personnes, surtout celles que j’ai rencontrées dans les premières années et qui m’ont véritablement inspiré à poursuivre des études supérieures. Particulièrement, j’aimerais mentionner André Languérand et Guillaume B. Chabot qui ont eu la lourde tâche de m’initier au travail en laboratoire. Plus que cela, cependant, vous m’avez montré, par l’exemple, ce qu’est le travail persévérant et intelligent qui est à la base de la recherche scientifique. Messieurs, le mouflet vous remercie.

Le reste de l’hétéroclite groupe Fontaine d’autrefois n’est pas non plus oublié. Le temps que j’ai passé avec Christian N. Garon (qui était toujours là pour me mettre au défi), Josée Boudreau, LN Staub et Patrick Ferland a été un des plus formateurs de ma vie. Je n’aurais jamais imaginé, à cette époque, que je déposerai un jour une thèse de doctorat. Merci à vous de m’avoir inspiré dans ce chemin !

Les remerciements sont étendus au professeur Tom K. Woo pour l’occasion de travailler dans son laboratoire à l’été 2010 et pour m’avoir enseigné les arts différents (mais bizzarement complémentaires) de la DFT et de la pêche. Merci également au professeur R. Tom Baker pour l’accueil lors du même stage et pour de sages conseils sur la suite de ma carrière. Je mentionne aussi chaleureusement le professeur T. T. T. Nguyen Dang pour ses cours de chimie théorique qui sont à la fois pertinents et enrichissant et pour plusieurs discussions intéressantes.

J’aimerais maintenant présenter un remerciement spécial à Marc-André Courtemanche pour une collaboration de plusieurs années. En travaillant avec toi, Marc, j’ai appris beaucoup sur la chimie, sur moi-même et j’ai trouvé un ami précieux. Même si ça n’a pas toujours été facile, nous avons accompli plus ensemble que nous n’aurions séparément. Je te souhaite le meilleur alors que nos chemins se séparent pour un temps! Tu es un excellent chercheur et je n’ai pas de doute que tu vas réussir ce que tu entreprendras.

Ambreen Mushtaq et Viridiana Perez, qui font partie des quatre doctorants de 2015 sont aussi remerciées chaleureusement. Les discussions scientifiques que j’ai eues avec vous deux ont été une grande source d’inspiration et de stimulation dans mes travaux. Votre présence dans le groupe (au bureau et au laboratoire) en ont fait ce qu’il est et je considère comme un privilège d’avoir travaillé avec vous.

Une mention spéciale aussi pour Étienne Rochette, avec qui j’ai eu le plaisir de travailler quelques temps. Merci pour tes efforts, ton intérêt. Tu t’apprêtes à voler de tes propres ailes et je suis sûr qu’elles te mèneront vers des découvertes de grand intérêt qui seront bien à toi.

Merci Maria Zakharova. Merci à ceux qui ont travaillé avec moi sur ces projets : Nicolas Bouchard, Julien Légaré-Lavergne, K. Cérine Nahi et Guillaume de Robillard. Ne lâchez pas.

Chapter 1 - Introduction

Catalysis represents one of the most promising ways of enabling useful chemical processes.[1] By definition, a catalyst lowers the energy barrier of a reaction, allowing it to proceed in milder conditions.[2] The use of selective catalysts makes high yields possible for otherwise difficult reactions, at a lower energy cost. Catalysts have been used and studied since the 18th century with great success, rapidly becoming a standard tool in the synthetic chemist's arsenal.[3] With growing concern and awareness over environmental matters and energy conservation, catalysis represents a field that will continue to grow throughout the 21st century. In fact, the very core of the green chemistry philosophy states that "catalytic reagents (as selective as possible) are superior to stoichiometric reagents."[4]

Transition metal catalysis is currently ubiquitous in most—if not all—fields of the chemical industry and is at the core of significant academic research efforts. In fact, from petrochemistry to fertilizer synthesis, including the production of polymers, pharmaceuticals and specialty chemicals, homogenous and heterogeneous transition metal species enable innumerable useful processes.[5]

The broad field of organic synthesis is also dependent on many catalytic processes. For decades now, reactions such as hydrogenation, oxidation, polymerization, metathesis and carbon-carbon cross-couplings can be mediated by highly efficient and convenient transition metal catalysts. For developments of catalysis of each of these classes of reactions, Nobel Prizes were awarded, recognizing the importance of catalysis to science and to the public.[6]

In the past few decades, a class of reactions that has been increasingly studied is the direct C-H functionalization by precious transition metals. While not (yet) honored with the Nobel Prize,[7] these useful processes open exciting new possibilities by transforming the ubiquitous and inert C-H bond into an active leaving group.[8]

However, the use of transition metals—especially of the reactive precious metals such as palladium, platinum, iridium and rhodium—suffers from some serious drawbacks due to their high cost and human and environmental toxicity. In fact, international instances regulate the amount of trace metals allowed to remain in products destined for human consumption.[9] As a result, catalyst scrubbing can be an expensive necessity for the pharmaceutical, food, and specialty chemicals industries. In addition, residual transition metal traces are known to

negatively affect the properties of opto-electronic materials and rigorous catalyst removal has to be performed by producers of electronic devices.[10]

The interest and potential impact of replacing transition metal catalysts with metal-free alternatives should thus appear evident. The less toxic and more abundant main-group elements offer an attractive and diverse bank of building blocks for the design of new, inexpensive, and green catalysts. Among these elements, boron has attracted considerable synthetic interest in recent years with the discovery of new reactions, most notably the hydroboration reaction.[11] With the rich chemistry of boron compounds, their application as organocatalysts is a promising entry into environmentally benign metal-free reactions.

1.1 Boron-Containing Molecules as a Replacement for Transition Metal Catalysts

Boron is an earth-abundant non-metal element of the main group. In the form of various mineral oxides,[12] it is extracted from the Earth's crust at the annual scale of four million tons, with the major producers being Turkey and the United States of America. Proven global reserves exceeding one billion tons of boron minerals make this element an abundant and commercially sustainable resource.[13,14]

After mineral extraction, refinement of boron-containing ore produces borax (various hydrates of sodium tetraborate – $Na_2B_4O_7.xH_2O$). This pure mineral can then, through various processes, be converted to boric oxide (B_2O_3) and boric acid ($B(OH)_3$) which in turn are versatile precursors to finished products.[15] This annual production of boron oxides has a wide range of applications, notably for the production of materials (fibers, glasses and ceramics), abrasives, coatings, semiconductors, optically active materials, and fertilizers.[16]

The use of boron in agricultural fertilization is a testimony to its environmental compatibility. In fact, boron is an essential micronutrient to plants and its deficiency negatively affects useful crops around the world.[17] In humans and mammals as well, boron intake has been well studied, with boron deficiency associated with reduced growth and a negative impact on hormonal concentrations.[18] At higher concentrations, boron oxides are very well tolerated by marine life and mammals. With a LD_{50} (oral, rat) of 6 g/kg, boric acid is less lethal to mammals than table salt (2 g/kg) and can effectually be considered non-toxic.[19] On the other hand, arthropods can suffer from acute poisoning when exposed to relatively concentrated solutions

of boron oxides, which can be used as domestic insecticides.[20] Plants can also suffer from reduced productivity when growing in seldom-occurring soil of high boron content.[21]

Because of the nontoxicity of boric acid to mammals, the incorporation of boron-containing molecules in medical materials and chemicals is a very attractive possibility. As such, modern applications of boron also include boron-based drugs and agents for boron neutron-capture therapy.[22]

As a nontoxic, earth-abundant, inexpensive and sustainable resource, boron thus becomes a highly attractive foundation to industrially relevant species. As such, organoboron compounds are widely used today as stoichiometric reagents in synthetic chemistry.[23] Reactions based on boron compounds require none of the special considerations coming from the use of precious metals and would come at very low cost. On the other hand, organoboron species cannot, at this time, compete with transition metals in the field of catalysis, as they cannot undergo the multi-electron processes that are at the core of many transition metal-mediated reactions. As such, new concepts, ideas, and paradigms have to be invented, explored, and implemented in order to develop efficient, metal-free, catalyst systems based on boron compounds. The work described in this thesis aims to participate in this exploration.

1.2 Outline of the Dissertation

This thesis explores the cooperative reactivity of boron-containing molecules with various Lewis bases, with a focus on the design of novel metal-free catalytic reactions. Using different case studies, we will show that through various mechanisms, the combination of Lewis bases and boron gives rise to certain properties which enable novel modes of reactivity. The thesis is divided in eight chapters. Four of them were written in the form of scientific papers that have been published or submitted. The candidate is the first author of all these papers.

In the current Chapter 1, we have briefly described the motivation behind the work of this thesis.

In Chapter 2, we make a more detailed review of the concepts that are at the core of the ideas presented in the thesis. In this chapter, we will also describe the state of the field as the work was performed.

In Chapter 3, we briefly summarize the methodology used in this research.

In Chapter 4, we describe an in-depth study of the bonding between borabenzene and neutral Lewis bases and of the reactivity modes of the complexes thus formed. The results presented therein have been published as: Légaré, M.-A.; Bélanger-Chabot, G.; De Robillard, G.; Languérand, A.; Maron, L.; and Fontaine, F.-G. "Insights into the Formation of Borabenzene Adducts via Ligand Exchange Reactions and TMSCl Elimination from Boracyclohexadiene Precursors" *Organometallics*, **2014**, 33, 3596-3606.

I wish to acknowledge the preliminary work performed by G. Bélanger-Chabot and A. Languérand upon which this study was built. I also recognize the work of G. De Robillard who worked under my supervision as an intern. Thanks are given to L. Maron for expert advice on computational studies.

Chapter 5 has been published as: Declercq[I], R.; Bouhadir, G.; Bourissou, D.; Légaré,[I] M.-A.; Courtemanche, M.-A.; Nahi, K. S.; Bouchard, N.; Fontaine, F.-G.; Maron, L. "Hydroboration of Carbon Dioxide Using Ambiphilic Phosphine–Borane Catalysts: On the Role of the Formaldehyde Adduct" *ACS Catal.* **2015**, *5*, 2513-2520.

This article describes the results of a collaborative project between our research group and that of Professor Didier Bourissou at the Université Paul-Sabatier in Toulouse. Our group performed the studies on the diphenylphosphino derivatives described in the paper. Furthermore, we can be credited for the mechanistic investigations, kinetic and isotope labelling experiments, computational work, and data interpretation. Prof. Laurent Maron is acknowledged for expert advice on computational calculations. Personally, the candidate did experimental work on said diphenylphosphino derivatives. He also directly supervised the work of undergraduate students N. Bouchard and K. S. Nahi who are listed as co-authors.

In Chapter 6, we explain lower catalytic efficiencies observed when using simple base catalysts for the reduction of carbon dioxide to methanol derivatives. A new activation mode is disclosed which offers interesting possibilities for reduction reactions using hydroboranes.

This work has been published as: Légaré, M.-A.; Courtemanche, M.-A.; Fontaine, F.-G. "Lewis base activation of borane–dimethylsulfide into strongly reducing ion pairs for the transformation of carbon dioxide to methoxyboranes" *Chem. Commun.* **2014**, *50*, 11362-11365.

[I] These authors contributed equally to the body of work.

In Chapter 7, we present the seminal contribution of this thesis: a highly efficient metal-free catalyst for the C-H borylation of heteroarenes. This system has been submitted and accepted in *Science* as: Légaré, M.-A.; Courtemanche, M.-A.; Rochette, E.; Fontaine, F.-G. “Metal-Free Catalytic C-H Bond Activation and Borylation of Heteroarenes”

The co-authors are acknowledged for their contribution to the experimental work and E. Rochette is particularly thanked for computational calculations performed on the final catalytic cycle.

The implications of this body of work will be discussed in Chapter 8 in the form of a conclusion and recommendations for future applications of this research, with special emphasis put on C-H functionalization chemistry.

Chapter 2 - Literature Review

In order for the reader to fully appreciate the full extent of the concepts developed in this thesis, it is important to first explore the general aspects of Lewis acidity and boron chemistry. The following chapter will thus include a discussion on their respective properties, with emphasis put on their synthetic applications.

2.1 Lewis Acids and Bases

2.1.1 Lewis Acids and Bases

The distinct properties of acids and bases have been recognized very early in the history of chemistry and have been described according to different formalisms along the years. [24–26]. In one of the most comprehensive and accurate assessments of the chemistry of acids and bases, Gilbert Lewis defined these classes of compounds with regard to their respective relations towards electrons and the octet rule.[27] According to his criterion, (Lewis) acids are defined as possessing an empty orbital and needing an electronic contribution from another molecule in order to reach the favored octet of electrons.

By contrast, Lewis bases are ions or molecules that possess a reactive lone pair of electrons available for bonding. In organic chemistry, the most common Lewis bases are amines, phosphines, ethers, carbonyls, thioethers, as well as anions such as alkoxides and amides, to name only a few. By virtue of their reactive lone pair, Lewis bases can be used as ligands for transition metals,[28] or as catalysts on their own quality.[29]

Lewis acids and bases can thus assemble into adducts. The concept of dative bonds emerges in the case of these adducts and is defined as a two-electron bond in which both electrons are contributed by a donor (the base) in its associations with an acceptor (the acid). In its definitions, the Lewis theory encompasses the earlier Brønsted-Lowry model, regarding the H^+ ion as the smallest possible Lewis acid. Protonation of bases corresponds in fact to the formation of a Lewis adduct **Figure 2-1**.[26]

Figure 2-1: Schematic representation of a Lewis base (left), acid (center) and of the proton as a Lewis acid (right).

Adducts formed by Lewis acids and bases vary in strength depending on many factors, both steric and electronic. As will be seen throughout this work, the properties of these adducts are at the core of acid and base reactivity.

2.1.2 Lewis Acids

Lewis acids have to possess an unoccupied valence orbital. For this reason, they are most commonly based on elements from the 13th group of the periodic table or from the transition metals. Many boron, aluminum, and metallic small molecules are routinely used by synthetic chemists as Lewis acids. Stronger Lewis acids can be prepared by surrounding the active atom with electron withdrawing groups, or by using cationic molecules. In this manner, tris(pentafluorophenyl)borane ($B(C_6F_5)_3$) is a very strong Lewis acid.[30] Even more so, carbocations[31] and silylium cations[32] are highly reactive Lewis acids capable of forcing difficult transformations in unreactive substrates.

Among such transformations is the Friedel-Crafts reaction, named after Charles Friedel and James Crafts, which includes a variety of Lewis acid-catalyzed C-H functionalizations of aromatic rings and unsaturated hydrocarbons. The most common variants of this reaction allow the alkylation or acylation of arenes. The basic principle of both the Friedel-Crafts alkylation and acylation is the use of a strong Lewis acid to activate the leaving group on a reagent, making it electrophilic and enabling a nucleophilic attack from an unactivated arene (**Figure 2-2**). The Friedel-Crafts reaction has been used extensively since 1877 and much development has been done on its scope and its applications. Many variants now exist that allow the formation of a great number of different products. The common denominator of these reactions—and what makes them Friedel-Crafts reactions—is the use of a Lewis acid to activate an electrophile.[33–36]

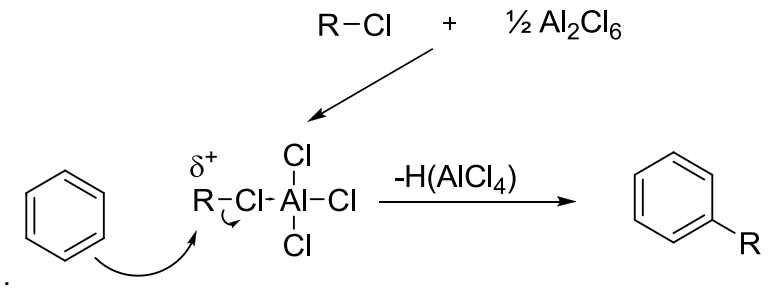

Figure 2-2: Example of the Friedel-Crafts alkylation or acylation of benzene.

2.1.3 Dissociated Borane-Base Cooperation: The Case of Frustrated Lewis Pairs

While the reactivity of Lewis acids and bases is rich and gives rise to many synthetic applications, the collaborative combination of acid and base behavior gives rise to new exciting possibilities. This cooperation can be found when the borane and the Lewis base do not interact and quench each other.

It has long been known that in some cases, steric bulk could prevent association and mutual quenching of combined Lewis acids and bases. As such, H. C. Brown reported as early as 1942 that 2,6-lutidine would not form adducts with bulkier trimethylborane, despite its propensity to associate with smaller acids.[37] Nobel Prize recipient Georg Wittig also showed that triphenylphosphine and triphenylborane retained their reactivity in the presence of each other and could react with benzyne in a 1,2 addition reaction (**Figure 2-3**).[38] Similar reactivity was observed more recently with stronger acids, evidencing the effect of steric bulk to prevent quenching in Lewis pairs and preserve their combined reactivity.[39]

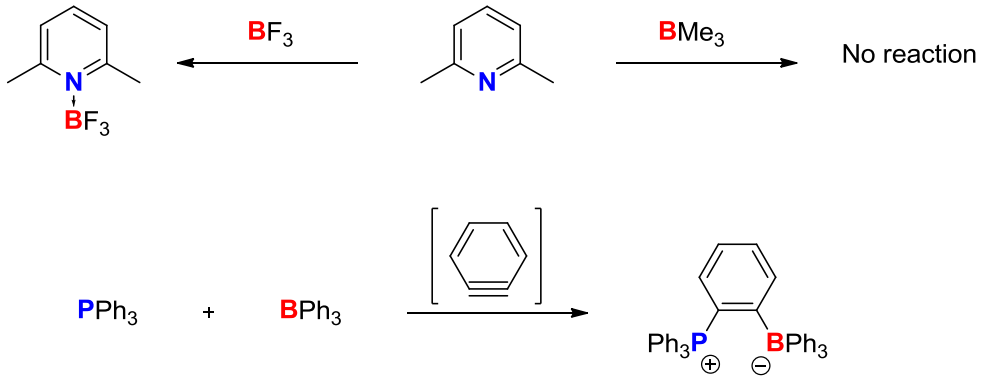

Figure 2-3: Early examples of steric frustration in Lewis pairs.

In fact, through steric constraints, Lewis acidic boranes and bases can be prevented to associate, even in the case of strong acids and bases. This effect, described as Frustrated Lewis Pairs (FLPs) allows the simultaneous interaction of both acid and base with substrates small enough to bind them in spite of the steric bulk (**Figure 2-4**).[40]

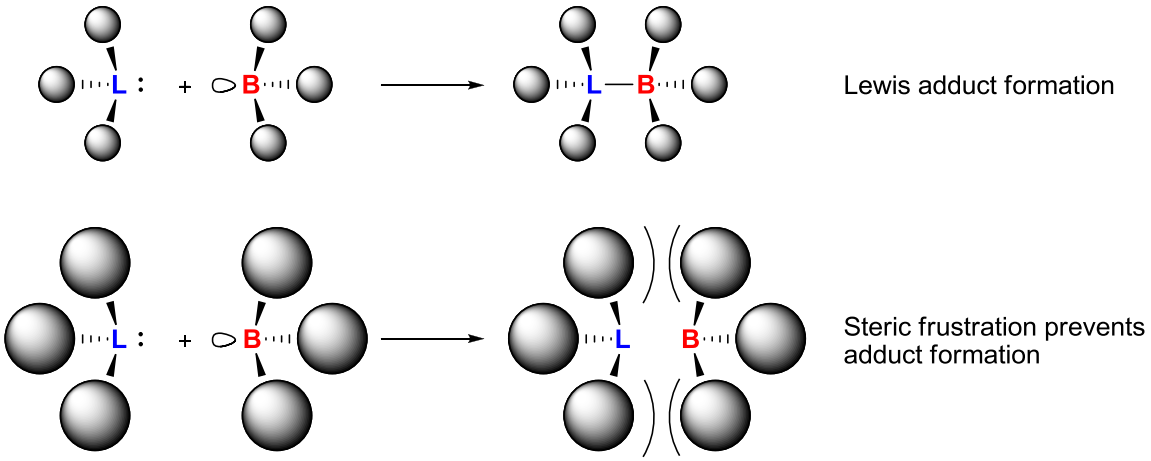

Figure 2-4: Schematic representation of the Frustrated Lewis Pair effect.

The FLP effect was first formulated by Stephan and coworkers in 2007 to describe their demonstration that a molecule bearing bulky alkylphosphine and perfluorophenylboryl moieties would not self-quench.[41] Instead, under an atmosphere of dihydrogen, the acid-base pair could cleave the hydrogen in a heterolytic manner to give a zwitterion-possessing phosphonium and borate functions.[42] In a Lewis formalism, the phosphonium is equivalent to an adduct between a phosphine and a proton, while the borate corresponds to the stabilization of a hydride by the borane group. Similar reactivity was observed when combining trimesitylphosphine or tri(*tert*-butyl)phosphine with perfluorophenylborane (**Figure 2-5**).[43]

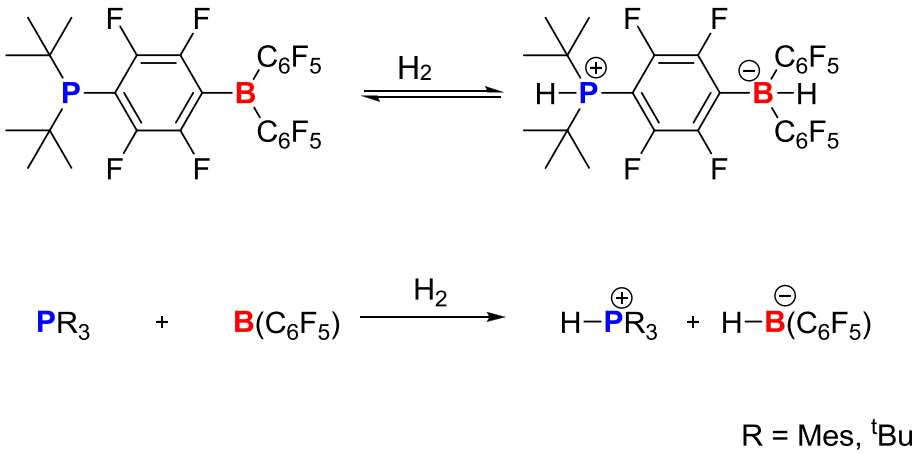

Figure 2-5: Heterolytic cleavage of molecular hydrogen by Frustrated Lewis Pairs.

This initial report quickly sparked considerable interest. The Frustrated Lewis Pair rapidly became an important research topic, with many systems being developed and reacted with hydrogen, showing the generality of the FLP principle for the activation of dihydrogen. Different classes of FLPs emerged with varied properties, and the fundamental aspects of their reactivity as well as their potential applications were studied and the subject has been abundantly reviewed in recent literature.[44,45]

While FLP reactivity was initially reported for intermolecular systems—i.e. the cooperating acid and base are located on different molecules—more recent advances have shown similar reactivity in intramolecular analogs. The latter case is distinguished from intermolecular FLPs by the mode of action for substrate activation as can be seen in (**Figure 2-6**).[46,47]

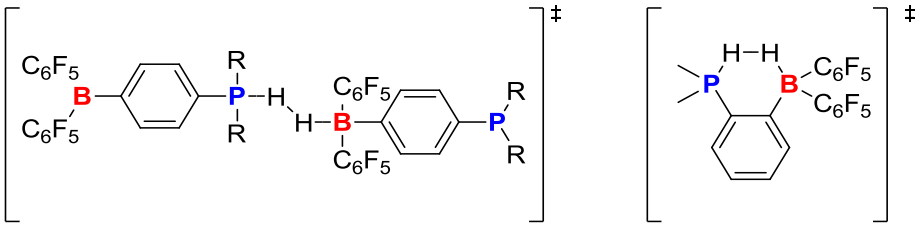

Figure 2-6: Mechanism of H_2 activation by intermolecular (left) and intramolecular (right) FLP systems.

Intramolecular FLPs feature proximal acidic and basic groups on a linking backbone that are still prevented from associating either intra- or intermolecularly through a combination of steric and geometric constraints. They possess a unique advantage over intermolecular FLPs: their

interaction with substrates involves one fewer molecule, reducing the entropic cost of association. Several linking backbones have been shown to be suitable for FLP chemistry and, in combination with the range of possible Lewis acids and bases, have given rise to a large FLP library (**Figure 2-7**).[48–52] It should be noted that for the rest of this dissertation, FLPs will be referred to with regard to the nature of their base and acid fragment as such: "base-acid."

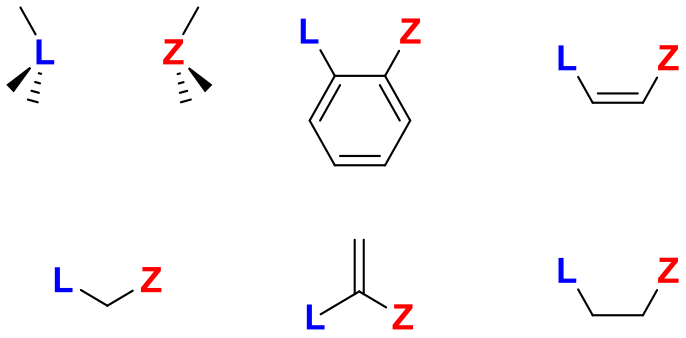

Figure 2-7: Range of typical intramolecular and intermolecular FLPs reported in the literature.

A wide range of amines, phosphines, and carbenes[53] can be used as Lewis bases in FLP systems. While FLP chemistry is dominated by perfluorophenylborane-based acids, alanes, carbocations, and other electrophiles are also used. The wide range of FLPs gives many examples capable of cleaving hydrogen.

The activation of hydrogen is archetypical of the collaborative acid-base reactivity of FLPs successfully applied to catalytic reactions in which a proton and a hydride can be transferred to an unsaturated substrate (**Figure 2-8**). With FLP methods, imines,[54] silyl enols,[55] and enamines[56] were first shown to be susceptible to metal-free hydrogenation.[57] These substrates are particularly well suited to hydrogenation by FLPs because of the polarity of their unsaturated bond and their affinity for protons.

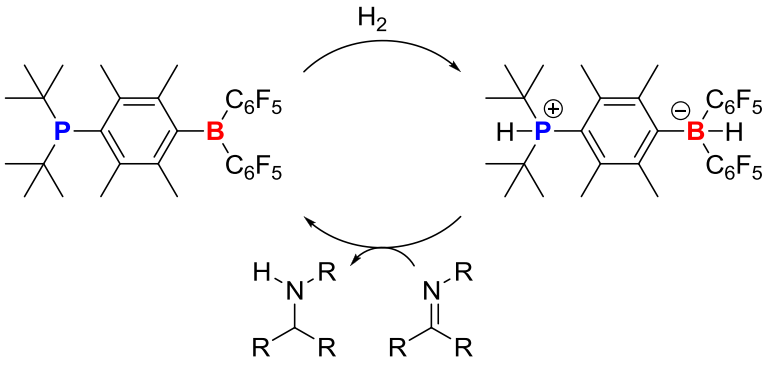

Figure 2-8: Hydrogenation of imines by phosphine-borane FLPs.

As can be seen in **Figure 2-8**, the protonation of the substrate by FLP-cleaved hydrogen allows for facile hydride transfer and is a key step in the hydrogenation mechanism. Consequently, inactivated alkenes and alkynes, as well as most carbonyl groups were found to be resistant to such hydrogenation. Alternative strategies had to be devised in order to hydrogenate these substrates. In the first case, using diethylether or electron-deficient phosphines as extremely weak bases, in combination with tris(perfluorophenyl)borane, enable the hydrogenation of 1,1-diphenylethylene and other alkenes, albeit at high catalyst loadings.[58,59] More recently, Stephan and Ashley independently reported the use of strongly Lewis acidic boranes in combination with ethers for the hydrogenation of carbonyls (**Figure 2-9**). Interestingly, in these cases, the cleavage of H_2 is not detected—being thermodynamically uphill—but occurs in sufficient amounts to generate the active species for the hydrogenation (**Figure 2-9**).[60,61]

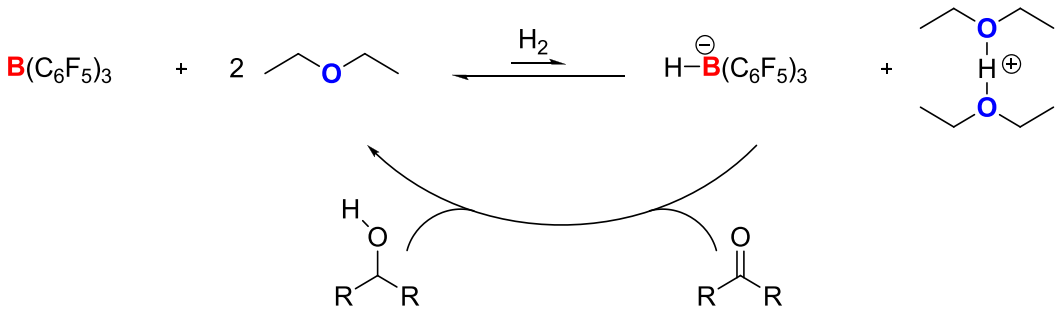

Figure 2-9: Hydrogenation of carbonyl compounds using a $B(C_6F_5)_3$-ether FLP.

In the case of the hydrogenation of alkynes, Repo and coworkers devised an elegant strategy relying on the H_2-induced protic elimination of substituents on the boron atom of an amine-

borane intramolecular FLP (**Figure 2-10**). The hydroboranes formed in this fashion can react with alkynes in a classical hydroboration step.[62]

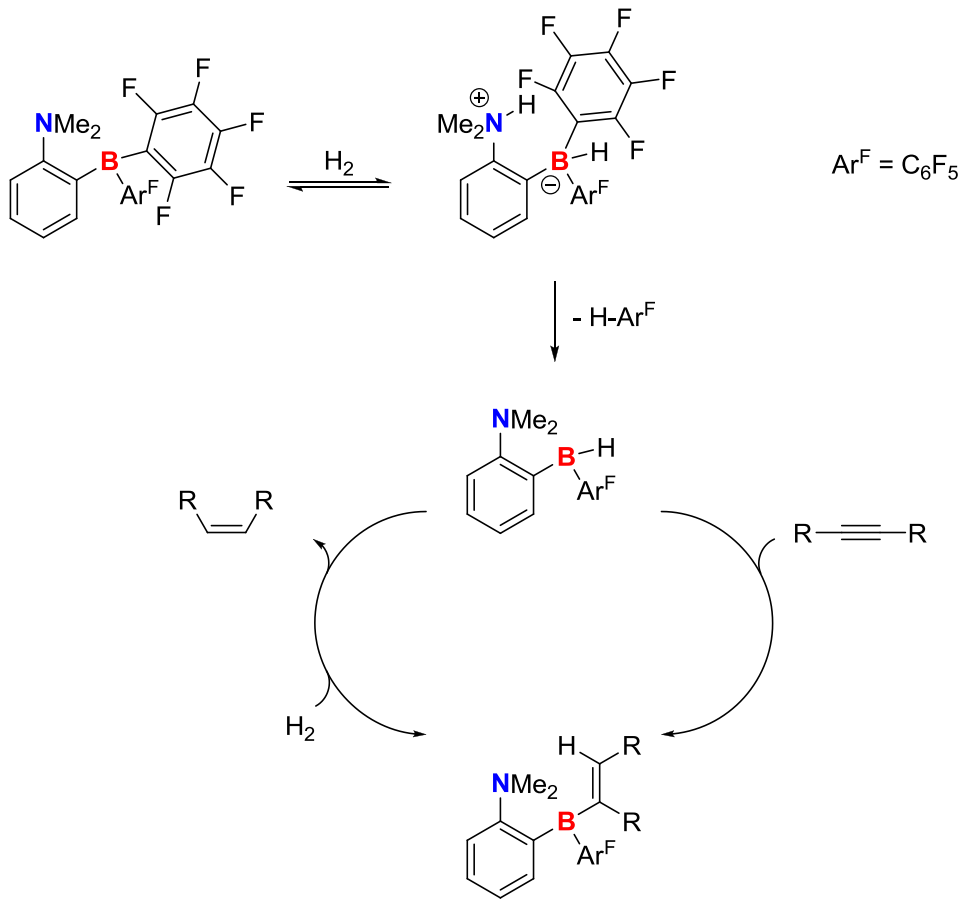

Figure 2-10: Mechanism of the FLP-catalyzed hydrogenation of alkynes as reported by Repo and coworkers.[62]

Other than their reaction with hydrogen, FLPs were also shown to bind unsaturated substrates such as alkenes, alkynes and carbon, sulfur, and nitrogen oxides in a 1,2-addition reaction. Although this mode of binding has yet to yield general catalytic systems for the activation of these substrates, there has been considerable interest in exploring these possibilities.[44]

2.1.4 Frustrated Lewis Pairs and Carbon Dioxide

As explained above, the combination of a Lewis acid and a Lewis base can, with the appropriate steric and geometric constraints, remain unquenched and react cooperatively. Using this Frustrated Lewis Pair approach, small molecules can be bound or cleaved by the concerted actions of the acid and the base.

As a polar, unsaturated small molecule, carbon dioxide is perfectly suited to interact with Frustrated Lewis Pairs. Indeed its carbon atom possesses an electrophilic character while the two oxygen atoms can bind Lewis acids (**Figure 2-11**).[63]

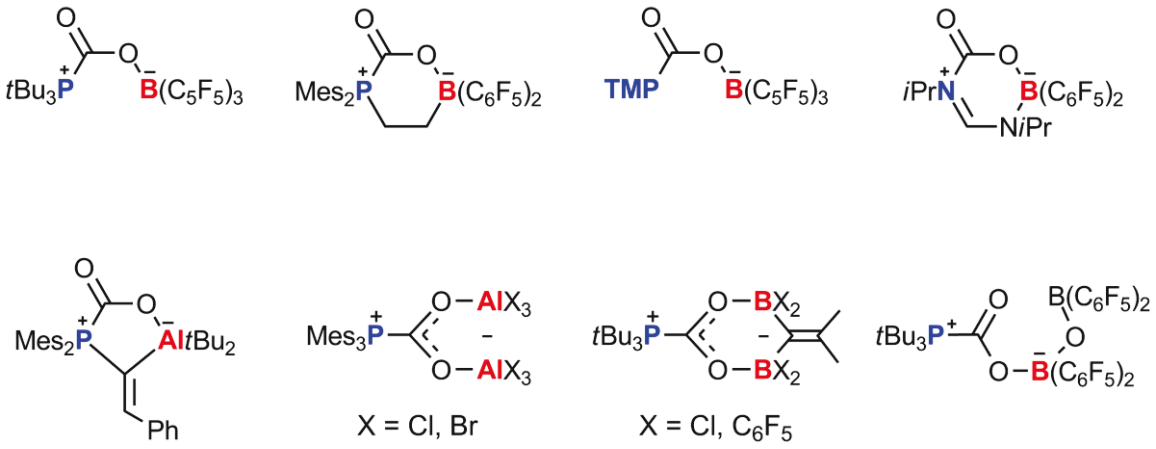

Figure 2-11: Examples of carbon dioxide fixation by FLP systems following the 1,2-addition mode.

Using this concept, several FLP systems have been shown to strongly bind carbon dioxide.[64] In its binding with FLPs, the linearity of carbon dioxide is broken and its properties change. As such, FLPs capable of binding carbon dioxide have long been considered a promising avenue for the catalytic reduction of carbon dioxide.[65,66] In fact, Stephan and coworkers showed that carbon dioxide bound in a FLP comprised of tris(mesityl)phosphine and aluminum chloride or bromide could be stoichiometrically reduced to methoxy products by BH_3•NH_3 (**Figure 2-12**).[67–69]

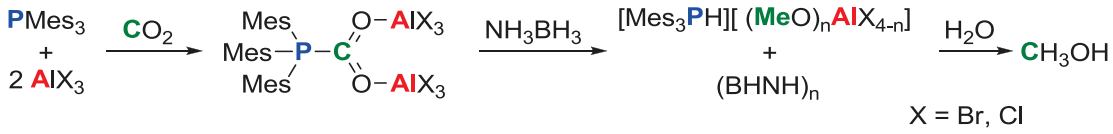

Figure 2-12: Stoichiometric reduction of FLP-bound carbon dioxide to methanol by ammonia-borane.

Another approach for the reduction of carbon dioxide using FLP systems consists of using the Lewis pair to activate the reducing agent instead of carbon dioxide. Ashley and O'Hare demonstrated that FLP activated hydrogen could stoichiometrically reduce carbon dioxide to a mixture of products.[70] This system consisting of tetramethylpyridine and tris(pentafluorophenyl)borane heterolytically cleaves molecular hydrogen into a proton and a

reactive hydride that can attack carbon dioxide (**Figure 2-13**). Using hydrosilanes, Piers and coworkers were able to use this system to catalytically reduce CO_2 to methane, albeit with low efficiency.[71]

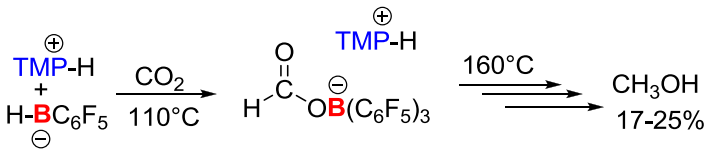

Figure 2-13: Stoichiometric hydrogenation of carbon dioxide as reported by Ashley and coworkers.[70]

2.1.5 Frustrated Lewis Pairs and Alkynes

Terminal alkynes make another class of compounds that can simultaneously interact with both members of a Frustrated Lewis Pair. In fact, in the case of alkynes, two modes of reaction are possible. On the one hand, similarly to CO_2, to alkenes, and to other unsaturated substrates, alkynes can undergo 1,2-addition from FLPs.[40]

On the other hand, and more relevant to the scope of this thesis, the C-H bond of terminal alkynes can be heterolytically cleaved (**Figure 2-14**).[72–74]

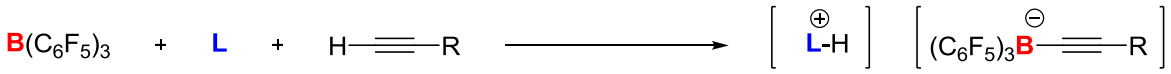

Figure 2-14: Heterolytic C-H bond cleavage of terminal alkynes.

In this reaction, the alkyne can be deprotonated by a weaker base than the alkynylide, owing to the precoordination and stabilization of the Lewis acid, illustrating yet again the collaborative behavior of the acid and base in FLP systems. This reality is similar to the copper-assisted deprotonation of alkyne that is a key step of Sonogashira coupling of sp and sp^2 carbons.[75]

The reaction between alkynes and FLPs show the potential of the latter to activate interesting substrates. In the activation product, the properties of the alkyne are modified and new reactions can occur. Indeed, the latter is a tetravalent alkynylborate. In these systems, nucleophilic migration of C_6F_5 groups to the alkyne was observed. The alkynylborate can also effect nucleophilic aromatic substitution on diazonium salts.[76]

Nevertheless, to this day, to the best of our knowledge, no catalytic or synthetically useful and practical transformation based on FLP-mediated C-H activation has been reported.

2.2 Chemistry of Boron-Containing Compounds

2.2.1 Bonding in Boron Compounds

Possessing five electrons, boron has a ground-state electronic distribution described as $1s^2 2s^2 2p^1$. With only three electrons in its valence shell, boron atoms cannot achieve a favorable octet configuration through the formation of classical covalent bonds. In fact, even after forming three covalent bonds with its three electrons, it remains with an empty orbital. For this reason, simple uncoordinated boron molecular species are generally planar, adopting an sp^2 hybridization and featuring a low-lying unoccupied orbital of p symmetry at boron. This orbital is prone to coordination by a neutral Lewis base to form adducts through the establishment of a dative bond. Anionic nucleophiles can also attack boron molecules to generate borates. Alternatively, the empty orbital can accept intramolecular π-donation from neighboring atoms possessing suitable orbitals (**Figure 2-15**). Boron can thus, in its different molecules, be described as a Lewis acid and a π-acceptor.[77,78]

Figure 2-15: Modes of electron acceptance by boron compounds.

On the other hand, boron is an electropositive element. Its low electronegativity value, as compared to that of other main group elements, often causes its covalent bonds to polarize away from it, with the bond`s electron density being located on the other element. Thus, in contrast to its π-accepting properties, boron is an electron donor with regard to inductive effects (**Table 2-1**).

While boron is mostly found in nature in the form of oxides, it can be transformed to compounds containing bonds with many other elements. Calculated bond dissociation energies of some diatomic species, as well as the electronegativity of involved elements allow us to predict some properties of the related molecules.[79] These energies confirm the exceptional stability of boron oxides based on the high strength of B-O bonds. This strong

oxophilicity of boron is a defining characteristic of boron chemistry, accounting for the selectivity of useful reaction steps as well as decomposition pathways.

Table 2-1: Dissociation enthalpy and electronegativity of various B-X bonds.[79]

Bond B-X	**Dissociation enthalpy at 0K** ($kJ.mol^{-1}$)	**Electronegativity of X**
B-B	293	2.04
B-O	782	3.44
B-C	444	2.55
B-H	326	2.20
B-N	385	3.04
B-F	759	3.98
B-Cl	531	3.16
B-Br	433	2.96

Boron also forms stable bonds with carbon and hydrogen. The chemistry of organoboranes, boranes, and boron hydrides is rich and has such considerable scientific interest that it is fitting to devote the next sections to their properties and reactivity.

2.2.2 Synthetic Applications of Boranes and Boron Hydrides

Like the other elements of the group 13, boron displays interesting properties in its bonding with hydrogen. In fact, contrary to the other main group elements and similarly to metals, it possesses lower electronegativity than hydrogen. The consequence of this property is the formation of a polar bond with hydrogen in which the electron density is principally on the hydrogen atom. For this reason, hydrogen atoms bound to elements from group 13 react as hydrides and are commonly used as nucleophiles and reducing agents.[80]

Boron hydrogen compounds are named boranes and this designation includes small molecules as well as large cluster-type structures. In fact, because of electron-deficient interactions[81] present in these compounds, diborane (B_2H_6) is the smallest isolable borane. This was shown to be applicable in many reactions of hydroboranes,[82] however, its ambient existence as a pyrophoric gas considerably diminishes the potential of diborane as an industrially relevant molecule. Instead, it is mostly used to prepare borane adducts of formula

BH_3•L (L = Lewis base). These molecules find many synthetic applications, notably for hydroboration and reduction reactions.

Hydroboration[83] is, as its name entails, the addition of a B-H to a molecule.[84,85] The most common variant of this reaction by far is the 1,2-hydroboration of alkynes and alkenes and involves the addition of the B-H bond across an unsaturated C-C bond. This reaction proceeds smoothly using a concerted mechanism that takes advantage of the nucleophilicity of boron-bound hydrogen, as well as the electron deficiency of boron. In such a mechanism, the boron atom coordinates with the most electron-rich carbon atom of the substrate, while a nucleophilic hydride is delivered.[86] Through hydroboration, various useful organoboranes can be generated. Combined with an oxidation step, the reaction allows for the easy production of alcohols (**Figure 2-16**).[11]

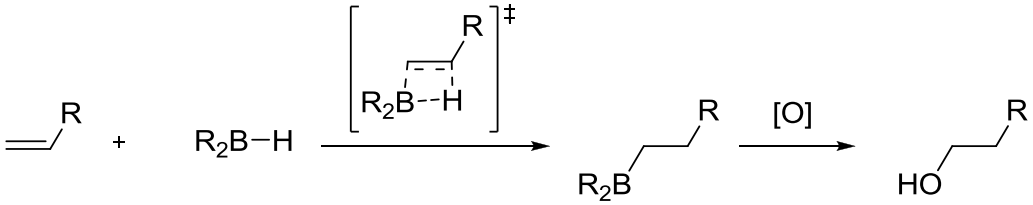

Figure 2-16: Hydroboration-oxidation of an alkene.

Various boron sources used for hydroboration are readily available. Among the least expensive, most reactive, and most convenient to use are the tetrahydrofuran (THF) and dimethylsulfide (SMe_2) adducts of monoborane which are also notable for possessing three reactive hydrides per molecule. Amine adducts of borane can also be used for the hydroboration reaction, although they suffer from diminished reactivity towards alkenes and alkynes. Indeed, the amine adducts are more stable and will not as readily release electron-deficient borane for the reaction with substrates.[87] This inhibition of reactivity is a prime example of the modulation of the properties of boranes by coordination to Lewis bases.

Alternatively, substituted boranes can be used. Catechol- and pinacolborane are used to form boronic esters by hydroboration. 9-Borabicyclo[3.3.1]nonane (9-BBN) is also a reactive boron source that primarily exists as a dimer because of its acidity. Interestingly, 9-BBN is itself prepared by hydroboration of cyclooctadiene by BH_3•SMe_2.[88]

Other unsaturated bonds are susceptible to hydroboration. Carbonyl compounds, notably, can be involved in the reaction. In this case, the reaction is generally known as a reduction and is

related to reactions using other reducing agents. Carbonyl groups differ significantly from alkenes and alkynes by their very high polarity. Indeed, the C=O double bond leaves the carbon atom electron-deficient, while the oxygen atom has a negative partial charge. For this reason, while the boron reagents are the same for both reactions, the mechanism of the reduction can be very different from that of the hydroboration.[89]

In carbonyl compounds, the carbon atom is prone to nucleophilic attack as can be illustrated by a wide range of textbook carbonyl substitution reactions. This property of carbonyls allows hydroboranes to reduce them through a nucleophilic attack of the hydride instead of a concerted mechanism. For this reason, anionic borohydrides are strong carbonyl reducing agents, while being inactive for the hydroboration of alkenes.[85] For its strong reduction potential and its convenience of use, sodium borohydride is produced on the kiloton scale annually.[90]

Contrary to the hydroboration reaction, the rates of reduction can be increased by the use of catalytic amounts of nucleophiles. Tetravalent boron adducts formed by interaction of the nucleophile with the hydroboranes possess more electron density on their hydrides, which can attack carbonyl compounds more easily.[91] These observations show the strongly nucleophilic nature of the reduction reaction by contrast to the hydroboration of alkenes and can be used to modulate the selectivity in the reaction of hydroboranes with carbonyl containing alkenes. The cooperation of hydroboranes with a Lewis base allows greater hydride nucleophilicity and thus greater reactivity in reduction reactions.

This concept has given rise to the asymmetric Itsuno-Corey reduction or Corey-Bakshi-Shibata reduction (CBS reduction) of ketones. In this reaction, an achiral ketone can be selectively reduced to a chiral alcohol by borane-dimethylsulfide, provided that a chiral oxazaborolidine catalyst is added to mixture. The broad scope of this reaction, and the high yields and enantiomeric excesses given by the process have made the CBS reduction a very important reaction in organic chemistry.[92–94] While the reduction of ketones by BH_3•SMe_2 can be achieved easily in ambient conditions, the chiral catalyst increases the rate of the prochiral reaction enough to obtain excellent isomer ratios. The mode of action of the CBS catalyst can be described as a double borane-base cooperation as illustrated in **Figure 2-17**.

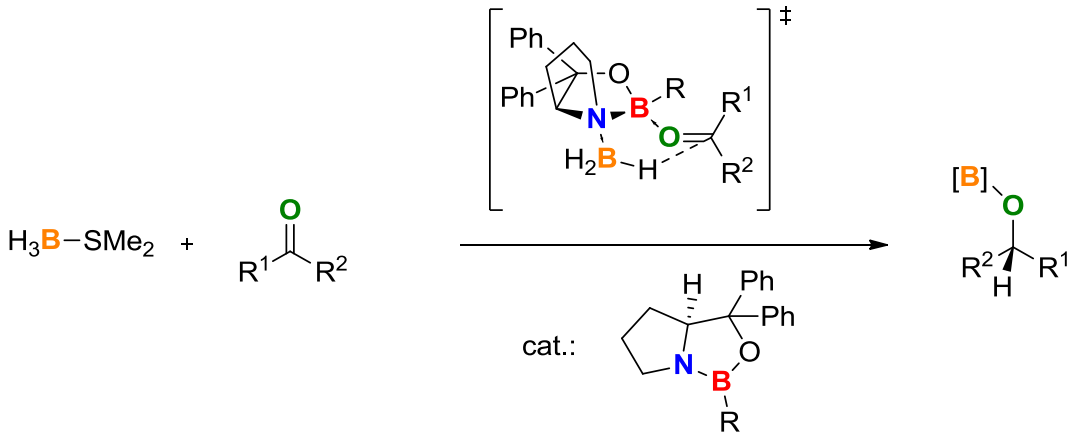

Figure 2-17: Mechanism of the Itsuno-Corey reduction of ketones.

On one hand, an amine group on the catalyst activates the BH_3 through the transfer of its electron density. Simultaneously, the acidic borane group of the oxazaborolidine catalyst is able to bind the ketone substrate, both activating it and directing it towards the reducing agent.[93,94] The proximity of the reagents bound to the chiral catalyst and their simultaneous acid and base activation considerably increase the rate of the prochiral reaction and explains the enantiomeric excesses observed. In the distinct and simultaneous reaction of unquenched acids and bases, the CBS catalyst is an unrecognized early example of the Frustrated Lewis Pairs that has been described previously.

On a final note for this section, it would be good to mention a challenge associated with the use of hydroborane reagents. If the non-hydrogen substituents at boron possess an accessible highest occupied molecular orbital (HOMO), they can participate in metathesis rearrangement with other similar hydroboranes. This reaction is particularly observable in the case of aryl, alkoxy, and haloboranes and cause scrambling of groups on boranes (**Figure 2-18**).[95]

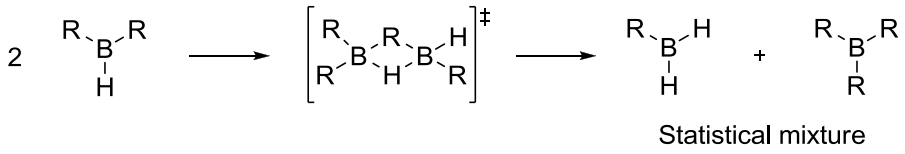

Figure 2-18: Functional group scrambling in boranes.

2.2.3 Chemistry of Organoboranes and Related Compounds

In order to fully appreciate the potential applications of the chemistry presented in this dissertation, something has to be said about the properties and reactivity of organoboranes.[96]

In its bonding with carbon, boron also displays interesting properties. The bond polarization makes boron electropositive and prone to nucleophilic attack, which opens up a rich reactivity for molecules that contain boron-carbon bonds (**Table 2-1**). For this reason, various methods have been developed to synthesize useful boron reagents.

One of the easiest methods (albeit an atom-inefficient one) for the laboratory scale production of organoboranes is the reaction of Grignard with organolithium reagents boron halides. Alternatively, for better selectivity, the less reactive organotin precursors can react with chloroboranes to create B-C bonds by transmetallation. Organosilanes are less reactive than their tin counterpart, although under the right conditions, they can react with boron tribromide in a transmetallation reaction. [96]

The aforementioned hydroboration reaction is also an interesting entry into various alkylboranes, provided that the suitable unsaturated precursors exist.[83]

Finally, catalytic borylation reactions are now included in the modern synthetic tools that allow the preparation of a wide range of organoboranes from stable and convenient precursors. While this reaction is going to be discussed in more depth in a later section, let us mention that this approach is one of the most promising, especially when speaking of C-H borylation, which is an atom-economical route into valuable materials.

The synthetic applications of organoboranes are varied and can be divided into two categories, namely the uncatalyzed reactions and the metal-catalyzed processes. While the latter provide the major parts of the modern synthetic use of organoboranes, an examination

of the intrinsic reactivity of organic boron species is primordial in order to assess the possibilities offered by boron chemistry.

As reagents, the chemistry of organoboranes is rich and versatile, allowing the manufacture of a vast range of products using stoichiometric amounts of stable and inexpensive boron products. Boron reagents can often be prepared *in situ* by hydroboration of Grignard reactions, before being made to react with a variety of substrates.[97] The principal organoboron reactions subsequently performed take roots in the aforementioned properties of boranes, namely their Lewis acidity and the polarity of their bonds.

Indeed, carbons attached to a boron group possess an augmented electron density through the polarization of the σ-bond. This makes them nucleophilic but, in most cases, not enough so to attack common electrophiles.[98] The boron atom, for its part, possesses an empty orbital which allows coordination of a nucleophilic Lewis base. The formation of a tetravalent borane-nucleophile complex further increases the nucleophilicity of the organic groups at boron and their propensity to migrate. If the substrate bound to boron possesses a suitable leaving group or unsaturation, a 1,2-migration can occur, forming new bonds (**Figure 2-19**).[99] By this type of reaction, C-C, C-N, C-O bonds and many others can be formed in mild conditions.[100] Albeit intramolecular, this reactivity constitutes another striking example of Lewis base enabled borane reactivity.

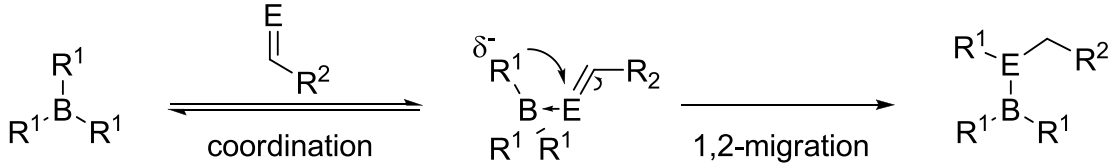

Figure 2-19: Boron-mediated bond formation by a coordination – 1,2-migration sequence (Ak = alkyl).

The propensity of the organic groups to migrate depends on their nucleophilicity. It varies according to their mode of hybridization with the general trend being: alkynyl > aryl / alkenyl > alkyl.[101]

Alternatively, anionic tetravalent borate complexes formed by a nucleophilic attack on boron can react with electrophiles without the need of a migration mechanism. While alkynyl borates[102] are particularly reactive in these conditions, ingenious oxidative homo- and cross-coupling reactions of aryl and alkyl groups were developed over the years.[103–110] By reacting

a tetravalent borate complex bearing at least one nucleophilic aryl group with an oxidant, a stoichiometric C-C coupling can be achieved with retention of stereochemistry (**Figure 2-20**).[103]

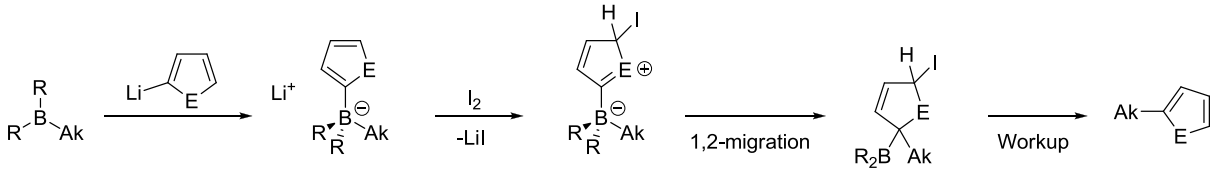

Figure 2-20: Boron-mediated (sp^2)C-C(sp^3) oxidative cross-coupling.

In most or all of the cases mentioned above, the intermediate organoboron product is treated in acidic or oxidative conditions to yield protonated products or alcohols respectively. This treatment decomposes the boron moieties.[111]

Despite the wide scope of their uncatalyzed reactions, the modern synthetic applications of organoboranes are dominated by the palladium-catalyzed Suzuki-Miyaura cross-coupling reaction. This process allows the C-C coupling of various organic halides with boronic acids in mild conditions. The use of non-toxic and earth abundant boronic acids as coupling partners to halides makes it the most environmentally benign of palladium-catalyzed, cross-coupling reactions. The usefulness of this process granted its principal inventor, Professor Akira Suzuki, the 2010 Nobel Prize for chemistry "for palladium catalyzed cross couplings in organic synthesis," along with R. F. Heck and E.-I. Negishi.[6,103]

The mechanism of the Suzuki-Miyaura reaction is similar to that of other palladium-catalyzed cross couplings. In a key step of the reaction cycle, however, a nucleophilic tetravalent boron complex is able to deliver an organic group to a palladium complex, thus allowing the cross coupling. Organoboranes are not able to transmetallate organic groups to palladium by themselves. With the collaboration of base, however, the generation of a tetravalent boron species is key to the reaction.[112,113]

The Suzuki-Miyaura coupling is now an extremely important synthetic reaction and its own research topic. Recent notable efforts have been made to substitute nickel for palladium catalysts.[114] Although not directly within the scope of this dissertation, it has to be hailed as one of the most important contributions to boron chemistry.

2.2.4 Borabenzene Chemistry

While the classical reactivity of organoboranes is of great interest, a particularly striking demonstration of the unique fundamental properties of the boron atom can be found in the borabenzene ring. This molecule, which has fascinated researchers since 1970, is defined as a six-membered unsaturated cycle containing formula C_5H_5B. Theoretical explorations of the structure and bonding in borabenzene have consistently affirmed its planarity and high aromaticity.[115–117]

Another prominent feature of the borabenzene ring is the exceptionally high electrophilicity of its boron atom. Indeed, in borabenzene, the empty orbital of boron is located in low-lying σ*. The particularly high reactivity of such an orbital makes borabenzene a theoretical molecule that never was successfully isolated. In fact, pyrolysis of six-membered boron heterocycle in argon or nitrogen matrixes never allowed even the detection of free borabenzene on solid matrix. Instead, a highly unstable dinitrogen adduct of borabenzene could be observed at 10K in these conditions, illustrating the propensity of this boron atom to bind to even weak nucleophiles.[118]

Stronger nucleophiles allow the isolation of stable aromatic adducts of borabenzene. In fact, since the first preparation of a complex of borabenzene in 1970,[119] a wide range of such adducts have been synthesized through various routes and their properties have been widely explored.[120–133] These complexes can be divided into two categories, depending on the nature of the nucleophilic substituent on the boron atom. While neutral ligands form classical Lewis adducts with borabenzene, anionic bases yield boratabenzenes—formal borates in nature—upon complexation of borabenzene. In the form of these neutral and anionic complexes, borabenzene is found to be a stable isoelectronic analogue of benzene and pyridine (**Figure 2-21**).

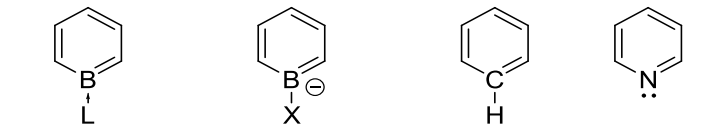

Figure 2-21: Isoelectronic relationship between six-membered heterocycles.

While boratabenzenes have been the object of considerable investigation, notably in view of their potential as ligands to transition metals, the properties of neutral borabenzene adducts are relatively less explored and have not been as formally defined. Work by Fu and coworkers have yielded a reliable and efficient synthetic method for the synthesis of neutral complexes by the ligand-induced aromatization of 2-trimethylsilyl boracyclohexadiene precursors (**Figure 2-22**).[123,134]

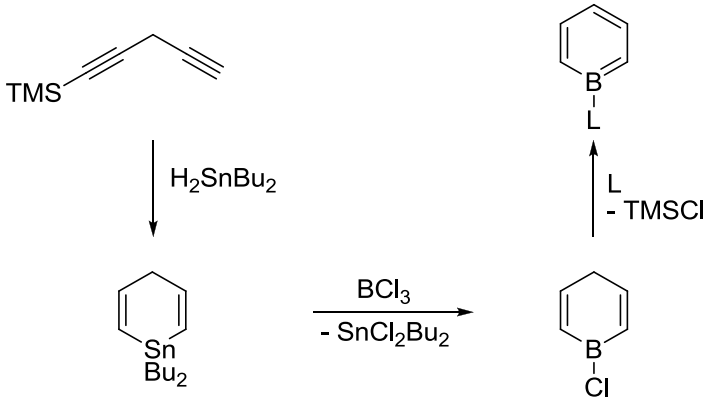

Figure 2-22: Synthesis of neutral borabenzene adducts.

Having been demonstrated with several ligands, the aromatization step is highly dependent on the capacity of the Lewis base to isomerize the 2,5-boracyclohexadiene precursor to the 2,4-boracyclohexadiene and to form a strong enough bond with boron to stabilize the aromatic product (**Figure 2-23**). Weak bases cannot perform such a step, as was shown by Herberich with his demonstration of the inertness of boracyclohexadienes towards reaction with phospholyl complex CpFe(3,4-$Me_2C_4H_2P$).[124]

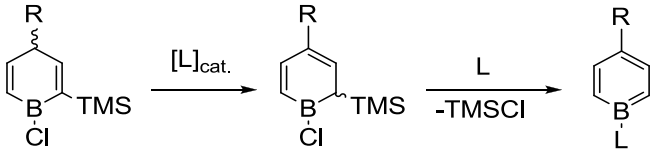

Figure 2-23: Proposed mechanism for the base-mediated aromatization of boracyclohexadiene into borabenzene.

Through this method, Piers and coworkers were able to prepare a wide range of neutral molecules containing one or several borabenzene moieties, some of which exhibit impressive optical properties. Some complexes thus prepared were studied to reveal the reactivity induced by the presence of boron in the molecule.[135–138]

Although the boron atom is electronically saturated, the Lewis acidic character of the molecule is believed to remain present. As such, neutral borabenzene adducts—especially borabenzene-PMe_3—react with anionic nucleophile to generate a broad range of boratabenzenes through an associative pathway (**Figure 2-24**-left). We also reported a unique example of the reverse reaction, the generation of pyridine and trimethylphosphine borabenzene species from an anionic chloroboratabenzene.[128] Although it has been reported that $(CO)_3Cr$(THF-borabenzene) can undergo substitution reactions at boron with neutral Lewis bases, to our knowledge no such reaction has been carried out on metal-free borabenzene species. On the contrary, it was even reported by Fu that the addition of d_9-PMe_3 to borabenzene-PMe_3 in THF at 20°C does not yield ligand exchange.[139]

By contrast, the presence of the boron atom in the six-membered aromatic cycle creates a certain nucleophilic component to the reactivity of borabenzene. This property was highlighted by Piers and colleagues who demonstrated that the borabenzene-pyridine adduct reacts with acids to yield cyclic borenium cations (**Figure 2-24**-right).[140] Although the reaction presumably occurs, *via* protonation of a nucleophilic aromatic carbon, the nature and the consequences of this nucleophilic character of borabenzene have never been formally investigated.

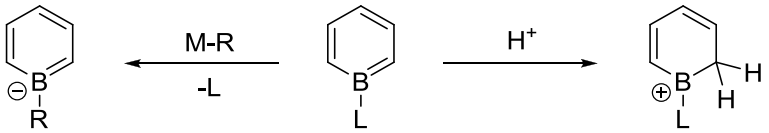

Figure 2-24: Comparison of the reported reactivity of borabenzene complexes towards nucleophiles (left) and electrophiles (right).

The chemistry of borabenzene is a rich field in which too few are laboring. While important discoveries remain to be made on its properties and reactivity, the arduous synthesis steps involved in this research limit the number of active groups on the subject. As will be presented in a later subject, we have ourselves conducted studies on borabenzene adducts that, we hope, contribute to the understanding of bora-aromatic molecules.

2.3 C-H Bond Activation and Functionalization

Having laid out the basic concepts behind the organoboron chemistry that we investigated in this work, we will now present one of the biggest challenges in modern synthetic chemistry and to which we hope to have contributed.

2.3.1 Interest and Impact of C-H Bond Activation

Classically, organic synthetic chemistry relies on the introduction and substitution of functional groups on organic hydrocarbon “backbones.” Functional groups are based on heteroatoms such as oxygen, nitrogen, halogens, sulfur, silicon, and boron. They serve both for functional and synthetic purposes. Indeed, some groups are introduced to organic molecules with the specific goal of being later substituted by another or for coupling using a known reaction (leaving groups). Other groups impart electronic, biological, or physical properties to a material. The selection, introduction, and interconversion of functional groups have been at the core of synthetic chemistry for centuries and have led to the development of innumerable chemical reactions. With the tools of their predecessors, modern chemists now are able to design and prepare molecules of incredible complexity using elegant and creative syntheses.

While the use of functional groups as leaving groups allows complex transformations in organic molecules, the necessity of introducing those to basic compounds prior to their substitution represents a certain waste of matter and energy. In view of the search for “greener” processes that are energy efficient and atom-economical, the use of leaving groups

in synthesis is not optimal. A more attractive way would consist of directly functionalizing molecules by the activation of bonds already present on the precursors.[7]

Organic precursors are built on hydrocarbon frameworks. By definition carbon-hydrogen bonds are ubiquitous in these compounds. Due to their stability and their often limited functional utility, hydrocarbyl groups are often considered as the unreactive part of an organic compound and viewed as a purely structural part of the molecule.

However, by reason of their natural abundance, C-H bonds represent, if they could be selectively activated, attractive reaction partners in green processes. Direct functionalization of C-H bonds represents a considerable shortcut when compared to classical organic chemistry, and it has the potential to open exciting new reaction possibilities. As such, the development of C-H activation methods has been the object of rapidly increasing research interest in the past two decades. Overcoming the stability of the C-H bond was found to be possible through interaction with transition metals, and completely new reactions were developed that allow critical late-stage transformation of big molecules as well as the green production of important compounds.[8]

In the following sections, an overview of the main metal-mediated C-H activation reactions will be presented. Such a vast subject could fill several much longer books than this dissertation. As such, only a selection of systems will be described. An excellent and deep review of the foundations of the subject can be found in a ACS Symposium Series from 2004.[141]

2.3.2 Abbreviated Timeline of C-H Activation Chemistry

The first formal description of the activation of C-H bonds by metal complexes was given by Chatt and Davidson who showed in 1965 that an electron-rich ruthenium-phosphine compound could reversibly cleave the C-H bonds of naphthalene.[142] Only a few years later, Alexander E. Shilov from the USSR disclosed a system for the platinum-catalyzed oxidation of methane in acidic medium that would bear his name and be later considered a comparison standard and textbook example of C-H bond functionalization.[143] In the Shilov system, the limiting step of the reaction is the C-H bond cleavage by a platinum(II) complex. The resulting platinum alkyl complex can be easily oxidized in the reaction conditions. Although of tremendous fundamental importance, Shilov-type systems use potassium hexachloroplatinate as stoichiometric oxidant or harsh conditions[144] and are consequently not applicable to synthesis.

In 1982, another seminal advance in the understanding of C-H activation was made when Bergman and Janowicz reported the cleavage of unactivated aliphatic C-H bonds by oxidative activation at a nucleophilic [Cp*Ir(PMe_3)] center generated photochemically from Cp*Ir(PMe_3)H_2.[145] In the same year, Graham and coworkers published an analogous photochemical reaction from Cp*Ir(PMe_3)$(CO)_2$ (**Figure 2-25**).[146] These important reports represent a great step towards the design of catalysts capable of functionalizing the unreactive C-H bonds.

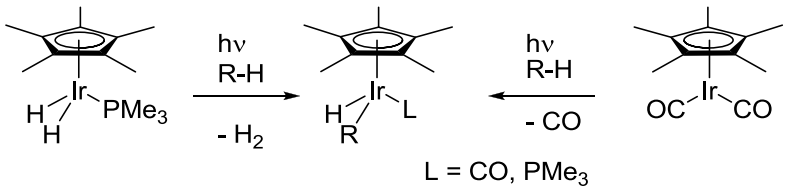

Figure 2-25: C-H bond cleavage of unactivated alkanes by iridium compounds, as reported by Bergman[145] (left) and Graham[146] (right).

The Cp*Ir(L) framework that was shown to activate alkanes provided an excellent platform to study the fundamentals of the oxidative addition of C-H bonds. These systems were examined in parallel with related 16-electron, square-planar complexes using extended Hückel calculations. These studies showed that in CpIr(L), as well as in distorted square-planar complexes, C-H activation of a substrate could occur through a two-fold electronic process: 1) the C-H σ-bond coordinates by donation to an empty orbital of the metal and 2) bonds are created to both carbon and hydrogen by interaction of these atoms with suitably positioned filled orbitals of the metal (**Figure 2-26**).[147]

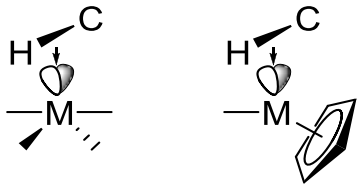

Figure 2-26: Orbitals involved in the C-H oxidative addition in distorted square-planar metal complexes and CpML complexes.

Precious metals in a d^8 state are particularly suited to this type of electron transfer. The Cp ligands also contribute to the transformation by restricting the geometry of the complexes. By contrast, an energy cost is associated with the distortion of square-planar complexes.

Cp*Ir(L) complexes perform the C-H bond activation of aromatic molecules with greater ease than that of alkanes. Interestingly, nucleophilic π-coordination of an aromatic C-C bond to the metal was found to be vital to the activation. W. D. Jones proved that this coordination was the limiting step through isotopic labelling experiments. Indeed, the kinetic isotope effect (KIE) for the stoichiometric activation of benzene and benzene-d_6 by Cp*Rh(PMe_3)(H)Ph was found to be quite small (1.05) suggesting that C-H bond-breaking was not rate-limiting. By contrast, a larger KIE was found for the oxidative addition of 1,3,5-$C_6H_3D_3$ showing that after π-precoordination, C-H bonds are activated faster than C-D bonds.[148,149] Relevant coordination complexes of arenes were later experimentally observed.[150,151]

In fact, isotopic studies are an incredible tool for the development of C-H bond activation reactions. Since the atomic mass of deuterium is about twice as large as that of naturally abundant protium, processes involving the breaking of X-H bonds as a rate-limiting step will display important KIE as a result of their different vibrational behavior. The measurement of KIE can thus yield important information about the mechanism of C-H functionalization reactions. Higher values of KIE are associated with processes in which the C-H bond cleavage is important in the transition state.[152]

More recently, Bergman and coworkers have extended the Cp*Ir C-H activation chemistry to more electron-deficient complexes. Indeed, cationic species of the general form $[Cp^*Ir(L)R]^+$ were shown to be capable of performing alkane metathesis. Extensive work by Hall, Tilley, and Bergman showed that the reaction still proceeded by oxidative addition, demonstrating that C-H bond addition is not exclusive to electron-rich iridium species.[153–155]

While we have discussed some of the results that have most impacted the current understanding of C-H activation reactions, many other metal complexes have been shown to activate C-H bonds in the last 30 years. The body of work and the knowledge that is being accumulated on the subject is very large and reveals many perspectives for the development of new, efficient catalytic reactions for the direct and selective functionalization of C-H bonds.

2.3.3 Catalytic C-H Functionalization

As mentioned before, economic and environmental incentives are pushing synthetic chemists to look for novel reactions with the aim of minimizing the waste of material associated with the reliance on an organic chemistry based on the substitution of leaving groups. It is for this reason that the beginning of the 21st century has seen direct C-H bond functionalization

emerging as a “revolutionary trend” in the synthetic sciences.[8] An ever growing number of catalytic reactions now use C-H bonds as the “active” group on substrates to give materials of high value. From the preparation of polymers to the late-stage functionalization of optical materials and bioactive pharmaceuticals, many processes now rely on metal-mediated C-H functionalization.[156]

The race to such processes was opened in 1983 by Eisenberg and coworkers who reported that $Rh(PPh_3)_2(CO)Cl$ can catalyze the insertion of carbon monoxide in benzene under photochemical conditions in an effectual formylation reaction.[157,158] Similar reactions were rapidly implemented, using arenes, alkanes,[159] aldimines, and ketenes for the insertion in various unsaturated substrates[160] in high yields and mild conditions. [161–163]

Of even greater impact in the synthetic sciences is the direct arylation cross-coupling that has been extensively studied in recent years. Using a wide range of metal catalysts, arenes and heteroarenes can be coupled to a variety of substrates for the atom-economical production of countless chemicals and the late-stage functionalization of important compounds.[8,164–166] One of the most notable expressions of this class of cross-coupling was studied in depth by Fagnou, Gorelsky, and coworkers and consists of the palladium-pivalate catalytic couple for the concerted metalation-deprotonation of arenes and heteroarenes. The use of pivalate as a co-catalyst interestingly actively contributes to the C-H activation step of the mechanism by acting as a base and a proton shuttle (**Figure 2-27**).[167,168]

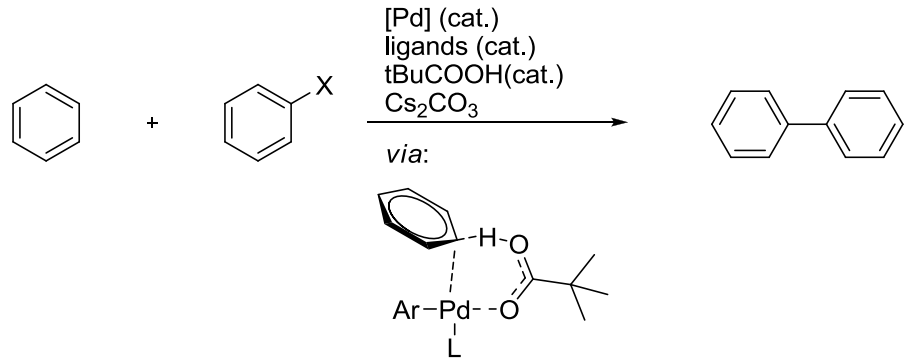

Figure 2-27: Palladium-pivalate catalyzed direct arylation cross-coupling with the key C-H activation transition state represented.

The C-H activation transition state modeled by Gorelsky is surprisingly reminiscent of intramolecular FLP activation of small molecules. In fact, the palladium(II) pyvalate is an ambiphilic complex that can be described as an FLP. Its reactivity towards arenes is a prime

example of acid-base collaboration: the electrophilic palladium(II) atom coordinates the arene though the π-electrons while the carboxylate ligand abstracts an activated proton. Interestingly, the selectivity of the reaction is dependant both on the nucleophilicity of arenes and on the acidity of its protons.[169,170]

Many variations of direct arylation currently exist and extensive work on these reactions has promoted it to its current position as a highly competitive alternative to traditional cross-coupling catalysis. As it has a wide range of suitable substrates, as well as the advantages of being able to directly functionalize C-H bonds, it is a very useful tool in the organic and industrial chemist's arsenal. Its high activity has allowed this direct arylation reaction to be adapted to the synthesis of conjugated polymers in a method developed and extensively studied at Université Laval by Leclerc and coworkers.[171,172]

2.3.4 Iridium-Catalyzed Borylation of Arenes

One last example of a C-H functionalization reaction that is of particular interest to this dissertation is the catalytic borylation of hydrocarbons. With the usefulness of organic boron reagents in many organic reactions—most notably for the Suzuki-Miyaura—methods used to prepare them are very useful for synthetic chemistry. It comes thus as no surprise that C-H borylation has received a special place—even among catalytic C-H functionalization—in the interests of catalysis chemists. In fact, at the time of writing, C-H borylation is a widely used technique to generate organoboron reagents, competing with less atom-economic methods like the Miyaura borylation of aryl halides.[173]

With the downside of being often reliant on the use of precious metals like iridium, the borylation continues to be the object of cutting-edge research and reports of its improvement continue to be regularly published in high-impact chemistry journals. The most notable recent improvements of the method include work towards the use of inexpensive base metals[174] and improvements of the reaction conditions and selectivity.

The pioneering research of Hartwig is at the foundation of metal-catalyzed borylations. He discovered early on that base-metal boryl complexes could easily substitute a variety of X-H bonds (X = NR_2, OR, Cl) with the boryl group acting as an electrophile.[175] Interestingly, the reaction could be extended to aryl then alkyl C-H bonds in photochemical conditions, using iron, ruthenium and tungsten compounds (**Figure 2-28**).[176] The metal fragments used in these

reactions were hitherto unknown to be able to perform C-H bond cleavage, suggesting an important role of the boryl ligand.

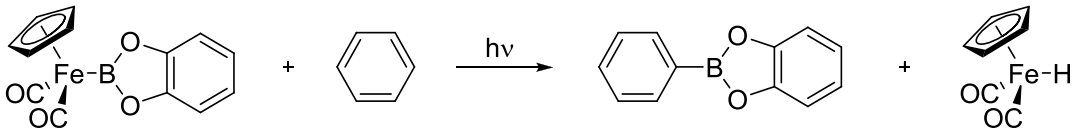

Figure 2-28: Stoichiometric borylation of benzene by an iron(II)-boryl complex in photochemical conditions.

Unfortunately, these metal-boryl complexes have to be prepared from highly reactive alkali metal salts.[175] This precludes their facile inclusion in a catalytic process. Instead, they should be generated by oxidative addition of B_2pin_2 reagent, a reaction that has several precedents in the literature.[177–181] Starting from $Cp^*Mn(CO)_3$ or $Cp^*Re(CO)_3$, they found that the oxidative addition was indeed possible and that the metal-boryl complexes thus found could activate the C-H bonds of alkanes under photochemical conditions. In fact, in catalytic conditions, these metals can mediate the C-H borylation of alkanes by B_2pin_2.[182]

With photochemical conditions impractical for chemical borylation, efforts were made to develop thermally activated processes for the mild borylation of hydrocarbons. For this, precious metals of Group 9 were found to be most active. Indeed, at 150 °C, rhodium and iridium catalysts gave good yields of borylation of alkanes and excellent activities in the case of arenes (**Figure 2-29**).[183,184]

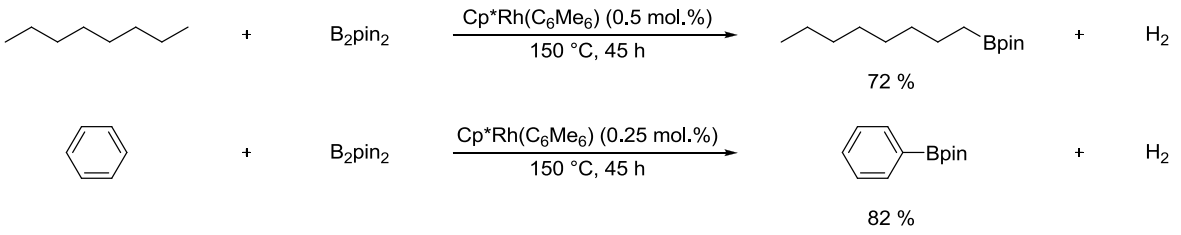

Figure 2-29: Catalytic borylation of arenes and alkanes by rhodium catalysts in thermal conditions.

While the initial arene-rhodium catalysts are not the most convenient reagents to use, subsequent work revealed high activity of the combination of the commercially available di(*tert*-butyl)2-bipyridine ligand with $[(cyclooctadiene)IrCl]_2$ precatalyst for the borylation of arenes (**Figure 2-30**). This system has been optimized for a wide range of interesting

substrates and works well in mild conditions.[185–189] In fact, it has rapidly become the golden standard of C-H borylation of arenes, against which other catalytic systems can be compared.[190]

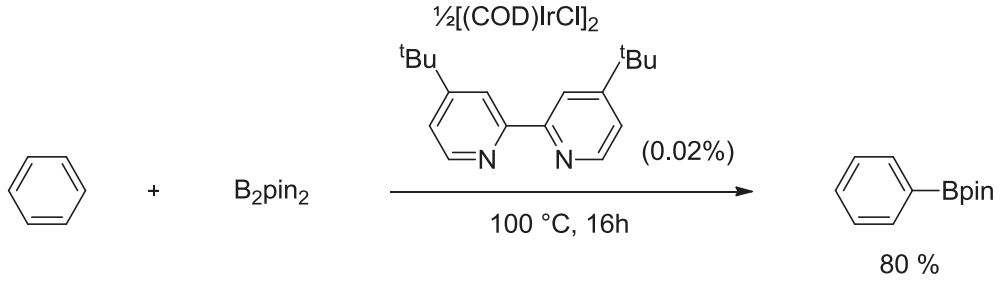

Figure 2-30: State-of-the-art iridium catalytic system for the efficient and mild borylation of arenes.

The mechanism of the reaction has been investigated to reveal evidence for a mechanism involving an active role of the boryl group on iridium in the C-H activation bond. In such a mechanism, the interaction between the boryl and the H atom of an arene is necessary for the activation (**Figure 2-31**).[189]

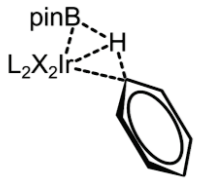

Figure 2-31: Mode of action of iridium-boryl catalysts for the cleavage of C-H bonds in arenes.

This mode of action explains the selectivity observed for the catalytic system that favors, when steric factors are not an issue, the substitution of the most acidic proton of the substrate. Indeed, the C-H activation step was proposed to be the rate-limiting step of the catalytic cycle, illustrating once again the difficulty of cleaving these inert bonds.[189,191] The full catalytic cycle of the borylation of benzene is presented in **Figure 2-32**.[191]

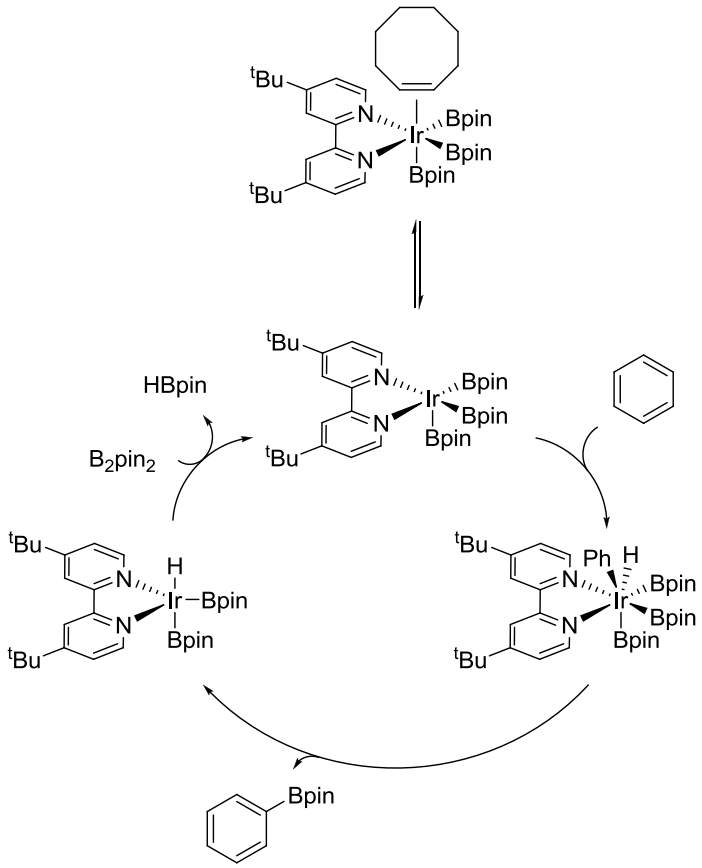

Figure 2-32: Catalytic cycle for the iridium-bipyridine-catalyzed borylation of benzene.

The scope of the iridium-mediated borylation of arenes was also studied and reaction optimization allowed the borylation of countless aromatic and heteroaromatic molecules. The generality of this method makes it indubitably a convenient and atom-economical entry into a vast number of useful chemicals.[189]

Finally, the reaction conditions have been and continue to be improved to the point where many aromatics can now be borylated at room temperature using pinacolborane instead of the expensive B_2pin_2. Thus, at the moment of writing, the iridium-bipyridine system described before has been convincingly demonstrated to be a highly efficient, selective, group-tolerant catalyst for the atom-efficient borylation of arenes in mild conditions.[185,188]

2.3.5 Non Precious Metal-Catalyzed Borylation

"One remaining challenge in the catalytic C–H borylation methodology is the development of base metal catalysts, driven by recent concerns regarding the limited availability of precious metals."[190] This comment was made in the very recent publication describing a system for the nickel-catalyzed borylation of arenes. Indeed, the use of iridium catalysis represents high catalyst costs, purification difficulties, and environmental concerns. Consequently, efforts are being made for the development of inexpensive base metal catalysts to replace, or at least complement, existing iridium-based protocols.

One of the first such systems was developed only in 2010 and consists of a Cp*Fe(carbene) active catalyst that was shown to activate C-H bonds of benzene and heteroarenes and to catalyze the borylation of thiophenes and furans (**Figure 2-33**). However, the low activity of the catalyst, combined with the necessity of using a hydrogen acceptor in this system limit its usefulness.[192]

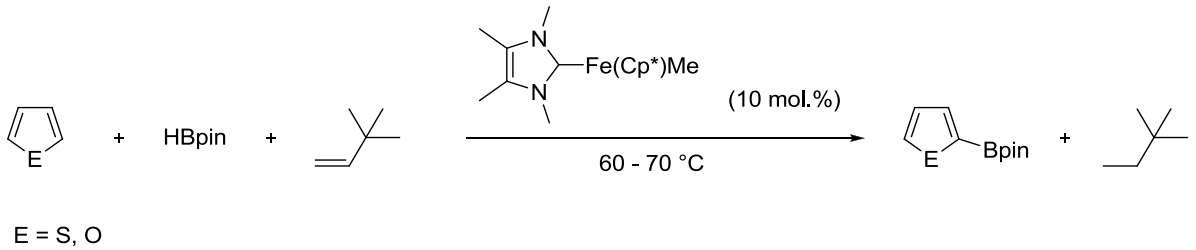

Figure 2-33: Catalytic borylation of heteroarenes by an iron-carbene catalyst in the presence of a hydrogen acceptor.[192]

A more active variation was found in bimetallic copper-iron complexes which were found to photochemically catalyze the borylation of arenes without the need of an acceptor.[193] More recently, Chirik and coworkers disclosed cobalt catalysts bearing redox-active ligands that were able to catalyze the reaction.[194] Sabo-Etienne, Darcel and coworkers also recently reported a new single-site iron catalyst for the same reaction.[174] Along with the nickel catalyst mentioned earlier, there exists today a number of base metal-mediated borylation of aryl and heteroaryl C-H bonds.[190] However, their reactivity remains limited when compared to iridium catalysts, which remain dominant in the field of C-H borylation.

2.3.6 Metal-Free Electrophilic C-H Borylation

Going a step further, the idea of completely removing transition metals from C-H borylation methods is a challenging, yet attractive idea. To this end, Ingleson and coworkers have studied highly electrophilic borocations as potential borylation agents for arenes. Indeed, they have found that catecholboron cations could rapidly borylate arenes at ambient temperature. These cations had to be produced *in situ* by halide abstraction of the corresponding halocatecholborane in the presence of a strongly Lewis acidic silylium, itself generated *in situ* from a silane and a tritylium cation.[195]

Interestingly, the boron cations thus formed were found to propagate the catalytic borylation of arenes by HBcat at temperature ranging from 80 to 140 °C. The impracticality of the method, however, as well as the highly reactive species involved, make this process less than competitive to iridium-based borylations.

Following this initial report, Ingleson and coworkers have showed the greater applicability of well-defined borenium cations for stoichiometric borylation.[196,197] It was also shown by

Prokofjevs and Vedejs that tetracoordinated boronium in a strained chelating environment could perform the same reaction.[198]

One of the most promising features of the stoichiometric borenium-based borylation of arenes is its selectivity which is different and complementary to that of iridium systems: instead of substituting the most acidic C-H bond, boron cations borylate the most nucleophilic position on the arene. In fact, by nature and by virtue of their selectivity, these reactions are related to Friedel-Crafts chemistry: they consist of the attack of an arene on a highly reactive electrophile generated by Lewis acid activation.

With that said, one must realize that the field of metal-free C-H borylation is but emerging. At the time we began our work, and still today, considerable work was needed to develop metal-free, convenient, selective, mild, and efficient catalysts for C-H activation and borylation of arenes.

2.4 Proposed Advancement of Knowledge

Considering the richness and variety of boron chemistry, we set our goals to expand it towards novel catalytic applications. Transition metal catalysis is a very powerful tool that is well known and widely used but that comprises downsides in terms of its high costs and contamination issues. In the quest for novel catalytic systems that do not rely on metals, we decided to investigate the factors that influence reactivity of boron and to develop new concepts to expand its chemistry. Foremost in our interests was, throughout the work presented here, the particular relationship that exists between organic boron compounds and Lewis bases. This collaborative reactivity is the core and the unifying concept of the very diverse reactions that will be presented in this thesis.

Chapter 3 - Methodology

In this chapter, we will give a brief overview of key methods that have been used in the context of this research. We will describe characterization, computational modeling, and synthetic methods.

3.1 Characterization Techniques

In our work on organoboron chemistry, the main characterization methods for new products are nuclear magnetic resonance spectroscopy and X-ray diffraction.

3.1.1 Nuclear Magnetic Resonance Spectroscopy (NMR)

NMR spectroscopy is a powerful tool for modern organic chemistry as it is used to gain information on the ubiquitous hydrogen and carbon atoms. In the hands of the organometallic chemist, NMR spectroscopy gains even more importance, as it allows the identification of atoms of many other nuclei (**Table 3-1**).

Table 3-1: Characteristics of the different nuclei that were analyzed by NMR in the course of this work.[199]

Isotope	Spin Number	Natural Abundance (%)	Frequency (MHz) (at 11.743 T)
^{1}H	1/2	99.98	500.0
^{2}H (D)	1	$1.5x10^{-2}$	76.753
^{13}C	1/2	1.108	125.721
^{11}B	3/2	80.42	160.419
^{31}P	1/2	100	202.404

Deuterium deserves an honorable mention in the list above, despite not having been directly analyzed by NMR. Rather, it can be used in labelling experiments as an isotope of hydrogen. Two properties of deuterium make it a valuable nucleus for reactivity studies.

First, the nuclear spin of 1 of deuterium can couple with that of other nuclei. This allows us to monitor the whereabouts of deuterium atoms in labelled systems. For example, in our work on dehydrogenative C-H borylation, the reaction of a deuterated substrate with a hydroborane evolves HD as a by-product. As shown in **Figure 3-1**, the HD resonance can be distinguished from that of H_2 by the H-D coupling which gives a triplet signal. Interestingly, HD also does not have the same chemical shift as H_2.

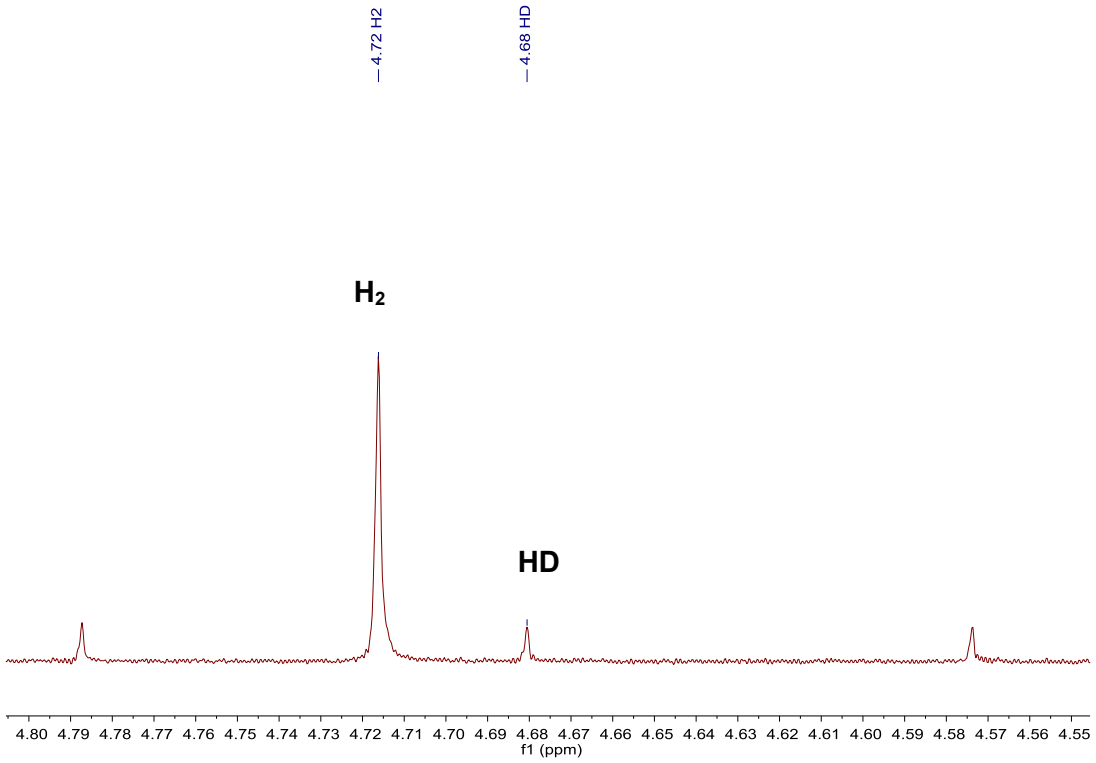

Figure 3-1: ^{1}H NMR spectrum of a dehydrogenative borylation reaction performed on an equimolar mixture of 1-methylpyrrole and 1-methylpyrrole-d_4 with pinacolborane. The region corresponding to the signal of H_2 and HD is represented.

Deuterium is also useful as an isotope of hydrogen with a different resonance frequency than the proton. Deuterated positions on organic molecules will not give signals in ^{1}H NMR. This property can be used to quantify the involvement of labelled molecules in a reaction as will be seen later.

In the context of our work on carbon dioxide, something has to be said of the use of labelled $^{13}CO_2$. Indeed, while natural carbon dioxide has a very low ^{13}C content, it is possible to purchase and to use isotopically enriched carbon dioxide. In this way, it becomes very easy to confirm $^{13}CO_2$ incorporation into reaction products by the hundredfold increase of the intensity of the ^{13}C NMR signal of the products coming from $^{13}CO_2$ reactions. Furthermore, the ^{13}C enrichment of molecules makes it possible to observe ^{13}C-X couplings that would not be seen otherwise **Figure 3-2**.

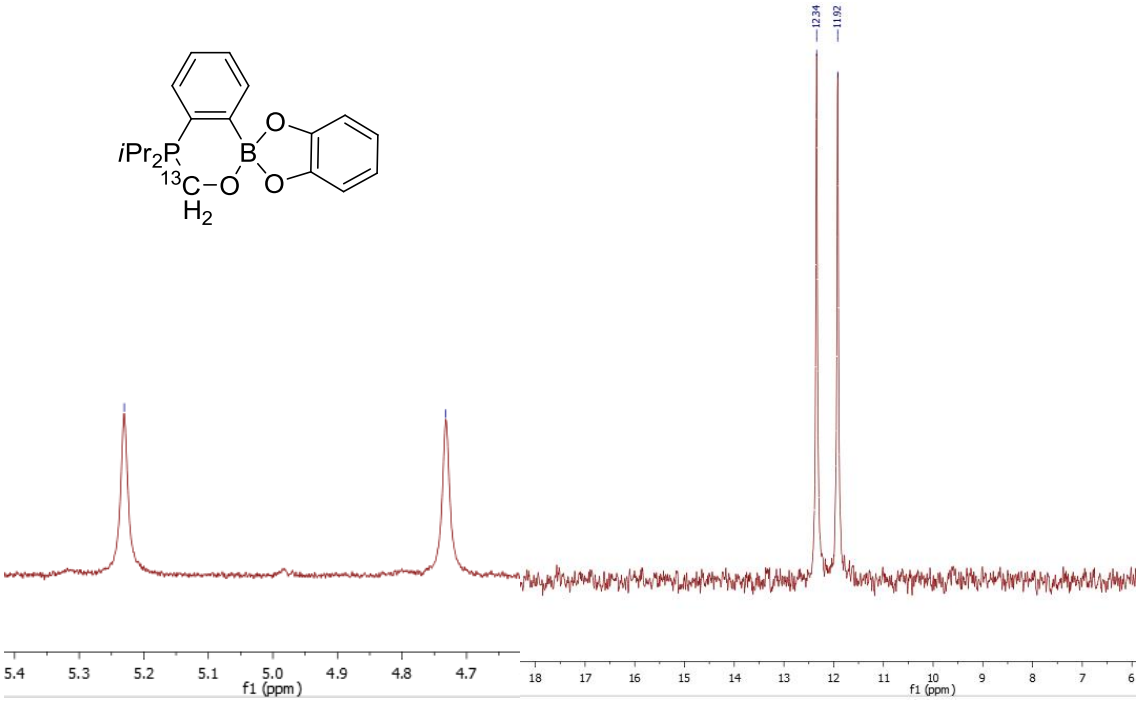

Figure 3-2: Left: ^{1}H NMR spectrum (chloroform-*d*, 300 MHz, zoom on formaldehyde resonance); Right: $^{31}P\{^{1}H\}$ (chloroform-*d*, 121 MHz) of a $^{13}CH_2O$ adduct of a phosphine-borane ambiphilic molecule. Both signals would be singlets without the ^{13}C enrichment.[200]

Finally, ^{11}B NMR spectrospcopy is a very powerful tool for the boron chemist, allowing facile characterization of relevant interactions in compounds. The chemical shift of the boron resonance varies strongly with its environment and gives information on the bonding environment of the boron atom. For example, the resonance of tetracoordinated boron complexes is typically found in the 10 – -60 ppm region. By contrast, the signals of tricoordinated complexes are generally located between 90 and 10 ppm, with stronger π-donation to boron associated to higher field resonances.

In its coupling with other atoms, ^{11}B also displays unique possibilities. In typical complexes, the quadrupolar moment of the elements interferes with the relaxation of nearby NMR active nuclei and causes broadening of their resonance signals. In the case of ^{13}C NMR, it is not uncommon to completely lose the signal associated with boron-bound carbon nuclei. This effect is cancelled, however, in the case of perfectly symmetrical tetrahedral boron complexes, as will be illustrated in a later chapter.

3.1.2 X-ray Diffraction Crystallography (XRD)

Another powerful characterization tool in organometallic chemistry is the analysis of single crystals by X-ray diffraction. On the one hand, this method rests on an elegant body of theory that is currently well understood by chemists. As described by Bragg's law, a crystal will diffract incoming X-rays according to a dependence on the incidence angle, the wavelength, and the arrangement of the crystal planes.

$$2d \sin\theta = n\lambda$$

Equation 3-1 Expression of Bragg's law. n is a positive integer, d is the interplanar distance, θ is the incidence angle and λ is the wavelength of the incoming X-ray.

On the other hand, the necessity of using single crystals for these analyses can make it a challenging tool to use. Indeed, the growth of high-quality, properly sized crystals is a difficult – and sometimes frustrating – endeavor that requires patience, finesse, and other indescribable qualities.

The reward is, however, worth the efforts as XRD allows us to precisely characterize the structure of new compounds in the solid state. In a typical experiment, a suitable crystal is introduced in a viscous organic matrix and installed on a goniometer that is set in front of an X-ray source. During irradiation, a detector based on a charge coupled device (CCD) collects the diffractions from different angles of the single crystals. This initial diffraction data allows the software associated with the diffractometer to calculate the unit cell parameters for the crystal.

If the unit cell is deemed interesting, a second acquisition phase can be started. This second phase can last up to 72 hours and will give precise data that, once processed by the software, describes the electronic density distribution in the unit cell. This information will then be interpreted by the experimentalist to determine the structure of the compound. It is also the

experimentalist's responsibility to ensure the validity of the structure that is obtained. As a matter of fact, it is not always the major product of a mixture that crystallizes and it is dangerous to assume that the crystallographic structure obtained is that of the relevant species in a system. Consequently, XRD should always be coupled with other characterization techniques, especially when studying the active species in a catalytic process.

Figure 3-3: Bruker Apex II Diffractometer that is operated by our group.

In our department, measurements are performed on a Bruker Apex II Diffractometer (**Figure 3-3**). Dr. Wenhua Bi is a valued crystallographer that I would like to acknowledge for his work on our crystal structures and for his useful insights and education on the matters of XRD and crystal growth.

3.2 Computational Methods

3.2.1 Density Functional Theory (DFT)

A large part of the body of experimental work presented in this thesis is supported, and sometimes based, on conclusions obtained through computational molecular modeling. To this end, we have applied methods that are based on the density functional theory.

While a complete description of the theory lies outside of the objectives of this thesis, it is pertinent to present a few key-aspects of the method that the reader may not be familiar with.[201]

DFT-based methods are a modern alternative to wave function-based calculations that rely on the Schrödinger equation. DFT is, in a way, an alternate way to represent atoms and molecules. Its definition is rooted in two theorems formulated by Hohenberg and Kohn that express the ground state of a system in terms of its electron density.[202] In fact, this electron density can itself be defined, in space, by a functional (i.e. a function of a function), with the ground state minimizing this functional.

This description of many-electron systems through only the electronic density is what makes DFT attractive as a modeling tool for molecules over wave function-based methods. Indeed, except for a few exceptional cases, the Schrödinger equation cannot be analytically resolved because of its electron-electron potential term that depends on two variables (**Equation 3-2**). Precise methods that give satisfactory solutions to this problem are typically resource-expensive for systems as big as molecules.

$$\hat{H}\Psi = \left[\sum_{i}^{N} -\frac{\hbar^2}{2m}\nabla_i^2 + \widehat{\sum_{i}^{N} V(\vec{r_i})} + \sum_{i<j}^{N} U(\vec{r_i},\vec{r_j})\right]\Psi = E\Psi$$

Equation 3-2: Schrödinger's equation for a N electron system, with the bielectron term evidenced in red.

By contrast, by defining the whole system in terms of an effective electron density potential, DFT gets rid of two-electron terms. In its core expression, the Kohn-Sham equation, no unresolvable term exists.[203]

$$\left[-\frac{\hbar^2}{2m}\nabla_i^2 + V_s(\vec{r})\right]\phi_s(\vec{r}) = \epsilon_i\phi_i(\vec{r})$$

Equation 3-3: Kohn-Sham equation.

As can be seen from **Equation 3-3**, in Kohn-Sham formalism, the system can be defined using only the global density that depends on spatial coordinates. The potential V_s is for a single particle and dependent on the electronic density. It can be developed as:

$$V_s = V + \int \frac{n_s(\vec{r}) n_s(\vec{r}')}{\left|\vec{r} - \vec{r'}\right|} d^3r' + V_{XC}[n_s(\vec{r})]$$

Equation 3-4: Development of the potential term V_s as dependent on the electronic density.

The density (n) can then be defined by a set of bases (orthogonal monoelectronic functions) as described in **Equation 3-5**. These functions are the Kohn-Sham orbitals, which are used to accurately model the electron density, but that do not correspond to actual molecular orbitals, since they are independent of the wave function.

$$n(\vec{r}) \stackrel{\text{def}}{=} n_s(r) = \sum_i^N |\phi_i(\vec{r})|^2$$

Equation 3-5: Definition of the electron density by a set of monoelectronic functions (Kohn-Sham orbitals).

Equation 3-4 and **Equation 3-5** are extremely important in DFT. They show both the advantages of Hohenberg-Kohn-Sham formalism and its challenges. Indeed, while all potential terms are monoelectronic and defined with regard to the density, they are interdependent because the φ_i functions (the Kohn-Sham orbitals) depend on the Vs potential (**Equation 3-3**). V_{XC} (the potential term that includes the many-particles interactions) is dependent according to the density (defined by the φ_i functions) that is in turn dependant on V_s. V_s depends on V_{XC} (**Equation 3-4**).

This complex interdependence of the potential terms can only be resolved through an iterative process. In such a method (called Self-Consistent Field (SCF)), an initial guess of the electronic density is produced for the system under consideration, which allows one to solve the Kohn-Sham equation and generate new φ_i functions which will be used to produce a new density. This cycle is repeated until convergence – i. e. when internally defined energy criteria.

To perform such calculations, the form of the bases used to define the density (the φ_i functions) has to be described. For this, various basis sets are available in the literature and provide a platform to build the Kohn-Sham orbitals for each atom of the system. Different degrees of complexity exist in basis sets and the appropriate functions should be chosen with regard to the size of the system, the elements involved and the type of calculation that is performed.

Another challenge of the DFT methods is that the exact nature of the dependency of the V_{XC} functional – which includes the exchange and correlation forces between electrons – on density is not known accurately. It has to be approximated. Many expressions of this functional for use in calculations have been published and can be used for molecular modeling with variable accuracy. It is important to review the literature carefully before choosing the functional to use for a set of systems.

3.2.2 Application of DFT in Molecular Modeling

In our case, our interest is in the modeling of molecules to our research and the calculation of their thermodynamic properties. We will now briefly describe the protocol that is followed to obtain relevant information.

Molecular modeling requires an educated understanding of chemical processes and molecular geometry. The first step to a successful model is the building of a reasonable initial structure using a 3D graphical interface. The atomic coordinates of the model are then combined to commands in an input file that is destined to the calculation software. The latter, in our case is the general quantum calculation program Gaussian[374, 375] that is installed on computer clusters operated by Compute Canada and Calcul Quebec.

This program first applies the SCF method presented above to represent the ground state of the system that is described by the initial structure that we generated. By this initial step, the electronic energy of the system can be known. The model is then subjected to another process in which the structure is modified according to different algorithms in a sequence of steps. For each new structure, the electronic energy is again calculated according to the Kohn-Sham equation with the process looking to converge to the lowest energy structure. Alternatively, the optimization can be made to converge on a saddle-point (minimum in all degrees of liberty but one) of the energy that will correspond to a transition state. This is a structure optimization calculation that produces a final structure that is more “real” – according to the level of theory implemented in the calculation – than the initial guess entered by the experimentalist.

With the optimized structure in hand, it is possible to request many other types of property calculations. Most notably, vibrational analysis of the structure gives a thermochemical energy calculation that can be correlated to the thermodynamic data of the molecule. In this process, the program analyzes the different vibration modes for the molecule and calculates the enthalpy and free energy of formation of the molecule.

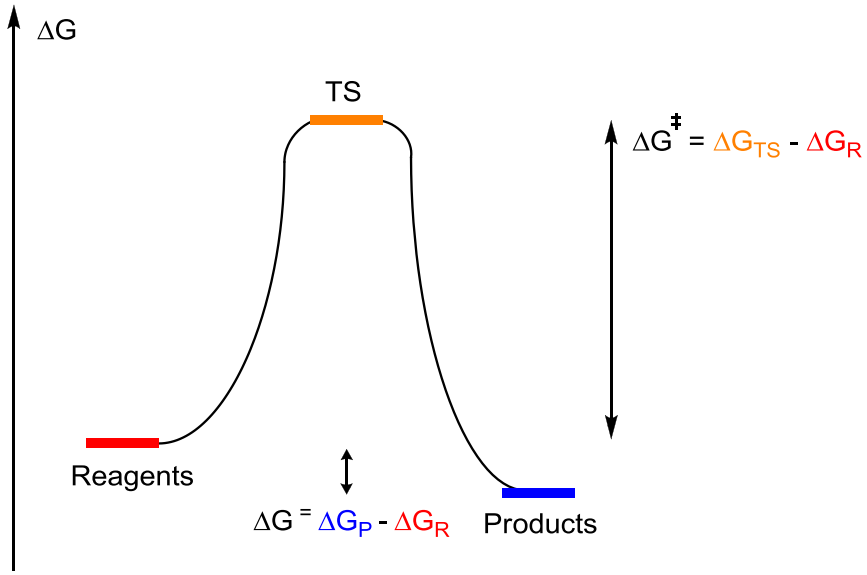

Figure 3-4: Representation of the energy profile of a reaction with simple formulas that allows for the calculation of reaction energies.

In summary, with these calculations, we can obtain a realistic structure for a molecule, as well as thermodynamic parameters for it. Using these parameters, reactions can be predicted. Indeed, by comparing the formation energies of the products with those of the modeled reagents, one can predict the endo- or exergonicity of the corresponding processes. The activation barrier can also be calculated in this way by taking the energy of the transition state.

3.3 Experimental methods

Most of the syntheses that were performed in the context of this work are rooted in analogous reactions that have been previously reported, either by our group or by others. For this reason, it does not seem pertinent to review them here. We will, however, briefly describe some specific techniques that were used in this research.

3.3.1 Inert Atmosphere Chemistry

The interest of our research is heavily weighted towards reactive organoboron compounds. Borabenzene derivatives are particularly sensitive to moisture and oxygen and FLP catalysts are designed to be able to activate such small molecules. For this reason, when working with such compounds, special care has to be taken to exclude even traces of water or oxygen from the reaction media. Consequently, we work using equipment that allows such conditions.

The main apparatus that allows us to work in inert atmosphere is the Schlenk line, which consists of the combination of nitrogen and vacuum inlets. The Schlenk line connects specially designed glassware to both a nitrogen source and a vacuum line simultaneously (**Figure 3-5**-right). This enables efficient purging of oven-dried glassware through vacuum-nitrogen cycles.

Once the reaction flask is purged from air and moisture, reagents can be introduced to it using syringes or cannulas and pressure differences. The Schlenk line, when properly used and maintained is one of the most reliable ways to perform atmosphere-sensitive chemistry in large scales.

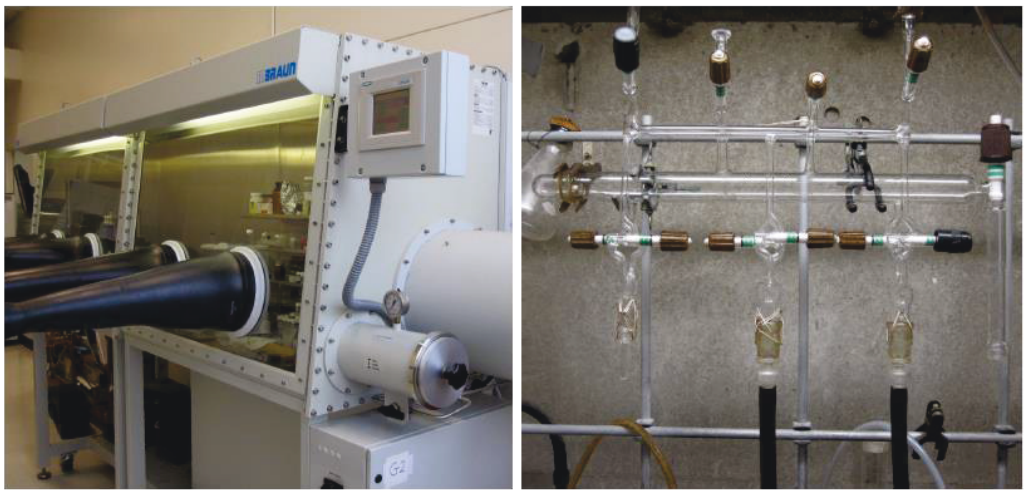

Figure 3-5: Glovebox (left) and Schlenk line (right) in operation in our laboratory.

For smaller scale reactions, for the preparation of NMR samples and the storing of products, gloveboxes can be used. They consist of an enclosed space filled with a controlled atmosphere of dry nitrogen. Their only access to the outside atmosphere is through an antechamber that can be purged through nitrogen-vacuum cycles. The experimentalist can access the contents of the glovebox through permanently installed gloves (**Figure 3-5** - left).

3.3.2 Handling of Gaseous Reagents

In the context of our interest in carbon dioxide chemistry, we performed many experiments using this gas. Once again, the Schlenk line is a remarkable tool for such work. The nitrogen supply can be switched for a CO_2 inlet in order to introduce it to reaction mixtures. In suitable glassware, the CO_2 can be condensed, using liquid nitrogen cooling, and pressurized upon thawing.

For this, we performed experiments in J-Young NMR tubes and Fisher-Porter flasks. The former is an NMR tube that is fitted at the top with a Teflon stopper that makes it gas-tight. J-Young tubes are fitted with joints that make them attachable to a Schlenk line. They are excellent for the monitoring of small-scale reactions that are either air-sensitive or that involve the use of gasses.

Fisher-Porter tubes, for their part, are thick-walled reaction vessels of various sizes that can be sealed and can tolerate internal pressures of several atmospheres. They were found to be suitable for the large-scale reduction of carbon dioxide in our studies.

In all cases, caution is required when using condensed and pressurized gases in closed glassware. J-Young tubes should not be loaded with more than five atmospheres of gas and Fisher-Porter flasks, depending of their size, should not be submitted to more than 12 atmospheres of internal pressure. Appropriate protective equipment, such as anti-explosion shields should be used during these reactions.

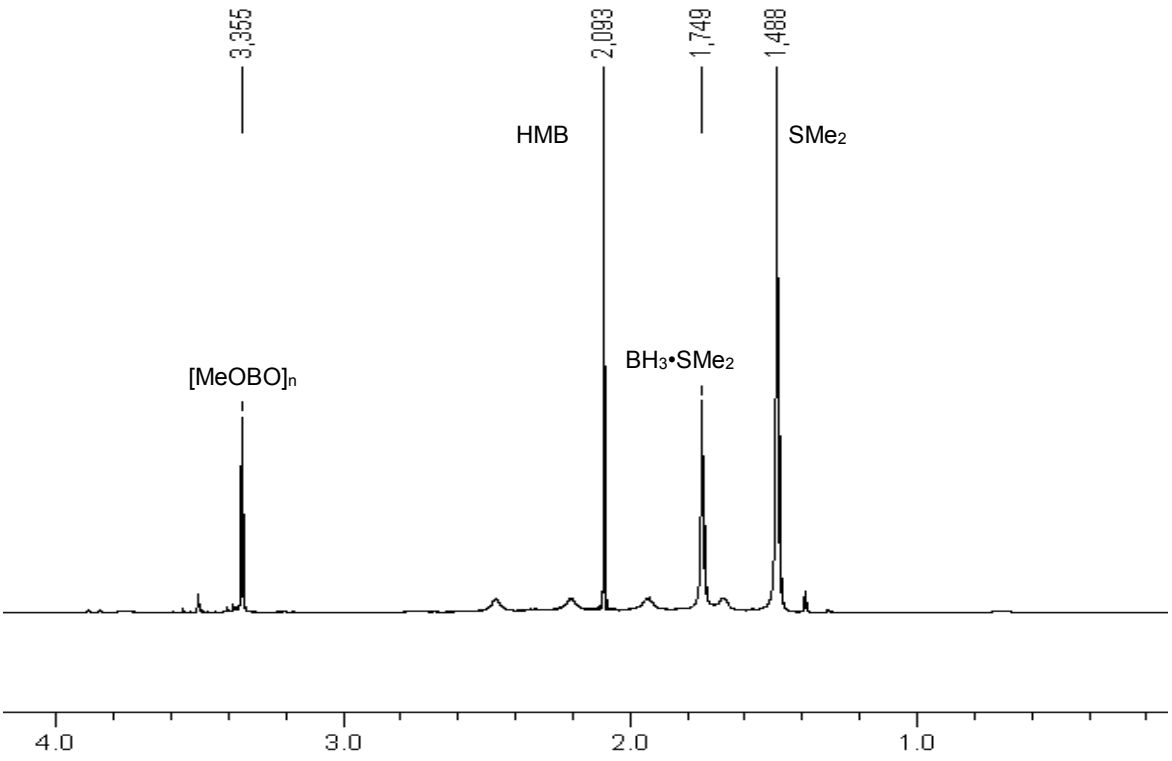

Figure 3-6: Typical ^{1}H NMR (benzene-d_6, 400 MHz) spectrum of the base-catalyzed reduction of carbon dioxide by BH_3•SMe_2 (zoom 0 – 4.2 ppm). HMB = hexamethylbenzene standard.

In a typical CO_2 reduction experiment on the NMR scale (**Figure 3-6**), a J-Young tube is loaded with a solution of catalyst and reductant in the nitrogen-filled glovebox. It is then attached directly to the Schlenk line using standard Schlenk techniques. The sample is subsequently frozen in liquid nitrogen and put under vacuum to remove the nitrogen atmosphere. Once degassed, the solution is allowed to warm up for one minute before the introduction of CO_2 to the tube.

3.3.3 Competition Experiments for the Determination of the Kinetic Isotope Effect

As was mentioned in an earlier chapter, isotope labelling experiments are a great tool in the context of C-H activation chemistry. The kinetics of the cleavage of C-H bonds will be greatly affected by the substitution of a proton by a deuterium atom. The change in reaction can be measured experimentally to yield information about the mechanism of reactions. This leads to define the kinetic isotope effect (KIE) as **Equation 3-6**.

$$KIE = \frac{k_H}{k_D}$$

Equation 3-6: Calculation of the kinetic isotope effect with regard to protium and deuterium. k_H and k_D are the rate constant of the reactions involving each isotope.

One of the most reliable ways of measuring the KIE of a process is the competitive reaction of the deuterated and non-deuterated substrates with a reagent and the measuring of the relative rate of reaction through the proportion of deuterated products. Alternatively, the direct measurement of the rate of reaction of the deuterated and non-deuterated substrate in identical, yet separate experiments can yield the same information, albeit within a greater error margin.

In our case, we performed competitive reactions. In a typical experiment, an equimolar mixture of the deuterated and non-deuterated substrate is added to a reagent in a J-Young NMR tube. An initial NMR analysis confirms the initial H/D ratio in the mixture, by comparison to an internal standard. After the reaction, the final H/D ratio in the final product is the basis to calculate the KIE as it correlates to the reaction rates of the respective species.

Chapter 4 - Insights into the Formation of Borabenzene Adducts via Ligand Exchange Reactions and TMSCl Elimination from Boracyclohexadiene Precursors

In this chapter, we present a study of the properties of neutral adducts of borabenzene.

4.1 Context of the Research

As mentioned in Chapter 2, neutral borabenzene adducts have been less studied than their anionic boratabenzene counterparts, to which they are precursors. Indeed, boratabenzenes can be prepared by nucleophilic attack of neutral borabenzene adducts, which implies an electrophilic behavior of borabenzene.

For their part, neutral borabenzene adducts can be synthesized in several steps by an elegant procedure reported by Fu and coworkers and that involves the base-mediated aromatization of boracyclohexadiene.

In order to shed light on the exact contribution of boron to the reactivity of organic molecules, we instigated a detailed study of the properties of neutral borabenzene adducts, highlighting the thermodynamics of Fu's borabenzene synthesis. We also present a broad investigation of the nature and the strength of the bonding between borabenzene and neutral ligands. Following that, we propose a novel procedure for the generation of borabenzene adducts through ligand exchange and discuss how its mechanism describes the nucleophilic character of borabenzene. This work follows our previous study of platinum-chloroboratabenzene adducts and the observation of ligand exchange in them.[128]

The results that comprise the core of this chapter have already been published in peer-reviewed press. The article describing our investigation will be included in this chapter in integral form.

4.2 Abstract

The bonding properties of borabenzene with various neutral Lewis bases have been investigated. 1-Chloro-4-*iso*propyl-2-trimethylsilyl-2,4-boracyclohexadiene reacts with a number of Lewis bases – notably pyridine, PMe_3, PCy_3 and PPh_3 – to afford 4-*iso*propylborabenzene-base adducts. These adducts can undergo ligand exchange to afford new borabenzene complexes. The scope and mechanism of the reaction, as well as the steric and electronic properties of different adducts were studied experimentally and computationally.

4.3 Résumé

Les propriétés des adduits formés par différentes bases de Lewis neutres avec le borabenzène ont été investiguées. 1-Chloro-4-*iso*propyl-2-trimethylsilyl-2,4-boracyclohexadiene réagit avec une variété de ligands neutres – notamment la pyridine, PMe_3, PCy_3 et PPh_3 – pour donner des adduits de forme 4-*iso*propylborabenzene-ligand. Ces complexes peuvent subir un échange de ligands pour donner de nouveaux adduits. La généralité de cette réaction, ainsi que son mécanisme et les propriétés stériques et électroniques de différents adduits de borabenzène ont été étudiées expérimentalement et par des méthodes de modélisation.

4.4 Introduction

Both the electron donating properties and the steric hindrance of a Lewis base can play a major role in the stability of a Lewis adduct.[204–206] On one hand work has been done to minimize the binding interactions of Lewis adducts in order to exploit the Lewis character of each individual component. It is notably the case in the now popular “Frustrated Lewis Pairs”[40] that can activate small molecules, such as hydrogen[42] and carbon dioxide,[52,64,69–71,207,208] and in the design of ambiphilic molecules,[48,209–211] notably as ligands for transition metals[212–221] and for ion sensing.[222–225] On the other hand some research has been aiming at increasing the strength of these interactions in order to stabilize very reactive Lewis acid sites from further transformations. Such strategy has been recently devised in the work of Braunschweig to stabilize the borolyl anion (**Figure 4-1A**),[226] of Piers to synthesize stable boraanthracene adducts (**Figure 4-1B**),[227,228] and of Bertrand to generate the highly reactive borylene fragment.[229]

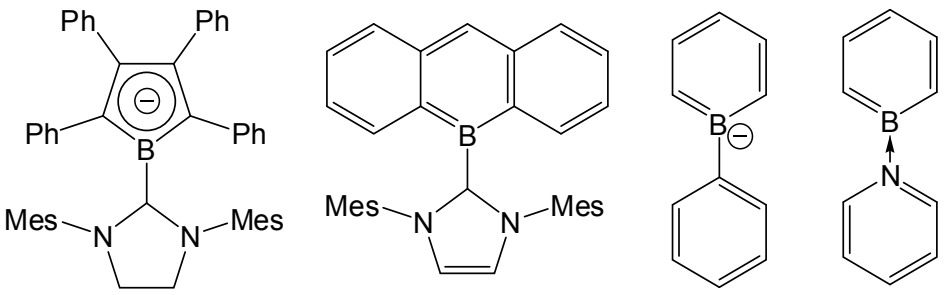

Figure 4-1: Carbene stabilized borolyl anion (**A**), boraanthracene adduct (**B**), phenylboratabenzene (**C**), and borabenzene-pyridine adduct (**D**).

Even when generated by flash thermolysis and condensed at 10 K in an argon matrix, the base-free borabenzene moiety has never been isolated or observed.[118] Base-free borabenzene has been calculated to possess a stable aromatic ring but the low lying σ* orbital on boron requires stabilization by a Lewis base.[117,230,231] Although the boratabenzene moiety, the anionic equivalent of borabenzene, was first reported by Herberich in 1970 (**Figure 4-1C**),[119] the pyridine-borabenzene adduct, the first stable neutral borabenzene, was only reported in 1985 (**Figure 4-1D**).[232] In 1996, an elegant general synthetic route for the generation of neutral borabenzene derivatives was designed by Fu where the aromatization of trimethylsilyl substituted chloroboracyclohexadiene derivatives is initiated by the addition of a Lewis base L which induces the elimination of TMSCl (**Figure 4-2**).[123] The aromatization, however, relies heavily on the capacity of the Lewis base to isomerize the 2,5-boracyclohexadiene precursor to the 2,4-boracyclohexadiene and to form a strong enough bond with boron to stabilize the aromatic product. In such regard, it was observed that the phospholyl complex CpFe(3,4-$Me_2C_4H_2P$) failed to react with the boracyclohexadiene precursor to generate a borabenzene adduct because of the lack of nucleophilicity at the phosphorous atom.[124]

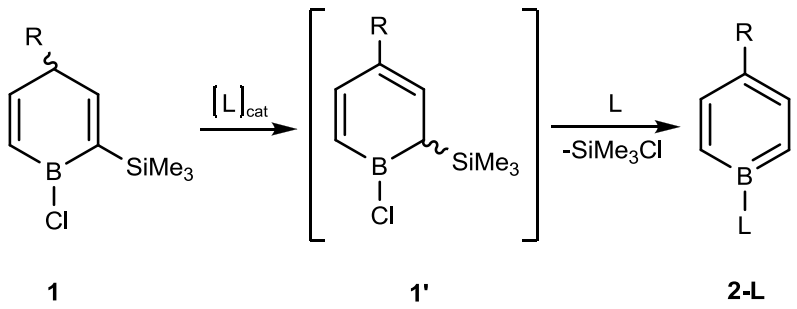

Figure 4-2: General synthesis of neutral borabenzene adducts.

In the past years, there have been a large number of reports on the properties of boratabenzene derivatives, notably as ligand for transition metals.[121,122,125,126,130–132,233–237,237–241] There are, however, only a limited number of transition metal adducts with neutral borabenzene analogues as ligands,[242–245] and although several boraaromatic adducts have been synthesized by Piers for their optoelectronic properties,[135,137,227,228,246] a limited number of studies have been reported on the reactivity of the neutral fragment.[120,140,242,247] It was observed that although the boron atom is formally electronically saturated in the borabenzene adduct, the Lewis acidic character remains prevalent in borabenzene complexes. The coplanarity between the borabenzene plane and the conjugated system of the acrolein in (3-(dimethylamino)acrolein-borabenzene)$Cr(CO)_3$ complex suggests that the borabenzene acts as a π-acceptor ligand.[243] However, the π-acidity of the metal-free borabenzene adducts has never been clearly determined.

It has been demonstrated on several occasions that the addition of anionic nucleophiles on borabenzene-PMe_3 cleanly generates the boratabenzene analogues by an associative pathway, and that other routes, such as the formation of a borabenzyne intermediate, were unlikely.[139] We reported that the reverse reaction, the generation of pyridine and trimethylphosphine borabenzene species from an anionic chloroboratabenzene, was also possible, presumably through an associative pathway.[128] Although it has been reported that $(CO)_3Cr$(THF-borabenzene) could undergo substitution reactions at boron with neutral Lewis bases, to our knowledge no such reaction has been carried out on the metal-free borabenzene species. It was even reported by Fu that the addition of d_9-PMe_3 to borabenzene-PMe_3 in THF at 20°C did not yield ligand exchange.[139]

Following our interest in the generation of novel coordination modes for bora(ta)benzene derivatives and in the generation of Z-type ligands for transition metals, we decided to

evaluate the possibility of synthesizing κ^B-borabenzene complexes. One possible route for making such complex is by substitution reaction between a neutral borabenzene adduct and a nucleophilic metal centre, to generate the metal-κ^B-boratabenzene species and the free Lewis base. In order to correctly probe the choice of borabenzene adduct to use for such a reaction, we report herein our study on the formation of neutral borabenzene adducts from the 1-chloro-2-trimethylsilyl-3,5-boracycloexadiene and the possibility to generate novel borabenzene adducts from ligand exchange reactions on a large array of borabenzene adducts.

4.5 Results and discussion

4.5.1 Synthesis and Characterization of Borabenzene Adducts.

The synthesis of borabenzene adducts 4-*i*Pr-C_6H_4B-L (**2-L**, L = PMe_3, pyridine (Py), lutidine (Lu), PCy_3, PPh_3, 1,3-dimesityl-imidazol-2-ylidene (IMes)) was carried out by aromatization of the boracyclohexadiene precursor (**1**) induced by the coordination of the corresponding Lewis bases L and driven by the release of TMSCl (see **Figure 4-2**, R = *i*-Pr). As expected, ^{1}H NMR spectra of species **2-L** exhibit two resonances at low field, confirming the aromatic character of the borabenzene adducts. All ^{13}C resonances for the borabenzene derivatives are in the expected range for this class of molecules. Interestingly, the ^{11}B chemical shift of neutral borabenzene adducts is highly dependent on the nature of the Lewis base ligand. Indeed, whereas **2-Lu** and **2-Py** both have resonances at 32.7 ppm, the carbene and phosphine adducts of borabenzene were found to have ^{11}B resonances in the 17 – 22 ppm range. Therefore, little correlation between the bond strength and the ^{11}B chemical shift was observed. In the case of the phosphine adducts, the ^{11}B NMR peaks are present as doublets whereas in the ^{31}P spectra the resonances appear as broad quadruplets. In both ^{11}B and ^{31}P NMR spectra, coupling constants of 97 and 110 Hz were measured for **2-PPh_3** and **2-PMe_3**, respectively, whereas no coupling constant was observed with **2-PCy_3**.

Addition of weaker Lewis bases (acetone, tetrahydrofuran, acetonitrile) to **1** did not afford any of the aromatized products and left the starting material unreacted. Interestingly, the reaction of **1** with excess diisopropylamine leads to the consumption of the boracyclohexadiene without the elimination of TMSCl. Indeed, NMR spectroscopy experiments showed complete disappearance of the signals associated with **1** and consumption of amine twelve hours after the addition of two equivalents HN*i*Pr_2. By ^{1}H NMR spectroscopy, **3a** shows the presence of

two doublets at δ = 6.87 and 6.51 (*J* = 12.3 Hz). Also present are two other signals at δ = 6.10 and 2.38 that were found to belong to adjacent protons according to COSY experiments. The TMS was still present as a singlet at 0.97 ppm. These results are consistent with the presence of a 2-TMS-3,5-boracyclohexadiene framework as shown in **Figure 4-3**.[248] The observation of four diastereotopic resonances for the methyl groups of the two *i*Pr substituents of the amido, both by ^{1}H and ^{13}C NMR spectroscopy, indicates that no rotation occurs around the B-N bond which suggests a double bond character. These findings are consistent with the formation of 1-diisopropylamido-2-trimethylsilyl-3,5-boracyclohexadiene (**3a**), which is reminiscent of the previously reported 1-(dimethylamino)-3-methylene-1,2,3,6-tetrahydroborinines.[127] This assignment was further supported by ^{11}B NMR spectroscopy which showed a ~10 ppm upfield shift of the signal from **1,** consistent with the substitution of a chlorine atom at boron with an amido group. Similar reactivity was observed with H_2N*t*Bu (**Figure 4-3**). In the latter case, only one regioisomer was observed for **3b**. Although there is no structural evidence for it, one would suspect the *t*Bu group to be further away from the bulky TMS substituent for steric reasons. As reported by our group recently in the generation of mesityl boratabenzene species, the first step in the generation of borabenzene and boratabenzene adducts is the nucleophilic attack on boron.[248] The strong π-donation of the electron lone pair on nitrogen to the empty p orbital on boron makes **3** a very stable conjugated-base. Therefore, the elimination of the acidic proton in **Int3** to generate the HCl salt of the corresponding amine is a strong driving force for the generation of derivatives of **3** rather than forming TMSCl and the expected borabenzene adduct.

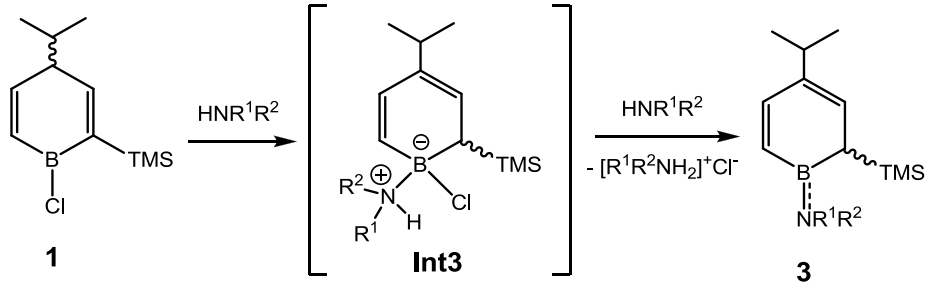

Figure 4-3: Reactivity of 1 with secondary amines generating derivatives **3** (**3a**: $R^1 = R^2$ = iPr; **3b**: R^1 = H, R^2 = tBu).

Single crystals were obtained for products **2-PMe$_3$**, **2-PCy$_3$**, and **2-IMes**. The ORTEP representations are shown in **Figure 4-4** to **Figure 4-6**, respectively, and the important structural data are in **Table 4-1**. Species **2-PCy$_3$** exhibits a disordered borabenzene moiety

that was easily resolved, but which is nevertheless affecting the precision of the atomic coordinates and of the structural data. The P-B bond lengths in **2-PMe$_3$** and **2-PCy$_3$** are 1.905(3) Å and 1.917(17) Å, respectively, which are in the expected range for phosphine-borabenzene species. The $C_{carbene}$-B distance in **2-IMes** of 1.570(5) Å is comparable to the B-C bond lengths observed by Herberich in 1-(1,3,4,5-tetramethylimidazol-2-ylidene)-3,5-dimethylborabenzene (1.596 Å)[129] and by Piers in a IMes-boranthracene adduct (1.607 Å).[228] The torsion angle of 25.5 ° between the plane of the borabenzene ring and the imidazolyl moiety of the carbene does not suggest any electronic communication. The B-C bond and C-C bond lengths in the structurally characterized species are unremarkable.

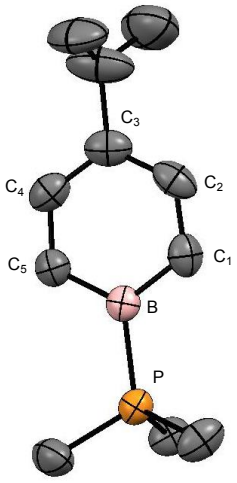

Figure 4-4: ORTEP drawing of **2-PMe$_3$**, with anisotropic atomic displacement ellipsoids shown at the 50% probability level. Hydrogen atoms are omitted for clarity.

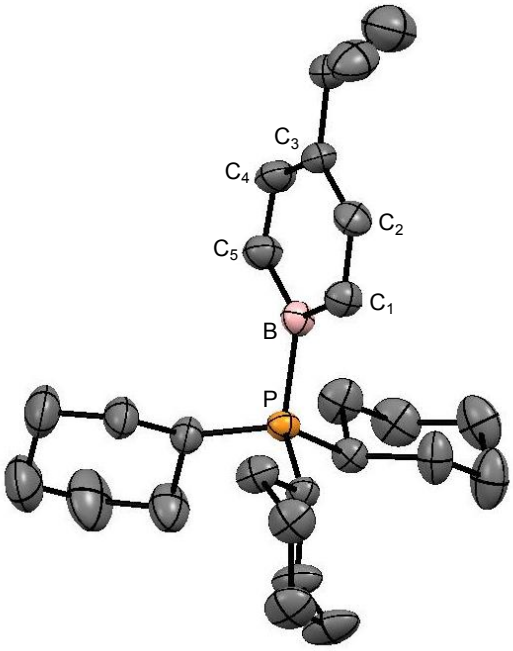

Figure 4-5: ORTEP drawing of **2-PCy$_3$**, with anisotropic atomic displacement ellipsoids shown at the 50% probability level. Hydrogen atoms are omitted for clarity.

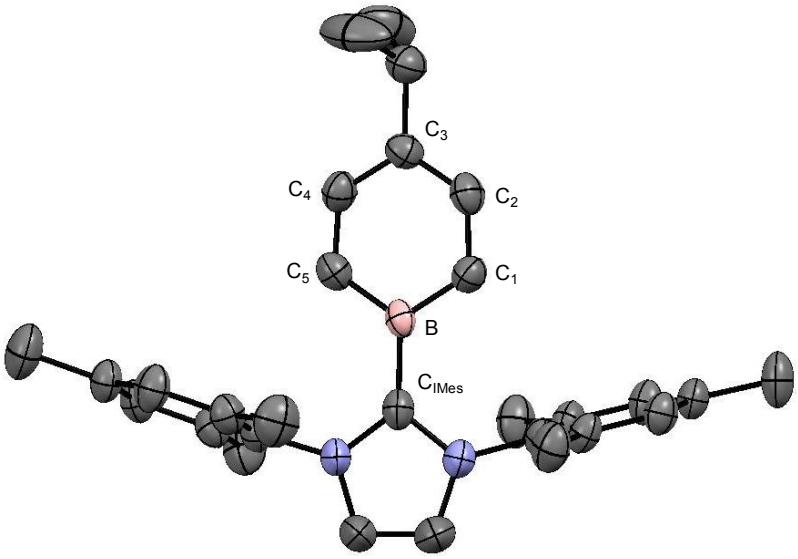

Figure 4-6: ORTEP drawing of **2-PCy$_3$**, with anisotropic atomic displacement ellipsoids shown at the 50% probability level. Hydrogen atoms are omitted for clarity.

Table 4-1: Selected structural data for **2-L**.

	2-PCy$_3$	**2-PMe$_3$**	**2-IMes**
Distances (Å)			
B-L	1.917(17)	1.905(3)	1.570(5)
B-C_1	1.44(2)	1.484(4)	1.482(5)
B-C_5	1.537(13)	1.479(4)	1.486(5)
C_1-C_2	1.358(13)	1.383(4)	1.393(4)
C_2-C_3	1.364(9)	1.380(5)	1.390(4)
C_3-C_4	1.409(8)	1.388(5)	1.400(4)
C_4-C_5	1.412(10)	1.394(4)	1.381(4)
Angles (º)			
L-B-C_1	124.6(10)	122.1(2)	122.2(3)
L-B-C_5	120.2(10)	120.8(2)	122.2(3)
C_1-B-C_5	114.9(12)	117.0(3)	115.5(3)

4.5.2 DFT Study on Borabenzene Adducts.

In order to better quantify the stabilizing ability of neutral Lewis pairs, a quantum chemical study was done on the binding energies of 49 neutral Lewis bases to base-free borabenzene (Step **b**, **Figure 4-7**) in the gas phase using DFT methods and the B3LYP hybrid functional.[249] Hess' law suggests that the thermodynamic values given in **Table 4-2** will be an indication of the overall trend observed in borabenzene adducts stability even in the absence of the base-free borabenzene species in solution. For simplicity, unsubstituted borabenzene adducts were modeled instead of the *i*Pr analogues synthesized and will be referred to as **2'-L**. In all cases, as expected, the association of Lewis bases to base-free borabenzene proved to be exothermic and exogenic. However, the formation of base-free borabenzene *via* aromatization of precursor **1** with the elimination of TMSCl was found to be endothermic by 18.2 kcal.mol^{-1} (Step **a**, **Figure 4-7**). Therefore, a ligand has to stabilize the borabenzene by at least 18 kcal.mol^{-1} in order for the overall process to be thermodynamically favorable. Otherwise, the reverse reaction – the addition of TMSCl on the borabenzene – is expected to be thermodynamically favored.[250]

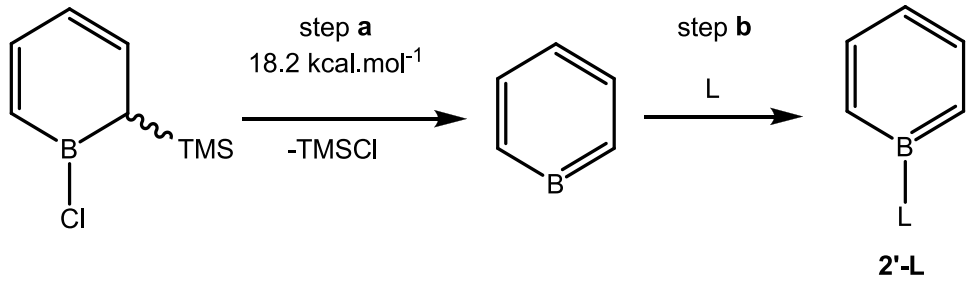

Figure 4-7: Formation of borabenzene adducts as modeled using DFT.

Table 4-2: Gas phase binding energies of selected Lewis bases (Ligand) with borabenzene at the B3LYP Level of Theory at 298 K using TZVP as a basis set for all atoms.

Ligand	ΔH° kcal/mol	ΔG° kcal/mol	Ligand	ΔH° kcal/mol	ΔG° kcal/mol
NMe_3	-40.1	-26.9	P(*p*-tolyl)$_3$	-38.1	-24.9
NEt_3	-34.0	-19.7	P(*p*-OMe)$_3$	-39.3	-26.0
$NiPr_3$	-22.6	-7.7	P(*p*-$C_6H_4CF_3$)$_3$	-34.9	-20.6
NEt_2H	-44.4	-31.2	P(*p*-C_6H_4F)$_3$	-36.4	-23.5
$NiPr_2H$	-36.5	-22.7	THF	-30.0	-18.3
$NiPrH_2$	-43.0	-30.8	DMSO	-35.4	-24.1
$NtBuH_2$	-42.1	-29.6	SMe_2	-29.0	-17.2
NH_3	-39.1	-26.7	Et_2O	-24.4	-13.4
pyridine	-45.8	-32.9	Ph_2O	-20.0	-10.0
2,6-lutidine	-41.6	-27.8	NCMe	-34.7	-24.3
2,4-lutidine	-43.7	-30.5	NCPh	-38.0	-26.3
2-picoline	-43.0	-29.7	acetone	-30.8	-19.1
3-picoline	-46.3	-33.5	acetone(anti)[a]	-30.6	-18.0
4-picoline	-44.8	-31.1	HC(O)H	-30.1	-18.3
aniline	-33.0	-21.6	HC(O)H(anti)[a]	-12.8	-9.0
quinuclidine	-43.9	-29.5	acetophenone	-34.5	-22.0
piperidine	-44.8	-32.2	Ph_2CO	-31.7	-19.4
PMe_3	-41.5	-30.2	IMe	-67.2	-55.9
PPh_3	-37.1	-24.0	IMes	-65.3	-50.4
PCy_3	-43.7	-30.9	N_2	-18.7	-8.2
P(tBu)$_3$	-36.1	-22.5	CO	-39.8	-29.1
P(iPr)$_3$	-41.2	-28.1	CNMe	-48.4	-38.1
P(OMe)$_3$	-36.4	-24.1	CNtBu	-49.2	-38.6
P(OPh)$_3$	-31.0	-17.9	CNPh	-50.3	-38.8
PF_3	-23.0	-11.4	CN(C_5H_{11})	-49.0	-38.4
PPh_2Cl	-34.2	-21.5	C_2H_4	-29.9	-17.4
P(*o*-tolyl)$_3$	-34.3	-20.2			

[a]Energy of the transition state corresponding to the rotation of the carbonyl ligand bound to borabenzene.

As can be visualized in **Figure 4-8**, a direct trend was observed between the Tolman's electronic parameter of the phosphines modeled and the binding energies for the various phosphine-borabenzene analogues, suggesting that the σ-donating capability of the Lewis pair plays an important role in the overall stability of the borabenzene adduct.[251] Indeed, strongly donating PCy_3 and $P(i\text{-}Pr)_3$ give respectively ΔG° values of -30.9 and -28.1 kcal.mol^{-1}, but electron deficient phosphines such as $P(OPh)_3$ and PF_3 have binding energies under -20 kcal.mol^{-1}. The steric hindrance of phosphines also seems to play a key role in their binding ability with borabenzene. Indeed, the three species having stronger binding energies than the trend observed are the ones with the smallest cone angles (PMe_3, $P(OMe)_3$, and PF_3), whereas $P(t\text{-}Bu)_3$ and $P(o\text{-tolyl})_3$, the two most encumbered phosphines with Tolman's cone angles superior to 180 °, clearly do not show the trend expected based on the electronic contribution. In both cases, the binding energies are lower than the expected trend by 7-8 kcal.mol^{-1}.

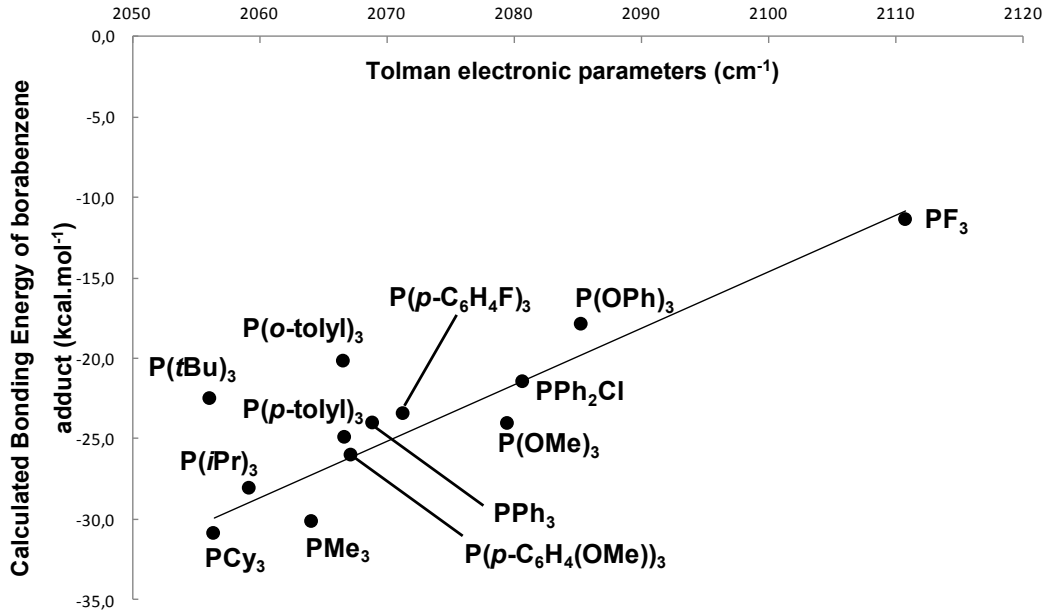

Figure 4-8: Diagram of the bonding energy of phosphine-borabenzene adducts (kcal.mol^{-1}) as determined by DFT methods in function of the Tolman electronic parameters calculated from $Ni(CO)_3L$ complexes.[204]

The steric influence of the amines seems to be much more important factor in the ΔG° of formation of borabenzene adducts than in the case of phosphines. Although NMe_3, NEt_3 and $Ni\text{Pr}_3$ have similar Lewis basicities,[206] there is a very significant difference in affinity between the various adducts formed between the borabenzene and the tertiary amines. Indeed, the

smallest amine NMe_3 possesses the highest affinity for borabenzene at -26.9 kcal.mol^{-1}, which is about 7 kcal.mol^{-1} more favorable than NEt_3 (-19.7 kcal.mol^{-1}), which in turn is more favorable than N*i*Pr_3 by 12 kcal.mol^{-1} (-7.7 kcal.mol^{-1}). The same trend can be observed with secondary amines. As for the primary amines, the formation of adducts, even with *t*$BuNH_2$, is highly exergonic with energies close to -30 kcal.mol^{-1}. N-Heterocyclic carbenes (NHCs) prove to be the strongest neutral donor, giving binding energies of -50.4 kcal.mol^{-1} in the case of IMes and of -55.9 kcal.mol^{-1} with the less hindered N-methyl containing carbene (IMe). The latter result is not surprising since NHCs are known to stabilize Lewis acid orbitals on boron, notably in the generation of highly reactive fragments such as the borolyl anion and boraanthracene.[226–228]

It is well documented that boratabenzene species possess π-accepting capabilities by the presence of an electrophilic p_z orbital on boron, notably evidenced by the planarization of the nitrogen atom on amidoboratabenzene species[121,122,125,126,130–132,233–237,237–241] η^6-borabenzene-transition metal complexes also exhibit some level of π-acidity as shown by the coplanarity between the borabenzene plane and the conjugated system of the boron coordinated 3-(dimethylamino)acrolein in a chromium(0) borabenzene complex.[243] However, to our knowledge there is no report on the π-acidity of metal-free borabenzene adducts. In that regard, we computationally investigated π-basic ketones and aldehydes as neutral ligands for borabenzene. We found that they do not bind significantly borabenzene and are in the low end of stability of borabenzene adducts with ΔG° values for MeC(O)Me, PhC(O)Ph, and MeC(O)Ph respectively of -19.1, -19.4, and -22.0 kcal.mol^{-1}. The optimized geometry of these species shows coplanarity between the aromatic borabenzene ring and the carbonyl moiety, suggesting some level of π-donation from the ketones to borabenzene. Modeling of an antiplanar structure for **2'-acetone** and **2'-formaldehyde** showed that the a free energy gain of respectively 1.1 and 9.3 kcal.mol^{-1} was associated with coplanarization of the borabenzene and ligand fragments. This energy value is representative of the amount of π-bond character but will include, especially in the case of acetone, a steric hindrance component. Therefore, it appears that B-O π-bond is highly dependent on the steric factors. Nevertheless, the strength of the π-bond is significantly less important than that observed in amido-borane species which are in the range of 30 kcal.mol^{-1}.[252]

We also modelled adducts of borabenzene and π-accepting ligands. These ligands were found to bind borabenzene more strongly than their Lewis basicity would suggest. The ΔG° values for the CO,[253] CNMe, CN^{t}Bu, CNPh, and CN(C_5H_{11}) adducts were found to be

respectively -29.1, -38.1, -38.6, -38.8, and -38.4 kcal.mol^{-1}. These results reveal that the borabenzene ring behaves more as a π-donor than a π-acceptor. This latter property is further shown by the geometry of the HOMO of the borabenzene adducts of π-acceptor ligands (**Figure 4-9**). This molecular orbital is strongly delocalized between the aromatic cycle and the antibonding π orbital of CO and CNMe. Therefore, these numeric data suggest that the borabenzene ring is a better π-donor than a π-acceptor. However, one should note that the values given in **Table 4-2** do not take into account the possible rearrangements for borabenzene adducts, that are numerous, as demonstrated by the formation **3** in presence of secondary amines or the lack of experimental evidence for the generation of the CO adduct.

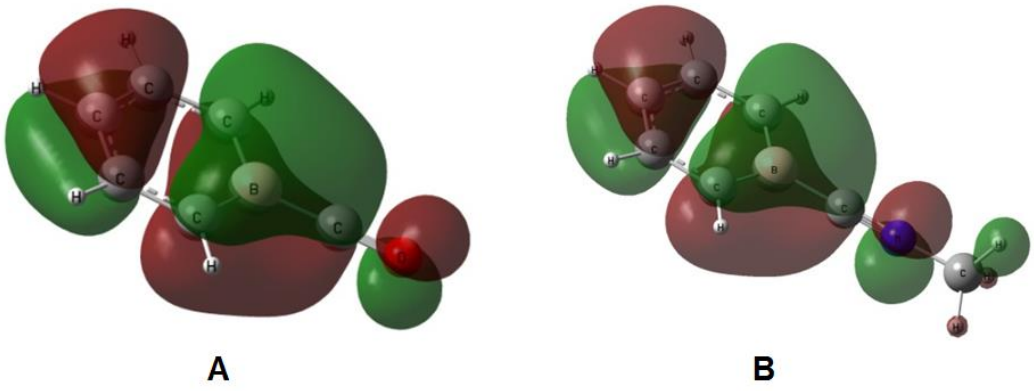

Figure 4-9: Representation of the highest occupied molecular orbital of **2'-CO** (MO = 27) and **2'-CNMe** (MO = 31) corresponding to the back donation of the π-system of the borabenzene ring to the π* orbitals of the ligand.

4.5.3 Experimental Validation of the Thermodynamic Stability of Borabenzene Adducts

It was previously demonstrated that the addition of anionic nucleophiles on borabenzene-PMe_3 adducts could lead to a large array of boratabenzene species.[139] However, no report of substitution of a neutral Lewis base on a metal-free borabenzene adduct was ever reported. In order to test the possibility of such reaction to occur, series of reactions were carried out where neutral Lewis bases (IMes, Pyridine (Py), PCy_3, 2,6-lutidine (Lu), and PPh_3) were added to species **2-L** (L = IMes, Py, PCy_3, Lu, PMe_3, and PPh_3) and heated in benzene-d_6 at 80 °C for three days or until equilibrium was reached (**Figure 4-10**), with the results displayed in **Table 4-3**.

Table 4-3: Outcome of the addition of various Lewis bases to species **2-L**. In benzene-d_6 at 80 °C for three days. X = reaction does not take place; O = complete substitution occurs; Eq. = Equilibrium has been reached.

	IMes	Py	PCy_3	Lutidine	PPh_3
2-IMes	-	X	X	X	X
2-Py	O	-	Eq.	X	X
2-PMe_3	O	Eq.	Eq.	X	X
2-PCy_3	X	Eq.	-	X	X
2-Lu	X	X	X	-	X
2-PPh_3	O	O	O	X	-

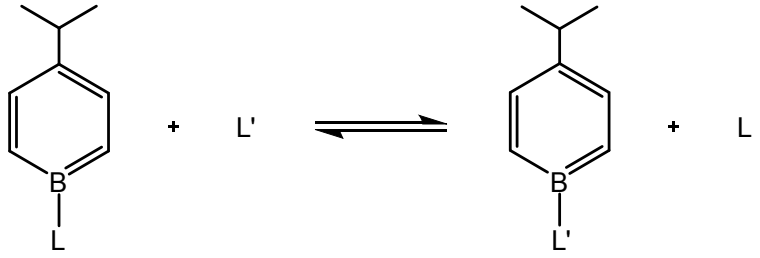

Figure 4-10: Exchange reaction of borabenzene adducts.

As can be expected from the DFT results, species **2-IMes** with a very strong carbene-boron interaction does not undergo any exchange reaction with any other ligand. On the other hand, the addition of IMes to **2-PMe_3**, **2-Py**, and **2-PPh_3** leads to the formation of **2-IMes**, which is again explained by the stability of the N-heterocyclic carbene adduct. However, **2-PCy_3** and **2-Lu** do not undergo exchange reaction with IMes. The later result suggests that the steric environment around boron is playing an important factor in the substitution reactions. This result is supported by the evidence that **2-Lu** does not undergo substitution reaction with any of the ligands that were used, or that the addition of 2,6-lutidine to any borabenzene adduct does not form new adducts. As can be seen on the DFT model of **2-Lu** (**Figure 4-11-B**), the boron p_z orbital is shielded on both sides by the methyl groups of the 2,6-lutidine which should prevent an associative substitution at the boron atom, especially when compared with **2-PMe_3** where the p_z orbital on boron is much more prominent (**Figure 4-11**).

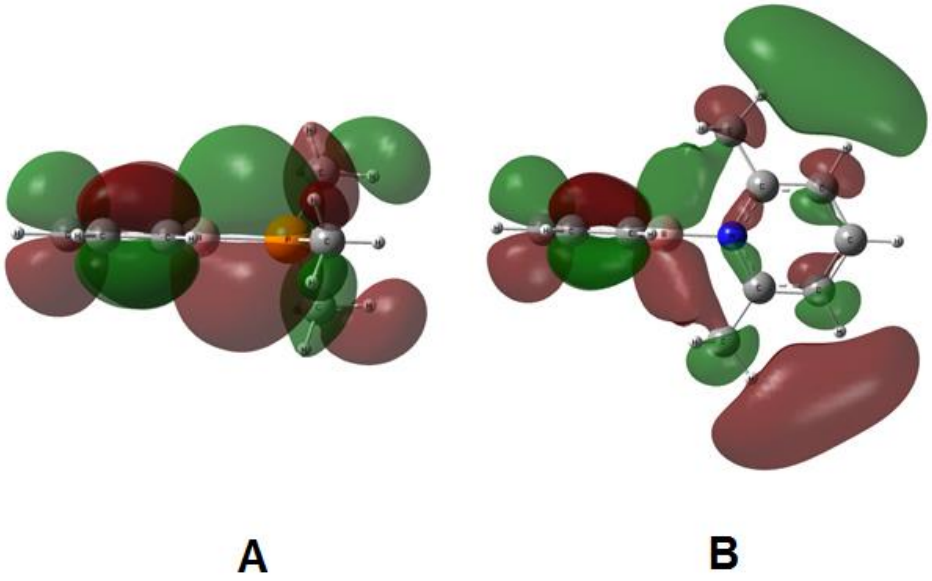

Figure 4-11: Representation of the molecular orbital of (**A**) **2'-PMe$_3$** (LUMO; MO = 42) and (**B**) **2'-Lu** (LUMO + 5; MO = 55) putting in evidence the p_z orbital on boron.

2-PPh$_3$, which according to the DFT results is the weakest of the synthesized borabenzene adduct with a ligand-borabenzene bond strength of 24 kcal.mol^{-1}, undergoes complete substitution with PMe_3, pyridine and IMes. **2-PPh$_3$** proved to be an excellent precursor for substitution reaction. Indeed, although borabenzene-NEt_3 and borabenzene-PMe_3 have both been used as starting reagents for accessing novel bora- and boratabenzene species and are useful by the fact that NEt_3 and PMe_3 are volatile side-products, borabenzene-PPh_3 proves to be easier to isolate and more stable in solution than borabenzene-NEt_3. Furthermore, PPh_3 is significantly less expensive and easier to handle than PMe_3. Interestingly, the addition of the Lewis bases L (L= PMe_3, Py, PCy_3) to species **2-L'** (L' ≠ L = Py, PMe_3, PCy_3) leads to an equilibrium between **2-L** and **2-L'**. A series of experiments was conducted in which various combinations of **L** and **2-L'** in different ratios and concentrations were combined in benzene-d_6 with hexamethylbenzene as an internal standard and allowed to reach equilibrium. The equilibrium constants were then calculated as the average of three equilibrium reactions and were used to calculate the difference in Gibbs' free energy between the studied systems (**Table 4-4**). The experimental results are in agreement with computations that indicated very small energy gap between those three adducts. PCy_3 is unsurprisingly found to form the strongest bond with borabenzene as the strongest donor of the studied ligands. The positive

ΔG° of 0.5 kcal.mol^{-1} found in the case of the substitution of trimethylphosphine by pyridine is opposed to the calculated energy gap of -2.9 kcal.mol^{-1} but remains in the error margin of the computational method.

Table 4-4: Determination of ΔG° between the various borabenzene adducts according to the equilibrium constants and the DFT calculations (B3LYP-TZVP). L and L' are represented in **Figure 4-10**.

Ligands	**ΔG° (DFT)** (kcal.mol^{-1})	**ΔG° (Experimental)** (kcal.mol^{-1})
L = PMe_3, L' = Pyridine	-2.7	0.5 ± 0.1
L = PMe_3, L' = PCy_3	-0.7	-0.6 ± 0.1
L = Pyridine, L' = PCy_3	-2.0	-1.0 ± 0.2

4.5.4 DFT Study on the Ligand Exchange Reaction

Our observations indicate that the exchange of the Lewis bases at boron is possible with borabenzene adducts. As expected, the NHC-boratabenzene adducts reveal to be the most thermodynamically favoured borabenzene species that can be obtained. Towards the lower end of thermodynamic stability, other than the NEt_3 which has been made on several occasions and proved to be quite labile, we can include the triphenylphosphine analogue, which undergoes full conversion to the PCy_3, pyridine, PMe_3, and IMes borabenzene adducts. However, these species tend to degrade slowly over time in solution, as we observed with the NEt_3 adduct. Once the bond energy gets closer to 30 kcal.mol^{-1}, as it is observed with the PCy_3, pyridine and PMe_3 adducts, the compounds get stable in solution for a prolonged period of time.

The absence of any exchange reaction when lutidine is added to a Lewis base-borabenzene adduct, or when a Lewis base is added to a borabenzene-lutidine adduct, suggests that an associative process is taking place at the boron atom. However, A DFT model of the transition state for a direct exchange reaction between borabenzene-pyridine and PMe_3 goes against such proposal since the activation barriers of 28.9 (enthalpy) and 40.4 (Gibbs free energy) kcal.mol^{-1}, respectively, are too important for such process to occur, even at 70 °C. Fu did mention in a previous report that the exchange of borabenzene-PMe_3 with borabenzene-

PMe_3-d_9 did not occur in THF at room temperature.[139] Our attempts to study the kinetics of this reaction are in accordance with the observations of Fu, since the rate of the reaction was highly dependent on the purity of the sample studied and the rates were highly irreproducible. In the case of the exchange reaction using **2-PMe$_3$** and pyridine to generate **2-Py** at 70 °C, the reaction with freshly sublimed starting material was very slow, whereas a sample that had been left in a freezer in a glove-box for two weeks underwent exchange reactions much more rapidly.

Therefore, it is highly likely that this exchange can be catalyzed by the presence of trace amount of some electrophile (notably some H^+ or B-containing species) in solution that could arise from thermal degradation of the borabenzene adducts when heated at 70 °C. Nevertheless, the observations made above suggest that it is still highly dependent on the steric hindrance around the boron atom. The most likely process for such exchange reaction would be the generation of borenium species that are generated readily in the presence of H^+, as previously reported by Piers, which would make the boron atom much more electrophilic and would reduce the energy of the transition state (**Figure 4-12**).[140]

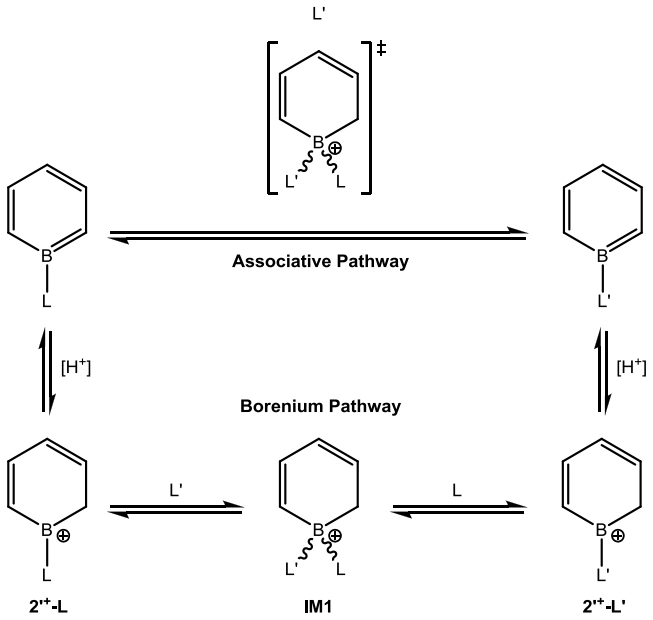

Figure 4-12: Possible pathways for the ligand substitution reaction on borabenzene.

Calculations were performed at the DFT level using the B3PW91 hybrid functional to investigate the possibility for the borenium ligand exchange pathway. The borenium **2$^+$-Py** was modeled and used as a starting point for the exchange reaction. Its formation energy from

2-Py could not be calculated since the electrophilic impurity reacting with **2-L** in our reaction conditions is unknown. However, this borenium cation has been reported by Piers as the product of the reaction of **2-L** with HCl and thallium tetraperfluorophenylborate.[140]

A stable tetracoordinated borenium structure (**IM1**) was found as the product of the association of PMe_3 on **2^+-Py**. This stable intermediate is reminiscent of $[C_5H_6B(Py)_2]^+[B(C_6F_5)_4]^-$ also reported by Piers.[140] Unsurprisingly, **IM1** is thermodynamically favoured, as the borenium fragment is then stabilized by two Lewis bases. Either pyridine or PMe_3 can easily dissociate from IM1 to give the corresponding monocoordinated borenium complex. The highest energy barrier found for the ligand exchange reaction of **2^+-Py** with PMe_3 to give **2^+-PMe_3** and free pyridine is 15.1 kcal.mol^{-1}, which is consistent with a reaction that occurs rapidly at room temperature. The reaction pathway is illustrated in **Figure 4-13**.

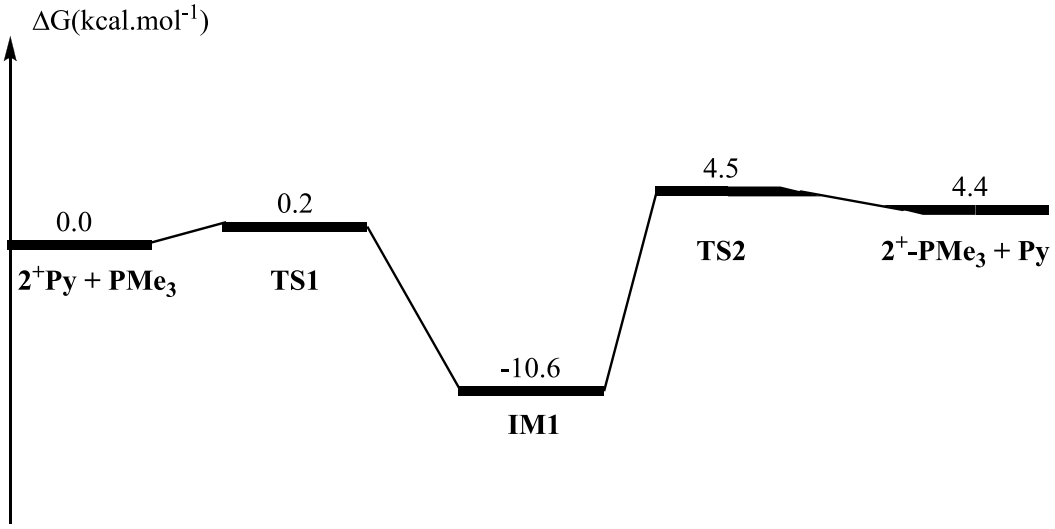

Figure 4-13: Reaction pathway for the ligand exchange between **2-Py** and PMe_3 to generate **2-PMe_3** and pyridine.

These results indicate that ligand exchange on borenium derivatives of borabenzene should be easy and proceed through an associative pathway. The rate of reaction is thus expected to be highly dependent on the steric properties of the ligands involved and their ability to form a tetracoordinated intermediate. Borenium complexes of bulky ligands, such as 2,6-lutidine, that completely protect the boron atom of the borenium are expected to be inert in regards to ligand substitution. Unfortunately, the thermodynamics of the relation between borenium derivatives **2^+-L** and borabenzene complexes **2-L** remain unknown. The main factors

governing the rate of the overall ligand substitution on neutral borabenzene adducts through a borenium pathway have to include the nature and concentration of the catalytic electrophile.

In order to experimentally verify this mechanistic hypothesis, 1-triphenylphosphine-4-H-borabenzene was reacted with an equivalent of PCy_3 in deuterated benzene in presence of 10 mol% of triphenylphosphonium bromide. A control experiment without the acidic phosphonium was conducted at the same time in similar conditions. Within 15 minutes, we observed complete conversion of borabenzene triphenylphosphine in the acid catalyzed reaction by ^{1}H and ^{31}P NMR (see Supporting Information). The control experiment did not show any conversion in these conditions. These findings give strong support to the idea that ligand exchange at borabenzene is an acid catalyzed process involving protonation of the aromatic cycle and formation of a borenium intermediate.

4.6 Conclusion

The borabenzene fragment has found applications in a large array of fields, from catalysis to material sciences. In that regard, the nature of the substituent on boron can play a large role in the activity and properties of the molecules of interest. While it is widely known that the borabenzene is kinetically reactive, we have quantified in this report, by computational and experimental results, the stability of the borabenzene adducts according to the nature of the substituents, and demonstrated that trace impurities can greatly enhance exchange reactions. We have also demonstrated that the neutral borabenzene fragment mostly acts as a π-donor rather than a π-acceptor, because of the availability of electron density from the aromatic ring. These results should be helpful in the design of more stable and durable boron heterocycles.

Added text:

We have also shown the potential of a ligand exchange reaction as a tool to generate new borabenzene adducts. The process is shown experimentally and computationally to occur through a borenium intermediate generated by the protonation or the electrophilic attack of a cyclic carbon.

In fact, it is interesting to consider that the exchange of a nucleophilic ligand is a process dominated by the *nucleophilic* character of borabenzene. The Lewis acidity involved in this exchange is not that of the electronically saturated boron atom of borabenzene but that of a borenium complex. In fact, throughout our investigation, borabenzene adducts of suitable

bases seem to behave as electron-rich species and have not revealed Lewis acidic properties. Rather, they act both as strong π-donors and nucleophiles. Interestingly, to the best of the author's knowledge, all published reactivity of neutral adducts with or without metals is dominated by a nucleophilic character.

An exception can be found in the reaction processes involved in the synthesis of boratabenzenes by associative nucleophilic substitution on the same substrates. In fact, one could be tempted to reevaluate the generally accepted mechanism of this last reaction. It is indeed conceivable that the metal counter-cations of the nucleophiles – as potential Lewis acids – could bind first to nucleophilic borabenzene and act as promoters of the nucleophilic attack through a borenium-like intermediate. One could propose to study the relative effect of different cations to the nucleophilic substitution as a tool to investigate the exact mechanism.

The coordination of Lewis bases to borabenzene thus radically modifies its properties and reactivity. While the hypothetical free borabenzene molecule is expected to be a strong Lewis acid, its adducts with Lewis bases can act as carbon-centered bases and nucleophiles. The acid-catalyzed ligand exchange constitutes a convincing example of Lewis base-borabenzene cooperative reactivity: electron density from the Lewis base is transferred to borabenzene and used in an otherwise impossible reaction. It can be proposed that appropriate modulation of the σ donation and π basicity or acidity of the ligand on borabenzene could allow the fine-tuning of the nucleophilic reactivity of borabenzene towards various substrates in order to generate a vast array of exciting new molecules.

End of added text

4.7 Experimental Section

General Procedures. All manipulations were conducted under a nitrogen atmosphere using standard Schlenk and glovebox techniques. Reactions were carried out either in a sealed J-Young NMR tube, in which case NMR conversions are indicated, or in standard flame dried Schlenk glassware. Dry deoxygenated solvents were employed for all manipulations. All solvents were distilled from Na/benzophenone. Benzene-d_6 and toluene-d_8 were purified by vacuum distillation from Na/K alloy. 1-chloro,2-TMS,4-^{i}Pr,2-5-boracyclohexadiene (**1**),[135] 1-pyridine-4-(isopropyl)borabenzene (**2-Py**)[140] and 1-tricyclohexylphosphine-4-(isopropyl)borabenzene (**2-PCy$_3$**)[121] were prepared and characterized according to literature

procedures. NMR spectra were recorded on a Varian Inova NMR AS400 spectrometer, at 400.0 MHz (^{1}H), 100.580 MHz (^{13}C), 161.923 MHz (^{31}P), Bruker Advance NMR 400 MHz spectrometer at 128.336 MHz (^{11}B), or on a Bruker NMR AC-300 at 300MHz (^{1}H), 75.435 MHz (^{13}C), 121.442 MHz (^{31}P). ^{1}H NMR and ^{13}C{^{1}H} NMR chemical shifts are referenced to residual solvent signals in deuterated solvent. Multiplicities are reported as singlet (s), doublet (d), triplet (t), quartet (q), multiplet (m), overlapping (ov.) or broad (br). Chemical shifts are reported in ppm. Peak assignment was confirmed using COSY (^{1}H) and gHSQC (^{13}C) 2D NMR experiments. Coupling constants are reported in Hz. HRMS characterization was performed with an Agilent Technologies 6210 LC Time of Flight Mass Spectrometer. Products in toluene solutions were introduced to the nebulizer by direct injection. Neutral borabenzene adducts were characterized using APPI ionization in positive mode.

4.7.1 Synthesis of Borabenzene Adducts

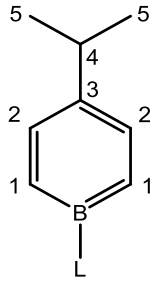

Figure 4-14: Atom labelling in borabenzene adducts.

1-Trimethylphosphine-4-(isopropyl)borabenzene (2-PMe$_3$)

Trimethylphosphine (0.23 mL, 168 mg, 2.21 mmol) was added dropwise at room temperature to **1** (500.3 mg, 2.21 mmol) in hexane (25 mL). The presence of a white precipitate was observed immediately and the mixture was stirred for 2 hours. Removal of the volatiles *in vacuo* and subsequent washing with hexane yielded 212.4 mg of a white solid (yield =50%). ^{1}H NMR (benzene-d_6) δ: 7.91 (br, 2H, H^2), 7.23 (dd, J = 8.7, 10.3 Hz, 2H, H^1), 3.20 (sept, $^{3}J_{H\text{-}H}$ = 6.9 Hz, 1H, CH(CH$_3$)$_2$), 1.53 (d, $^{3}J_{H\text{-}H}$ = 6.9 Hz, 6H, -CH(CH_3)$_2$), 0.65 (d, $^{2}J_{H\text{-}P}$ = 10.8 Hz, 9H, PMe_3). ^{13}C{^{1}H} NMR (benzene-d_6) δ: 140.0 (s, C^3), 132.0 (d, 18.1 Hz, C^2), 129.3 (br. d, C^1), 36.2 (s, C^4), 25.8 (s, C^5), 10.9 (d, $^{2}J_{C\text{-}P}$ = 41.8 Hz, PMe_3). ^{31}P{^{1}H} NMR (benzene-d_6) δ: -23.2 (q, ^{1}J$_{P\text{-}B}$ = 110 Hz). ^{11}B NMR (benzene-d_6) δ: 19.8 (d, ^{1}J$_{B\text{-}P}$ = 110 Hz). DI-MSTOF (APPI, m/e): [M + H]$^{+}$ 195.1714 (calc: 195.0691).

1-Triphenylphosphine-4-(isopropyl)borabenzene (2-PPh_3)

A saturated solution of triphenylphosphine (526.6 mg, 2.02 mmol) in hexane was added dropwise at room temperature to **1** (455 mg, 2.02 mmol). The presence of a white precipitate was observed immediately and the mixture was stirred for 1 hour. Removal of the volatiles *in vacuo* and subsequent washing with hexane yielded 347.2 mg of a white solid (yield =45%). ^{1}H NMR (benzene-d_6) δ: 7.98 (dd, $^3J_{H\text{-}H}$ = 10.3, $^4J_{P\text{-}H}$ = 4.7, 2H, H^2), 7.58 (m, 6H, PPh_3), 7.46 (dd, $^3J_{H\text{-}H}$ = 10.3, $^3J_{P\text{-}H}$ = 7.8, 2H, H^1), 6.98 (m, 3H, PPh_3), 6.90 (m, 6H, PPh_3), 3.21 (sept, $^3J_{H\text{-}H}$ = 6.9, 1H, C*H*$(CH_3)_2$), 1.53 (d, $^3J_{H\text{-}H}$ = 6.9, 6H, -CH(C*H*$_3)_2$). ^{13}C{^{1}H} NMR (benzene-d_6) δ: 140.4 (s, C^3), 134.6 (d, $J_{C\text{-}P}$ = 10.3 Hz, P*Ph*$_3$), 132.5 (d, $^3J_{C\text{-}P}$ = 17.3 , C^2), 131.6 (d, $J_{C\text{-}P}$ = 2.4 Hz, P*Ph*$_3$), 131.5 (d, $J_{C\text{-}P}$ = 3.0 Hz, P*Ph*$_3$), 128.5 (br, C^1), 36.2 (s, C^4), 25.7 (s, C^5). ^{31}P{^{1}H} NMR (benzene-d_6) δ: 8.2 (br). ^{11}B NMR (benzene-d_6) δ: 18.8 (d, $^1J_{B\text{-}P}$ 96.7). DI-MSTOF (APPI, m/e): [M + H - ^{i}Pr]$^+$: 339.2670 (calc: 339.1468).

1-(2,6-Lutidine)-4-(isopropyl)borabenzene (2-Lu)

2,6-lutidine (0.30 mL, 272 mg, 2.54 mmol) was added dropwise at room temperature to a saturated hexane solution of **1** (575.8 mg, 2.54 mmol). The reaction mixture was stirred for 3 hours and all volatiles were removed *in vacuo*. The resulting bright yellow solid was washed with hexane to yield 342.7 mg of a white solid (yield = 60%).^{1}H NMR (benzene-d_6) δ: 8.00 (d, $^3J_{H\text{-}H}$ = 10.2 Hz, 2H, H^2), 6.47-6.52 (m, 1H, lut(p-*H*)), 6.49 (d, $^3J_{H\text{-}H}$ = 10.2 Hz, 2H, H^1), 6.11 (d, $^3J_{H\text{-}H}$ = 7.7 Hz, 2H, lut(m-*H*)), 3.29 (sept, $^3J_{H\text{-}H}$ = 7 Hz, 1H, C*H*$(CH_3)_2$), 2.22 (s, 6H, lut(C*H*$_3$)), 1.62 (d, $^3J_{H\text{-}H}$ = 7 Hz, 6H, CH(C*H*$_3)_2$). ^{13}C{^{1}H} NMR (benzene-d_6) δ: 156.9 (s, lut(o-*C*)), 139.0 (s, lut(p-*C*)), 133.9 (s, C^2), 123.5 (s, lut(m-*C*)), 116.9 (br, C^1), 35.9 (s, C^4), 26.3 (s, C^5), 26.0 (s, lut(C*H*$_3$)), not located (C^3). ^{11}B NMR (benzene-d_6) δ: 32.7 (s). DI-MSTOF (APPI, m/e): (M^+): 225.1435 (calc: 225.1689).

1-(1,3-Dimesitylimidazolin-2-ylidene)-4-(isopropyl)borabenzene (2-IMes)

A saturated solution of 1,3-dimesitylimidazoline-2-ylidene (310.2.9 mg, 1.01 mmol) in hexane was added dropwise at room temperature to **1** (231.3 mg, 1.01 mmol). The yellow reaction mixture was stirred for 2 hours. Removal of the volatiles *in vacuo* and several washings in hexane yielded 212.4 mg of a pale solid. ^{1}H NMR (benzene-d_6) δ: 7.51 (d, $^{3}J_{H\text{-}H}$ = 10.5 Hz, 2H, H^{2}), 6.68 (s, 4 H, Mes(m-*H*)), 6.53 (d, $^{3}J_{H\text{-}H}$ = 10.5 Hz, 2H, H^{1}), 5.92 (s, 2 H, Im(C*H*)), 2.91 (sept, $^{3}J_{H\text{-}H}$ = 6.9 Hz, 1H, C*H*(CH$_3$)$_2$), 2.08 (s, 6H, Mes(*p*-C*H*$_3$)), 1.96 (s, 12H, Mes(*o*-C*H*$_3$)), 1.26 (d, $^{3}J_{H\text{-}H}$ = 6.9 Hz, 6H, CH(C*H*$_3$)$_2$). ^{13}C{^{1}H} NMR (benzene-d_6) δ: 146.1 (s, Mes(*ipso*)), 139.3 (s, Mes(p-*C*)), 135.5 (s, *C*^{3}), 135.0 (s, Mes(o-*C*)), 131.9 (s, *C*^{2}), 129.8 (s, Mes(m-*C*)), 121.3 (s, Im), 35.9 (s, *C*^{4}), 25.6 (s, *C*^{5}), 21.1 (s, Mes(p-*C*H$_3$)), 17.9 (s, Mes(o-*C*H$_3$)), not located (*C*^{3} and carbene). ^{11}B NMR (benzene-d_6) δ: 21.0 (s). DI-MSTOF (APPI, m/e): (M^{+}): 422.2892 (calc: 422.2893).

1-Di(*iso*-propyl)amido-2-trimethylsilyl-4-isopropyl-3,5-boracyclohexadiene (3a)

To a solution of **1** (8.6 mg, 0.04 mmol) in 0.5 mL of benzene-d_6 was added di(*iso*-propyl)amine (55 µL, 0.2 mmol) by syringe. A white precipitate was immediately formed. The reaction mixture was kept at room temperature for 16 hours and analyzed by NMR spectroscopy. The assignation was confirmed based on COSY experiments and with comparison to similar compounds.[124]

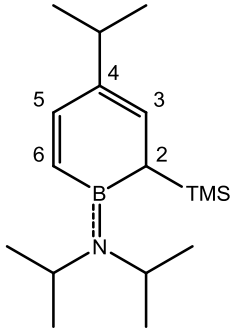

^{1}H NMR (benzene-d_6) δ: 6.87 (d, $^{3}J_{H\text{-}H}$ = 12.3 Hz, 1H, *H*^{5}), 6.51 (d, $^{3}J_{H\text{-}H}$ = 12.3 Hz, 1H, *H*^{6}), 6.10 (s, 1H, H^{3}), 3.74 (br s., 1H, N(C*H*Me$_2$)$_2$), 3.21 (br s., 1H, N(C*H*Me$_2$)$_2$), 2.38 (br. ov. s., 1H, C*H*Me$_2$), 2.38 (br. ov. s., 1H, H^{2}), 1.31 (br. s., 3H, N(CH*Me*$_2$)$_2$), 1.28 (br. s., 3H, N(CH*Me*$_2$)$_2$), 1.10 (br, 6H, CH*Me*$_2$), 1.01 (br, 3H, N(CH*Me*$_2$)$_2$), 0.91 (br, 3H, N(CH*Me*$_2$)$_2$), 0.10 (s, 9H, TMS); signals for excess di(*iso*-propyl)amine are present at δ: 2.78 and 0.94. ^{13}C{^{1}H} NMR (benzene-d_6) δ: 143.3 (s, C^{5}), 138.8 (s, C^{4}), 131.6 (br, C^{6}), 129.8 (s, C^{3}), 48.8 (s, N(*C*HMe$_2$)$_2$), 44.9 (s, N(*C*HMe$_2$)$_2$), 34.5 (s, *C*HMe$_2$), 25.5 (s, CH*Me*$_2$ or N(CH*Me*$_2$)$_2$), 24.8 (s, CH*Me*$_2$ or N(CH*Me*$_2$)$_2$), 23.0 (s, CH*Me*$_2$ or N(CH*Me*$_2$)$_2$), 22.8 (s, CH*Me*$_2$ or N(CH*Me*$_2$)$_2$), 22.7 (s, CH*Me*$_2$ or N(CH*Me*$_2$)$_2$), 21.2 (s, CH*Me*$_2$ or N(CH*Me*$_2$)$_2$), 0.0 (s, TMS); signals for excess di(*iso*-propyl)amine are present at δ: 45.3 and 23.7. ^{11}B NMR (benzene-d_6) δ: 41.2 (s).

1-*tert*-Butylamido-2-trimethylsilyl-4-isopropyl-3,5-boracyclohexadiene (3b)

To a solution of **1** (8.7 mg, 0.04 mmol) in 0.5 mL of benzene-d_6 was added *tert*-butylamine (20 µL, 0.2 mmol) by syringe. A white precipitate was immediately formed. The reaction mixture was kept at room temperature for 24 hours and analyzed by NMR spectroscopy.

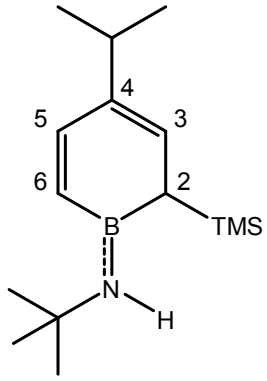

^{1}H NMR (benzene-d_6) δ: 7.00 (d, $^3J_{H\text{-}H}$ = 12.3 Hz, 1H, H^5), 6.48 (d, $^3J_{H\text{-}H}$ = 12.3 Hz, 1H, H^6), 6.07 (d, $^3J_{H\text{-}H}$ = 4.9 Hz, 1H, H^3), 3.44 (br, 1H, N*H*), 2.40 (sept, $^3J_{H\text{-}H}$ = 6.9 Hz, 1H, C*H*Me$_2$), 1.80 (d, $^3J_{H\text{-}H}$ = 5.4 Hz, 1H, H^2), 1.09 (m, 6H, CH*Me*$_2$), 0.66 (s, 9H, NC*Me*$_3$), 0.04 (s, 9H, TMS); signals for excess *tert*-butylamine are present at δ 1.20 (s) and 0.98 (s). ^{13}C{^{1}H} NMR (benzene-d_6) δ: 146.4 (s, C^5), 139.5 (s, C^4), 130.2 (s, C^3), 129.2 (br, C^6), 50.0 (s, N(*C*Me$_3$)), 35.5 (br, C^2), 34.7 (s, *C*HMe$_2$), 22.9 (s, CH*Me*$_2$ or N(C*Me*$_3$)), 23.0 (s, CH*Me*$_2$ or N(C*Me*$_3$)), -1.3 (s, TMS). ^{11}B NMR (benzene-d_6) δ: 40.9 (s).

4.7.2 General Procedure for Ligand Exchange

Qualitative ligand exchange reactions were performed at the NMR scale with **2-L** (L = 2,6-lutidine, pyridine, PMe$_3$, PCy$_3$, PPh$_3$, IMes). In these experiments, a molar equivalent of **L'** (L' = 2,6-lutidine, pyridine, PMe$_3$, PCy$_3$, PPh$_3$, IMes) was added to a benzene-d_6 solution of **2-L**. The reaction mixtures were heated to 60 °C overnight. NMR analysis was then used to verify if the exchange reaction occurred. Reaction mixtures that did not undergo reaction were heated 80 °C for up to five more days to make sure no exchange occurred.

Quantitative analysis of the exchange reaction was done for L = pyridine, PMe$_3$, PCy$_3$ and L' = pyridine, PMe$_3$, PCy$_3$. These reactions were done at the NMR scale in benzene-d_6 with hexamethylbenzene (HMB) as an internal standard. 4.2 mol.L^{-1} solutions of (**2-L** + HMB) and **L'** were prepared. These solutions were mixed in air-tight NMR tubes in 1:2, 1:1, and 2:1 ratios. The reaction mixtures were heated to 80 °C for 72 hours and the equilibrium constants were measured by NMR spectroscopy. Gibb's free energy variation for these systems was calculated as the average of the measurements taken for the 1:2, 1:1, and 2:1 mixtures.

4.7.3 Acid Catalyzed Ligand Exchange Reaction

Two benzene-d_6 (*ca.* 0.4 mL) solutions of **2-PPh$_3$** (4.4 mg, 0.012 mmol) and tricyclohexylphosphine (3.3 mg, 0.012 mmol) were prepared. To one of them was added 0.4 mg (0.001 mmol) of triphenylphosphonium bromide. The solutions thus prepared were introduced into J-Young NMR tubes and analyzed by NMR spectroscopy after 15 minutes.

4.7.4 Computational Details

The density functional theory calculations were carried out with the B3LYP/B3PW91 hybrid functional as implemented in the G03 program. B3LYP is Becke's three parameter functionals (B3)[254] with the non-local correlation provided by the LYP expression[255,256] and VWN functional III for local correlation.[257] The TZVP basis set was used for all atoms.[258] The tight geometry optimizations were performed without symmetry constraints and with the use of the modified GDIIS algorithm.[259,260] Vibrational analyses were performed to confirm the optimized stationary points as true minima on the potential energy surface or as transition states, and to obtain the zero-point energy, thermodynamic data and orbital analysis. The free Gibbs energies, G, were calculated for T = 298.15 K. For every transition state, the reaction path in both directions was followed using the intrinsic reaction coordinate (IRC).[261,262]

ACKNOWLEDGEMENTS

We are grateful to NSERC (Canada), CFI (Canada), CCVC (Québec), and C3V (Université Laval) for financial support; M.-A.L. and G. B.-C. are grateful to NSERC and FQRNT for scholarships. Prof T. Woo and S. Goreslky are acknowledged for the training of M.-A. L and G. B.-C. and their help with DFT calculations. We also acknowledge Prof A. Hill for his insightful input.

Supporting Information Available. Spectroscopic data for all compounds. Cartesian coordinates for numerical models. This material is available free of charge via the Internet at http://pubs.acs.org.

Chapter 5 - Metal-free Catalytic Reduction of Carbon Dioxide

In the next two chapters, we will consider a difficult reaction: the reduction of carbon dioxide. This chapter will describe the problematic of carbon dioxide as a greenhouse gas, as well as lay out its principal properties. We will present a brief timeline of the development of reduction systems, and we will then describe and discuss two novel catalytic systems that, relying on the cooperation of Lewis bases with boranes, allow the facile and mild reduction of carbon dioxide to methanol.

5.1 Carbon Dioxide

5.1.1 Carbon Dioxide as a Greenhouse Gas and a Renewable Resource

The 18th and 19th centuries saw important changes in the very fabric of society throughout the Western world. The effect of technological advances on the daily lives of billions of people at this time cannot be overstated. As such, this period of history is well known as the Industrial Revolution. During these times, the gradual yet rapid replacement of wood to coal and then later to petroleum as fuel allowed revolutions in transportation, mechanized production, agriculture, and a plethora of other fields. With the increased availability of these energy sources, energy consumption increased in the West first, and then throughout the world.

While the positive impact of industrialization on society is incalculable, a consequence of the energetic reliance on fossil fuel that became plain only later is the increase of the concentration of atmospheric carbon dioxide caused by anthropogenic emissions. While carbon dioxide is a nontoxic compound and could appear harmless, its properties as a greenhouse gas and its potential as a climate changing agent are now a cause of global concern.

Indeed, continuous monitoring of the level of atmospheric CO_2 performed at Mauna Loa, Hawaii since 1958 have shown an inexorable increase in the concentration of this gas up to now. In fact, while below 320 ppm of CO_2 could be quantified in 1958, it had breached the threshold average value of 400 ppm for the month of March 2015.[263] According to the National

Oceanic and Atmospheric Administration (United States of America) responsible for these measurements, this current concentration of carbon dioxide is 120 ppm above that of the pre-Industrial period.[264]

The use of fossil fuel, deforestation, and agricultural practices are generally regarded as the main reasons behind the anthropogenic emissions of carbon dioxide that total 25.6 gigatons annually.[265] Considerable work would be necessary to replace the existing infrastructure which relies on current technology with carbon neutral solutions. In the case of the use of fossil fuel, a good fraction of the human population is dependent on liquid energy media to operate important pieces of machinery, most notably for transportation. Adapting emerging "green" sources of energy to the current technology may seem an insurmountable goal. For this reason, the use of methanol as an alternative fuel was advocated by Nobel Prize recipient Georges A. Olah.[266] According to him and other scientists, methanol produced from the reduction of carbon dioxide represents a viable alternative to fossil fuels both as an energy vector compatible with current technology and as a potential source of synthetic building blocks. In principle, the reduction of carbon dioxide to methanol should be performed using green energy sources and clean processes to be a carbon neutral energy vector: no *new* carbon dioxide is produced by the combustion of methanol produced from atmospheric CO_2.

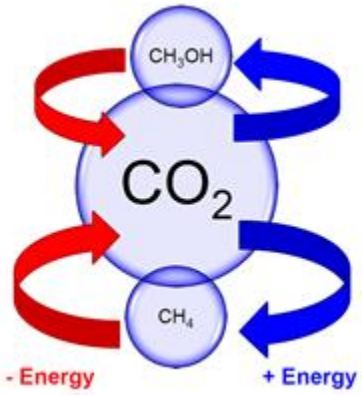

Figure 5-1: Conversion of CO_2 to energy vectors (blue). The combustion of these vectors regenerate CO_2 and releases energy (red).[II]

The reduction of carbon dioxide to methanol and water by molecular hydrogen is both thermodynamically and economically feasible. By producing hydrogen from green energy sources, the hydrogenation of carbon dioxide can be made feasible in a renewable manner.

[II] Used with permission from N. Bouchard who designed this figure that is commonly used in our group to illustrate this concept.

Unfortunately, the CO_2 reduction reaction is not feasible in ambient conditions due to the exceptional stability of carbon dioxide. For this reason catalysts have to be used.

5.1.2 Catalytic Reduction of Carbon Dioxide to Methanol Derivatives

The field of catalytic reduction of carbon dioxide to methanol is currently dominated by heterogeneous catalysts based on transition metals and transition metal oxides. This type of system, which allows the gas phase reagents (CO_2 and H_2) to react together on the surface of a solid catalyst, is the only kind used today on the industrial scale.[267,268] The leading commercial example of this process is found in the Georges Olah Plant, belonging to the Icelandic company Carbon Recycling International, that has a yearly production capacity of renewable methanol of 5 million liters.[269]

The downside of modern heterogeneous catalysts comes from their lack of selectivity. When reducing carbon dioxide with hydrogen, several products can be formed by side-reactions and over- or under-reduction.[270–272] Where heterogeneous catalysts are concerned, the complex processes occurring on metal surfaces are difficult to characterize and it can be difficult to optimize the catalysts for the desired selectivity. As such, optimization of the conditions, as well as the use of harsh conditions, is often the best way to obtain satisfactory methanol yields on sub-optimal catalysts.

While extensive research focuses on the development of new homogeneous catalysts, homogeneous catalysis in solution offers a convenient platform to study the fundamentals of carbon dioxide reduction and to develop catalysts with better selectivity. Higher selectivity can indeed be obtained for the transformation of carbon dioxide to various useful chemicals using homogenous transition metal-catalyzed processes.[273–286] However, the field being relatively new, only two ruthenium homogeneous catalytic systems have yet been reported to yield methanol by hydrogenation of carbon dioxide, with unfortunately very low efficiency. Indeed, in solution chemistry, the cascade reduction of CO_2 to formic acid then to formaldehyde and to methanol is a considerable challenge (**Figure 5-2**). The transformation of carbon dioxide to formic acid is endergonic and formic acid is as difficult to hydrogenate as carbon dioxide, but possesses different properties.

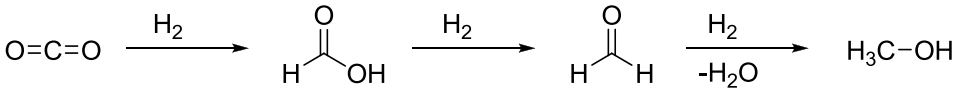

Figure 5-2: Stepwise hydrogenation of carbon dioxide to methanol.

Since hydroboranes can be conveniently used for the reduction of carbonyl compounds, they can be seen as an alternative to hydrogen as a reducing agent for carbon dioxide. One of the first uses of hydroboranes in a catalytic reduction of carbon dioxide to methanol was shown by Guan and coworkers who used a nickel pincer-complex to catalyze the reaction between carbon dioxide and catecholborane (**Figure 5-3**). Under ambient pressure and temperature, the reaction yielded methoxycatecholborane in high yields with close to 100% selectivity and with a turnover frequency (TOF) of 495 h^{-1}. The methoxyboranes thus formed are precursors to methanol by simple hydrolysis.[273]

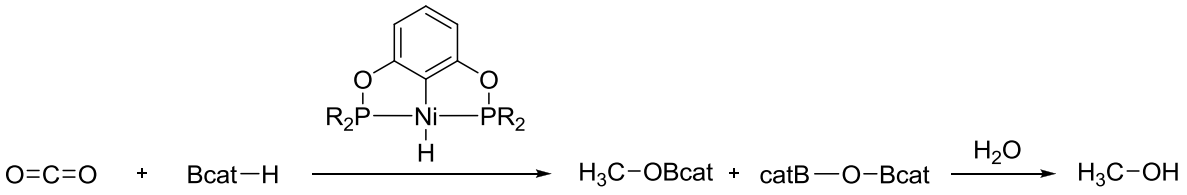

Figure 5-3: Nickel pincer-catalyzed reduction of carbon dioxide using catecholborane.

Using hydrosilanes as reducing agents, transition metal-free systems were also reported for the production of methanol from carbon dioxide. As mentioned above, alumenium[287] and silylium[288] cations were shown to catalyze the reduction of carbon dioxide to a mixture of products including methanol derivatives, with their lack of selectivity coming from their extreme Lewis acid character. As of June 2013, in fact, the only efficient organocatalysts for the reduction of CO_2 were highly Lewis basic N-heterocyclic carbenes that diphenylsilane used as a hydrogen source with turnover frequencies (TOF) of 25 h^{-1} at 25 °C.[289] Mechanistic studies on the carbene-catalyzed hydrosilylation of carbon dioxide reveal that the Lewis basic catalysts can bind to silanes and increase the nucleophilicity of their hydrides (**Figure 5-4**). This mode of action is analogous to the alkoxide activation of hydroboranes mentioned above.[289,290]

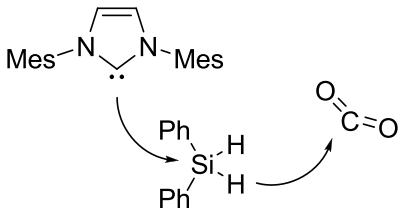

Figure 5-4: N-heterocyclic carbene activation of diphenylsilane for the activation of carbon dioxide.

5.1.3 Frustrated Lewis Pairs and Carbon Dioxide

As explained in an earlier chapter, the combination of a Lewis acid and a Lewis base can, with the appropriate steric and geometric constraints, remain unquenched and react cooperatively. Using this Frustrated Lewis Pair approach, several systems have been shown to strongly bind carbon dioxide. These systems have long been considered a promising avenue for the catalytic reduction of carbon dioxide, but empirical evidence has shown that using FLP systems to activate the reducing agent instead of carbon dioxide was a better approach. Indeed, Piers and coworkers were able to use this concept to catalytically reduce CO_2 to methane using hydrosilanes, albeit with low efficiency.[71]

5.2 Phosphine-borane Catalyzed Reduction of Carbon Dioxide

5.2.1 An Ambiphilic Catalyst for the Reduction of Carbon Dioxide to Methanol

As of 2013, the aforementioned systems represented the most notable examples of metal-free carbon dioxide reduction to methanol derivatives. At this time, following extensive research on FLP systems comprised of weakly acidic and basic moieties for collaborative reactivity, our group studied and reported the possible interactions between phosphine-alane and carbon dioxide. In these studies Boudreau, Courtemanche and Fontaine showed that alkyl-bridged phosphine-alanes tend to decompose in the presence of carbon dioxide or of reducing agents.[208,291] In the case of phenyl-bridged phosphine-alane, however, we found that the decomposition product in the presence of catecholborane a phosphine-borane **4b**.[291]

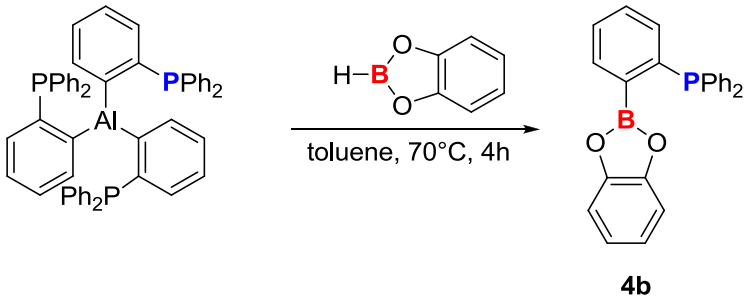

4b

Figure 5-5: Conversion of phosphine-alane FLP to catalytically active phosphine-borane **4b**.

The reaction mixture, if exposed to carbon dioxide, was shown to reduce it to methoxycatecholborane in mild conditions. With these results in hand, we studied the reactivity of **4b** as a catalyst for the reduction of carbon dioxide using hydroboranes. The author of this dissertation personally demonstrated the exceptionally high activity of this catalyst by showing that several boranes were suitable for the reduction, and that inexpensive borane-dimethylsulfide was especially reactive in the reaction conditions. In fact, he was able to report an unprecedented and yet unsurpassed turn-over frequency of 853 h^{-1} at 80 °C. In addition he showed that the reaction could be scaled up and that the catalyst would reliably react even in loadings as low as 0.1 mol.%. Interestingly, the high activities observed for ambiphilic molecule **4b** did not emulate those of transition-metal catalysts. Instead, it surpassed them by a large margin.

In the course of this study, we also observed the formation of a formaldehyde adduct of **4b**, as well as an induction period for the catalysis.

5.2.2 Mechanism of Phosphine-borane Catalyzed Carbon Dioxide Reduction

Having obtained these record-breaking results, we set out to investigate the mechanism of action of the catalyst and to uncover how such high activity could be attained. A detailed computational investigation of possible mechanisms allowed us to determine that a cooperative behaviour of the unquenched phosphine and boryl moieties of the catalyst was responsible for the reduction of carbon dioxide. On the one hand, the phosphorus atom is able to bind stoichiometric catecholborane, transferring to it electron density. On the other hand, the boryl moiety of the catalyst can simultaneously bind carbon dioxide, acting like a Lewis acid. We determined this simultaneous ambiphilic activation to be the most plausible mode of

action of the catalyst. Interestingly, this mode of action did not involve CO_2 binding by the FLP molecule as would have been predicted by the then-dominant hypothesis.

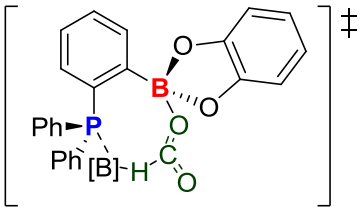

Figure 5-6: Transition state for the simultaneous activation of catecholborane and carbon dioxide in the phosphine-borane-catalyzed reduction of CO_2.

However, these calculations could not explain the induction period observed for the catalysis at room temperature. Furthermore, the influence of the steric and electronic properties of the phosphine and boryl moieties of the catalyst remained unknown. We thus decided to synthesize a range of phosphine-borane compounds and evaluate their efficiency as catalysts for the reduction of carbon dioxide to methoxyboranes. In the course of the project, a priority was given to the elucidation of the mechanism of the reaction. The results obtained in the course of this study will be the subject of this chapter.

5.3 Abstract

Ambiphilic phosphine-borane derivatives 1-$B(OR)_2$-2-PR'_2−C_6H_4 (R' = Ph (**4**), *i*Pr (**5**); $(OR)_2$ = $(OMe)_2$ (**4a, 5a**); catechol (**4b, 5b**) pinacol (**4c, 5c**), $OCH_2C(CH_3)_2CH_2O$- (**4d**)) were tested as catalysts for the hydroboration of CO_2 using HBcat or BH_3•SMe_2 to generate methoxyboranes. It was shown that the most active species were the catechol derivatives **4b** and **5b**. In the presence of HBcat, without CO_2, ambiphilic species **4a**, **4c**, and **4d** were shown to transform to **4b**, whereas **5a** and **5c** were shown to transform to **5b**. The formaldehyde adducts **4b.CH_2O** and **5b.CH_2O** are postulated to be the active catalysts in the reduction of CO_2 rather than being simple resting states. Isotope labelling experiments and DFT studies show that once the formaldehyde adduct is generated, the CH_2O moiety remains on the ambiphilic system through catalysis. Species **5b.CH_2O** was shown to exhibit turn-over frequencies for the CO_2 reduction using BH_3•SMe_2 up to 228 h^{-1} at ambient temperature and up to 873 h^{-1} at 70 °C, mirroring the catalytic activity of **5b**.

5.4 Résumé

Les dérivés ambiphiles phosphine-borane de forme 1-$B(OR)_2$-2-PR'_2−C_6H_4 (R' = Ph (**4**), *i*Pr (**5**); $(OR)_2$ = $(OMe)_2$ (**4a, 5a**); catéchol (**4b, 5b**) pinacol (**4c, 5c**), $OCH_2C(CH_3)_2CH_2O$- (**4d**)) ont été évalués quant à leur activité catalytique pour la réduction du dioxyde de carbone en methoxyboranes par HBcat ou BH_3•SMe_2. Il est démontré que les dérivés catéchol **4b** et **5b** sont les plus actifs. En présence de HBcat, et sans CO_2, les composés ambiphiles **4a**, **4c** et **4d** sont convertis en **4b**, alos que **5a** et **5c** sont transformés en **5b**. Les adduits de formaldéhyde **4b.CH_2O** et **5b.CH_2O** sont proposés comme espèces catalytiquement actives pour la réduction du CO_2, plutôt que n'être que des intermédiaires de la réaction. Des expériences de marquage isotopique et des études basées sur la DFT montrent que, une fois que l'adduit formaldéhyde est formé, le groupement CH_2O reste lié au système ambiphile durant toute la réaction catalytique. Globalement, l'espèce **5b.CH_2O** est le catalyseur le plus actif, donnant une fréquence catalytique de 228 h^{-1} pour la réduction du dioxide de carbone par BH_3•SMe_2 à température ambiante, et de 873 h^{-1} à 70 °C. Ces activités sont comparables à celles du catalyseur **5b** rapportées précédemment.

5.5 Introduction

The general consensus of the scientific community on the role of green-house gases on global climate changes has led to several initiatives to limit their emissions. As a consequence, a large number of contributions on the search for economical and efficient ways to sequester and valorize carbon dioxide, the principal gas which causes global warming, have appeared. Nowadays, several technologies are used in order to capture carbon dioxide from flue exhausts of major producers but sequestration remains a costly solution.[292] One way to make the capture of CO_2 more economically viable is in its valorization by using this molecule as a C-1 building block for the synthesis of valuable chemicals.[293] One transformation that has attracted much attention is the reduction of carbon dioxide to methanol, which is at the core of the methanol economy, as promoted by Nobel laureate George A. Olah.[294] Several heterogeneous systems are known to catalytically reduce carbon dioxide to methanol and some of these technologies are now commercialized.[294] Nevertheless, the search for novel catalysts is still ongoing, notably using homogeneous systems which give the promise for more active and selective processes. In that regard, some transition metal-based systems have been used for the reduction of carbon dioxide to formic acid,[295–297] formates,[280–283,286,295,298,299] formaldehyde,[274,300–302] methanol,[273,275,276,282,302] methane,[277,280,285,286] acetals,[303] and carbon monoxide.[283,284,304]

In the past few years, there have been many important developments in the design of metal-free catalytic systems for the reduction of carbon dioxide. Indeed, some highly reactive species such as aluminum[287,305] and silyl cations[288] have been shown to reduce carbon dioxide with low selectivity to methane, methanol and other alkylation side-products. FLP (Frustrated Lewis Pair) systems, although known to bind carbon dioxide,[52,64,306] have demonstrated very limited efficiency in its reduction.[68–71,307–309] Since the seminal report by Ying and co-workers that *N*-heterocyclic carbenes can reduce carbon dioxide in the presence of hydrosilanes to methoxysilanes,[289] which upon hydrolysis yield methanol, there have been few other organocatalytic systems reported for carbon dioxide reduction. Among these figures the report by Stephan that some phosphine-borane systems derived from 9-BBN catalyze the hydroboration of CO_2.[310] For their part, Cantat and co-workers demonstrated that strong nitrogen bases, such as guanidines and amidines can be used as organocatalysts for the reduction of CO_2 to formamides using hydrosilanes[311] or to methoxyboranes using 9-borabicyclo[3.3.1]nonane (9-BBN) and, although with very low turn-over frequency, HBcat (cat

= catechol).[312] It was recently reported that bidentate Lewis bases, such as proton sponge, can also act as a catalyst for the reduction of carbon dioxide using BH_3•SMe_2 as a reductant[313,314] and that even $NaBH_4$ can catalyse the reduction of carbon dioxide using BH_3 adducts.[315] Moreover, Cantat and co-workers reported the methylation of amines with carbon dioxide and 9-BBN mediated by proazaphosphatrane superbases.[316] However, these last systems, although active, exhibit either low turn-over numbers or low turn-over frequencies.

One of the most active metal-free systems for the reduction of carbon dioxide to date is 1-Bcat-2-PPh_2−C_6H_4 (**4b**), which can be generated *in situ* from the addition of HBcat to precatalyst Al(2-PPh_2-C_6H_4)$_3$.[291] **4b** can generate methoxyboranes of general formula CH_3OBR_2 from several hydroboranes (HBR_2), such as catecholborane, pinacolborane, and BH_3•SMe_2, which in turn can be hydrolyzed to methanol.[63,207] Although such process has limited commercial potential because of the cost of boranes, it serves as an excellent model to understand the mechanism of FLP-derivatives in the catalytic functionalization of unsaturated substrates such as carbon dioxide. Indeed, the very high turn-over frequency (TOF), which can reach 973 h^{-1}, and the turn-over numbers (TON), which exceeds 2950 at 70 °C, obtained surpass that of the most active transition metal catalysts. An in-depth DFT study of this system using HBcat as reductant allowed postulating that the activation of both the catecholborane and CO_2 in a concerted fashion led to much lower transition state energies than classical reduction pathways, a process that does not occur without catalyst.[317] In order to optimize this class of catalyst, we were interested at looking at the influence of the substituents on the phosphine and borane parts. Herein, we report that the influence of the phosphine and the borane moieties on the catalyst is of limited importance because of substitutions that occur prior to the beginning of the catalytic activity. Notably, the formaldehyde generated forms an adduct with the phosphine-borane that turns out to be an active catalyst for the reduction of carbon dioxide rather than only a resting state as previously postulated. DFT calculations suggest that the dual activation of the borane and carbon dioxide plays a key role in the reduction process.

5.6 Results and Discussion

5.6.1 Efficiency of 1-B(OR)$_2$-2-PR'$_2$-C$_6$H$_4$ Derivatives as Catalysts for the HBcat Hydroboration of CO_2

Phosphine-boranes of the general structure 1-BR$_2$-2-PR'$_2$−C$_6$H$_4$ have been reported before and used extensively as ligands for transition metals. Some of these metal-free species have shown a large range of activities, notably in the fixation, splitting and transfer of singlet dioxygen, [23a] in the bifunctional organo-catalyzed Michael addition[23b] and in the trapping of reactive intermediates of organic transformations. In order to better understand the importance of structural parameters of these phosphine-borane derivatives on the catalytic activity, the synthesis of 1-B(OR)$_2$-2-PR'$_2$−C$_6$H$_4$ derivatives with diphenyl- and di*iso*propyl-phosphine moieties (R' = Ph and *i*Pr) was envisioned (**Figure 5-7**).

The 1-B(OR)$_2$-2-PPh$_2$−C$_6$H$_4$ derivatives (R$_2$ = catechol (**4b**), pinacol (**4c**), and OCH$_2$C(CH$_3$)$_2$CH$_2$O- (**4d**)) were easily synthesized from the addition of the corresponding diols to *in situ* generated 1-B(OMe)$_2$-2-PPh$_2$−C$_6$H$_4$ (**4a**).[318] The isolation of the latter compound was also possible on the gram scale, but proved to be quite sensitive to hydrolysis. On the other hand, the reaction of catechol with 1-B(OMe)$_2$-2-P(*i*Pr)$_2$−C$_6$H$_4$ (**5a**) surprisingly did not yield the expected 1-Bcat-2-P(*i*Pr)$_2$−C$_6$H$_4$ (**5b**), although the generation of the pinacol derivative 1-Bpin-2-P(*i*Pr)$_2$−C$_6$H$_4$ (**5c**) was successful using a similar reaction pathway. It was however possible to synthesize the desired analogue **5b** by the electrophilic trapping of 1-Li-2-P(*i*Pr)$_2$-C$_6$H$_4$ with ClBcat. Unfortunately, species **5b** proved to be particularly unstable in solution, which might be caused by redistribution of the catechol moiety promoted by the nucleophilic phosphine, which had to be protected by coordination to borane, generating species 1-Bcat-2-[P(*i*Pr)$_2$•BH$_3$]−C$_6$H$_4$ (**5b.BH$_3$**).

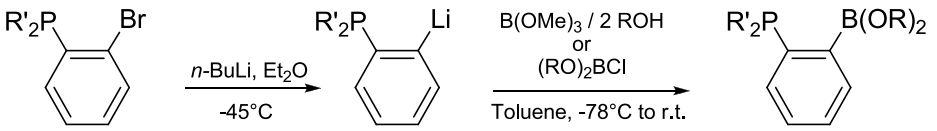

$(OR)_2$	$(OMe)_2$			
R' = Ph	**4a**	**4b**	**4c**	**4d**
R' = *i*Pr	**5a**	**5b**	**5c**	

Figure 5-7: Synthesis of the various derivatives of general formula 1-$B(OR)_2$-2-R'_2P-C_6H_4 tested in the course of this study.

Table 5-1: Catalytic hydroboration of 2 atm of CO_2 using HBcat.[a]

Entry	Catalyst	Borane	Time (min)	TON[b]	TOF[b] (h^{-1})
1	**4a**	HBcat	105	92	53
2	**4b**	HBcat	98	98	56
3	**4c**	HBcat	105	81	46
4	**4d**	HBcat	105	1	<1
5	**4d**	HBcat	240	48	12
6	**5a**	HBcat	105	84	48
7	**5b.BH_3**	HBcat	105	0	0
8	**5b.BH_3**	HBcat	720	74	6
9	**5c**	HBcat	105	75	43

[a]Reaction conditions: In a J-Young NMR tube, 530 µmol of catecholborane (56.4 µL) was added to a mixture of 5.3 µmol of catalyst (~0.6 mL of mother liquor at ~8.8 mmol/L) and an internal standard of hexamethylbenzene (2 mg, 3.3 g/L) in benzene-d_6. The final concentration of catalyst is 8.1 mM. The J-young NMR tube was placed under ~2 atm of CO_2 and was heated at 70 °C. The catalysis was followed by ^{1}H NMR spectroscopy. [b]Turnover numbers (TON) and turnover frequencies for the formation of CH_3OBcat according to the number of

hydrogen atoms transferred to CO_2 based on NMR integration of the corresponding resonance with internal standard.

The catalytic activity of **4a-d**, **5a**, **5b.BH$_3$**, and **5c** was evaluated first using HBcat as a reducing agent under approximately 2 atm of CO_2 in benzene-*d*$_6$.[III] As can be seen in **Table 5-1** (entries 1-3, 6, and 9), species **4a-c**, **5a** and **5c** exhibit similar catalytic activity for the formation of methoxyboranes, sustaining turn-over frequencies between 46 to 56 h^{-1} range in the first 105 minutes of reaction. A stoichiometric amount of catBOBcat was also formed during the process, as previously characterized for this system.[207] The exception is **5b-BH$_3$**, presumably because of the BH_3 protection of the phosphine moiety (entry 7). However, this problem is circumvented after some time since a TON of 74 was observed after 12 hours of reaction (entry 8). Species **4d** is very slow to start (entry 4), showing insignificant production of methoxyboranes after 105 minutes of reaction, but with increasing activity as time goes, reaching TON of 48 after 4 hours (entry 9).

5.6.2 Spectroscopic Monitoring of the Reduction Process

In order to rationalize the similarities in catalytic activity of the different phosphine-borane species, and explain the difference of reactivity for the neopentyl glycol derivative **4d**, the CO_2 reduction using HBcat was monitored using ^1H and $^{31}P\{^1H\}$ NMR spectroscopy. As previously reported, one species at -1.0 ppm was observed by $^{31}P\{^1H\}$ NMR spectroscopy when **4b** was used as catalyst, which was attributed to the formaldehyde adduct 1-Bcat-2-PPh_2−C_6H_4.CH_2O (**4b.CH$_2$O**). Interestingly, it was observed that **4b.CH$_2$O** was also present at the end of the CO_2 reduction catalytic experiments when using any of the **4a-d** derivatives as catalyst. In order to account for possible transformations of the catalyst during the reduction process, the reactions of species **4a-d** with HBcat were carried out. It was found that **4a**, **c** and **d** readily convert to species **4b** when 5 equiv of catecholborane was added to these species in the absence of CO_2. However, species **4d** was shown to undergo such replacement more slowly than the other ambiphilic species. Monitoring the catalytic reduction of CO_2 with **4d** as a catalyst showed that catalysis did not begin until it transforms to **4b**. Similarly, the CO_2

[III] The exact protocol described in the experimental section was carried out for all catalytic reactions. However, since the volume of the NMR tubes differ slightly and some small difference in temperature or pressure can occur when the CO_2 is transferred in the J-Young tube, the exact pressure cannot be known. In a typical experiment with HBcat, the CO_2 will be in significant excess, but in the case of the reactions with BH_3•SMe_2, about 1.5 atm is needed for full conversion, which might alter the activity after more than 200 TON.

reduction reactions using **5a**, **5b.BH$_3$**, or **5c** as catalysts allowed the observation of a single phosphorus containing species by $^{31}P\{^1H\}$ NMR at δ = 14.8 as the resting state of the reaction. The addition of HBcat to **5b.CH$_2$O** (*vide infra*) in solution without the presence of CO_2 gave the same resonance observed under catalytic conditions at ≈ 14 ppm, suggesting that the latter species consist in a Lewis adduct between **5b.CH$_2$O** and HBcat, presumably by an interaction between the HBcat and one O adjacent to B, although the exact mode of interaction could not be determined experimentally. This transformation implies the reduction of CO_2 to formaldehyde, as previously reported for the PPh_2 derivatives, but also the substitution of the pinacol moiety on boron by a catechol moiety. Similarly to the case of the -PPh_2 catalysts, the formaldehyde adduct **5b.CH$_2$O** is the resting state of the CO_2 reduction reaction.

5.6.3 Synthesis of the Formaldehyde Adducts and Labelling Experiments

As observed in **Figure 5-8**, the formaldehyde adduct of **4b** can be prepared and isolated by heating the phosphine-borane **4b** in the presence of excess paraformaldehyde. Unfortunately, other phosphine-borane formaldehyde adducts based on the PPh_3 framework could not be isolated. In fact, **4a** decomposed when heated with paraformaldehyde. While **4c** is stable in the presence of paraformaldehyde, its binding of formaldehyde was found to be reversible and the adduct **4c.CH$_2$O** could not be isolated in the solid form. Consequently, **4c.CH$_2$O** could be prepared *in situ* and characterized by NMR spectroscopy, but its catalytic activity could not be quantified. In chloroform-*d*, the methylene resonances were observed by ^1H NMR spectroscopy at 5.37 ppm for both **4b.CH$_2$O** and **4c.CH$_2$O**, which is consistent with the change in hybridization of the carbon atom and with the loss of planarity of the aldehyde. In the $^{31}P\{^1H\}$ NMR spectra, **4c.CH$_2$O** was characterized by a singlet at -5.5 ppm, while **4b.CH$_2$O** resonates at δ = -3.5. The ^{11}B NMR spectra show signals consistent with tetravalent boron atoms at 5.7 and 8.8 ppm for **4c.CH$_2$O** and **4b.CH$_2$O**, respectively. The formaldehyde adducts of the P*i*Pr$_2$ derivatives appeared to be more stable than their PPh_2 counterparts. Species **5b.CH$_2$O** was isolated in quantitative yield by the addition of 3 equiv of HBcat to **5c** under 1 atm of CO_2 in benzene-d_6 or by the addition of 30 equiv of HBcat to species **5c.CH$_2$O** (**Figure 5-8**). This species has a ^{31}P NMR chemical shift of δ = 12.2 and the CH_2 resonance was observed at δ = 4.96 in the ^1H NMR spectrum**. 5c.CH$_2$O** was isolated by the addition of paraformaldehyde to species **5c** in toluene at 70 °C and was characterized by ^{31}P NMR spectroscopy (δ = 7.7).

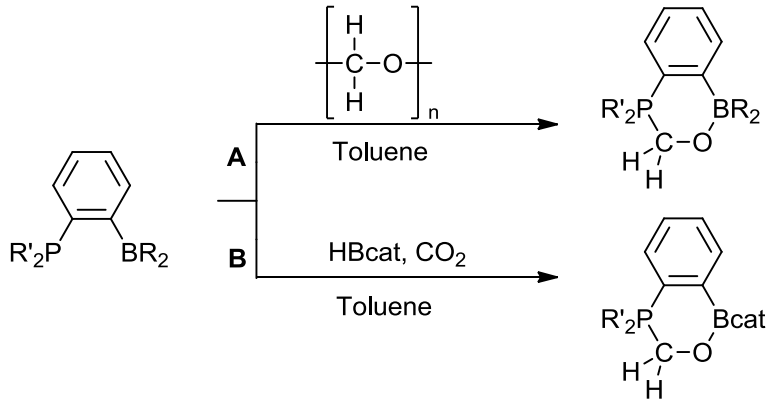

Figure 5-8: Synthesis of formaldehyde adducts of phosphine boranes. **4b.CH_2O** : path **A** using **4b**, 80 °C, 16 h; **4b.$^{13}CH_2O$**: path **B** using **4b**, $^{13}CO_2$, 5 HBcat, 80 °C, 16 h; **4c.CH_2O**: path **A**, using **4c**, 70 °C, 15 min; **5b.CH_2O**: path **B** using **5c**, 3 HBcat, 80 °C, 12 h; **5c.CH_2O**: path **A**, using **5c**, 70 °C, 15 min.

In order to verify if the aldehyde adduct is only a resting state or a significant part of the active catalyst, labelled **4b.$^{13}CH_2O$** and **5b.$^{13}CH_2O$** were prepared directly from $^{13}CO_2$. **4b.$^{13}CH_2O$** was synthesized by exposing **4b** to *ca.* 2 atm of $^{13}CO_2$ in a closed Schlenk vessel in the presence of 5 equivalents of catecholborane. The resulting white precipitate was isolated and washed several times with toluene to yield pure **4b.$^{13}CH_2O$**. The $^{31}P\{^1H\}$ NMR spectrum for **4b.$^{13}CH_2O$** shows a characteristic doublet at -3.5 ppm with a $^1J_{C\text{-}P}$ of 57 Hz. In the ^1H NMR spectrum, the CH_2O resonance was found as a doublet at 5.37 ppm with a $^1J_{C\text{-}H}$ of 151 Hz. Interestingly, when this species was used as catalyst for the hydroboration of CO_2 using HBcat (**Figure 5-9**, equation 1), no ^{13}C incorporation was observed in the methoxyborane formed and the ^{13}C-^{31}P coupling within the formaldehyde adduct could be observed by NMR spectroscopy throughout the catalytic process. Consistently, when **4b.CH_2O** and **5b.CH_2O** were used to reduce $^{13}CO_2$, no ^{13}C incorporation was observed in the formaldehyde adducts. These experiments demonstrate that the CH_2O fragment bridging P and B is not reduced but stays coordinated on the ambiphilic molecule. Thus the formaldehyde adduct is more than a resting state and is in fact the active species responsible for the fast reduction of CO_2 in the presence of ambiphilic phosphine-boranes compounds **4** and **5**.

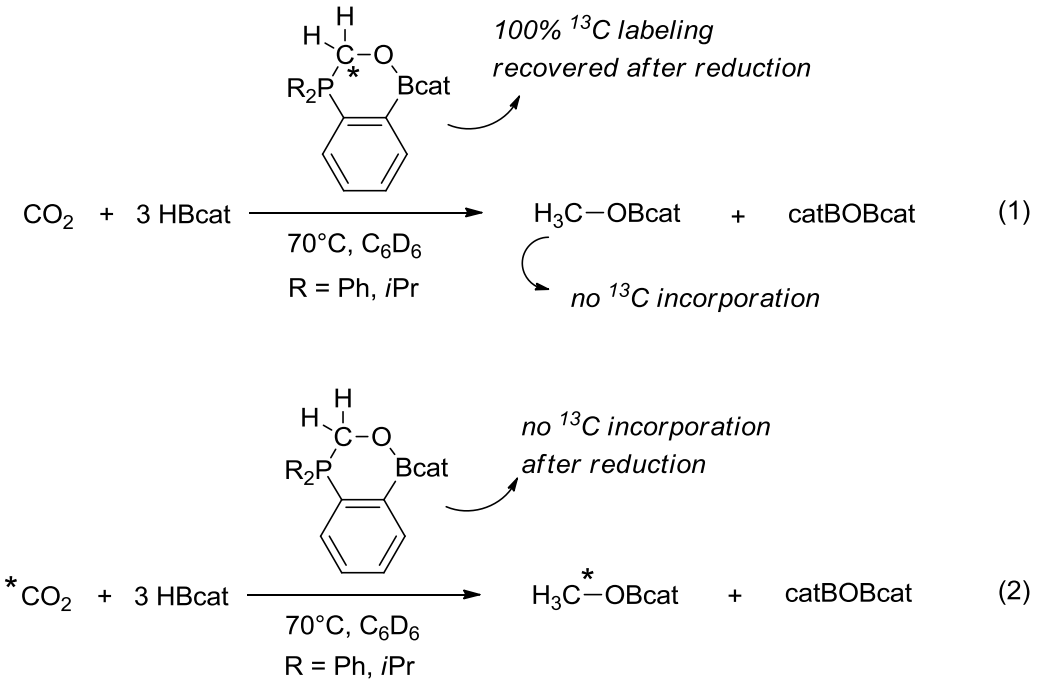

Figure 5-9: Labeling experiments carried out with the phosphine-borane formaldehyde adducts **4b.CH_2O** and **5b.CH_2O**.

5.6.4 DFT Studies of CO_2 Reduction using Formaldehyde Adducts

In order to determine whether formaldehyde adduct **4b.CH_2O** and **5b.CH_2O** in the catalytic transformation, the possible interactions between HBcat and these species were studied using computational chemistry. In order to compare the energies with our previous computational studies, calculations were performed at the same level of theory (B97D/6-31G**) with the solvation effects (benzene) accounted for by the SMD model. As shown in **Figure 5-10**, several possible adducts could be optimized where the borane interacts with one of the oxygen on the phosphine-borane species, notably from the catechol and the aldehyde moieties. Although the previously reported formaldehyde adduct remains the most thermodynamically stable adduct, many other minima could be located on the energy surface. Unsurprisingly, all the isomers have very similar energy values, making difficult the identification of one ground-state structure, especially when keeping in account the uncertainty of the method (± 5 kcal.mol^{-1}), and the possible involvement of fluxional processes and conformational changes.

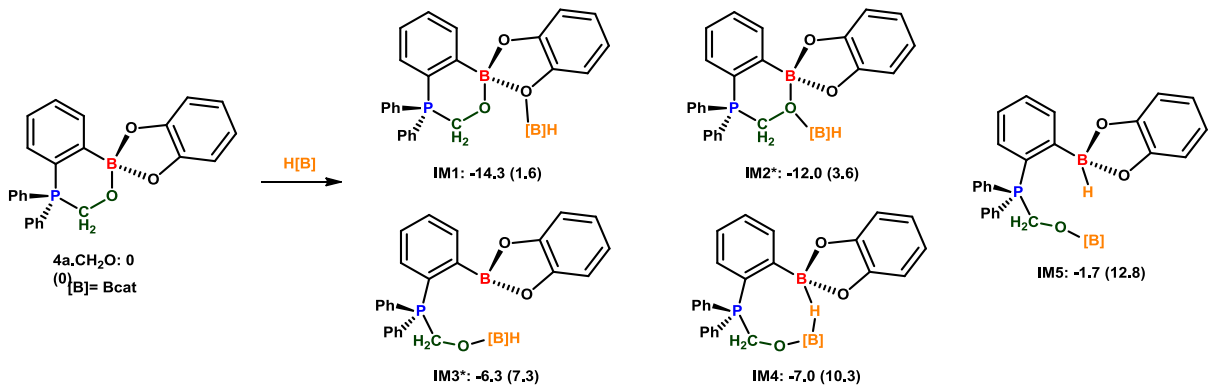

Figure 5-10: Some of the calculated adducts between the boranes (**[B]H** = HBcat) and species **4b-CH_2O** with calculated free enthalpy and free energy (kcal.mol^{-1}) computed at the B97D/6-31G** with the experimental solvent (benzene) accounted for the SMD model. *Indicates that two minima were observed for two rotamers.

Intrigued by the important number of isomers identified and by the possibility for the aldehyde adduct to be an active catalyst rather than a resting state, pathways for CO_2 reduction were investigated with **4b.CH_2O** acting as a catalyst. In the study of the reduction of CO_2 by **4b**, the lowest energy barriers were found upon simultaneous activation of the catecholborane by the Lewis base and of carbon dioxide by the Lewis acid. Direct reduction of carbon dioxide, once bound in a classical fashion by the phosphine and the borane of the catalyst, was found to require a much higher barrier (**Figure 5-11**).

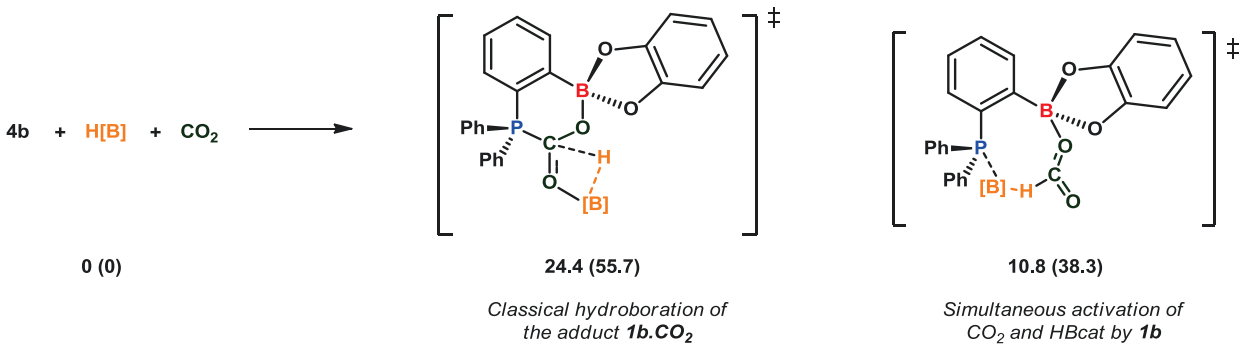

Figure 5-11: Previously reported transition states (and energies in kcal.mol^{-1}) for the hydroboration of CO_2 by **4b**; H[B] = catecholborane.[317]

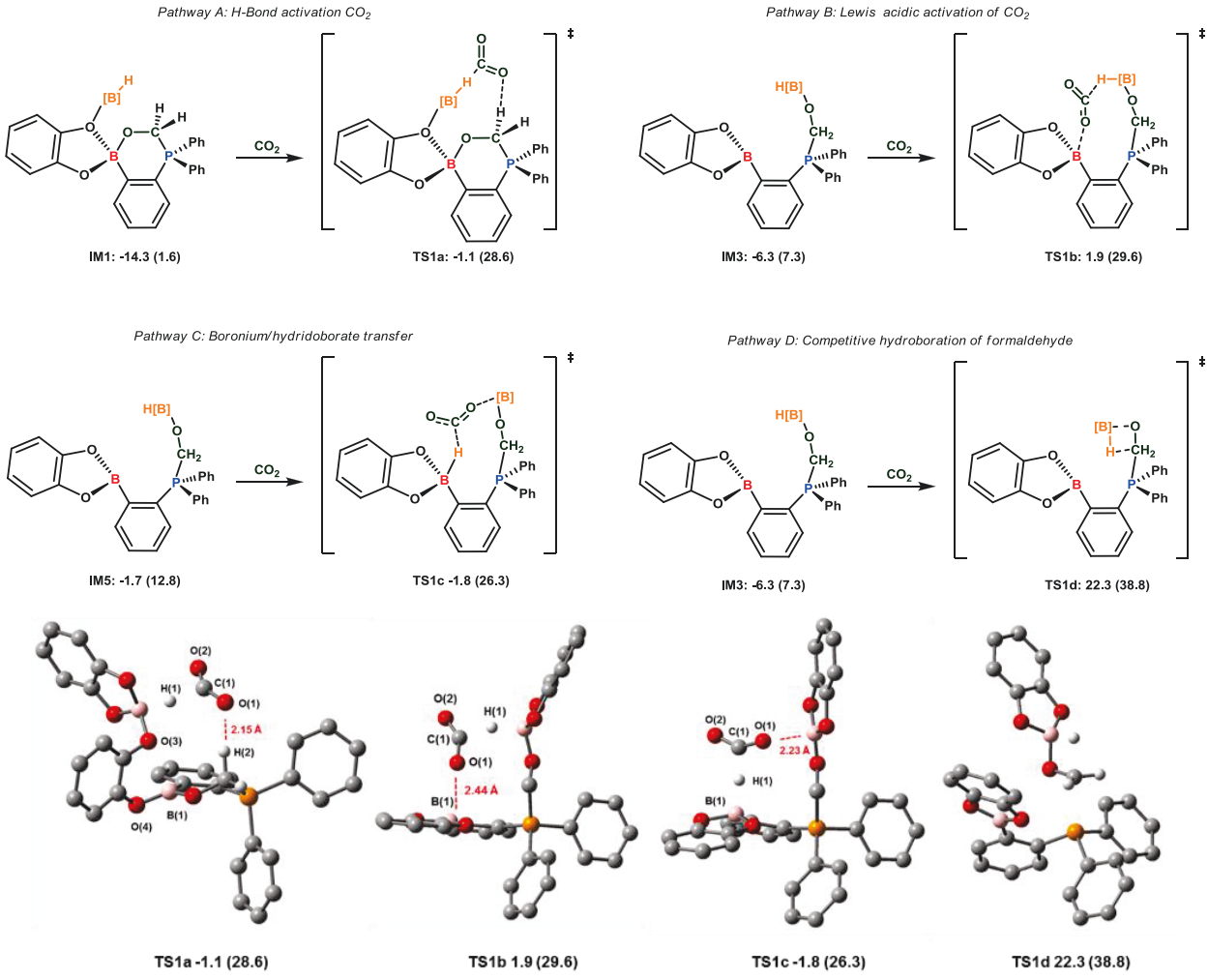

Figure 5-12: Transition states structures for the hydroboration of CO_2 by **4b.CH$_2$O** and HBcat. Calculated free enthalpy and free energy (kcal.mol^{-1}) computed at the B97D/6-31G** with the experimental solvent (benzene) accounted for the SMD model.

After a thorough investigation of the possibilities for **4b.CH_2O** to act as a catalyst for CO_2 reduction, it was possible to find three new transition states which all involve simultaneous activation of HBcat and CO_2. In the first transition state, **TS1a (-1.1 (28.6))**, the H(2)-O(1) distance of 2.15 Å suggests that the Lewis acidic activation is achieved through hydrogen bonding with one of the hydrogen atoms of the bound-formaldehyde (**Figure 5-12**). Although unusual, the activation of CO_2 by hydrogen bonding was suggested before in the Ni(II)(cyclam) electrochemical reduction of CO_2 to CO by Sauvage and co-workers and in the reduction of CO_2 to sodium formate by an Ir(III) pincer complex by Hazari and co-workers. Another interesting aspect of this transition state is the difference in B-O bond lengths. While the B(1)-O(4) bond of 1.38 Å is in the expected range, the B(1)-O(3) bond of 2.27 Å is significantly elongated, showing that the catechol group is disconnected and that the B-catechol ring is opened. The second transition state also involved the formation of an oxygenate species with HBcat, but this time from the opening of the formaldehyde adduct (**IM3**) (**TS1b**; 1.9 (29.6) kcal.mol^{-1}). The oxygen atom of CO_2 is perfectly aligned with the Lewis acidic boron center. The B-O bond distance of 2.44 Å and the planar geometry around the boron center (sum of angles = 358.7°) suggests weak interaction with the carbon dioxide molecule. The third transition state with similar energy values than the two other transition states was also located starting from intermediate **IM5**, (**TS1c** -1.8 (26.3) kcal.mol^{-1}). It was found to occur by a simultaneous delivery of a boronium/hydridoborate ion pair which would be formed from the transfer of the hydride from one B-catechol moiety to the other. In all these intermediates, the formaldehyde adduct plays an important role, either by activating the borane or the carbon dioxide. Once the hydride and the Bcat moieties are transferred to generate the catBOC(O)H species, the B-O bond that was broken in the transition state (from the Bcat in pathway A and from B-OCH_2 in pathways B and C) is regenerated to reform species **4b.CH_2O**.

Comparing these transition states with the direct reduction of formaldehyde (**TS1d**, 22.3 (38.8 kcal.mol^{-1}) supports the experimental observation that formaldehyde remains bound to the ambiphilic framework during catalysis. The transition states **TS1a**-**TS1c** were found to have free energies that are respectively 9.7, 8.7, and 12.0 kcal.mol^{-1} lower than the activation by the phosphine that was originally reported. Although it is likely that the initial formation of the aldehyde occurs through the phosphine-borane mechanism, the results reported herein show that the oxygen atoms are more potent than phosphorus in the activation of hydroboranes.

5.6.5 Catalytic Efficiency of Aldehyde Adducts in the Reduction of CO_2 using BH_3•SMe_2

The efficiency of the aldehyde adducts was then evaluated in the reduction of CO_2 using the dimethylsulfide-borane adduct as a reducing agent. BH_3•SMe_2 is a reagent of choice for the hydroboration of CO_2 since it is less reactive and dangerous than the diborane reagent B_2H_6 while possessing high hydrogen content by having three transferable hydrides per boron atom. Interestingly, no transition metal system has been reported to use BH_3 adducts for the reduction of carbon dioxide and only a limited number of organocatalysts can do such reaction, including **4b** that proved the most active to date, with TOF of 973 h^{-1} at 70 °C.[63,207] To follow up on known literature, the values of TON and TOF were calculated according to the number of hydrogen atoms transferred on CO_2.

The catalytic reduction of CO_2 was carried out using **4a**-**4d** as catalysts (**Table 5-2**, entries 1-4). In these experiments, about 2 atm of CO_2 was added to a 8 mM solution of the catalyst in benzene-d_6 containing 100 equiv of BH_3•SMe_2 in a J-Young NMR tube. As can be observed, both species **4a** and **4b** showed good activities, reaching TOF of 257 and 242 h^{-1} in the first hour of reaction (**Table 5-2**, entries 1 and 2, respectively). There is a significant decrease in activity when the pinacol derivative was used, since only a TOF of 43 h^{-1} was observed (**Table 5-2** entry 3), whereas catalyst **4d** did not show significant activity (**Table 5-2**, entry 4). While the reduction of CO_2 using BH_3•SMe_2 and **4b** as catalyst proceeds rapidly at 70 °C, it was shown to be much slower at room temperature. As it was reported, the spectroscopic monitoring of the latter reaction reveals that it suffers from a long induction period before reaching its peak turnover frequency. The intermediates of the reaction were monitored using ^{1}H and ^{31}P NMR spectroscopy. As long as species **4b.BH$_3$** is the only one in solution, no significant reduction process is taking place. However, as soon as the presence of the formaldehyde adduct was observed, the catalytic reduction rate was shown to increase significantly, confirming that **4b.CH$_2$O** is playing a significant role in the catalytic reduction.

Table 5-2: Catalytic hydroboration of 2 atm of CO_2 using BH_3•SMe_2.[a]

Entry	Catalyst	Time (min)	T (°C)	TON[b]	TOF[b] (h^{-1})
1	**4a**	60	70	257	257
2[207]	**4b**	67	70	271	242
3	**4c**	60	70	43	43
4	**4d**	60	70	<1	<1
5	**4b.CH_2O**	35	25	84	144
6	**5b.CH_2O**	30	20	114	228
7	**5b.CH_2O**	90	20	204	136
8	**5b.CH_2O**	30	70	297	594
9[c]	**5b.CH_2O**	30	70	435	873
10[c]	**5b.CH_2O**	90	70	1005	670

[a]Reaction conditions: In a J-Young NMR tube, 530 µmol of BH_3•SMe_2 (56.4 µL) was added to a mixture of 5.3 µmol of catalyst (~0.6 mL of stock solution at ~8.8 mmol/L) and an internal standard of hexamethylbenzene (2 mg, 3.3 g/L) in benzene-d_6 for entries 1-5, but in chloroform-*d* for entries 6-10. The final concentration of catalyst is ~8.1 mM. The J-young NMR tube was placed under 2 atm of CO_2 and was heated at 70 °C. The catalysis was followed by ^{1}H NMR spectroscopy. [b]Turnover numbers (TON) and turnover frequencies for the formation of $[B(OMe)O]_n$ according to the number of hydrogen atoms transferred to CO_2 based on NMR integration of the corresponding resonance with internal standard. [c]The reaction was performed under the same conditions but with a catalyst concentration of ~1.8 mM.

When carrying out the reduction of CO_2 in benzene at *room temperature* with **4b.CH_2O** as the catalyst, the rapid reduction of CO_2 was observed in the first minutes of reaction. In fact, within the five minutes needed for the acquisition of the first NMR spectrum, it was possible to ascertain a nominal TON value of 26 for the conversion of CO_2 to $[MeOBO]_n$, which can be associated with an initial TOF of > 520 h^{-1} (**Figure 5-13**). This reaction rate is significantly superior to previously observed catalytic activities at ambient temperature when using **4b** as

the starting catalyst, especially when considering that a significant amount of the catalyst was not dissolved at this time. After 35 minutes, a TON of 84 was observed, corresponding to a TOF of 144 h^{-1} (**Table 5-2**, entry 5).

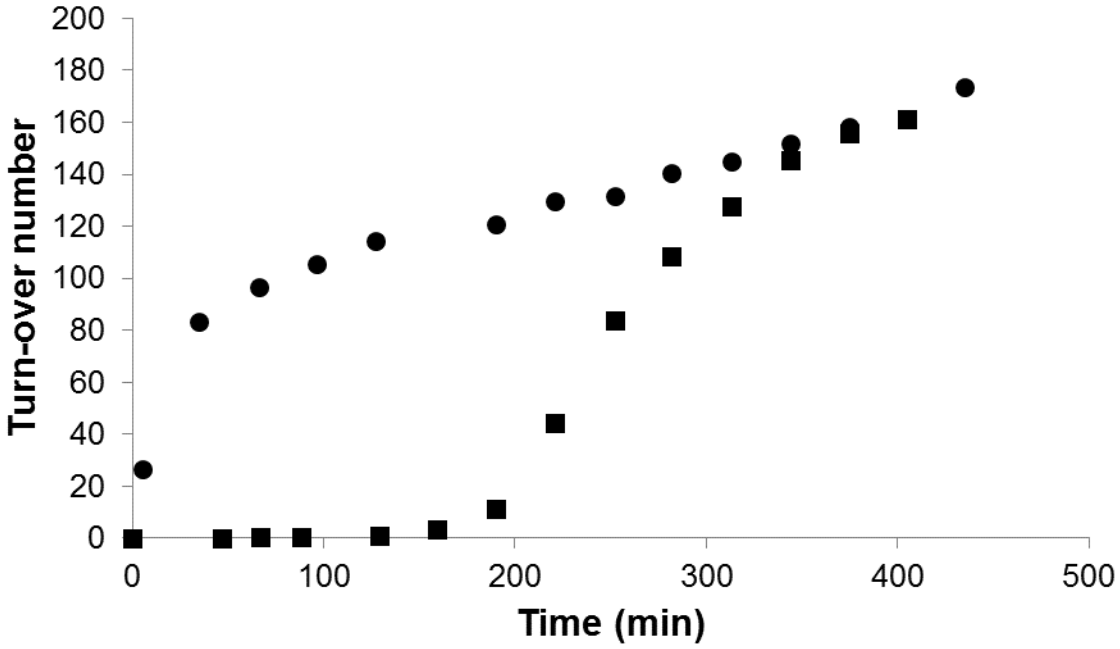

Figure 5-13: Number of turn-overs for the reduction of CO_2 in $[B(OMe)O]_n$ in the presence of 100 equiv of BH_3•SMe_2 as a reductant using 9 mM solution of (●) **4b.CH_2O** and (■) **4b** in benzene-d_6. The reaction was carried out at room temperature using about 1-2 atm of CO_2 in a J-Young NMR tube. The exact pressure could not be measured, but under the loading present it is expected that CO_2 will be the limiting reagent since 1.5 atm is needed to obtain 100% yield (300 TON), explaining the lower rate at high conversion.

The formaldehyde adduct **5b.CH_2O** was also evaluated with BH_3•SMe_2 as a reductant. The catalytic tests were performed in chloroform-*d* to ensure good solubility. Accordingly, it was found that a 1 mol% of species **5b.CH_2O** could give over 99% of the conversion expected within 30 min, giving TON of 114 and TOF over 228 h^{-1} at ambient temperature, which is slightly higher that the activity of **4b.CH_2O** (**Table 5-2**, entry 6). Letting the reaction run for 90 minutes increased the TON value to 204, while reducing the TOF to 136 h^{-1} (**Table 5-2**, entry 7). Looking at the reactivity at 70 °C it was possible to observe that catalyst **5b.CH_2O** converted almost quantitatively BH_3•SMe_2 to methoxyboranes in 30 min, giving TON and TOF of 297 and 594 h^{-1} (**Table 5-2**, entry 8), respectively, which under NMR tube conditions surpass that of catalyst **4b**. Decreasing catalyst loading to 1.8 mM but keeping all the other parameters identical, it was possible to observe that catalyst **5b.CH_2O** could give a TON of

435 in the first 30 min (TOF of 873 h^{-1}), while running the reaction for 150 min increased the TON to 1005 (**Table 5-2**, entries 9 and 10). These results are of significant interest since some of the formaldehyde adducts exhibit higher stability than their phosphine-borane precursors, notably in the case of **5b**. Also, the high activity at ambient temperature and the absence of induction period contrasts drastically with all systems reported to date to reduce CO_2 using BH_3 derivatives which usually need induction periods and higher temperatures to proceed efficiently.

It should be noted that the increase in activity of the formaldehyde adducts compared to the ambiphilic phosphine-boranes is really counterintuitive, especially when comparing with the usual chemistry of Frustrated Lewis Pairs. Indeed, in latter systems, the activation of substrates such as molecular hydrogen and carbon dioxide is possible by preventing the formation of Lewis adducts between the two components of the FLP. Although such process is particularly important in hydrogen activation, it does not seem to play a similar role in the catalytic reduction of carbon dioxide. Indeed, the most important factor seems to be the activation of the reducing agent, which is done in the current system by interaction of the hydroborane with O atoms of the formaldehyde adduct; something that can be related to the activity of several borates in the reduction of carbon dioxide, including notably the BH_4^- salts that are well-known to reduce CO_2 in a stoichiometric fashion. It seems however that the simultaneous activation of the carbon dioxide by either hydrogen bonding or by a weak Lewis acid such as the boroncatecholate moiety is helping to lower significantly the transition state energy. As it was stated before, such weak Lewis acid can also prevent the formation of very stable formate adducts which might make difficult the release of the reduced species and high catalytic turn-overs. The formaldehyde adducts **4b.CH_2O** and **5b.CH_2O** presented in this system have also the advantage to be quite stable to both air and water, which are significant advantages compared to some ambiphilic species, notably **5b**.

5.7 Conclusion

Ambiphilic species reported in this study all show the ability to hydroborate catalytically CO_2 to CH_3OBR_2 derivatives using catecholborane and BH_3•SMe_2. However, in the presence of catecholborane, all species undergo transformations to generate respectively **4b.CH_2O** or **5b.CH_2O**, which are believed to be the active catalysts in the latter reaction. Although the exact mechanism for such transformation is unknown, derivatives of **4b** and **5b** seem to be the favored species in such system. The latter reaction also puts in evidence the importance

of possible redistribution occurring in such systems with the B-O bonds being quite kinetically labile. As it was demonstrated by using **4b.$^{13}CH_2O$** and **5b.$^{13}CH_2O$** as catalysts, the interaction between the formaldehyde and the phosphine-borane moiety seems to remain intact throughout catalysis. DFT modeling of possible transition states show that the ambiphilic activation remains possible, as it was proposed for species **4b**, but this time one oxygen atom, either from the formaldehyde or the catechol moieties, acts as Lewis base to activate the reducing agent, whereas the CO_2 is activated either by one borane or by hydrogen bonding with one hydrogen of the formaldehyde adduct. Species **5b.CH_2O** was shown to be the best catalyst at room temperature reported for this system, obtaining TOF of 228 h^{-1}. Although it represents a much harder challenge, we are currently interested in using this concept for the hydrogenation of carbon dioxide.

5.8 Experimental Details

General comments: All reactions and manipulations were carried out under an atmosphere of dry argon using standard Schlenk techniques. All solvents were sparged with argon and dried using an MBRAUN Solvent Purification System or distilled from Na/benzophenone. ^{1}H, ^{13}C and ^{31}P NMR spectra were recorded on NMR spectra were recorded on Agilent Technologies or Bruker Avance 500 NMR spectrometers at 500 MHz (^{1}H), 125.758 MHz (^{13}C), 202.456 MHz (^{31}P) 160.46 MHz (^{11}B), on a Varian Inova NMR AS400 spectrometer, at 400.0 MHz (^{1}H), 100.580 MHz (^{13}C), 161.923 MHz (^{31}P), or on Bruker NMR AC-300 at 300MHz (^{1}H), 75.435 MHz (^{13}C), 121.442 MHz (^{31}P). Chemical shifts are expressed with a positive sign, in parts per million, calibrated to residual solvent signals (^{1}H, ^{13}C), 85% H_3PO_4 (^{31}P, 0 ppm), and $B(OMe)_3$ (^{11}B, 0 ppm). Mass spectra were recorded on a Waters GCT mass spectrometer. 1−bromo−2−diisopropylphosphinobenzene,[319] **4b**,[207] **4b.CH_2O**,[207] **4c,**[318] and **4d**[318] were prepared as previously described.

5.8.1 Synthesis of Phosphine-Borane Derivatives

Compound 4a

To a solution of (2-bromophenyl)diphenylphosphine (1.95 g, 5.72 mmol) in tetrahydrofuran (20 mL) was added dropwise *n*-BuLi (2.3 mL, 2.5 M in hexane, 5.72 mmol) at -78 °C and the reaction mixture was warmed up to -40 and stirred for 1 hour. Trimethylborate (1.78 g, 1.9 mL, 15.6 mmol) was then added by syringe. The reaction mixture let to warm up to room temperature in its cold bath and stirred at room temperature overnight. The volatiles were removed under a vacuum and the mixture was extracted with hexanes (3 x *ca*. 20 mL). Compound **4a** was obtained as a white solid with a yield of 94% after *in vacuo* evaporation. ^{1}H NMR (500 MHz, benzene-d_6) : 7.44-7.37 (m, 5H), 7.37-7.28 (m, 2H), 7.10-6.99 (m, 7H), 3.48 (s, 6H, $BOMe_2$); $^{13}C\{^{1}H\}$ NMR (125 MHz, chloroform-*d*): 133.9 (d, J_{C-P} = 19.5 Hz, C_{arom}), 133.8 (s, C_{arom}), 131.5 (d, $^{1}J_{C-P}$ = 15.7 Hz, C_{arom}), 128.9 (s, C_{arom}), 128.7 (d, J_{C-P} = 6.2 Hz, C_{arom}), 128.6 (s, C_{arom}), 128.6 (s, C_{arom}), 52.3 (d, J_{C-P} = 57.7 Hz, *MeO*); $^{31}P\{^{1}H\}$ NMR (202 MHz, benzene-d_6): -6.0 (s); $^{11}B\{^{1}H\}$ NMR (161 MHz, benzene-d_6) : 29.7 (br).

Compound 4a.$^{13}CH_2O$

A solution of **4a** (550 mg, 1.45 mmol) in toluene (15 mL) was prepared and introduced in a sealable Schlenk tube. Catecholborane (867 mg, 7.25 mmol) was added and the reaction vessel was immediately frozen in a liquid N_2 bath. $^{13}CO_2$ (ca 2 atm.) was added and the tube was sealed, thawed then heated to 70 °C overnight. A white solid precipitated during the heating, was collected by filtration and washed four times with toluene to afford **4a.$^{13}CH_2O$** as a white solid. ^{1}H NMR (500 MHz, chloroform-*d*) : 7.87 (dd, 1H), 7.77-7.70 (m, 6H), 7.64-7.60 (m, 5H), 7.36 (ddt, 1H, J = 1.5, 3.7, 7.6 Hz), 7.30-7.24 (m, 1H), 6.78 (m, 2H, catechol), 6.66 (m, 2H, catechol), 5.37 (d, 2H, $^{1}J_{C-H}$ = 151 Hz, CH_2O). $^{13}C\{^{1}H\}$ NMR (125 MHz, chloroform-*d*): 152.6 (s, C_{arom}), 134.5 (d, J_{C-P} = 2.8 Hz, C_{arom}), 134.3 (br), 133.7 (d, $^{1}J_{C-P}$ = 9.5 Hz, C_{arom}), 130.7 (d, J_{C-P} = 9.5 Hz, C_{arom}), 130.1 (d, J_{C-P} = 11.4 Hz, C_{arom}), 127.9 (d, J_{C-P} = 12.9 Hz, C_{arom}), 118.1 (s, *cat*), 109.3 (s, *cat*), 60.3 (d, J_{C-P} = 57.7 Hz, CH_2O); $^{31}P\{^{1}H\}$ NMR (202 MHz, chloroform-*d*) : -3.5 (d, $^{1}J_{C-H}$ = 57 Hz); $^{11}B\{^{1}H\}$ NMR (161 MHz, chloroform-*d*) : 8.7 (br).

In situ characterization of 4c.CH_2O

4c (*ca*. 5 mg) was dissolved in chloroform-*d* and placed in a J-Young NMR tube along with excess paraformaldehyde. The mixture was heated for 30 minutes at 80 °C and subsequently analyzed by NMR.^{1}H NMR (500 MHz, chloroform-*d*) : 8.12 (dd, 1H), 7.77-7.45 (m, 11H), 7.37-7.05 (m, 2H), 5.37 (d, 2H, $^{1}J_{C-H}$ = 151 Hz, CH_2O), 1.32 (s, 12H, pinacol); $^{31}P\{^{1}H\}$ NMR (202 MHz, benzene-d_6) : -5.5 (s); $^{11}B\{^{1}H\}$ NMR (161 MHz, chloroform-*d*) : 5.7 (br).

Compound 5a

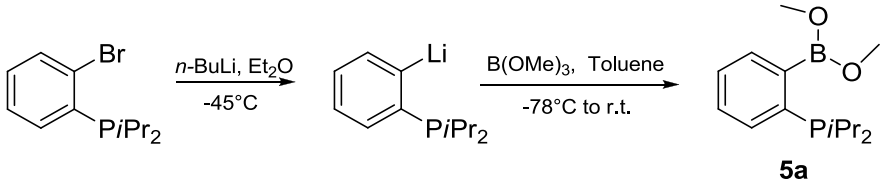

5a

Figure 5-14: Preparation of compound **5a**.

To a solution of (2-bromophenyl)diisopropylphosphine (1.11 g, 4.06 mmol) in diethylether (5 mL) was added dropwise *n*-BuLi (2.5 mL, 1.60 M in hexane, 4.06 mmol) at -40 °C and the reaction mixture was stirred 1 h at this temperature. The mixture was decanted and the supernatant was removed by filtration at -40 °C. The resulting white solid was washed with diethylether (2 x 5 mL) at -40 °C. The solid was then dissolved in 5 mL of toluene at -78 °C, and added to a solution of trimethylborate (2.7 mL, 24.7 mmol) in 5 mL of toluene at the same temperature. The reaction mixture was stirred at rt overnight. The solution was filtrated through a plug of Celite, and volatiles were removed under a vacuum. The resulting oil was distilled using Kugelrohr apparatus (vacuum: 0.05 mbar, T°= 90 °C). Compound **5a** was obtained as colorless oil with a yield of 70 %.^{1}H NMR (300 MHz, benzene-d_6): 7.30 (m, 2H), 7.14 (m, H), 3.57 (s, 6H, OC*H*3), 1.97 (septd, 2H, $^{3}J_{H-H}$ = 7.0 Hz, $^{2}J_{H-P}$ = 2.8 Hz, C*H*$(CH_3)_2$), 1.10 (dd, 6H, $^{3}J_{H-H}$ = 7.0 Hz, $^{3}J_{H-P}$ = 14.7 Hz, CH(C*H*$_3)_2$), 0.92 (dd, 6H,$^{3}J_{H-H}$ = 7.0 Hz, $^{3}J_{H-P}$ = 11.7 Hz, CH(C*H*$_3)_2$); $^{31}P\{^{1}H\}$ NMR: (161 MHz, benzene-d_6): 8.8 (s); $^{11}B\{^{1}H\}$ NMR: (96 MHz, benzene-d_6) : 29.7 (s).

Compound 5b.BH_3

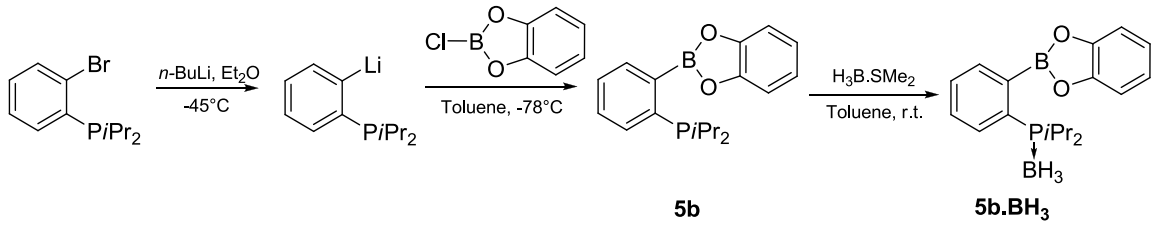

Figure 5-15: Preparation of compound **5b.BH_3**.

To a solution of (2-bromophenyl)diisopropylphosphine (505 mg, 1.85 mmol) in diethylether (5 mL) was added *n*-BuLi (1.15 mL, 1.60 M in hexane, 1.85 mmol) dropwise at -40 °C and the reaction mixture was stirred 1 h at this temperature. The mixture was decanted and the supernatant was removed by filtration at -40 °C. The resulting white solid was washed with diethylether (2 x 5 mL) at -40 °C. The solid was then dissolved in 5 mL of toluene at -78 °C, and added to a solution of chlorocatecholborane (257 mg, 1.66 mmol) in 5 mL of toluene at -78 °C. The reaction mixture was stirred at rt overnight. The solution was filtrated through a plug of Celite, and dried under a vacuum. The resulting solid was dissolved in 5 mL of pentane and stored at -80 °C overnight allowing the precipitation of a white solid. The solution was then filtrated and dried. The resulting solid was dissolved in 5 mL of toluene and borane dimethylsulfide complex (0.83 mL, 2.0 M in THF, 1.66 mmol) was added to the solution. The mixture was stirred 30 min and then volatiles were removed under vacuum. The resulting solid was dissolved in 2 mL of pentane and stored at -80 °C overnight. Compound **5b.BH_3** was obtained as a white powder after filtration with a yield of 49%. HRMS (DCI-CH_4) calcd for $[M-H]^+$ $(C_{18}H_{24}B_2O_2P)^+$: 325.1700, Found: 325.1702. ^{1}H NMR (300 MHz, benzene-d_6): 7.72 (t, 1H, $^3J_{H-H}$ = 1.5 Hz, J_{H-P} = 8 Hz, H_{arom}), 7.64 (m, 1H), 7.08 (m, 4H), 6.84 (m, 2H), 2.33 (septd, 2H, $^3J_{H-H}$ = 7.0 Hz, $^2J_{H-P}$ = 12.0 Hz, C*H*$(CH_3)_2$), 1.17 (dd, 6H, $^3J_{H-H}$ = 7.0 Hz, $^3J_{H-P}$ = 15.0 Hz, CH(C*H*$_3)_2$), 0.89 (dd, 6H,$^3J_{H-H}$ = 7.0 Hz, $^3J_{H-P}$ = 15.0 Hz, CH(C*H*$_3)_2$). Signals attributed to BH_3 are very broad (multiplet from 0.7 to 1.5 ppm); ^{13}C{^{1}H} NMR (75 MHz, chloroform-*d*): 148.8 (s, 2C, C_{arom}), 136.0 (d, J_{C-P} = 10.0 Hz, CH_{arom}), 134.4 (d, J_{C-P} = 7.8 Hz, CH_{arom}), 133.0 (d, $^1J_{C-P}$ = 45.3 Hz, C_{arom}), 130.1 (d, J_{C-P} = 8.6 Hz, CH_{arom}), 130.0 (d, J_{C-P} = 2.4 Hz, CH_{arom}), 123.3 (s, 2C, CH_{arom}), 113.0 (s, 2C, CH_{arom}), 23.6 (d, J_{C-P} = 32.8 Hz, *C*HCH_3), 17.8 (s, *C*H_3), 17.7 (d, J_{C-P} = 1.5 Hz, CH_3). The quaternary carbon connected to the boron atom was not observed; ^{31}P{^{1}H} NMR: (161 MHz, benzene-d_6): 39.0 (m); ^{11}B{^{1}H} NMR: (96 MHz, benzene-d_6) : 32.0 (s, Bcat), -43.8 (d, $J_{B-P} \approx 30.0$ Hz, BH_3).

Compound 5c

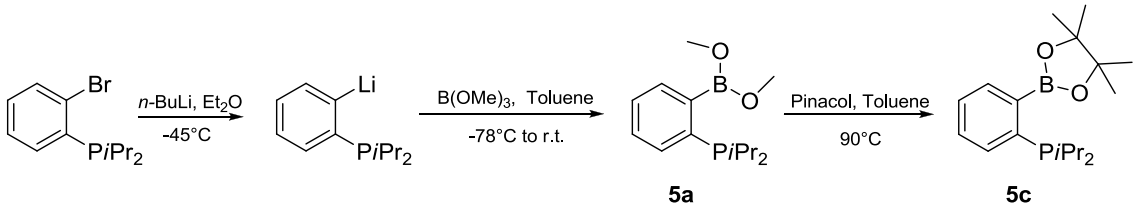

Figure 5-16: Preparation of compound **5c**.

To the solution of (2-bromophenyl)diisopropylphosphine (558 mg, 2.04 mmol) in diethylether (5 mL) were added *n*-BuLi (1.3 mL, 1.60 M in hexane, 2.04 mmol) dropwise at -40 °C and the reaction mixture was stirred 1 h at this temperature. The mixture was decanted and the supernatant was removed by filtration at -40 °C. The resulting white solid was washed with diethylether (2 x 5 mL) at -40 °C. The solid was then dissolved in 5 mL of toluene at -78 °C, and added to a solution of trimethylborate (1.4 mL, 12.2 mmol) in 5 mL of toluene at the same temperature. The reaction mixture was stirred at rt overnight. The solution was filtrated through a plug of Celite, and the volatiles were removed from the supernatant under a vacuum. The resulting oil was dissolved in 5 mL of toluene and added to a solution of pinacol (200 mg, 1.69 mmol) in toluene (5 mL). The mixture was heated during 1h at 90 °C. The volatiles were removed under a vacuum. The resulting solid was dissolved in 10 mL of pentane and stored at -80 °C overnight. The exces of pinacol was precipitated and eliminated by filtration. The supernatant was concentrated and placed at -80 °C overnight. Compound **5c** was obtained as a white powder after filtration with a yield of 76%. HRMS (DCI-CH_4) calcd for $[M+H]^+$ $(C_{18}H_{30}BO_2P)^+$: 321.2155, Found: 321.2159. ^{1}H NMR (300 MHz, benzene-d_6): 7.77 (m, 1H, H_{arom}), 7.39 (m, 1H), 7.18 (m, 2H), 2.04 (septd, 2H, $^3J_{H-H}$ = 7.0 Hz, $^2J_{H-P}$ = 4.5 Hz, C*H*$(CH_3)_2$), 1.24 (s, 12H, Hpin), 1.15 (dd, 6H, $^3J_{H-H}$ = 7.0 Hz, $^3J_{H-P}$ = 13.9 Hz, CH(C*H*$_3)_2$), 1.0 (dd, 6H, $^3J_{H-H}$ = 7.0 Hz, $^3J_{H-P}$ = 11.9 Hz, CH(C*H*$_3)_2$); ^{13}C{^{1}H} NMR (76 MHz, benzene-d_6): 141.8 (d, $^1J_{C-P}$ = 20.0 Hz, CH_{arom}), 133.8 (d, J_{C-P} = 13.8 Hz, CH_{arom}), 131.7 (d, J_{C-P} = 2.3 Hz, CH_{arom}), 128.9 (s, CH_{arom}), 127.99 (d, J_{C-P} = 1 Hz, C_{arom}), 83.9 (s, 2C, Cpin), 25.2 (s, CH_3pin), 25.1 (s, CH_3pin), 24.6 (d, $^1J_{C-P}$ = 14.5 Hz, *C*HCH_3), 20.3 (d, $^2J_{C-P}$ = 18.0 Hz ,CH_3), 20.1 (d, $^2J_{C-P}$ = 12.0 Hz, CH_3) The quaternary carbon connected to the boron atom was not observed; ^{31}P{^{1}H} NMR (161 MHz, benzene-d_6): 6.4 (s); ^{11}B{^{1}H} NMR (96 MHz, benzene-d_6): 31.7 (s, Bpin).

Compound 5b.CH_2O

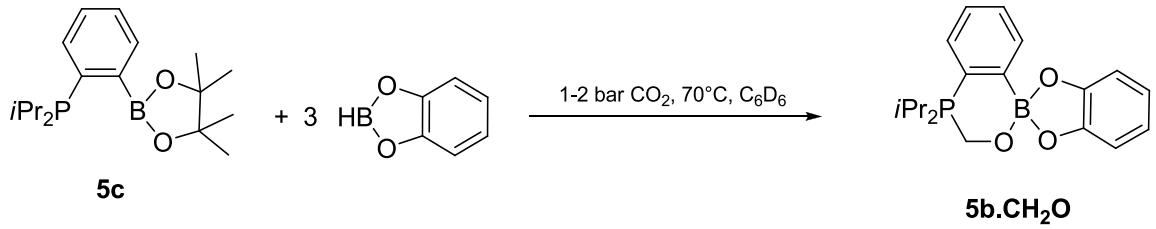

5c **5b.CH_2O**

Figure 5-17: Preparation of compound **5b.CH_2O**.

Catecholborane (123.8 µL, 1.16 mmol) was added to **5c** (124 mg, 0.39 mmol) in benzene-d_6 solution (15 mL) and the mixture was transferred to a *Fisher-Porter tube at rt. T*he tube was placed under vacuum in the liquid nitrogen bath during ≈ 10 seconds. Then, the cold bath was removed and the *tube was placed* at room temperature. After ≈ *30 seconds the tube was placed under 1 atm of* CO_2. The solution was stirred and heated at 70 °C. The consumption of catecholborane was followed by ^{1}H NMR. After one night of reaction under CO_2, the mixture was filtrated. The solid was washed with pentane (2 x 15 mL) and dried under vacuum. Compound **5b.CH_2O** was obtained as a white powder with a yield of 96%. Anal. Calcd. for $C_{19}H_{24}BO_3P$; C, 66.69; H,7.07. Found: C,66.57; H, 7.30. HRMS(DCI-CH_4) calcd for $[M+H]^+$ $(C_{19}H_{25}BO_3P)^+$: 343.1634, Found: 343.1631. ^{1}H NMR (300 MHz, chloroform-*d*): 7.82 (m, 1H), 7.56 (m, 1H), 7.33 (m, 2H), 6.71 (m, 4H, Hcat), 4.965 (s, 2H, CH_2O), 2.75 (septd, 2H, $^3J_{H-H}$ = 7.0 Hz, $^2J_{H-P}$ = 12.0 Hz, C$H$$(CH_3)_2$), 1.43 (dd, 6H, $^3J_{H-H}$ = 7.0 Hz, $^3J_{H-P}$ = 16.3 Hz, CH(C$H_3)_2$), 1.37 (dd, 6H, $^3J_{H-H}$ = 7.0 Hz, $^3J_{H-P}$ = 16.3 Hz, CH(C$H_3)_2$); ^{13}C{^{1}H} NMR (75 MHz, chloroform-*d*): 152.8 (s, Ccat), 135.4 (d, J_{C-P} = 11.7 Hz, CH_{arom}), 133.8 (d, J_{C-P} = 3 Hz, CH_{arom}), 128.8 (d, J_{C-P} = 8.8 Hz, CH_{arom}), 127.6 (d, J_{C-P} = 11.9 Hz, CH_{arom}), 118.2 (s, CHcat), 115.8 (d, $^1J_{C-P}$ = 77.0 Hz, C_{arom}), 109.4 (s, CHcat), 52.3 (d, J_{C-P} = 51.5 Hz, CH_2O), 21.9 (d, J_{C-P} = 40.9 Hz, $C$$HCH_3$), 17.1 (d, J_{C-P} = 3.1 Hz ,CH_3), 16.4 (d, J_{C-P} = 2.3 Hz, CH_3). The quaternary carbon atom connected to the boron atom was not observed; ^{31}P{^{1}H} NMR (161 MHz, chloroform-*d*): 12.2 (s); ^{11}B{^{1}H} NMR (96 MHz, chloroform-*d*): 8.6 (s).

Compound 5b.$^{13}CH_2O$

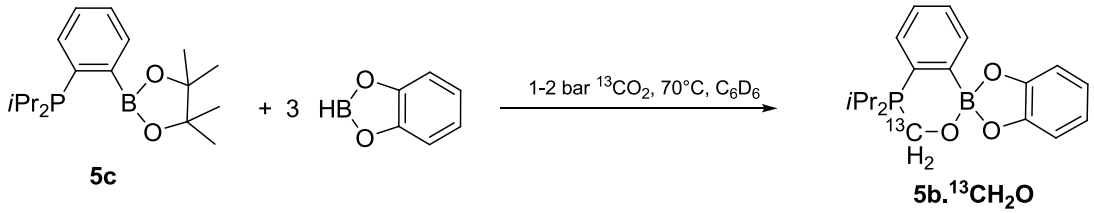

Figure 5-18: Preparation of compound **5b.CH_2O**.

Catecholborane (123.8 µL, 1.16 mmol) was added to **5c** (124 mg, 0.39 mmol) in benzene-*d_6* solution (15 mL) and the mixture was transferred to a Fisher**-**Porter tube *at rt. T*he tube was placed under vacuum in the liquid nitrogen bath during ≈ 10 seconds. Then, the cold bath was removed and the *tube was placed* at room temperature. After ≈ *30 seconds the tube was placed under 1 atm of* $^{13}CO_2$. The solution was stirred and heated at 70 °C. The consumption of catecholborane was followed by ^{1}H NMR. After one night of reaction under $^{13}CO_2$, the mixture was filtrated. The solid was washed with pentane (2 x 15 mL) and dried under vacuum. Compound **5b.$^{13}CH_2O$** was obtained as a white powder with a yield of 96%. ^{1}H NMR (300 MHz, chloroform-*d*): 7.82 (m, 1H), 7.56 (m, 1H), 7.33 (m, 2H), 6.71 (m, 4H, Hcat), 4.90 (d, 2H, $^1J_{H\text{-}C}$ = 148.5 Hz, $^{13}C\mathit{H}_2O$), 2.76 (septd, 2H, C*H*$(CH_3)_2$), 1.43 (dd, 6H, $^3J_{H\text{-}H}$ = 7.0 Hz, $^3J_{H\text{-}P}$ = 16.3 Hz, CH(C*H*$_3)_2$), 1.37 (dd, 6H, $^3J_{H\text{-}H}$ = 7.0 Hz, $^3J_{H\text{-}P}$ = 16.3 Hz, CH(C*H*$_3)_2$); $^{13}C\{^1H\}$ NMR (75 MHz, chloroform-*d*): 152.8 (s, Ccat), 135.5 (d, $J_{C\text{-}P}$ = 11.6 Hz, CH_{arom}), 133.9 (d, $J_{C\text{-}P}$ = 2.8 Hz, CH_{arom}), 128.7 (d, $J_{C\text{-}P}$ = 8.7 Hz, CH_{arom}), 127.6 (d, $J_{C\text{-}P}$ = 11.8 Hz, CH_{arom}), 118.2 (s, CHcat), 109.4 (s, CHcat), 52.4 (d, $J_{C\text{-}P}$ = 51.5 Hz, $^{13}CH_2O$), 21.9 (d, $J_{C\text{-}P}$ = 40.8 Hz, *C*HCH_3), 17.1 (d, $J_{C\text{-}P}$ = 3.1 Hz ,CH_3), 16.5 (d, $J_{C\text{-}P}$ = 2.2 Hz, CH_3). The quaternary carbon atom connected to the boron atom and to the phosphorus atom were not observed; $^{31}P\{^1H\}$ NMR (161 MHz, chloroform-*d*): 12.1 (d, $^1J_{P\text{-}C}$ = 51.5 Hz); $^{11}B\{^1H\}$ NMR (96 MHz, chloroform-*d*): 8.5 (s).

Compound 5c.CH_2O

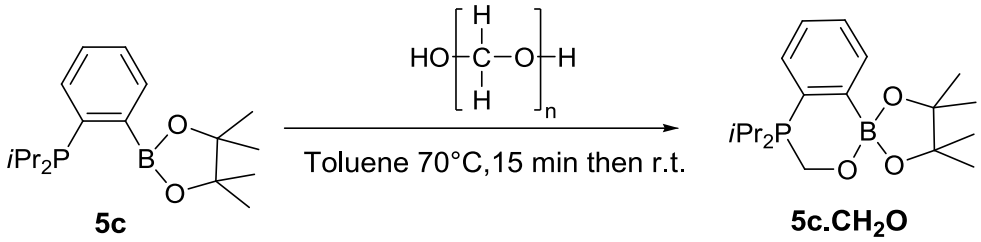

Figure 5-19: Preparation of compound **5c.CH_2O**.

To an excess of paraformaldehyde in toluene (5 mL) was added a solution of **5c** (300 mg, 0.62 mmol) in toluene (5 mL). The reaction mixture was stirred at 70 °C and followed by $^{31}P\{^1H\}$ NMR until the complete conversion. The mixture was then filtrated, and volatiles were removed from supernatant under vacuum. The resulting solid was dissolved in 0.2 mL of dichloromethane and 2 mL of pentane and stored at -80 °C overnight. Compound **5c.CH_2O** was obtained as a white powder after filtration and drying with a yield of 93%. Anal. Calcd. for $C_{19}H_{32}BO_3P$; C, 65.16; H,9.21. Found: C, 65.30; H, 9.46. ^1H NMR(300 MHz, benzene-d_6): 8.57 (dd, $^3J_{H-H}$ = 7.5 Hz, J_{H-P} = 4.5 Hz, 1H), 7.39 (pseudot-t,$^3J_{H-H}$ = 7.5 Hz, $^4J_{H-H}$ = J_{H-P} = 1.2 Hz, 1H), 6.99 (pseudot-dd, $^3J_{H-H}$ = 7.5 Hz, $^4J_{H-H}$ = 1.2 Hz, J_{H-P} = 3.4 Hz, 1H), 6.65 (dd, $^3J_{H-H}$ = 7.5 Hz, J_{H-P} = 10.0 Hz, 1H), 4.75 (d, $^2J_{H-P}$ = 1.5 Hz, 2H, CH_2O), 1.75 (s, 6H, CH_3pin), 1.62 (s, 6H, CH_3pin), 1.53 (septd, 2H, $^3J_{H-H}$ = 7 Hz, $^2J_{H-P}$ = 12.0 Hz, C*H*$(CH_3)_2$), 0.62 (dd, 6H,$^3J_{H-H}$ = 7.0 Hz, J_{H-P} = 16.0 Hz, CH(C*H*$_3)_2$), 0.61 (dd, 6H,$^3J_{H-H}$ = 7.0 Hz, J_{H-P} = 16.0 Hz, CH(C*H*$_3)_2$); $^{13}C\{^1H\}$ NMR (75 MHz, benzene-d_6): 135.3 (d, J_{C-P} = 12.0 Hz, CH_{arom}), 132.1 (d, J_{C-P} = 2.8 Hz, CH_{arom}), 129.0 (d, J_{C-P} = 9.0 Hz, CH_{arom}), 125.5 (d, J_{C-P} = 12.0 Hz, CH_{arom}), 117.7 (d, $^1J_{C-P}$ = 77.3 Hz, C_{arom}), 79.6 (s, 2C, C_{pin}), 53.2 (d, $^1J_{C-P}$ = 45.2 Hz, CH_2O), 27.8 (s, CH_3pin), 27.3 (s, CH_3pin), 21.4 (d, $^2J_{C-P}$ = 39.9 Hz, *C*HCH_3), 16.3 (d, $^3J_{C-P}$ = 3.0 Hz ,CH_3), 15.8 (d, J_{C-P} = 2.0 Hz, CH_3) The quaternary carbon atom connected to the boron atom was not observed; $^{31}P\{^1H\}$ NMR (161 MHz, benzene-d_6): 7.8 (s); $^{11}B\{^1H\}$ NMR (96 MHz, benzene-d_6): 6.0 (s).

5.8.2 Catalytic Reduction of Carbon Dioxide

General procedure for catalytic reduction of carbon dioxide with HBcat as reducing agent at 70 °C:

In a J-Young NMR tube, catecholborane (56.4 µL, 530 µmol) was added to a mixture catalyst (0.6 mL of stock solution at 8.8 mmol/L, 5.3 µmol) and an internal standard of hexamethylbenzene (2 mg, 3.3 g/L) in benzene-d_6. The tube was placed under vacuum in the liquid nitrogen bath during ≈ 10 seconds. Then, the cold bath was removed and the *tube was placed* at room temperature. After ≈ *30 seconds the tube was placed under 1-2 atm of* CO_2. The J-young NMR tube was heated at 70 °C and the catalysis was followed by ^{1}H NMR spectroscopy. ^{1}H NMR (500 MHz, benzene-d_6): 6.9 (m, 2H), 6.7 (m, 2H), 3.37, (s, 3H). δ ^{11}B{^{1}H} (160.46 MHz, benzene-d_6): δ 23.4 (s). ^{13}C{^{1}H} (101 MHz, benzene-d_6)**:** δ 148.5 (s), 122.5 (s), 112.2 (s), 53.1 (s) ppm.

General procedure for catalytic reduction of carbon dioxide with BH_3 as reducing agent at 70 °C:

In a J-Young NMR tube, BH_3•SMe_2 (50 µL, 530 µmol) was added to a mixture of **5b.CH_2O** (0.6 mL of stock solution at 8.8 mmol/L, 5.3 µmol) and an internal standard of hexamethylbenzene (2 mg, 3.3 g/L) in benzene-d_6. The solution was degassed before adding to CO_2: the tube was placed under vacuum in the liquid nitrogen bath during ≈ 10 seconds (to avoid the evaporation of solvent). Then, the cold bath was removed and the *tube was placed* at room temperature. After ≈ *30 seconds the tube was placed under 1-2 atm of* CO_2. The J-young NMR tube was heated at 70 °C and the catalysis was followed by ^{1}H NMR spectroscopy. ^{1}H NMR (500 MHz, benzene-d_6): 3.37, (s, 3H) δ ^{11}B{^{1}H} (160.46 MHz, benzene-d_6): δ 19.1 (s, br). ^{13}C{^{1}H} (101 MHz, benzene-d_6)**:** δ 51.3 (s) ppm.

5.8.3 Computational Details

All the calculations were performed on the full structures of the reported compounds. Calculations were performed with the GAUSSIAN 03 and GAUSSIAN 09 suite of programs. The B3PW91[254,320] functional was used in combination with the 6-31G** basis set for B, C, H, and O atoms[321,322] and the SDD basis set with an additional polarization function (one d function with a 0.34 exponent and a 1.0 contraction coefficient) for the P atom.[323] The transition states were located and confirmed by frequency calculations (single imaginary

frequency). The stationary points were characterized as minima by full vibration frequencies calculations (no imaginary frequency). All geometry optimizations were carried out without any symmetry constraints. The energies were then refined by single point calculations to include dispersion at the B97D/6-31G** level of theory.[324] The energies were further refined by single point calculations to account for solvent effects using the SMD solvation model[325] with benzene. Bond rotations and their associated transition states were not calculated as it is clear that their energy will be much lower than the energy barriers associated with the reduction steps in such a system and are therefore trivial.

ACKNOWLEDGMENTS

This work was supported by the National Sciences and Engineering Research Council of Canada (NSERC, Canada) and the Centre de Catalyse et Chimie Verte (Quebec). M.-A. C., M.-A. L, and N.B. would like to thank NSERC and FQRNT for scholarships. The Centre National de la Recherche Scientifique (CNRS), the Université Paul Sabatier (UPS) and French MESR (PhD grant to R. D.) are acknowledged for financial support of this work.

Supporting Information

Additional DFT information (other calculated reaction pathways, cartesian coordinates, free enthalpies and energies). This material is available free of charge via the Internet at http://pubs.acs.org.

Chapter 6 - Lewis Base Activation of Borane-Dimethyl Sulfide into Strongly Reducing Ion Pairs for the Transformation of Carbon Dioxide to Methoxyboranes

In this chapter, we discuss the reduction of carbon dioxide catalyzed by simple Lewis bases.

6.1 Context of the Research

In the previous chapter, we discussed the development of a highly active ambiphilic catalyst for the reduction of carbon dioxide using hydroboranes, and the thorough investigation of its mode of action. While we revealed a mechanism of action involving formaldehyde, the formaldehyde formation involved the phosphine-borane catalyst. In all cases, a double collaboration of Lewis bases and boranes was found to be a key factor in the reduction of carbon dioxide. Indeed, on one hand, a phosphine moiety of the catalyst binds and activates a reducing hydroboranes. On the other hand, a pending boryl group acts outside of the coordination influence of the phosphine to activate carbon dioxide as a Lewis acid. The formaldehyde-mediated mechanism, while more complex, involves the same type of interactions.

With these results in hand, we decided to study the exact contribution of these two collaborative processes. Namely, we decided to investigate whether either the Lewis acidic activation of carbon dioxide or the Lewis base activation of hydroboranes was sufficient to yield an efficient system for the reduction of carbon dioxide to methanol. Strong Lewis acids had already been used to catalyze the reduction of carbon dioxide by silanes. Indeed it was found that extremely electrophilic silylium cations generated *in situ* by the reaction of an acid with a hydrosilane could bind carbon dioxide and make it prone to reduction. The reaction thus catalyzed was found to suffer from a lack of selectivity, with methane being the major reduction product.

At the start of our research project, it was known that N-heterocyclic carbenes, as strong Lewis bases, were capable of catalyzing the reduction of carbon dioxide to methanol precursors using hydrosilanes as reductants. The catalysts were proposed to bind hydrosilanes and

activate them by making their hydrides more nucleophilic. Along the same lines, this chapter will describe the use of different Lewis bases to activate borane-dimethylsulfide for the reduction of carbon dioxide.

During the redaction of the article, and as has been mentioned in the previous chapter, three metal-free catalytic systems were reported for the reduction of carbon dioxide to methanol using Lewis basic catalysts, which provided insight into the reactivity of boranes that did not previously exist.[310,312,326] These reports show the broad interest given to carbon dioxide reduction in this decade.

6.2 Abstract

The hydroboration of carbon dioxide into methoxyboranes by borane-dimethylsulfide using different base catalysts is described. Non-nucleophilic proton sponge is found to be the most active catalyst, with TOF reaching 64 h^{-1} at 80 °C, and is acting *via* the activation of $BH_3 \bullet SMe_2$ into a boronium-borohydride ion pair.

6.3 Résumé

Ici est décrite La réaction d'hydroboration du dioxide de carbone par le complexe borane-diméthylsulfure catalysée par différentes bases. La molécule non-nucléophile « Proton Sponge » se révèle être le catalyseur le plus actif pour la transformation, avec une fréquence catalytique de 64 h^{-1} à 80 °C. Le mode d'action est postulé être l'activation de $BH_3 \bullet SMe_2$ en une paire d'ions boronium-borohydride.

6.4 Introduction

Due to its availability and its role in climate change, carbon dioxide has attracted considerable interest in recent years. Although several sequestration technologies are known,[327] chemical storage of CO_2 in the form of valuable hydrogen containing molecules, such as methanol, is highly desirable since these chemicals could be a green alternative to fossil fuels, both as a source of organic building blocks and as energy media. [266,327]

Although they are costly and not economically viable for large scale processes, hydroboranes are amongst the most efficient reagents for the catalytic reduction of carbon dioxide to methanol. [63,71,207,265,289,291,310,312,326,328,329] While the hydroboration of C=O bonds is a well-

studied reaction for a large variety of substrates,[330] carbon dioxide remains resistant to uncatalyzed hydroboration by neutral hydroboranes, even when using the most reactive BH_3 adducts. It has been shown that sodium or lithium borohydride can reduce CO_2 with low selectivity to a mixture of formate and methoxy products without the use of a catalyst, illustrating the superior reducing power of these anionic boron hydrides.[331,332] In order to facilitate the reaction of neutral hydroboranes with CO_2, transition metal catalysts have been used to activate the B-H bonds and reduce CO_2 via a hydrometallation reaction.[273,274,333] The most notable example of this type of catalysis is a nickel pincer complex developed by Guan *et al.* that catalyzes the hydroboration of CO_2 to methoxyboranes with a TOF of 495 h^{-1} using HBcat.[273] Recently, Cantat has shown that one of the most reactive boranes, 9-borabicyclo[3.3.1]nonane (9-BBN), can be used as a reductant in the presence of some nitrogen bases to generate methoxyboranes from CO_2.[312] It was proposed that the role of the catalysts was to activate the borane, either in a Frustrated Lewis Pair (FLP) fashion or by the formation of ion pairs. A similar reaction with 9-BBN was also reported using phosphines as catalysts to reduce carbon dioxide into methoxyboranes.[326] However, the most active metal-free organocatalyst to date is a phosphine-borane complex reported by our group that activates borane-dimethylsulfide ($BH_3{\bullet}SMe_2$) and CO_2 to yield methoxyboranes ($(MeOBO)_n$) with a TOF exceeding 900 h^{-1} at 70 °C.[207] The transformation was proposed to occur through simultaneous nucleophilic activation of the borane and electrophilic fixation of carbon dioxide.[317] In such a mechanism, the reductant is made more nucleophilic by receiving electron density from the phosphine moiety. It is important to note that it is one of the only two CO_2 reduction systems reported to use $BH_3{\bullet}SMe_2$ as a hydrogen source, the other being a more recent report by Stephan of an ambiphilic catalyst for the hydroboration of CO_2.[310] BH_3 adducts are by far the most interesting boranes to use, since they have the highest hydrogen content of any hydroboranes in addition of being less expensive than most of them. Their reactivity, however, tends to be limited by its strong tendency to form stable borane adducts with Lewis bases.

6.5 Results and Discussion

In an effort to broaden the scope of $BH_3{\bullet}SMe_2$ as a reducing agent for the functionalization of CO_2, the effect of various commercially available bases on the catalytic activity was studied. We thus decided to monitor by ^1H NMR spectroscopy the reaction between the bases and 25 equiv of $BH_3{\bullet}SMe_2$ under one atm of CO_2 at 80 °C in a J Young NMR tube. The yields were

calculated using the integration of the $(MeOBO)_n$ generated in comparison to the internal standard (hexamethylbenzene) present in the solution. Contrary to the reactivity observed using 9-BBN as a reductant,[326] phosphines (PPh_3, P*t*Bu_3 and PCy_3) proved ineffective for the CO_2 reduction, as they are known to generate stable BH_3•PR_3 adducts.[334] Inorganic bases such as CsF, KCN and $CsCO_3$ also did not have any effect on the reduction of CO_2. However, sodium alkoxides (MeONa, EtONa, and *t*BuONa) proved to convert some of the CO_2 to $(MeOBO)_n$, notably getting up to 3 turn-overs in the first hour of reaction with *t*BuONa (**Table 6-1**, entries 1-3). It is known that the addition of alkoxides to BH_3 leads to the generation of alkoxyborohydrides.[335] These species possess increased nucleophilicity when compared to neutral BH_3 adducts and can disproportionate to give sodium borohydride.[336] The low activity of sodium alkoxides can either be attributed to their low solubility or to the low rate of the disproportion reaction in benzene-d_6. On the other hand, anionic amides (lithium diisopropylamide and lithium dimethylamide) were found to be inactive in the reduction of CO_2.

Several nitrogen Lewis bases also proved to be inefficient under the conditions tested, including triethylamine, diisopropylethylamine, 2,2,6,6-tetramethylpiperidine, pyridine, 4-dimethylaminopyridine, 2,6-lutidine, 4-pyrrolopyridine and 2,6-di*tert*butylpyridine. However, as shown in **Table 6-1**, some species proved to exhibit significant activity in the generation of methoxyboranes.

Table 6-1: Catalytic activity of different bases for the hydroboration of CO_2 by BH_3•SMe_2.

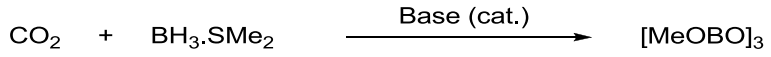

Entry	Base (mol. %)	t(h)	T (°C)	Yield (%) (TON)	TOF
1	MeONa (4)	1	80	1.3 (1)	1
2	EtONa (4)	1	80	2.6 (2)	2
3	^{t}BuONa (4)	1	80	4.0 (3)	3
4	DBU (4)	1	80	23 (17)	17
5	TBD (4)	1	80	25 (19)	19
6	Terpyridine (4)	1	80	47 (35)	35
7	**6** (4)	1	80	68 (51)	51
8[a]	**6** (4)	1	25	4.0 (3)	3
9[a]	**6** (4)	24	25	39 (29)	1
10[a]	**6** (4)	1	80	85 (64)	64
11[a]	**6** (4)	21	80	>99 (75)	4
12[a]	**6** (1)	24	80	7.6 (23)	1
13	**7-BH$_4$** (4)	0.16	25[b]	24 (18)	108
14[a]	**7-BH$_4$** (1)	3	25[b]	21 (62)	62
15[a]	**7-BH$_4$** (1)	24	25	28 (84)	4
16[a]	**7-BH$_4$** (1)	1	80	21 (64)	64
17[a]	**7-BH$_4$** (1)	24	80	25 (75)	3

Conditions: 0.01 mmol of base catalyst in benzene-d_6 (0.4 mL), the number of equivalents of BH_3•SMe_2 was calculated to obtain the desired catalytic loading, 1 atm CO_2. The yield was measured by NMR spectroscopy using hexamethylbenzene as an internal standard. TONs and TOFs are given in regard to the number of hydrides transferred. [a] Solvent = Dichloromethane-d_2. [b] Although the tube was kept at room temperature, the exothermic reaction caused internal heating of the system.

Some reduction products were observed when BH_3•SMe_2 was added to strong Lewis bases, such as DBU (1,8-diazabicycloundec-7-ene) and TBD (triazabicyclo[4.4.0]dec-5-ene), giving

respective TOF of 17 and 19 h^{-1} (**Table 6-1**, entries 4 - 5). However, multidentate amines, such as terpyridine and proton sponge (PS; **6**) gave the best activity, with observed TOF of 35 and 51 h^{-1} when the reaction was carried out at 80 °C in benzene-d_6 (**Table 6-1**, entries 6 - 7). When the reaction was carried out in the presence of **6** as catalyst at ambient temperature a lower activity was observed. The TON and TOF dropped to reach in the best conditions, 29 (**Table 6-1**, entry 9) and 3 h^{-1}, respectively (**Table 6-1**, entry 8). It is good to note that under these conditions **6** did not present any activity in the presence of 9-BBN, as reported by Cantat *et al.*[312] Running the reaction in dichloromethane-d_2 (**Table 6-1**, entry 10) did increase the TON (64) and the TOF of the reaction (64 h^{-1}), presumably by increasing the solubility of the reaction intermediates (*vide infra*). Letting the reaction run for a longer time period allowed for complete conversion of the BH_3•SMe_2 (**Table 6-1**, entry 11).

In order to shed light on the mode of activation of BH_3 by bidentate ligands, the reaction was studied using **6** since it proved to be the most active catalyst. This exceptionally basic amine is thus called because of its almost exclusive affinity for protons, a result of the unique steric environment around its nitrogen atoms which prevents the coordination of larger electrophiles. The notable exceptions include the fixation of a handful of boron cations,[198,337–343] as well as two transition metal complexes and group XIII species.[344–346] **6** was reported to react rapidly with B_2H_6 or boron trifluoride gas to afford species identified as $[PS(BX_2)]^+[BX_4]^-$ (X = H, F)[338] or $[PS(BH_2)]^+[B_2H_7]^-$,[339] but were not structurally characterized. These species are reminiscent of the "diammonia of diborane" that was proposed as a key intermediate in the deshydrogenation of ammonia-borane.[340–342] Interestingly, Vedejs and coworkers were able to prepare a 9-BBN derived PS stabilized boronium by a more aggressive method.[198] The cation thus formed was found to be a highly reactive electrophile, contrary to classical boronium cations. This property was proposed to arise from the steric demands of the proton sponge framework. It is important to note that no catalytic activity was ever reported for these species.

The hydroboration of CO_2 using BH_3•SMe_2 was very slow when catalyzed by **6** at room temperature in benzene-d_6. However, a solution of BH_3•SMe_2 and 1 heated to 70 °C for an hour in the absence of CO_2 was found to react rapidly and exothermically upon exposure to CO_2 at room temperature. These observations suggest that a reaction between **6** and BH_3•SMe_2 is the limiting step in the catalytic transformation. It was possible to isolate single crystals from a reaction mixture between **6**, 50 equiv of BH_3•SMe_2 and CO_2. Although the

limited solubility prevented NMR characterization, the solid state structure consisted of the boronium salt $[PS(BH_2)]_2[B_{12}H_{12}]$ (**7-$B_{12}H_{12}$**) (**Figure 6-1***).* the resolved solid state structure of the boronium cation is similar to a previously reported structure of $[PS(BH_2)][B_{19}H_{22}]$.[343] Since the $B_{12}H_{12}^{2-}$ dianion is generally isolated as a product of the disproportionation of $[B_3H_8]^-$, which is prepared in oxidative conditions from BH_4^-,[347] it could be suggested that the initial step in the catalytic transformation involves the generation of the ion pair $[PS(BH_2)][BH_4]$ (**7-BH_4**).

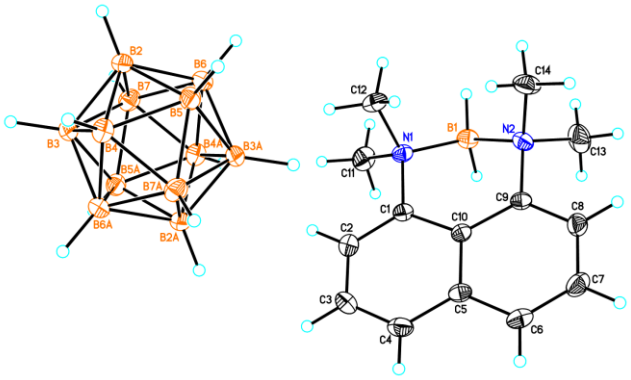

Figure 6-1: The ORTEP plot of $[PS(BH_2)]_2[B_{12}H_{12}]$ (**7-$B_{12}H_{12}$**) with thermal ellipsoids set at the 40% probability level. Selected bond lengths (Å) and angles (°): N1-B1: 1.601(2), N1-C1: 1.511(2), N2-B1: 1.600(2), N1-B1-N2: 111.62(13), C1-C10-C9: 126.11(15), C1-N1-B1: 111.07(12), C9-N2-B1: 111.07(13).

In order to better understand the reaction between **6** and $BH_3{\bullet}SMe_2$, the products formed were characterized using ^{11}B NMR spectroscopy while controlling the stoichiometry of the reagents. Over the course of the reaction, three different boronium salts were observed, depending on the reaction conditions. In all cases, the formation of the dihydroboronium cation is supported by ^1H NMR by a significant downfield shift for the proton sponge resonances to a doublet of doublets at 7.78 ppm (J = 8 Hz) and two doublets at 8.23 and 8.08 ppm (J = 8 Hz) in dichloromethane-d_2, with a slight variation on the chemical shift depending on the counterion (see Supporting Info). Although the resonances of the $[BH_2]^+$ were not observed by ^1H NMR spectroscopy, the ^{11}B NMR spectra of derivatives of **7** did show a broad resonance at *ca* 1.5 ppm, which is similar to that of previously reported $[PS(BH_2)][B_2H_7]$.[339] Stirring **6** in diethyl ether with 2 equiv of $BH_3{\bullet}SMe_2$ for 16 hours allowed us to obtain colourless crystals. ^{11}B NMR spectroscopy for this compound showed, in addition to the resonance at 1.57 ppm for the borenium species $[PS(BH_2)]^+$, a sharp quintuplet at -38.4 ppm due to the $[BH_4]^-$ anion. The latter was confirmed by observation of a sharp 4-line ^1H NMR resonance at δ -0.06 (**Figure 6-2**).

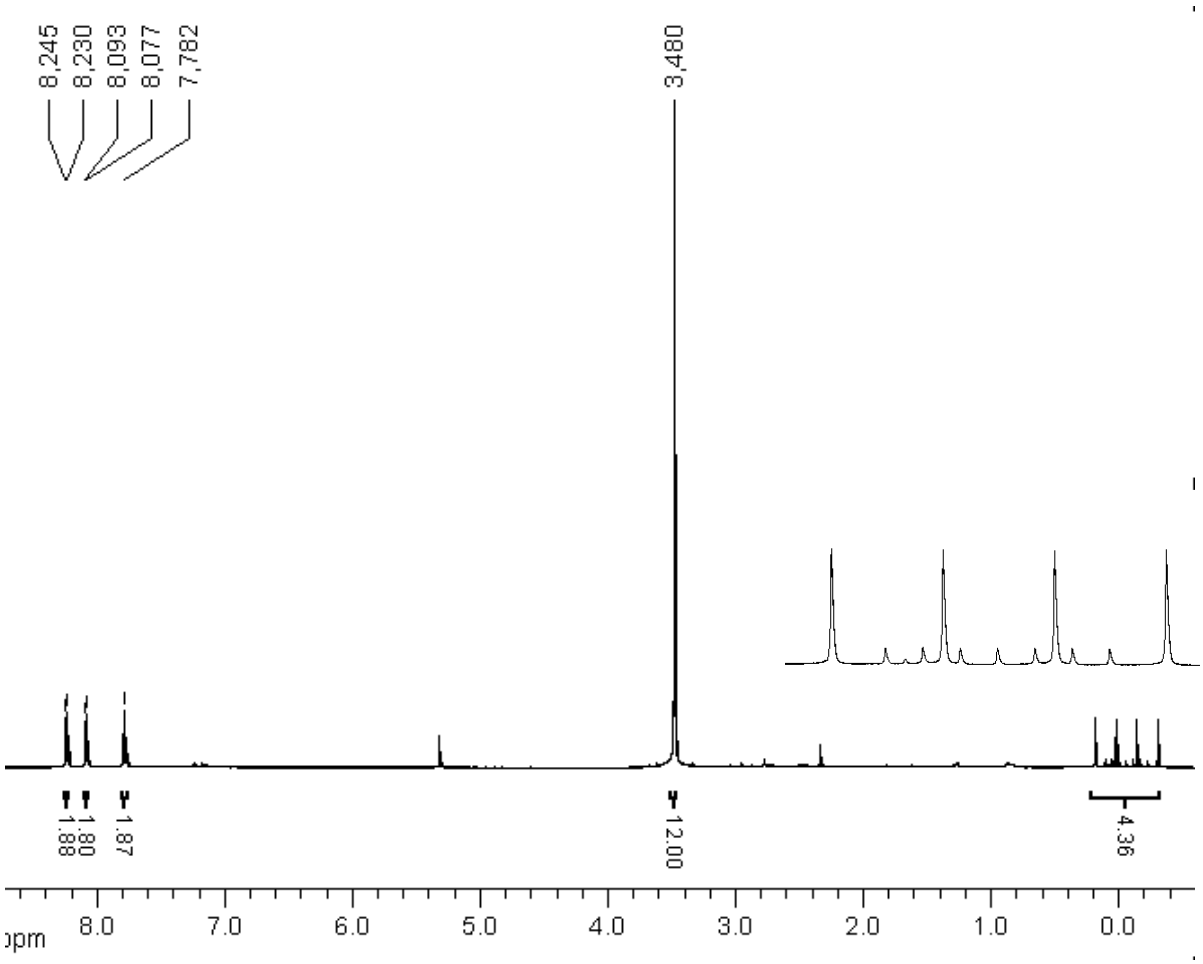

Figure 6-2: ^{1}H NMR Spectrum of **7-BH_4** displaying the characteristic quadruplet of a soluble BH_4^- anion.

These spectroscopic findings strongly suggest the presence of the $[BH_4]^-$ anion and the formation of salt **7-BH_4** ($[PS(BH_2)][BH_4]$). However, using 10 equiv of $BH_3{\bullet}SMe_2$ in presence of **6** in toluene afforded $[PS(BH_2)][B_3H_8]$ (**7-B_3H_8**) as the main product (**Figure 6-3**) after heating. The $[B_3H_8]^-$ anion was characterized by the presence of a nonuplet at -30.0 ppm in the ^{11}B NMR spectrum.[348]

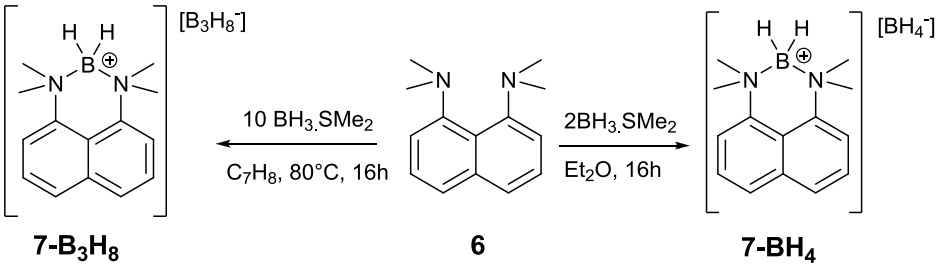

Figure 6-3: Reaction of PS with BH_3•SMe_2 to give boronium salts.

Altough the $[B_{12}H_{12}]^-$ anion could not be observed by NMR spectroscopy, the crystallization of all samples of $[PS(BH_2)][B_3H_8]$ consistently yielded **7-$B_{12}H_{12}$**. It is rational to propose that initial activation of BH_3•SMe_2 by proton sponge affords the ion pair **7-BH_4**, which can degrade to **7-B_3H_8** by reaction with BH_3•SMe_2 and to **7-$B_{12}H_{12}$**. The activity of these compounds was studied by treating them with an atmosphere of carbon dioxide. In this manner, $[PS(BH_2)][B_3H_8]$ was found to be unreactive towards CO_2. Unsurprisingly, a dichloromethane-d^2 solution of **7-BH_4** in the absence of additional boranes reacted instantaneously at room temperature with carbon dioxide. Within five minutes, two different signals appeared in the ^{1}H NMR spectrum at 8.27 and 8.33 ppm, assigned to the formation of formate products, along with the complete disappearance of the BH_4^- resonances. No products of higher reduction level were observed in this manner, suggesting that the catalyst is only active in the reduction of carbon dioxide. Similarly, a solution of **7-BH_4** and 25 equiv of BH_3•SMe_2 reacted within minutes with carbon dioxide to give methoxyboranes at room temperature (**Table 6-1**, entry 13). The heat produced by the exothermic hydroboration of carbon dioxide likely contributed to the increase in catalytic activity, obtaining a TOF of 108 h^{-1}. However, when looking at its reactivity at 80 °C or for a longer time period, the catalytic activity **7-BH_4** was found to be similar to that of **6** (**Table 6-1**, entries 14-17).

From these observations, it is possible to propose a catalytic cycle, as shown in **Figure 6-4**. In a first step that is rate-limiting, the bidentate ligand activates borane-dimethylsulfide to generate a highly reactive boronium-borohydride ion pair. Similar boronium species has been synthesized with TBD,[349] but under catalytic conditions, thus explaining the need for higher reaction temperature in order to achieve the catalytic reduction of CO_2 since no activity was observed between DBU and TBD in presence of BH_3•SMe_2 at 25 °C.[310] The $[BH_4]^-$ generated can in turn react with carbon dioxide to give formate derivatives. The formate generated can abstract the BH_2^+ fragment generating reduced species such as $HCOOBH_2$. In turn, BH_3•SMe_2

can very efficiently reduce formatoboranes into $(MeOBO)_n$, thus explaining the highest TOF obtained using $BH_3{\bullet}SMe_2$ instead of other organic hydroboranes.

In summary, the use of $BH_3{\bullet}SMe_2$ as a reducing agent for CO_2 hydroboration is possible in the presence of strong Lewis bases. Although limited activity is observed with monodentate species such as DBU and TMP, bidentate amines such as proton sponge proved to be the active catalysts in this reaction. It was possible to isolate single crystals that demonstrated the presence of the boronium species $[PS(BH_2)]^+$. ^{11}B NMR studies demonstrate that the most likely active species for the CO_2 reduction into formates was the borate ion, BH_4^-, whereas the $BH_3{\bullet}SMe_2$ in solution can reduce the formatoborane derivatives into methoxyboranes. Optimization of this system is currently underway.

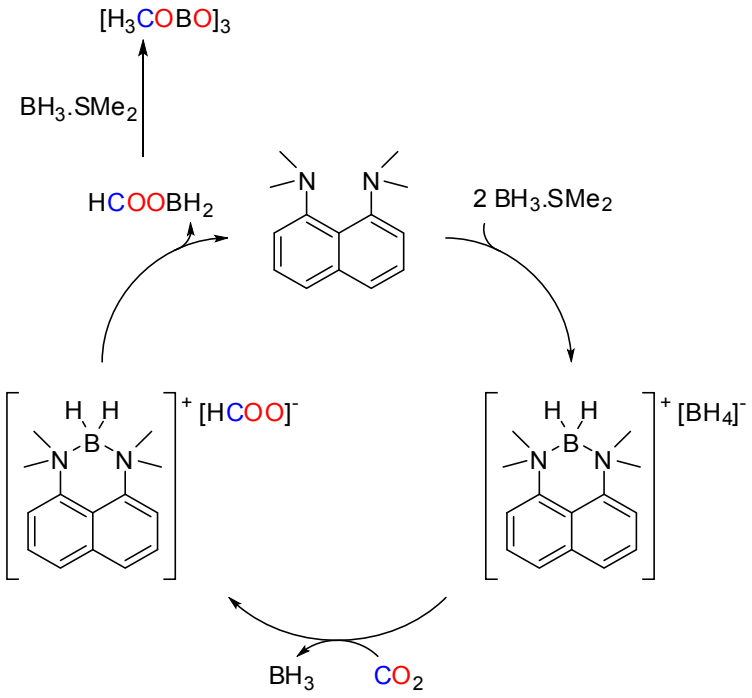

Figure 6-4: Proposed mechanism for the reduction of CO_2 to methoxyboranes catalyzed by **6**.

6.6 Experimental Details

General Procedures: Unless otherwise specified, manipulations were carried out under an atmosphere of dinitrogen, using standard glovebox and Schlenk techniques. Catalytic reactions were carried out in a sealed J-Young NMR tube, in which case NMR conversions are indicated, or in standard flame-dried Schlenk glassware. All solvents were distilled from

Na/benzophenone, benzene-d_6 was purified by vacuum distillation from Na/K alloy, dichloromethane-d_2 was dried over 4Å Molecular sieves. Proton sponge, DBU, TBD, terpyridine and borane-dimethylsulfide were purchased from Sigma-Aldrich and used as provided.

NMR spectra were recorded on an Agilent Technologies NMR spectrometer at 500 MHz (^{1}H), 125.76 MHz (^{13}C), 202.46 MHz (^{31}P), 160.46 MHz (^{11}B), and on a Varian Inova NMR AS400 spectrometer, at 400.0 MHz (^{1}H), 100.58 MHz (^{13}C), 161.92 MHz (^{31}P). ^{1}H NMR and ^{13}C{^{1}H} NMR chemical shifts are referenced to residual protons or carbons in deuterated solvent. ^{11}B{^{1}H} was calibrated using an external reference of $B(OMe)_3$ (set at +18.1 relative to BF_3 etherate solution). Multiplicities are reported as singlet (s), broad signal (br) doublet (d), triplet (t), quadruplet (q), quintuplet (qt) nontuplet (n), multiplet (m). Chemical shifts are reported in ppm.

6.6.1 General Method for the Hydroboration of Carbon Dioxide

0.01 mmol of base catalyst was dissolved in *ca.* 0.4 mL of benzene-d_6 or dichloromethane-d_2 containing an internal standard of hexamethylbenzene. The BH_3•SMe_2 was added to the solution and the mixture was introduced in a J-Young NMR tube. The J-young NMR tube was frozen in a liquid nitrogen bath and its atmosphere was removed under vacuum after which the headspace was filled with CO_2. The reaction was then followed by NMR spectroscopy. Yields are reported using ^{1}H NMR spectroscopy according to the integration of the $[MeOBO]_n$ moieties at 3.36 ppm and compared to that of the internal standard.

6.6.2 Synthesis and Characterization of Boronium Salts

[PS(BH$_2$)][BH$_4$] (7-BH$_4$). 300 mg of proton sponge (1.40 mmol) were dissolved in 20 mL of diethylether. To this solution was added 0.3 mL (3.1 mmol) of BH_3•SMe_2. The resulting mixture was stirred for 16 hours at room temperature after which the volatiles were removed *in vacuo* to afford colourless crystals, which were rinsed with hexanes. 291 mg (86%) of **7-BH$_4$** were collected in this manner. The spectral data are consistent with those of the $[PS(BH_2)]^+$ and $[BH_4]^-$ which were reported previously.[339] ^{1}H NMR (500 MHz, dichloromethane-d_2): 8.23 (d, 2H, $^{1}J_{H-H}$ = 7.7 Hz, *p*-PS), 8.08 (d, 2H, $^{1}J_{H-H}$ = 8.4 Hz, *o*-PS), 7.78 (dd, 2H, $^{1}J_{H-H}$ = *ca* 8 Hz, *m*-PS), 3.48 (s, 12H, NMe_2), -0.06 (q, 4H, $^{1}J_{B-H}$ = 81.4 Hz, BH_4), the BH_2 was not located; ^{13}C{^{1}H} (101 MHz, dichloromethane-d_2): 140.2 (s, C_{quat}), 135.8 (s, C_{quat}), 130.9 (s, *o*-PS), 127.5 (s, *p*-

PS), 121.3 (s, *m*-PS), 56.5 (s, NMe_2), one quaternary signal was not located; ^{11}B (160.46 MHz, dichloromethane-d_2): 1.7 (br , BH_2), -38.4 (qt, $^1J_{B-H}$ = 81.4 Hz, BH_4).

[PS(BH$_2$)][B$_3$H$_8$] (7-B$_3$H$_8$). 300 mg of proton sponge (1.40 mmol) were dissolved in 30 mL of toluene. To this solution was added 1.3 mL (14 mmol) of BH_3•SMe_2. The resulting mixture was stirred for 16 hours at 80 °C. The resulting yellow suspension was filtered and the residue was rinsed twice with toluene to afford a yellow powder (194 mg. (52%). The spectral data are consistent with those of the $[PS(BH_2)]^+$ and $[BH_4]^-$ which were reported previously.[348] ^1H NMR: (400 MHz, dichloromethane-d_2): 8.11 (d, 2H, $^1J_{H-H}$ = 8.2 Hz, *p*-PS), 8.03 (d, 2H, $^1J_{H-H}$ = 7.8 Hz, *o*-PS), 7.79 (dd, 2H, $^1J_{H-H}$ = *ca* 8 Hz, *m*-PS), 3.48 (s, 12H, NMe_2), 0.17 (br m, B_3H_8); $^{13}C\{^1H\}$ (101 MHz, dichloromethane-d_2): 140.1 (s, C_{quat}), 136.0 (s, C_{quat}), 131.2 (s, *o*-PS), 127.5 (s, *p*-PS), 120.7 (s, *m*-PS), 56.5 (s, NMe_2), one quaternary signal was not located; ^{11}B (160.46 MHz, dichloromethane-d_2): 1.5 (br m , BH_2), -30.0 (n, $^1J_{B-H}$ = 81.4 Hz, B_3H_8).

(PS(BH$_2$)])$_2$[B$_{12}$H$_{12}$] (7-B$_{12}$H$_{12}$). 2.1 mg (0.01 mmol) of proton sponge was dissolved with 38 mg (50 equiv, 0.5 mmol) of BH_3•SMe_2 in benzene-d_6 and transferred to a J-Young NMR tube. The tube was frozen in liquid nitrogen and put under vacuum. Its atmosphere was then replaced with carbon dioxide. The reaction mixture was heated at 70 °C for 20 hours. A single crop of crystals suitable for X-ray diffraction study was collected at the bottom of the tube at the end of the reaction.

ACKOWLEDGEMENTS

The authors would like to acknowledge National Sciences and Engineering Research Council of Canada (NSERC, Canada) and the Centre de Catalyse et Chimie Verte (Quebec) for financial support. M.-A. C. and M.-A. L. would like to thank NSERC and FQRNT for scholarships. We acknowledge W. Bi for the resolution of the crystal structure.

Supplementary Information Avaible:

Electronic Supplementary Information (ESI) available: Solution NMR data and crystallographic information. See DOI: 10.1039/C4CC04857A

6.7 Conclusion and Perspectives

Thus, Lewis base activation is shown to enable reduction of carbon dioxide by borane-dimethylsufide to methoxy products. Interestingly, and in contrast to reported reduction of ketones, alkali metal alkoxides are shown to be poor catalysts for the reduction of carbon dioxide. On the other hand, neutral nitrogen bases are able to provide the necessary electron density to borane dimethylsulfide and sufficiently increase its nucleophilicity to enable the reduction of carbon dioxide. With strong bases such as amidines and guanidines, TOFs can reach $17h^{-1}$ and $19h^{-1}$, respectively.

While it is interesting that such activity can be obtained, these results rather highlight the superiority of dual acid-base cooperation that is at the core of the phosphine-borane catalyzed reduction of carbon dioxide discussed in the previous chapter. Indeed, the TOF of 873 h^{-1} reported for the ambiphilic catalyst is an order magnitude higher than that of simple base catalysis. It continues to show the potential of Frustrated Lewis Pairs as the unquenched collaborative combination of an acid and a base to easily perform difficult reactions in mild conditions. In fact, while strong bases give moderate activity, as shown in this chapter, weak ones will outperform them if combined with suitable unquenched boryl moieties.

We have also identified the superior activity of bidentate bases, which allows us to propose a different mechanism of activation of borane-dimethylsufide. In this mechanism, the Lewis base forces the displacement of a hydride from BH_3 that is bound by another to form the BH_4^- borohydride. This strong reducing agent can rapidly reduce carbon dioxide at room temperature. In a way, this reaction can be seen as a *hydride activation* of BH_3•SMe_2. The hydride involved is a strong base that strongly binds to BH_3 and makes the resulting tetravalent boron species extremely nucleophilic. The displacement of a hydride can be rationalized on thermodynamic grounds when considering the enthalpy effect of the net formation of two strong N-B bonds and the entropic gain associated with the displacement of two SMe_2 bonds in the binding of BH_3 to rigid bidentate bases.

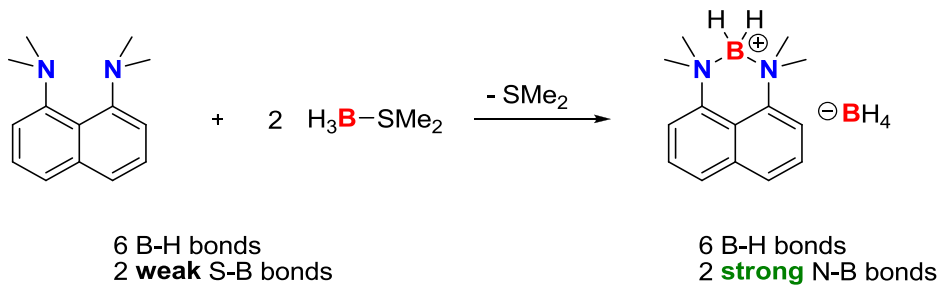

Figure 6-5: Representation of the reaction of **6** with BH_3•SMe_2 with emphasis on the breaking and forming of bonds.

In combination with our ambiphilic catalyst, these results constitute our group's contribution to the reduction of carbon dioxide using hydroboranes. While the topic was of great interest at the time of the beginning of our research program, our results have contributed to demonstrate the main mechanisms by which hydroboranes could be activated to perform the hydroboration of carbon dioxide. Our report that simple Lewis bases can activate BH_3•SMe_2 to form the BH_4 anion has prompted additional research in its use for the reduction carbon dioxide and new studies have been developed for the borane reduction of carbon dioxide using BH_4^-. While the efficiency of BH_4^- does not compete with ambiphilic catalysis for the reduction of carbon dioxide, it reveals the strongly electrophilic character of carbon dioxide in its reduction chemistry.

The reality of the high costs of hydroboranes and the commercial unviability of using them as stoichiometric reductants for carbon dioxide remains, however. As the fundamental aspects of hydroboranes reduction reactions are being uncovered, the amount of research aimed at the reduction of carbon dioxide using boranes understandably diminishes. While new systems continue to be reported, cutting-edge research is more and more directed towards the use of inexpensive silanes and molecular hydrogen for the reduction of CO_2. We estimate that our work on hydroboranes and carbon dioxide chemistry has contributed to the collective understanding of their reactivity to reach its current state. While the decline of interest in hydroboration of carbon dioxide in the last year cannot be denied, we believe it comes about because of advancement in the fundamental knowledge of the field rather than because of the nature of the reaction.

Our group has also begun to focus its efforts towards the use of silanes of hydrosilanes and molecular hydrogen for the reduction of carbon dioxide. As such, conform to a proposition from the author of this dissertation, we have shown that strong phosphazene organobases

can activate silanes for the reduction of carbon dioxide. The mechanism is proposed to involve Lewis base activation of the silane by the catalyst, enabling the nucleophilic reduction of carbon dioxide with a TOF of 32 h^{-1}.[350] This study has also highlighted the important role of dimethylformamide as a solvent for silane reduction of carbon dioxide. Conform to the high rates of reaction observed with ambiphilic catalyst coming from the intramolecular activation of carbon dioxide, a logical next step to this study would consist of investigating ambiphilic phosphazene catalysts.

We have also recently reported a new system for the hydrogenation of carbon dioxide. Our findings show that the compound phenylene-bridged NMe_2-BAr_2 (Ar = 1,2,4-trimethylphenyl) reacts with molecular hydrogen and carbon dioxide to give a mixture of acetals, methoxides and formates. The main product could be identified as an acetal compound of the ambiphilic compound (**Figure 6-6**).[351]

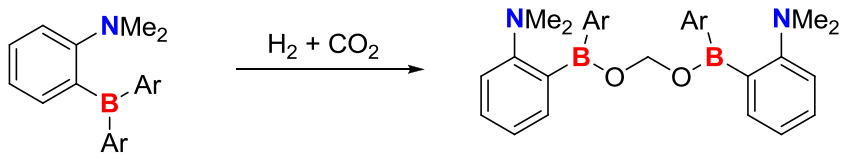

Figure 6-6: Stoichiometric hydrogenation of CO_2 using an amine-borane FLP system.

This hydrogenation reaction is stoichiometric in FLPs. This fact highlights one of the main challenges regarding FLP mediated hydrogenation of carbon dioxide: typical Lewis acids from the main group are highly oxophilic and cannot release the CO_2 reduction products.

In summary of the previous two chapters, we have developed a range of new systems for the reduction of carbon dioxide that rely on the cooperation between Lewis bases and boron-containing molecules. Ambiphilic molecules in combination with hydroboranes are found to give the best catalytic efficiency and durability, illustrating the potential of FLPs to challenge the hegemony of transition metal catalysis.

The fundamental understanding of the reactivity of hydroboranes is beginning to be adapted in our group to hydrogen and silane chemistry as new catalytic and stoichiometric systems are developed.

Chapter 7 - Metal-Free Catalytic C-H bond Activation and Borylation of Heteroarenes

In the two previous chapters, we have shown that organocatalysts and ambiphilic molecules can emulate and even surpass the activity of transition metal catalysts for reactions involving hydroboranes, such as the reduction of carbon dioxide to methanol derivatives. In the following chapter, we present a part of our work which is aimed at one of the most challenging problems of modern synthetic chemistry: the activation and selective functionalization of organic C-H bonds.

In the present chapter, we describe the approach that used applied in the search for novel C-H activation modes. This description serves as an introduction to the last section of the chapter in which we will discuss results we have obtained in the catalytic functionalization of heteroaryl C-H bonds.

7.1 Objectives and Strategy

Motivated by our interest to emulate the reactivity of precious metal complexes using inexpensive and environmentally benign metal-free systems, we decided to investigate the potential of organoboron compounds for C-H activation. Indeed, as repeatedly demonstrated, the collaborative action of boron products with Lewis bases enables a rich range of elegant reactivity. One of the most exciting expression of this cooperation is found in the FLP activation of molecular hydrogen, in which a formal four-electron process can be performed by the combination of an acid and a Lewis base for the heterolytic cleavage of a relatively inert molecule.

While the splitting of H_2 is of great interest in its own right, the infinite synthetic possibilities represented by C-H activation appeared to us as a potentially revolutionary application of simple FLP organocatalysts.[40,44,63,317,352] In fact, instead of H_2, FLPs seem perfectly fitted to activate polar bonds in a four-electron process (**Figure 7-1**).

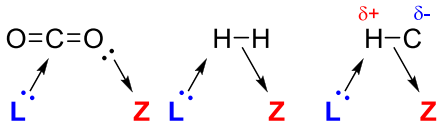

Figure 7-1: Analogy between the FLP binding of CO_2 and the cleavage of H_2 and of C-H bonds. The arrows represent electron transfers.

In fact, we acknowledged the already discovered reactivity of FLP systems with alkynes that has been described above. This interesting activation consists of the heterolytic cleavage of the C-H bond of terminal alkynes. However, presumably because of the well-known reactivity of alkynes, the heterolytic splitting by FLPs was not recognized as a promising avenue for general C-H bond activation. Furthermore, no catalytic process involving the FLP cleavage of alkynes has been hitherto reported. However, alkynes are related to arenes, which are very important substrates for C-H functionalization applications in synthetic chemistry. Both classes of molecule possess a nucleophilic π-electron density that can coordinate electrophiles. While aryl C-H bonds have never been selectively functionalized using FLP protocols, they are known to react stoichiometrically with electrophiles such as Friedel-Crafts intermediate[33] and even borenium ions.[195–198]

Inspired by the possibilities offered by boron chemistry in the field of C-H bond activation, we instigated a research program focused on three main axes:

1) Computational identification of suitable FLP systems for the cleavage of aryl C-H bonds.
2) Construction of a molecular framework allowing the confirmation of the C-H bond cleavage.
3) Design of a FLP system capable of catalytic functionalization of arenes.

These goals keep as a priority the advancement of knowledge regarding boron species and their potential applications in modern synthesis. Frustrated Lewis Pairs will possibly become a major paradigm in future green chemistry, and systematic investigation of their chemistry is of prime importance for the understanding of organic chemistry as a whole.

7.1.1 Computational Identification of Suitable FLP Systems for the Cleavage of Aromatic C-H Bonds

The first step of our research program relied on the rational design and computational evaluation of different Frustrated Lewis Pairs. Our goal was to determine both the kinetics and thermodynamics of a C-H bond cleavage by Frustrated Lewis Pairs. Any given reaction step is comprised of a starting structure, a transition state, and a final structure. Computational calculations based on the density functional theory (DFT) allow efficient and accurate modeling of these structures and of their relative energies.[353] As such, DFT calculations, at the ωB97xd/6-31G** level,[321,322,354] were deemed a suitable tool to predict the reactivity of different FLP systems towards C-H bonds.

In terms of FLP design, we considered ambiphilic molecules, i.e. intramolecular FLPs in which both the Lewis acid and the base are included in the same molecule but remain unquenched due to steric and geometric constraints. Suitably constructed ambiphilic molecules can interact with substrates without the entropic cost associated with intermolecular FLPs.

More specifically, we decided to explore the chemistry of phenylene-bridged phosphine- and amine-boranes. The former have already been extensively studied by our group as catalysts for the reduction of carbon dioxide, as was presented earlier.[200,207,317] The latter have been shown to possess remarkable qualities as hydrogenation catalysts by Repo and coworkers.[62,351] The arene linker between boron and the Lewis base moiety provides remarkable stability to the ambiphilic molecule, as well as excellent geometrical features for the FLP to remain unquenched and possess the right geometry to interact with substrates.[318,355]

As mentioned previously, ambiphilic molecules often exist in two forms. One of them, that is often the ground-state, features an intramolecular interaction between the acid and the base that effectually quenches the acidity and the basicity of the pair. Fortunately, in FLPs, the strength of this interaction is reduced by the geometric constraints of the backbone and the steric features of the active sites, making the active “open form“ thermodynamically accessible.[44,351,356] The strength of the intramolecular adduct will depend on many factors, such as the nature of the linker, the respective acidity, and basicity of the active groups and their steric bulk. Nevertheless, it is of prime importance to accurately represent the real ground-state of a molecule when performing energy calculations. For this reason, in the

following study, we have optimized the structures of both open and closed forms of each FLP. In order to present accurate energy profiles, the energy of the ground state of the reagent is presented, unless stated otherwise.

With these concerns in mind, our first priority was to determine the thermodynamics of the aryl C-H bond cleavage reaction by intramolecular FLPs. For this purpose, we modeled the species involved in the simple C-H bond cleavage reaction of benzene and thiophene (position 2) and calculated the energy change in the process. Results are presented in **Table 7-1** and are compared with analogous calculations performed on the C-H bond activation of phenylacetylene. Indeed, while the aryl C-H bond cleavage was yet unreported, the activation of terminal alkynes by FLPs is a well-known reaction that is exergonic in many cases.

Table 7-1: Enthalpies and Gibbs free Energies (kcal.mol^{-1}) of C-H bond cleavage of phenylacetylene, thiophene (position 2), benzene by phenylene-bridged ambiphilic molecules as calculated by DFT at the ωB97xd/6-31G** level.

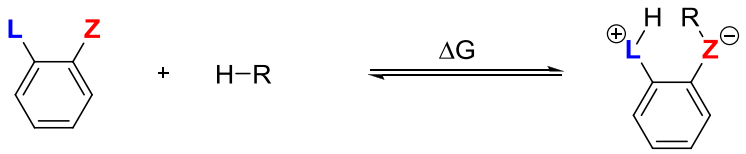

cat = catechol
Fpin = perfluoropinacol
Scat = thiocatechol

ox = oxalato

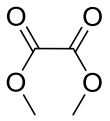

thio = 2-thienyl

		Phenylacetylene		Thiophene		Benzene	
L	**Z**	ΔH	ΔG	ΔH	**ΔG**	ΔH	ΔG
PMe_2	BMe_2	-2.8	10.0	8.3	**22.5**	12.9	27.7
NMe_2	BMe_2	-6.7	4.8	1.4	**14.7**	6.9	20.6
NMe_2	$B(OMe)_2$	-4.7	7.3	3.7	**17.9**	6.8	21.8
NMe_2	Bcat	3.2	15.9	8.4	**21.6**	9.5	22.8
NMe_2	BScat	0.1	11.5	6.3	**19.8**	10.5	24.1
NMe_2	BFpin	-6.5	9.0	-0.9	**12.3**	2.1	15.1
NMe_2	Box	-11.3	0.3	-6.1	**6.0**	-3.1	9.0
NMe_2	Box*	-13.0	-0.6	-7.8	**5.1**	-4.8	8.1
NMe_2	BPh_2	-12.4	-0.4	-0.6	**13.5**	4.1	18.1
NMe_2	B(H)Ph	-12.7	-0.3	-1.0	**10.7**		
NMe_2	Bthio	-11.3	0.8	-1.1	**12.0**	4.2	18.2
NMe_2	B(h)thio	-12.4	-0.1	-1.4	**10.3**		
NMe_2	$B(C_6F_5)_2$	-15.5	-3.4	-3.8	**9.1**	-0.4	12.7
NMe_2	BH_2	-12.3	-1.4	-3.6	**7.9**	1.6	13.5
NMe_2	BH_2*	-18.5	-6.3	-9.8	**3.1**	-4.5	8.7
NMe_2	BCl_2	-12.7	-1.5	-7.1	**5.6**	-4.1	8.7

*The open form of the FLP was used as a reference.

Taking a first look at these results, we see that phenylacetylene can indeed be cleaved by FLPs. In many cases in which the ambiphilic molecules featuring a strongly acidic boron center, the reaction was found to be exergonic. In contrast, in the case of weakly acidic boronates, and alkoxyboryl groups, the C-H bond cleavage is unsurprisingly endergonic. We also see that, for the same acidic partner, a phosphine moiety does not stabilize the C-H

activation product as much as a nitrogen base. This can be rationalized by the larger orbitals of phosphorus which will favor intramolecular interactions with boron despite the geometric constraints imposed by the backbone. Phosphines are also known to be poorer Brønsted-Lowry bases, forming weaker bonds with the small and hard H^+ present in the C-H bond activation.

Looking now at thiophene and benzene, we find that, in all cases, the FLP cleavage of their C-H bond is endergonic, with benzene activation being less stable than those of the more nucleophilic thiophene. These results are hardly surprising, considering that FLP-mediated C-H bond activation has never been observed for these species. Some trends can however be rationalized when considering the results.

1) More acidic boron centers favor the C-H bond cleavage.
2) Steric bulk at boron disfavors the reaction.

Indeed, the small and strongly acidic dichloroboryl group gives the most stable C-H activation products, along with dihydridoboryl and oxalatoboryl. Bulkier bis(pentafluorophenyl)boryl, by contrast, is less apt to the aryl C-H bond cleavage, despite being better for the activation of phenylacetylene and molecular hydrogen.[62]

This effect of the steric bulk, however, is not straight-forward. On the one hand, smaller acid fragments will maximize the access of the aryl group to the boron site and favor activation. On the other hand, unencumbered acids will not be protected against intramolecular deactivation. As can be seen in **Table 7-1**, the NMe_2-BH_2 FLP would be one of the best systems for C-H activation from its open form. However, the inactive closed form lies a full 4.8 kcal.mol^{-1} lower.

With the establishment that the C-H bond cleavage of thiophene and benzene is endergonic for phenylene-bridged FLP molecules, we investigated the kinetics of the reaction. In fact, we modelled the transition state of the C-H bond cleavage of thiophene, with its energy corresponding to the activation barrier of the reaction. For comparison, we also modelled the transition states for phenylacetylene for a few key systems (**Table 7-2**).[357]

Table 7-2: Enthalpies and Gibbs free energies (kcal.mol^{-1}) of the transition state of the C-H bond cleavage of phenylacetylene and thiophene (position 2) by phenylene-bridged ambiphilic molecules as calculated by DFT at the ωB97xd/6-31G** level.

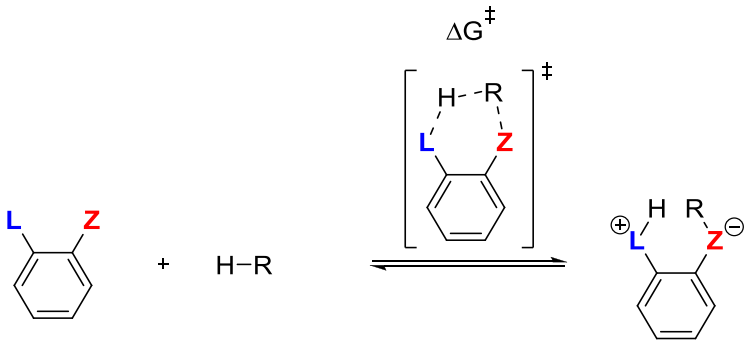

		Phenylacetylene		Thiophene	
L	**Z**	**ΔH‡**	**ΔG‡**	**ΔH‡**	**ΔG‡**
PMe_2	BMe_2	10.0	24.2	16.2	30.3
NMe_2	BMe_2	6.5	19.1	11.4	25.0
NMe_2	Bcat			16.0	30.6
NMe_2	BScat			16.1	31.0
NMe_2	BpinF			12.9	28.0
NMe_2	Box	3.1	16.0	7.1	**20.9**
NMe_2	Box*	1.4	15.1	5.4	**20.0**
NMe_2	BPh_2	2.1	15.3	11.0	24.9
NMe_2	B(H)Ph			9.5	23.0
NMe_2	Bthio			11.6	25.5
NMe_2	B(h)thio			9.5	22.7
NMe_2	$B(C_6F_5)_2$			7.1	**21.1**
NMe_2	BH_2	4.2	16.4	8.2	**21.1**
NMe_2	BH_2*	-1.9	11.5	2.1	**16.3**
NMe_2	BCl_2			8.9	22.9

*The open form of the FLP was used as zero-point energy reference.

Interestingly, these results (**Table 7-2**) for the activation barrier follow trends similar to those of the thermodynamic aspect of the reaction. Once again, we find that phenylacetylene is much easier to activate. Also, the more acidic boryl moieties are once again found to be those that favor C-H bond cleavage with energy barriers that are quite accessible. $B(C_6F_5)_2$, Box and BH_2 are, once again, found to be the best groups for C-H bond activation. In fact, these calculations reveal that the problem of C-H bond cleavage by FLP systems does not come from kinetic difficulties of C-H activation, but rather from the endergonic nature of the process.

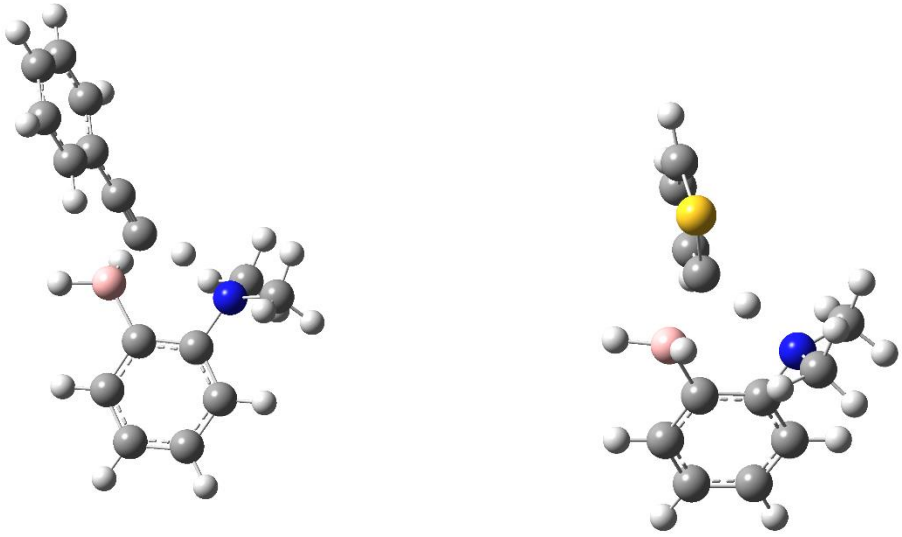

Figure 7-2: Transition state for the C-H bond cleavage of phenylacetylene (left) and thiophene (right) by a NMe_2-BH_2 intramolecular FLP.

Looking now at the structure the transition state (**Figure 7-2**), we see that the nature of the C-H bond cleavage process can be rationalized as a precoordination of the alkyne or the arene to the Lewis acidic organoboryl moiety with the deprotonation performed by the basic group. The drainage of electrons from the triple bond by boron increases the acidity of the proton and the geometry of the FLP is perfect for a simultaneous deprotonation. Reflecting this cooperative behavior, the energy of the transition state is found to be quite low, despite the fact that our FLP molecule is based on a relatively base moiety. This mode of action is reminiscent of several transition metal mediated processes (**Figure 7-3**), namely the Sonogashira coupling, the palladium-catalyzed direct arylation, and the C-H bond activation of arenes by iridium Cp* complexes discussed above.[148,149,160] While in the Sonogashira coupling an alkyne is activated by copper for deprotonation by an external base,[75] in direct arylation, a palladium carboxylate coordinates an arene through its π-system and deprotonates it at the same time.[169,170,172,358,359]

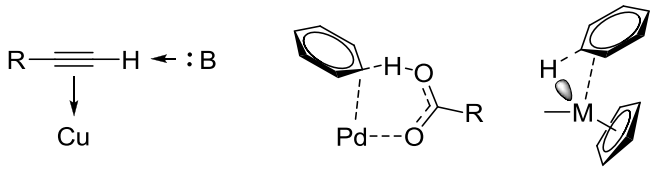

Figure 7-3 Left: Sonogashira activation of terminal alkynes (B = base); center: concerted metalation-deprotonation of arenes; right: precoordination-bond cleavage of arenes by precious metal complexes (M = Ir, Rh).

This bank of calculations, revealing the thermodynamics and kinetics of the C-H bond cleavage by ambiphilic molecules, is at the core of the following sections which explain the design of a metal-free system for the activation of arenes.

7.1.2 Construction of a Molecular Framework Allowing the Confirmation of the C-H Bond Cleavage

As was concluded from the computational results, the C-H bond activation by phenylene-bridged amine-boranes is endergonic. Just as it is for numerous metal systems, the thermodynamic strength of the C-H bond makes its cleavage unfavorable, despite easy kinetics. In fact, as we found, this thermodynamic challenge is even harder for arenes than for the more nucleophilic phenylacetylene. Consequently, it comes to no surprise that the inverse reaction – C-H bond formation – was previously reported by Repo and coworkers in their work on FLP-catalyzed hydrogenation of internal alkynes.[356] In this seminal work, a phenylene-bridged dimethylamino-bis(pentafluorophenyl)boryl FLP eliminates pentafluorophenylbenzene in a “protodeborylation” reaction after hydrogen activation (**Figure 7-4**).

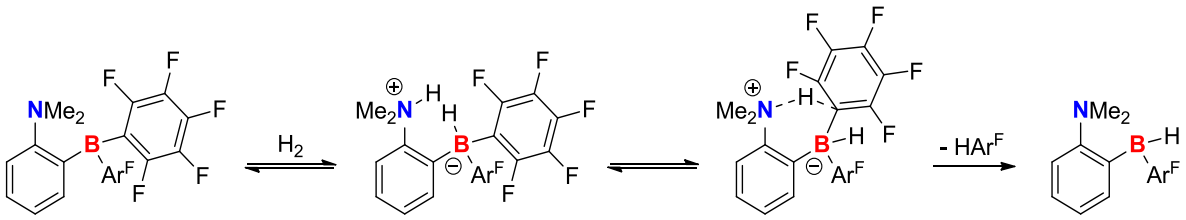

Figure 7-4: Hydrogen activation-protodeborylation as reported by Repo and coworkers.[356]

The protodeborylation transition state is, if looking at the reaction in reverse direction, the transition state for the endergonic C-H bond cleavage of pentafluorobenzene by a

dimethylamino-hydrido(pentafluorophenyl)boryl FLP. In fact, by simple C-B bond rotation of the zwitterionic H_2 complex of the FLP allows for proto-elimination of any group at boron provided that it has a suitable orbital to attack the proton on nitrogen. Hypothetically, the activation-elimination sequence is driven by thermodynamic factors until the most stable product is formed. This reaction was investigated further by our group in a study of the stoichiometric hydrogenation of carbon dioxide.[351]

In order to prove aromatic C-H activation, our goal thus became to find a suitable leaving group at boron that would be easily replaced by an aryl group. Certain limitations exist for this case, however, as was shown by our computational experiments. First, the acid site should not be sterically encumbered, as the interaction of an arene with it should be maximized. Also, it has to be sufficiently acidic to activate the inert arene towards deprotonation. On the other hand, a bulky base group is desirable in order to preserve the FLP character of the ambiphilic molecule. Since the role of the base is presumably the abstraction of a proton from the arene, steric bulk should not limit its reactivity.

With these constraints in mind, we had to design a FLP that would:

1) Be suitable (according to calculations) for the endergonic C-H activation of arenes.
2) Possess a leaving group that would be eliminated after arene activation.

Based on our previous calculations, we selected TMP-BH_2 as one of the best candidates for the C-H activation of thiophene as it was found to have an energy barrier of 21.0 kcal.mol^{-1} for the reaction (**Figure 7-5**). Upon protodeborylation, the hydrides on boron would yield hydrogen gas which could be easily evacuated under a flow of nitrogen, thus driving the reaction towards the desired product. We also expected the bulky TMP group to prevent the formation of dimers that were calculated to be extremely stable in the case of the dimethylamino analog.[351]

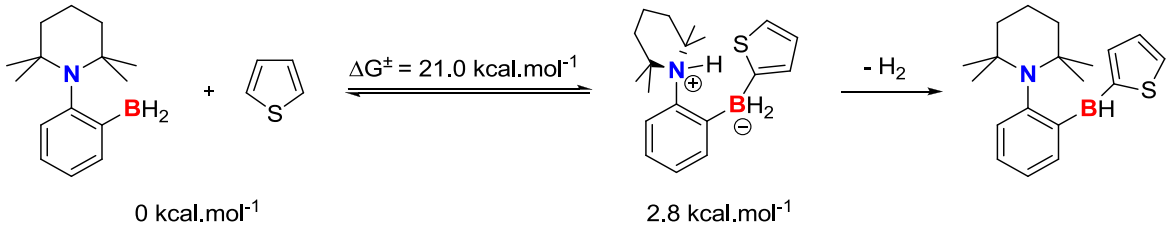

Figure 7-5: Hypothetical C-H activation of thiophene by a TMP-BH_2 Intramolecular FLP with computed energies (ΔG) for the reaction.

Unfortunately, despite the computed barrier of TMP-BH_2 for the C-H bond activation of thiophene, we found that product was unreactive when put in the presence of this substrate. This unexpected result was soon explained as, during the course of these studies, Chernichenko, Papai, Repo, and coworkers reported the crystal structure of **8** as well as its behavior in solution.[356] Their work demonstrated that **8** is in fact a H-bridged dimer both in the solid state and in solution (**Figure 7-6**). Calculations by this group showed that the dimeric resting state of **8** was in fact located 8.7 kcal.mol^{-1} below the monomeric open form.[356] This amount of energy thus has to be supplied in order to reach the C-H activation transition state. In fact, as they found, **8** can still react with molecular hydrogen in an FLP fashion.

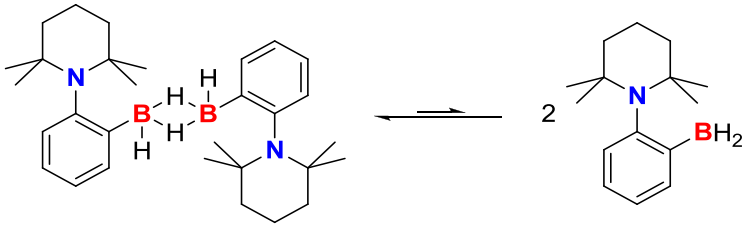

Figure 7-6: Dimeric character of 8 as described by Repo and coworkers.[356]

While the dimeric form of **8** represented a hurdle on the path to C-H activation of arenes, the BH_2 moiety was so promising in terms of its potential to eliminate H_2 that we decided to investigate the ability of **8** to activate more nucleophilic heteroarenes. Simple computations allowed us to determine that furans and pyrroles were easier to activate than thiophene (**Figure 7-7**).

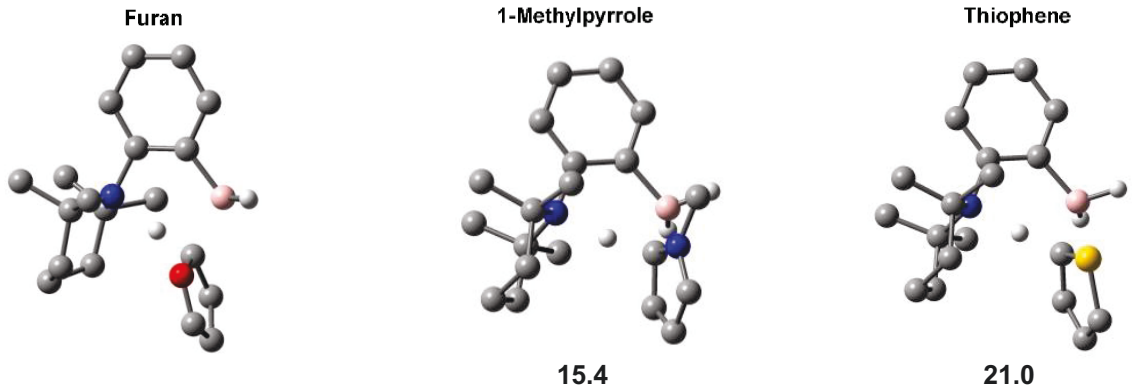

Figure 7-7: Transition state for the C-H bond cleavage of various heteroarenes and the ΔG (kcal.mol^{-1}) associated with them.

As a matter of fact, we found that 1-methylpyrrole reacted with **8** in the course of five hours at 80 °C to give the hitherto unreported compound **9** with release of H_2. While **9** could not be successfully isolated, ^{1}H, ^{13}C and ^{11}B NMR, as well as correlation studies confirm its structure unambiguously (**Figure 7-9**). This stoichiometric reaction was found to be very selective with the main product coming from the C-H activation in the 2-position of 1-methylpyrrole. This selectivity is explained by electronic factors, as this is the most nucleophilic position of pyrrole rings, and supported by calculations described above.

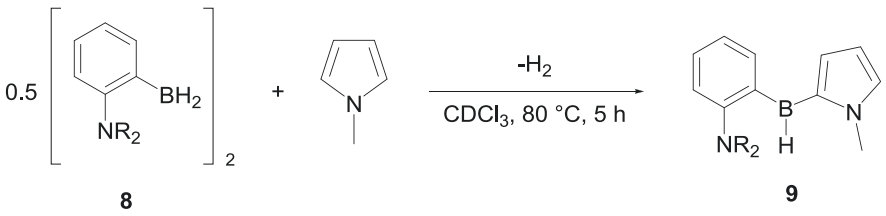

8 **9**

Figure 7-8: Experimentally observed C-H activation-protodeborylation of 1-methylpyrrole by **8**.

This tremendous result confirms the first characterized cleavage of sp^2 C-H bond by an ambiphilic molecule and is a vital step towards selective catalytic C-H functionalization of arenes using metal-free systems. The reaction could be reproduced using 1-methyl-2,3,4,5-tetradeuteropyrrole which allowed the observation of HD.

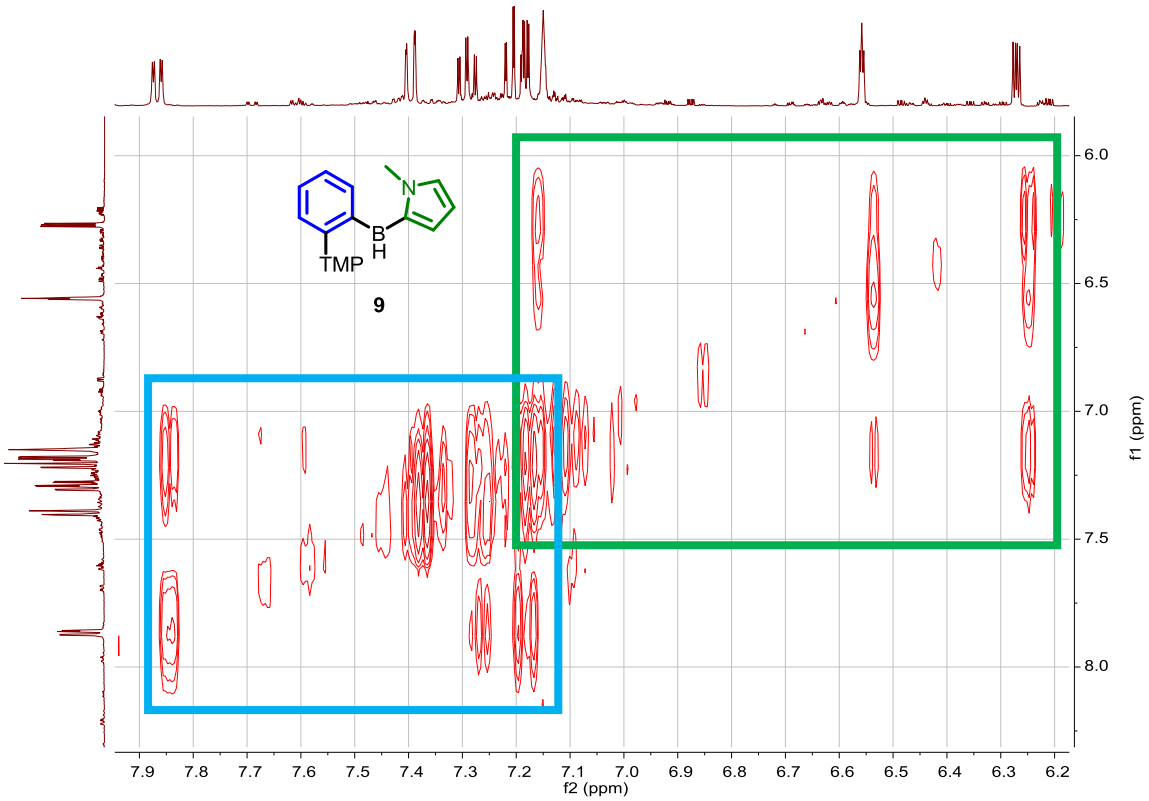

Figure 7-9: ^{1}H COSY NMR (500 MHz, benzene-d_6) spectrum of the aromatic region of **9**.

On a fundamental note, we would like to comment on the contribution of this result to broader synthetic and catalytic chemistry. We find that a well-known though often overlooked aspect of reaction thermodynamics is that even if certain key steps are endergonic a reaction can proceed as long as the intermediates can react further in overall exergonic processes. While one cannot observe the actual zwitterionic arene-FLP intermediate, we were able to prove that C-H activation occurs reversibly in the case of some mild ambiphilic molecules. In our case, we merely trapped the C-H activation intermediate using a simple strategy. By this method, we did not necessarily make the first C(sp^2)-H activating FLP system, but we showed a process that is likely to occur, albeit undetectably, in many ambiphilic systems. It is of prime importance to the experimental chemist to be open to the existence of such intermediates and to take advantage of them in the design of desirable systems.

7.1.3 Design of a FLP System Capable of Catalytic Functionalization of Arenes

While catalytic results obtained for the C-H functionalization of arenes are discussed in the next chapter, a word has to be said about the actual design of the catalytic systems. With the

proof of C-H activation in hand, we considered several options. One idea that the author of this dissertation wished to investigate was that of a N-directed "boryldeborylation." Namely, this reaction was envisioned as an analog to the H_2 activation – protodeborylation sequence by FLPs, but with hydroboranes. In this potential reaction, a hydroborane (R_2BH = BH_3, catecholborane, pinacolborane or 9-BBN) would bind to the nitrogen atom of a N-B(Ar) FLP along with hydride abstraction by the B(Ar) fragment. A C-B bond rotation would then place the aryl group on boron in front of the R_2B^+ on nitrogen, which would allow elimination (**Figure 7-10**).

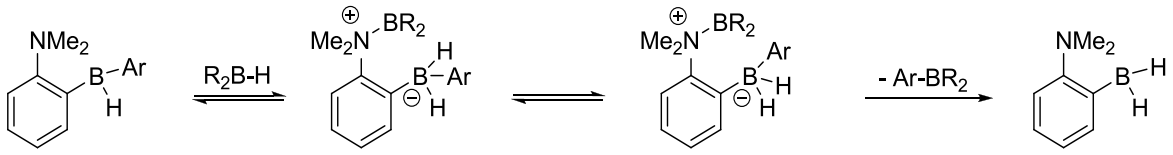

Figure 7-10: Initially proposed C-H activation-boryldeborylation sequence in an intramolecular FLP.

The whole C-H activation, H_2 elimination, B-H activation, and C-B elimination is the equivalent of a typical metal-catalyzed cross-coupling reaction.

With hopes to concretize this idea, we investigated the reactivity of arenes and hydroboranes catalyzed by phenylene-bridged TMP-BH_2 FLP. While we were successful in designing a metal-free catalytic borylation of heteroarenes, the bulk of the TMP moiety precludes any interaction with hydroboranes, making the "boryldeborylation" mechanism impossible. In fact, we have shown that the catalyst could not interact with any borane but BH_3. The actual mechanism by which the borylation takes place will be presented in the next chapter.

Said chapter will be presented in the form of an article that concisely reports our seminal contribution to metal-free activation of C-H bonds.

7.2 Abstract

Transition metal complexes are efficient catalysts for the C-H bond functionalization of heteroarenes to generate useful products for the pharmaceutical and agricultural industries. However, the costly need to remove potentially toxic trace metals from the end products has prompted great interest in developing metal-free catalysts that can mimic metallic systems. We demonstrate here that the borane (1-TMP-2-BH_2-C_6H_4)$_2$ (TMP = 2,2,6,6-

tetramethylpiperidine) can activate the C-H bonds of heteroarenes and catalyze the borylation of furans, pyrroles, and electron-rich thiophenes. The selectivities complement those observed with most transition-metal catalysts reported for this transformation.

7.3 Résumé

De nombreux complexes de métaux de transition sont d'efficaces catalyseurs pour la fonctionnalisation des liens C-H d'hétéroarènes dans le but de générer des produits utiles aux industries pharmaceutique et agricoles. Les coûts associés à la séparation des résidus métalliques en traces des produits finaux a suscité un intérêt important pour le développement et l'utilisation de catalyseurs sans métaux. Dans ce rapport, nous montrons que le borane (1-TMP-2-BH_2-C_6H_4)$_2$ (TMP = 2,2,6,6-tetramethylpiperidine) peut activer les liens C-H d'hétéroarènes et activer la borylation des furanes, des pyrroles et des thiophènes enrichis en électrons. La sélectivité observée pour la borylation est complémentaire à celle observée pour la majorité des catalyseurs organométalliques.

7.4 Introduction

Transition metal catalyzed reactions are ubiquitous tools in the pharmaceutical and agrochemical industries despite the costs associated with removing residual catalysts; trace metals in products for human consumption are heavily regulated by international bodies.[9] Similar concerns exist in the modern electronic industry where metals need to be removed from organic electronic devices to avoid loss of efficiency.[10] Nevertheless, the importance of selectively forming bonds between carbon and other atoms using transition metals has been acknowledged by three Nobel Prizes in Chemistry in the past 15 years. More recently, the catalytic functionalization of C-H bonds using transition metals has emerged as an atom-economical way to generate new bonds without the need for activated precursors.[8,166] Through such an activation process, the catalytic C_{sp2}-H borylation of aromatic molecules generates organoboronates,[185,360,361] which are important species for the pharmaceutical industry and in the field of modern organic materials, notably as building blocks for the creation of new bonds using the Suzuki-Miyaura cross-coupling reaction.[100,362] Although some base metal complexes have been used as catalysts for the borylation of arenes[174,190,193] the most efficient systems to date rely on noble metals, most notably iridium.[185,361] Alternatively, borenium or boronium species generated by highly reactive precursors can promote the

electrophilic borylation of arenes but stoichiometric quantities of amine derivatives are needed to generate the active boron reagents.[195,196,198]

Noble metals are well suited to cleave aromatic C-H bonds in catalytic processes because they can easily mediate two-electron transfer processes. In the borylation reaction using iridium catalysts, this transformation is usually assisted by the boryl substituents present on the metal centre which facilitate the proton transfer (**Figure 7-11A**).[189] An analogous process is the direct arylation through palladium carboxylate complexes, a process in which the electron transfer is helped by the basic carboxylate group abstracting the proton on the aromatic molecule while the aryl group coordinates the metallic center (**Figure 7-11B**).[167,168] Herein, we report that intramolecular "Frustrated Lewis Pairs" (FLPs) can be used as catalysts for the C-H bond cleavage and dehydrogenative borylation of heteroarenes. Replacing current metal-catalyzed technologies by FLP processes offers exciting possibilities because of the abundance, low cost and low toxicity of most organoboranes, especially in comparison with noble metals.[363] The metal-free activation of hydrogen reported in 2006 using the concept of FLPs[40,42] led to an important breakthrough in the metal-free hydrogenation reaction.[352] In FLP processes, cleavage of H_2 occurs during the transition state via the cooperation of a Lewis acid and a Lewis base that are prevented from forming a Lewis adduct by steric or geometrical constraints. We now report the design of a FLP catalyst capable of cleaving and functionalizing C_{sp2}-H bonds. In this process, a Lewis basic amine putatively serves to abstract a proton while the electron density of the C_{sp2}-H bond is transferred to a Lewis acidic borane (**Figure 7-11C**). This concept is thus reminiscent of the transformations observed with transition metal complexes.

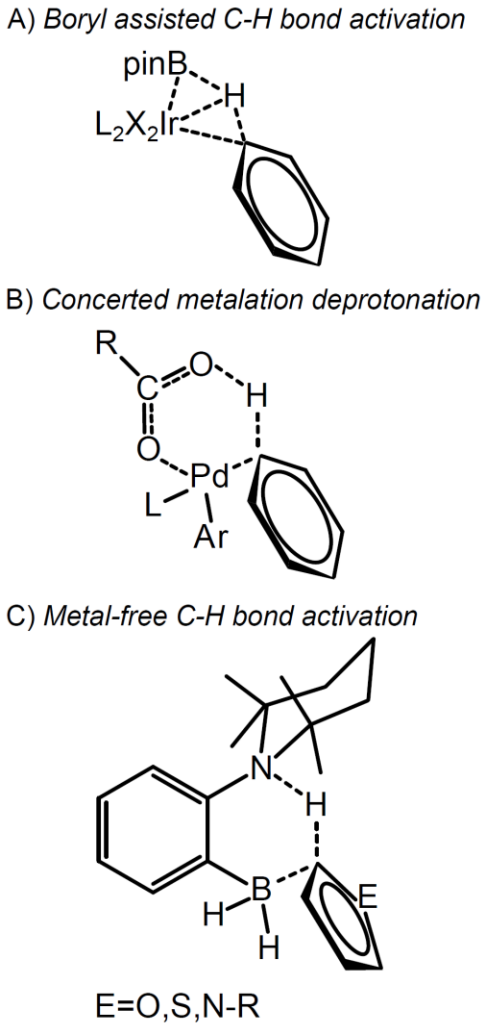

Figure 7-11: Representative transition states for the C-H activation of arenes. **A**) Activation of C-H bonds in borylation transformations using Ir catalysts. **B**) Carboxylate-assisted metalation deprotonation at palladium. **C**) Metal-free C-H activation of heteroarenes using FLP catalysts. The dashed lines represent bonds formed and cleaved during the electron transfer.

7.5 Results and Discussion

The catalyst presented in **Figure 7-11-C** was designed to afford the nucleophilic carbon of the heterocyclic substrate close access to the Lewis acidic BH_2 moiety. In concert, the bulky amine moiety favors the abstraction of the proton from the C_{sp2} while preventing possible head-to-tail dimerization. The phenyl linker between the Lewis moieties has been shown to be quite durable in FLP catalysis.[62,207,355,356] Compound **8** [(1-TMP-2-BH_2-C_6H_4)$_2$ (TMP = 2,2,6,6-tetramethylpiperidine)] was therefore a promising candidate for the metal-free C_{sp2}-H

activation of aromatic molecules in addition to being synthetically easily accessible. While we were carrying out this work, compound **8** was shown to be in equilibrium with the monomeric form and was reported to be an active species for hydrogen activation.[356]

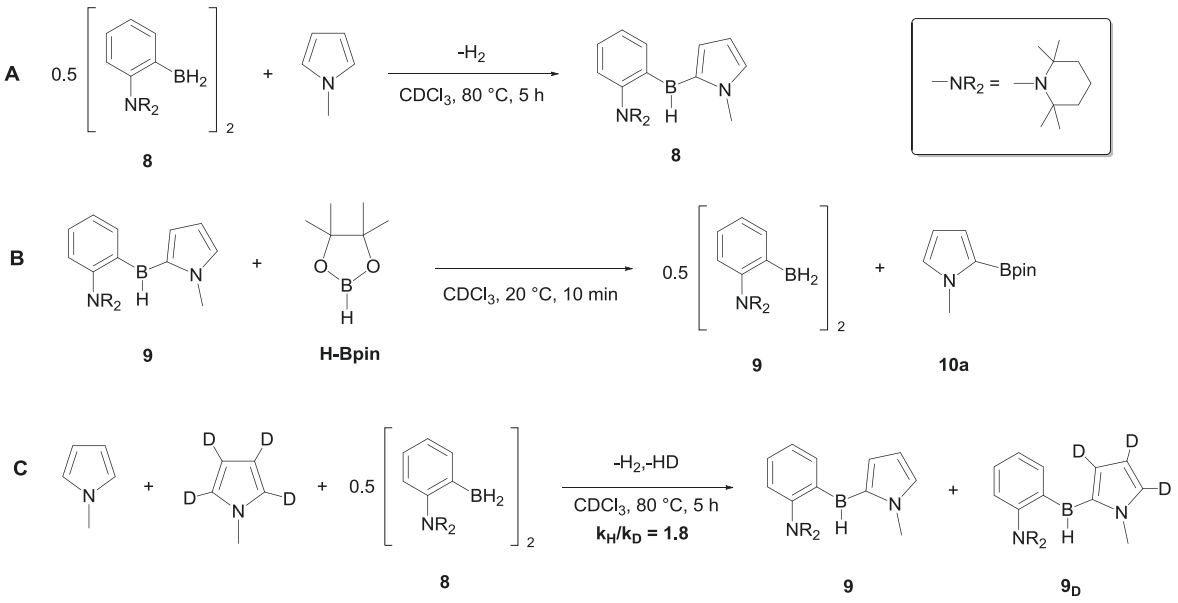

Figure 7-12: Stoichiometric transformations observed in the course of this study using ^{1}H, ^{13}C, and ^{11}B NMR spectroscopy. **A**) Reaction of species **8** with 1-methylpyrrole generating **9**. **B**) Reaction of **9** with HBpin generating **9** and **10a**. **C**) Competitive experiment between 1-methylpyrrole and 1-methylpyrrole-*d*$_4$ allowing determination of the kinetic isotope effect for the generation of **9**.

^{1}H Nuclear magnetic resonance (NMR) monitoring of the addition of 1-methylpyrrole to a solution of **8** in chloroform-*d* at 80 °C revealed the evolution of H_2 (δ = 4.63) and the formation of product **9** over a period of 5 hours, resulting from the C-H activation of 1-methylpyrrole at the 2 position (**Figure 7-12-A**). Conducting a similar reaction with 1-methylpyrrole-*d*$_4$ allowed the observation of HD and the unambiguous assignment of the resonances associated with the 1-methylpyrrole activation products (**Figure 7-12-C**). Compound **9** was shown to react with HBpin (pin = pinacolato) in a chloroform-*d* solution over the course of 10 minutes at ambient temperature, regenerating **8** by releasing 1-Me-2-Bpin-pyrrole (**10a**) (**Figure 7-12-B, Figure 7-13**).

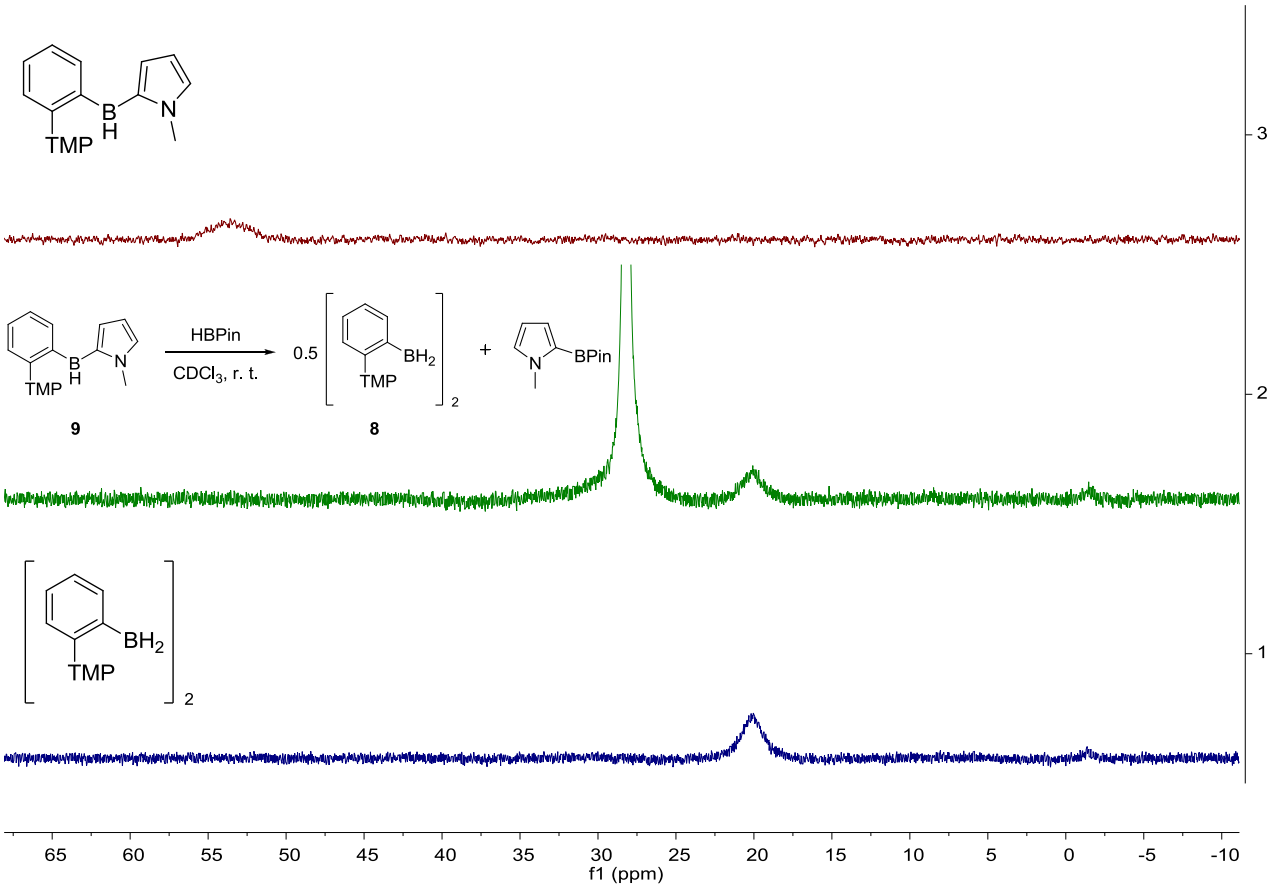

Figure 7-13: Stacked $^{11}B\{^{1}H\}$ NMR (160 MHz, benzene-d_6) spectra of **9** (top), the reaction of **9** and HBpin (middle) and **8** (bottom).

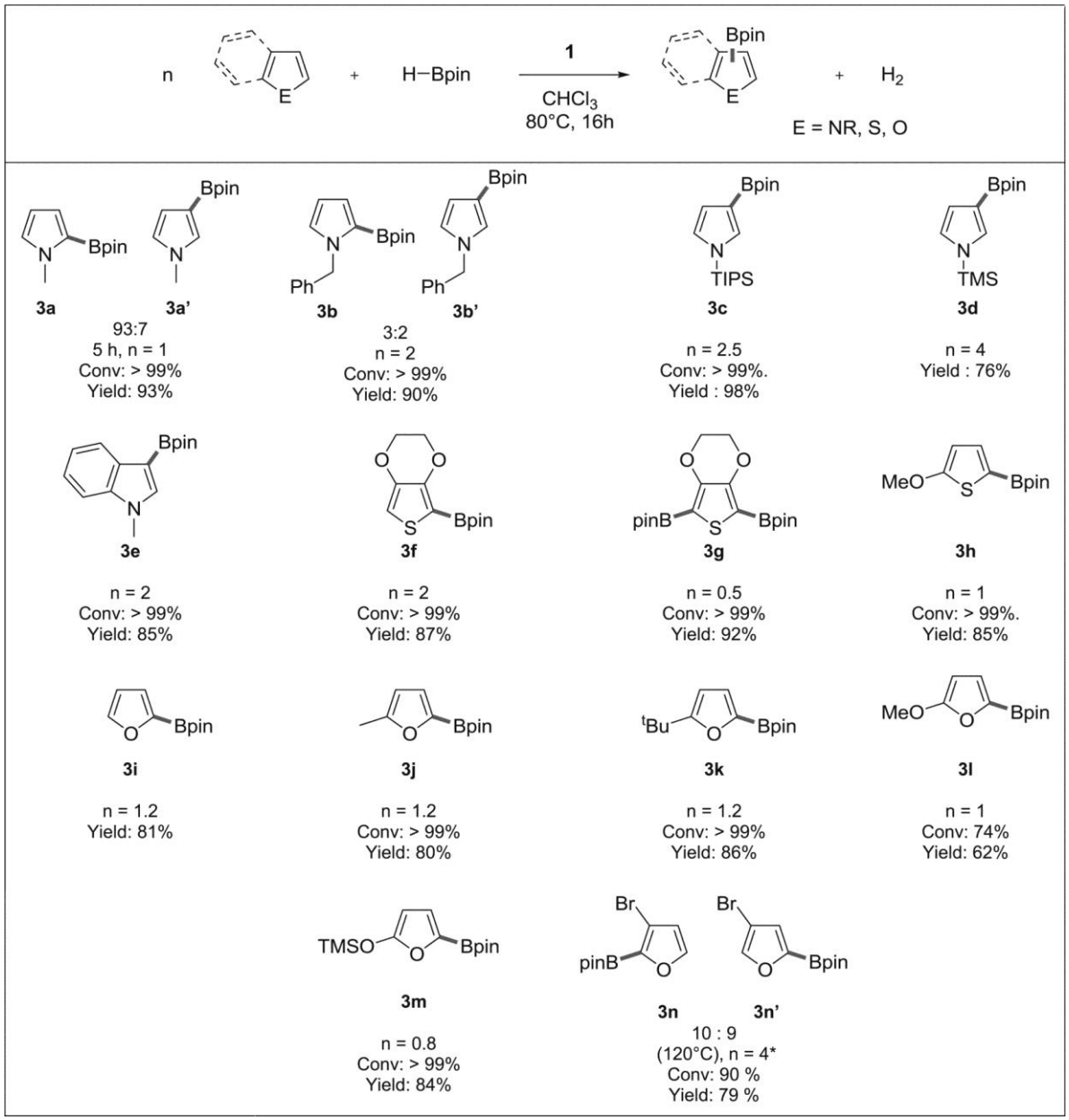

Table 7-3: Scope of the borylation reaction catalyzed by **8**. Unless specified otherwise, the reactions were run using **8** (14.0 mg, 0.0305 mmol, 2.5 mol. %), HBpin (156 mg, 1.22 mmol), and the substrate (n x 1.22 mmol) in 5 mL of $CHCl_3$ at 80 °C. The conversions (conv.) are given with respect to the transformation of the limiting reagent to the borylated product as measured by ^{1}H NMR spectroscopy at the end of the reaction. Yields and isomer ratios refer to isolated quantities. Unless specified otherwise, a single isomer was isolated and detected. * **8** (2.1 mg, 0.045 mmol, 5 mol. %), 3-bromofuran (32.9 µL, 53.9 mg, 0.367 mmol) and HBpin (12.8 µL, 11.7 mg, 0.092 mmol), benzene-d_6 (0.4 mL), 100 °C, 36 hours.

When equimolar amounts of 1-methylpyrrole and HBpin (1.22 mmol) were added to a 2.5 mol. % solution of **8** in $CHCl_3$, we observed quantitative conversion of the reagents to a 93 : 7 ratio of **10a** and **10a'** by ^{1}H NMR spectroscopy, confirming that **8** is a catalyst for the

borylation reaction. We obtained the isolated products in a yield of 93% by passing the reaction mixture over a short pad of silica to remove the catalyst. The same protocol was used on a multigram scale reaction (0.22 mol) to isolate 3.76 g of the desired product (yield = 81 %). With a catalytic loading as low as 0.5 mol %, we isolated species **10a** and **10a'** in an overall 72 % yield. The borylation of 1-methylpyrrole was also possible with catecholborane and 9-borabicyclo[3.3.1]nonane, but these gave yields of 42 and 60%, respectively. In addition, we tested functional group tolerance by conducting the borylation of 1-methylpyrrole in the presence of additives. The reaction was shown to be tolerant of aryl or alkyl halides, epoxides, ethers, hexamethylphosphoramide, and less basic amines, but inhibition was observed in the presence of basic amines, carbonyl groups, or unsaturated hydrocarbons (**Table 7-3**).

The scope of the borylation is displayed in **Table 7-3**. The reaction does not proceed for the parent pyrrole because of the reactive N-H bond that presumably inhibits the catalyst. Protection of the pyrrole with the N-benzyl group allowed us to isolate a 3:2 mixture of **10b** and **10b'** in 90% yield. Not only are the TIPS (TIPS = triisopropylsilyl) and TMS protecting group also tolerated, but they allow the formation of the 3-substituted isomer, giving **10c** and **10d** in good yields. However, the presence of the electron-withdrawing *tert*butyloxycarbonyl group (BOC) inhibits the reaction completely. The latter results suggest that the electronic parameters are critical for the reaction to proceed. Indeed, the quantitative borylation for 1-methylindole at the most electron-rich 3-position to generate **10e** rather than in the 10-position as observed for the iridium catalysts[187] is reminiscent of the regioselectivity observed in electrophilic borylations.[196,198]

Whereas our investigation revealed that thiophene is not reactive, the borylation proceeds rapidly for electron rich 3,4-ethylenedioxythiophene. By adding 0.5 or 2 equiv of HBpin, it was possible to observe quantitative conversion to the mono- (**10f**) or diborylated (**10g**) products. Similarly, 2-methoxythiophene was borylated successfully once more suggesting that electron-rich substrates are required for catalysis to occur.

Many furan derivatives are challenging to isolate since they tend to be light sensitive and degrade on silica but our simple purification methods allows rapid isolation of the products. Although furan gave only limited conversion to **10i** by NMR spectroscopy, we were able to isolate borylated 2-alkylfurans **10j** and **10k** in excellent yields. Once again, electron-rich substrates react readily, giving methoxide and siloxide species **10l** and **10m** in good yields

and thus expanding the scope to the use of protected alcohol functionalities. **8** is tolerant of bromide-containing substrates and generates **10n** and **10n'** in a close to statistical 1:0.9 ratio.

Density functional theory (DFT) calculations were carried out at the ωB97xd/6-31+G** level (with the SMD solvation model to account for chloroform solvent) to propose a reliable mechanism for this transformation using 1-methylpyrrole as the model substrate, as shown in **Figure 7-14**. After dissociation of the dimer **8**, the rate-determining step was calculated to be the C-H activation of the substrate by **Int1**, generating the zwitterionic species **Int2**. Once **Int2** is generated, the calculations predict a rapid release of H_2 to generate **9**.[62] The formation of **10a** in the presence of HBpin was calculated to proceed via a four-centre sigma-bond metathesis, regenerating **8** in the process.

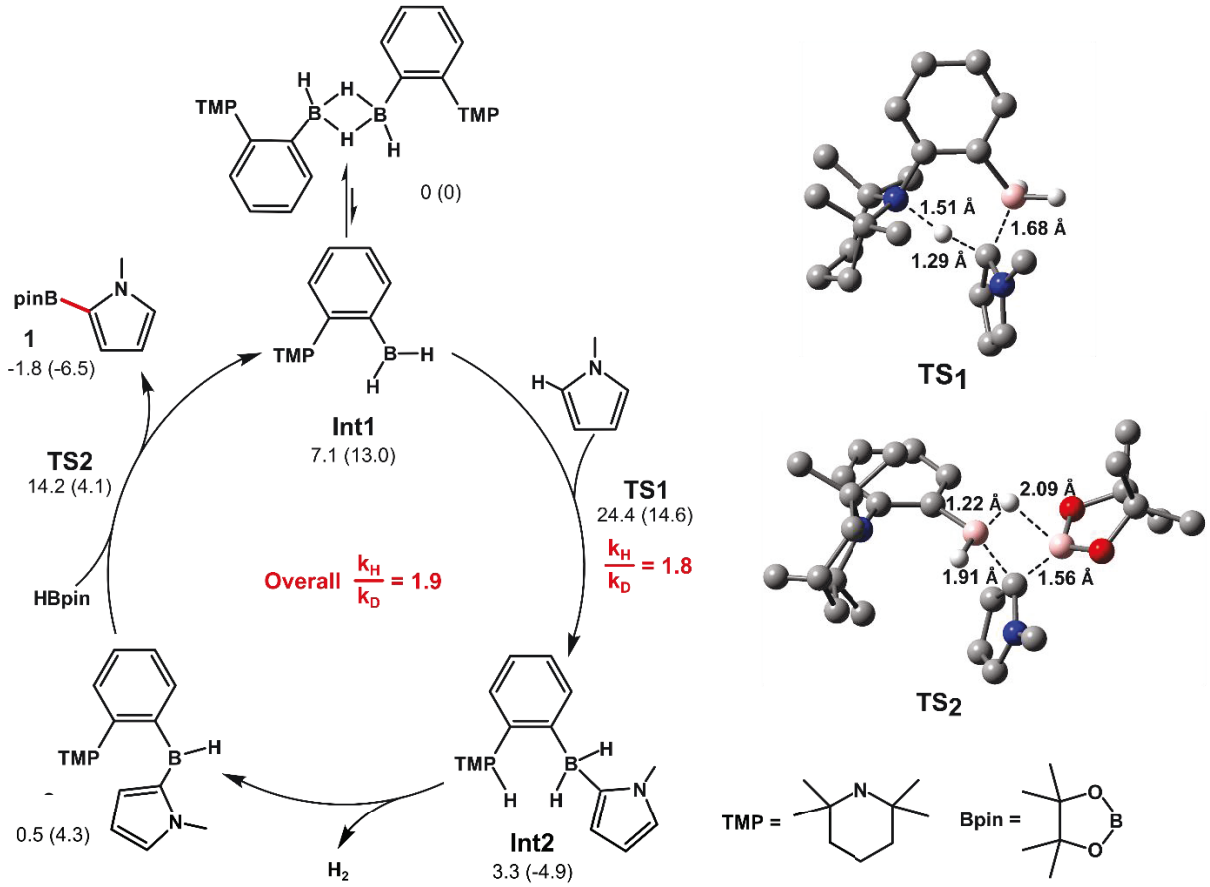

Figure 7-14: Proposed mechanism of the borylation of 1-methylpyrrole using catalyst **8**, with calculated (ωB97xd/6-31+G**) energies ΔG^{273K} (ΔH^{273K}) given for each structure in kcal.mol^{-1} in chloroform phase. The formation of **9** from **8** (KIE of 1.8 when was obtained using 1-methylpyrrole-d_4) and **10a** from **9** were observed using NMR spectroscopy, with an overall

KIE of 1.9 for the catalytic transformation. Int1 and Int2 were not observed and transition states TS1 and TS2 are represented, based on DFT calculations.

Whereas the 24.4 kcal.mol^{-1} barrier for C-H activation of the proton in the 2-position of the pyrrole is favored, the activation on the 3-position is also possible, requiring only 0.4 kcal.mol^{-1} of additional activation energy, justifying the minor amount of **10a'** produced during catalysis. These barriers are consistent with catalysis operating at 80 °C. We performed competition experiments at 80 °C between 1-methylpyrrole and 1-methylpyrrole-d_4 to measure a kinetic isotope effect (KIE) of 1.8 for the stoichiometric C-H activation with formation of **9** and of 1.9 for the catalytic borylation. The relatively low KIE value of 1.8 to 1.9 is similar to that observed for the concerted metalation-deprotonation of the palladium-catalyzed arylation reaction with similar substrates (KIE of 2.1 at 100 °C).[359,364]

It is well established that the C-H activation processes using iridium catalysts correlate well with the acidity of the proton.[365,366] In contrast, the ease of activation of C-H bonds using carboxylate-assisted palladium catalysts can be attributed to both the acidity of the proton and the nucleophilicity of the carbon.[170,358] The regioselectivity observed for the borylated indole **10e** and the KIE values support the transition-state calculations indicating that the C-H bond activation by catalyst **8** is directed by the most nucleophilic carbon, therefore acting in a complementary fashion when compared to transition-metal systems. Although thiophene and 1,3,5-trimethoxybenzene are more difficult to activate since these molecules have higher aromatic stabilization and hence lower nucleophilicity than pyrroles, the DFT results suggest that the C-H activation transition state energies of these molecules are, respectively, only 3.3 and 6.7 kcal.mol^{-1} higher than for the activation of 1-methylpyrrole, suggesting that the borylation of these substrates might be accessible with further catalyst optimization. Furthermore, it is expected that the FLP mediated activation of C-H bonds could be exploited for a plethora of C-H functionalization reactions.

7.6 Experimental Details

General Procedures: Unless specified otherwise, manipulations were carried out under a nitrogen atmosphere using standard glovebox and Schlenk techniques. Toluene and hexanes were purified by distillation over Na/benzophenone. Chloroform used in catalytic reactions was dried by distillation over P_2O_5. chloroform-*d* used for the test catalytic reactions was

similarly treated. benzene-d_6 was dried over Na/K alloy and distilled. Catalytic reactions, unless specified otherwise, were carried out in oven-dried sealable vials.

NMR spectra were recorded on an Agilent Technologies NMR spectrometer at 500 MHz (^{1}H), 125.758 MHz (^{13}C), 160.46 MHz (^{11}B) and on a Varian Inova NMR AS400 spectrometer, at 400.0 MHz (^{1}H), 100.580 MHz (^{13}C). ^{1}H NMR and ^{13}C{^{1}H} NMR chemical shifts are referenced to residual protons or carbons in deuterated solvent. ^{11}B{^{1}H} was calibrated using an external reference of $BF_3.Et_2O$. Multiplicities are reported as singlet (s), broad singlet (s, br) doublet (d), triplet (t), multiplet (m). Chemical shifts are reported in ppm. Coupling constants are reported in Hz. ICP-MS measurements were conducted on an Agilent Technologies Triple Quadrupole 8800 ICP-MS. Mass Spectrometry analyses were carried out on an Thermo-Fisher Trace GC Ultra with a ITQ 900 MS, using electronic impact as an ionization source (precision +/- 0.2 uma).

Al_2O_3 was purchased from Sigma-Aldrich and activated by heating in a Schlenk flask at 300 °C under vacuum (20 millitorr) for 16 hours. Heteroaromatic substrates were purchased from Sigma-Aldrich or Alfa Aesar or prepared according to literature procedures[367,368] and stored in a glovebox over 4 Å molecular sieves. 1-methylpyrrole was distilled from KOH and flame-dried $MgSO_4$. 2-Methoxyfuran (Alfa), 2-silyloxyfuran (Aldrich), 2-methoxythiophene (Alfa), 3-bromofuran (Aldrich), furan (Aldrich), 2-methylfuran (Aldrich), and 1-benzylpyrrole were passed through a short pad of alumina before use. 3,4-Ethylenedioxythiophene was distilled before use. Pinacolborane was purchased from Sigma-Aldrich and used as received.

7.6.1 Synthesis of Catalyst

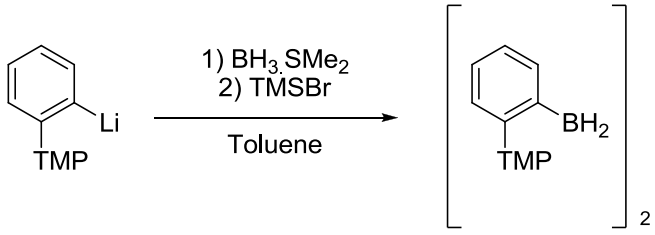

8

Figure 7-15: Preparation of **8** according to the procedure reported by Repo and coworkers.

8 was synthesized using the procedure reported by Repo and coworkers with minor modifications.[356] In a Schlenk tube, 4.2 g of [2-(2,2,6,6-tetramethylpiperidin-1-yl)phenyl]lithium

(18.8 mmol) were suspended in *ca.* 90 ml of dry toluene and cooled to -80 °C. Borane dimethyl sulfide complex (3.6 ml, 37.6 mmol, 2 equiv) was added via syringe in one portion. The reaction was stirred at -80 °C for 2 h, then allowed to warm to room temperature within 1 h and stirred overnight. Trimethylsilyl bromide (2.6 ml, 19.7 mmol, 1.05 equiv) was added in one portion via syringe and the reaction was stirred for another 4 h at room temperature after which volatiles were removed in vacuum (1 mbar). The residue was dispersed in *ca.* 50 mL of hot hexane and was filtered hot. The filter cake was washed two times with additional *ca.* 25 mL of hot hexanes, and the combined liquors were left to crystallize at -35 °C. After *ca.* 48 h the supernatant was removed by filtration and the crystals washed twice with cold hexanes (2 x 25 mL, -60 °C). After evaporation of the volatiles *in vacuo*, 2.24 g (52% yield) of a white crystalline powder was obtained. Spectroscopic measurements corresponded to that of pure **8**.

^{1}H NMR (500 MHz, chloroform-*d*): δ 7.71 (br. d, *J* = 7.3 Hz, 2H), 7.43 – 7.32 (m, 4H), 7.25 (br. t, *J* = 7.1 Hz, 2H), 5.10 (br, 1H, BH), 2.36 (br, 1H, BH), 1.96 – 1.83 (m, 2H, TMP), 1.67 – 1.52 (m, 10H, TMP), 1.33 (s, 12H, TMP(Me_2)), 0.81 (s, 12H, TMP(Me_2)). ^{13}C{^{1}H} NMR (126 MHz, chloroform-*d*) δ 151.7, 142.1, 134.6, 131.8, 129.1, 125.2, 55.4, 42.1, 32.9, 26.0, 18.8. ^{11}B{^{1}H} NMR (160 MHz, chloroform-*d*) : 20.0.

7.6.2 Stoichiometric Reactions

Preparation of 9 by C-H activation

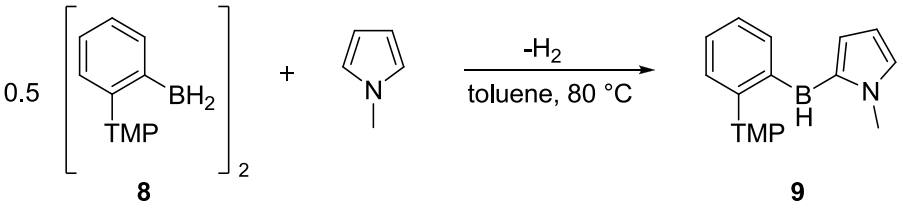

Figure 7-16: Preparation of **9** by the C-H bond activation-H_2 release sequence.

In a glovebox, 300 mg (1.654 mmol) of **8** was dissolved in *ca.* 25 ml of toluene and placed into a Schlenk tube. 116 µL (106 mg, 1.31 mmol) of 1-methylpyrrole was subsequently added by pipet. The reaction mixture was heated under nitrogen to 80 °C for 5h and then evaporated to dryness *in vacuo*. The resulting thick orange oil proved to be difficult to handle and attempts to isolate **9** from the small impurities failed (presumed to be the activation of 1-methylpyrrole

at the 3 position and/or a double activation of 1-methylpyrrole). Instead, it was characterized as is and used without further purification. The structure of the product could be unambiguously assigned as that of **9** by its ^{1}H and ^{13}C NMR signature. A similar reaction using a mixture of 1-methylpyrrole and 1-methylpyrrole-*d*$_4$ confirmed the assignation of the aromatic pyrrole (NC_4H_3) since they do not integrate for the unity as expected for a D-containing product.

^{1}H NMR (500 MHz, benzene-*d*$_6$) δ 7.85 (dd, *J* = 7.3, 1.8 Hz, 1H, C_6H_4), 7.37 (dd, *J* = 8.0, 1.1 Hz,1H, C_6H_4), 7.27 (ddd, *J* = 8.0, 7.2, 1.9 Hz, 1H, C_6H_4), 7.19 (dt, *J* = 7.3, 1.1 Hz, 1H, C_6H_4), 7.17 (dd, *J* = 3.9, 1.5 Hz, 1H, NC_4H_3), 6.54 (t, *J* = 1.9 Hz, 1H, NC_4H_3), 6.25 (dd, *J* = 3.9, 2.3 Hz, 1H, NC_4H_3), 3.35 (s, 3H, NCH_3), 1.30 (s, 6H, TMP(Me_2)), 0.95 (s, 6H, TMP(Me_2)), cyclic TMP signals were found as poorly resolved multiplets in the 2.0 - 0.9 ppm area. $^{13}C\{^{1}H\}$ NMR (126 MHz, benzene-*d*$_6$) δ 152.8, 136.1, 132.2, 131.4, 129.7, 128.4, 125.2, 110.5, 55.4, 42.5, 34.6, 26.0, 19.1. $^{11}B\{^{1}H\}$ NMR (160 MHz, chloroform-*d*) : 54.3 (br).

^{11}B NMR monitoring of the reaction of 9 and pinacolborane

20.0 mg (0.0649 mmol) of **9** was dissolved in chloroform-*d* and placed into a J-Young NMR tube. HBpin (0.129 mmol, 16.6 mg, 18.2 µL) was added by pipet and the resulting mixture was immediately analyzed by $^{11}B\{^{1}H\}$ NMR (total acquisition time: 30 minutes). The analysis revealed complete conversion of **9** to **8**. The concomitant generation of **10a** could not be confirmed by ^{11}B NMR because of the overlap of the signal with HBpin but could be seen by ^{1}H NMR. The ^{1}H NMR spectrum was taken before the ^{11}B NMR spectrum and within 10 minutes of the addition of HBpin to **9**.

7.6.3 Catalytic Results and Analytics

For the following study, a solution of catalyst **8** (11.2 mmol.L^{-1}) and hexamethylbenzene (42.6 mmol.L^{-1}) in chloroform-*d* was prepared and used for the NMR experiments.

Optimization of the catalytic borylation of N-Methypyrrole

Table 7-4: Optimization of the yields for the metal-free borylation of 1-methylpyrrole.

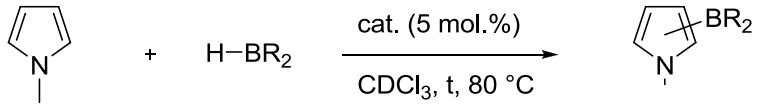

3a + 3a'

Entry	Catalyst	HBR_2	t (h)	Yield (%)
1	-	HBpin	24	0
2	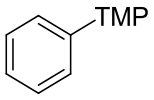	HBpin	24	0
3	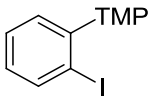	HBpin	24	0
4	**8 (2.5 mol. %)**	**HBpin**	**5**	**> 95**
5	**8** (2.5 mol. %)	HBcat	12	42
6	**8** (2.5 mol. %)	9-BBN	12	60

These results led us to use pinacolborane for the borylation of heteroaromatic molecules. Pinacolboronates are the most useful boronates to the synthetic chemist for their superior stability and their interesting reactivity.

Evaluation of Functional Group Tolerance.

In order to evaluate the tolerance of the catalytic process towards various functional groups, the catalytic borylation of 1-methylpyrrole was performed in the presence of additives containing various functional groups. Such study was recently performed for testing the functional group tolerance in the silylation of heterocycles catalyzed by KO*t*Bu.[369] For such a study, a solution of catalyst **8** (11.3 mmol.L^{-1}) and hexamethylbenzene (42.6 mmol.L^{-1}) was prepared.

In a typical experiment, 0.4 mL of solution (0.0045 mmol) was introduced by automatic pipet into a J-Young or normal NMR tube, followed by HBpin (26.1 mL, 23.0 mg, 0.18 mmol), 1-methylpyrrole (19.1 mL, 17.5 mg, 0.22 mmol) and an additive (0.18 mmol). The resulting solution was heated to 80 °C in an oil bath for 5 hours before being analyzed by ^{1}H NMR. Results are given in **Table 7-5**.

Table 7-5: Tolerance of the catalytic system to various additives.

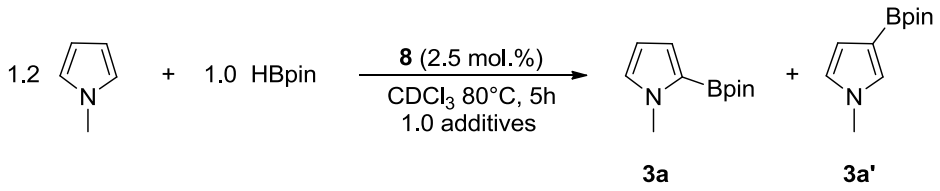

Entry	Additive	Yield(%)	Entry	Additive	Yield(%)
1[a]	-	95	12	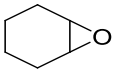	48
2		4	13		88
3	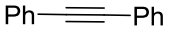	0	14	THF	98
4	PhF	>99	15	DMF	0
5	PhCl	93	16	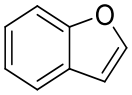	12
6	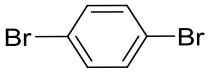	90	17	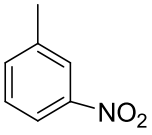	31
7	Br-(C)$_{10}$-Br	88	18	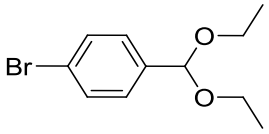	68
8	Ph_3N	92	19	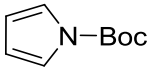	64
9	Ph_2NH	0	20	$PhCF_3$	94
10	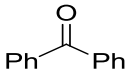	0	21	HMPA	87
11	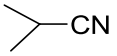	0	22	TMEDA	24

Conditions: 0.4 mL chloroform-*d*, 0.0045 mmol cat (2.5 mol%), 0.18 mmol additive (1.0 equiv), 0.22 mmol 1-methylpyrrole (1.2 equiv.), 0.18 mmol HBpin 80 °C, 5 hours. Yields (based on HBpin) determined by NMR integration with respect to the internal standard of hexamethylbenzene which was introduced before the start of the reaction.[a] Control reaction without the presence of any additive

ICP-MS quantification of trace metals in catalytic mixture

The catalytic borylation of 1-methylpyrrole was performed using the exact conditions specified below (see **Part IV**). At the end of the reaction, an aliquot of the reaction mixture was taken to ascertain the completion of the reaction. Instead of purifying, isolating and quantifying the product, the reaction mixture was dried *in vacuo* and an aliquot of 100 mg was taken and added to a mixture 18 mL of concentrated HNO_3 and 2 mL concentrated HCl. This mixture was heated to 175 °C under a pressure of 120 psi for 20 minutes before being diluted and analyzed by ICP-QQQ-MS to quantify their metal contents. Results are reported as the average of two sample solutions analyzed 10 times each. Results are given in **Table 7-6**.

Table 7-6: Concentration of various metals in the unpurified reaction mixture of the borylation of 1-Methylpyrrole by HBpin catalyzed by **8**.

	Concentration (ppm)
Co	0,00 ± 0,03
Mo	0.000 ± 0.002
Ru	0,000 ± 0,002
Rh	0,00 ± 0,01
Pd	0,13 ± 0,02
Ag	0,04 ± 0,03
Os	0,4 ± 0,3
Ir	0,03 ± 0,01
Pt	0,4 ± 0,4
Au	3 ± 2
Tl	0,00 ± 0,05

7.6.4 Borylation of Heteroarenes

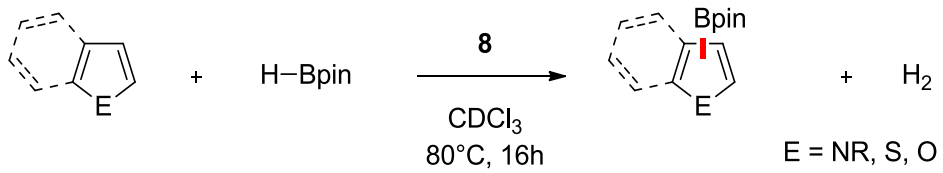

Figure 7-17: General formulation of the catalytic borylation of heteroarenes.

General Procedure: In a nitrogen-filled glovebox, a 0.0305 M stock solution of **8** in $CHCl_3$ was prepared. 1 mL of this solution was introduced by pipet to a sealable 25 mL microwave vial equipped with a magnetic stirring bar and diluted in 4 mL additional $CHCl_3$. Warning: using smaller vials may lead to hydrogen overpressure and explosion hazard. To this was added HBpin and the heteroaromatic substrate in the specified quantities. The vial was subsequently sealed and heated with stirring to 80 °C for 16 hours, after which the mixture was cooled down to room temperature and 60 µL of p-xylene or mesitylene was added. An aliquot of the reaction mixture was analyzed by ^1H NMR to determine the conversion, which was measured with regard to the resonance of the pinacol moieties. Heteroaromatic boronates were often found to be of dubious stability, especially in the case of furyl boronates. For this reason, the reaction mixture was purified by rapid passage through a *very short* pad of silica with vacuum suction along with CH_2Cl_2 for rinsing. Such a treatment proved sufficient to remove the catalyst and yield the borylated product with good purity after vacuum evaporation of solvents and volatiles. Longer flash chromatography columns, on the other hand, tended to reduce the yields of obtained products. The reaction with the parent pyrrole was shown not to work because of activation of the N-H bond. The reaction with N-BOC-pyrrole was shown not to work because of the electron withdrawing character of the BOC group.

Description of the Flash Legare Apparatus

In order to efficiently purify material that decomposes on the silica gel, we decided to design an apparatus that would allow the purification of crude mixtures rapidly and using small quantities of silica. This setup, which came to be known as the *Flash Legare* consists of a 9 mm pastor pipet inserted in a short column set on a round bottom flask and connected to a vacuum line (**Figure 7-18**). The pipet is fitted in a joint that is made from a reused rubber pipe. Cotton is set at the bottom of the pipet that is then filler with *ca.* 4 cm of silica.

Figure 7-18: Picture of a typical Flash Legare setup used for the purification of 1.22 mmol of borylated material on a silica pad.

With vacuum suction, the crude mixture is *rapidly*[IV] poured on the silica and subsequently rinsed with several portions of solvent. The manipulation has to be done rapidly in order to minimize contact with the silica. Such a treatment was sufficient for the purification of our products.

Borylation of 1-methylpyrrole

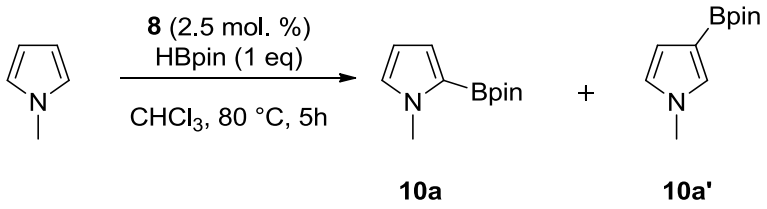

Figure 7-19: Borylation of 1-methylpyrrole catalyzed by **8**.

The general procedure was followed with the reaction time reduced to **5 hours**. 1-methylpyrrole (109 µL, 99.1 mg, 1.22 mmol) was reacted with HBpin (177 µL, 156 mg, 1.22 mmol). Complete conversion was observed by NMR and 235 mg (93 %) of a 93:7 mixture of 1-methyl-2-(4,4,5,5-tetramethyl-1,3,2-dioxaborolan-2-yl)pyrrole and 1-methyl-3-(4,4,5,5-

[IV] We have found that the following rule of thumb was appropriate for the handling of the *Flash Legare*: from start to finish, all manipulations should be done while listening to "Flash Gordon" by Queen and be over before the end of the song.

tetramethyl-1,3,2-dioxaborolan-2-yl)pyrrole was isolated as a white solid. NMR characterization was conform to that of the reported products. [196] M^+: 207.1 (calc.: 207.14).

1-methyl-2-(4,4,5,5-tetramethyl-1,3,2-dioxaborolan-2-yl)pyrrole (**10a**): ^{1}H NMR (400 MHz, chloroform-*d*) δ 6.81 (m, 2H), 6.15 (m, 1H), 3.84 (s, 3H), 1.31 (s, 12H); ^{13}C{^{1}H} NMR (101 MHz, chloroform-*d*): δ 128.3, 122.0, 108.6, 83.2, 36.7, 25.0; ^{11}B{^{1}H} NMR (160 MHz, chloroform-*d*) : δ 28.1.

1-methyl-3-(4,4,5,5-tetramethyl-1,3,2-dioxaborolan-2-yl)pyrrole (**10a'**): ^{1}H NMR (400 MHz, chloroform-*d*) δ 7.06 (m, 1H), 6.64 (m, 1H), 6.47 (m, 1H), 3.81 (s, 3H), 1.29 (s, 12H).

While **10a'** can be identified by its ^{1}H NMR spectrum, it was not found in sufficient concentration to be characterized by ^{11}B and ^{13}C NMR.

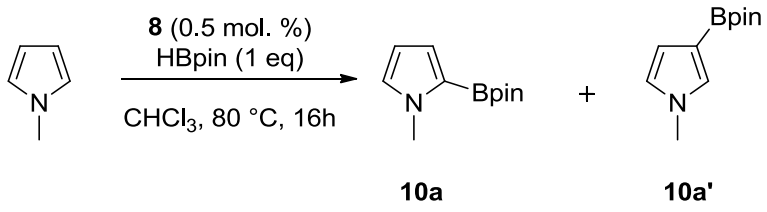

Figure 7-20: Borylation of 1-methylpyrrole catalyzed by **8** at 1 mol.%.

The catalyst loading for the borylation of 1-methylpyrrole could be decreased to 0.5 mol. **%**. To assess this, we performed the catalytic reaction using 0.2 mL of our 0.305 M stock solution of catalyst. 1-methylpyrrole (109 µL, 99.1 mg, 1.22 mmol) and HBpin (177 µL, 156 mg, 1.22 mmol) were subsequently added by pipet and the sealed vial was heated to 80 °C with stirring. A conversion of 92 % was observed by NMR after 16 hours and 182 mg (72 %) of a 86:14 mixture of **10a** and **10a'** was isolated as a white solid.

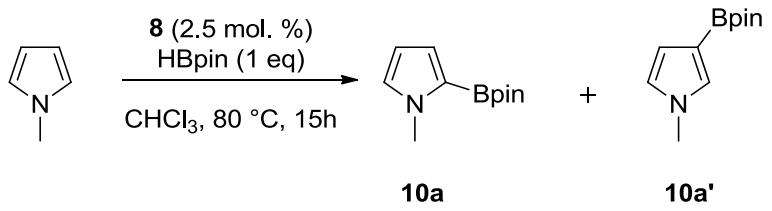

Figure 7-21: Large scale borylation of 1-methylpyrrole catalyzed by **8**.

The reaction was scaled up: in a glovebox, **8** (257 mg, 1.12 mmol) was introduced in a Schlenk tube and dissolved in *ca.* 100 mL of $CHCl_3$. HBpin (2.87 g, 22.4 mmol) and 1-methylpyrrole (2,00 g, 24.7 mmol) were subsequently added. The closed Schlenk was heated to 80 °C under a flow of N_2 for 15 hours. After 15 hours, the reaction mixture was cooled down and an aliquot was analyzed by ^1H NMR. This analysis showed a conversion of 90 % as showed by the pinacol resonances (see below). The mixture was then vacuum-filtered through a pad of silica, which was rinsed with CH_2Cl_2. Evaporation of the volatiles afforded the borylated products as a white solid (3.76 g, 81%).

Borylation of 1-benzylpyrrole

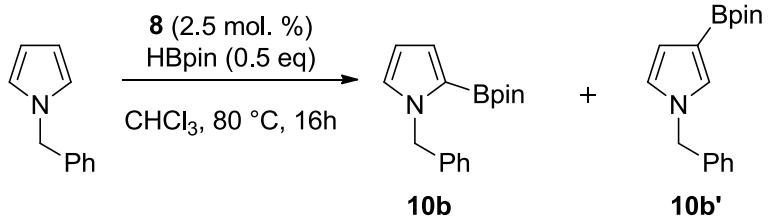

Figure 7-22: Borylation of 1-benzyllpyrrole catalyzed by **8**.

The general procedure was followed with 1-benzylpyrrole (377 µL, 384 mg, 2.44 mmol) and HBpin (177 µL, 156 mg, 1.22 mmol). Complete conversion was observed by NMR and 311 mg (90 %) of a 3:2 mixture of 1-benzyl-2-(4,4,5,5-tetramethyl-1,3,2-dioxaborolan-2-yl)pyrrole and 1-benzyl-3-(4,4,5,5-tetramethyl-1,3,2-dioxaborolan-2-yl)pyrrole was obtained after thorough evaporation of volatiles as a colorless oil which rapidly became light pink. NMR characterization was conform to that of the reported compound for 1-benzyl-3-(4,4,5,5-tetramethyl-1,3,2-dioxaborolan-2-yl)pyrrole.[370] 1-benzyl-2-(4,4,5,5-tetramethyl-1,3,2-dioxaborolan-2-yl)pyrrole is a new compound. M^+: 283.2 (calc.: 283.17).

1-benzyl-2-(4,4,5,5-tetramethyl-1,3,2-dioxaborolan-2-yl)pyrrole (**10b**): ^{1}H NMR (400 MHz, chloroform-*d*) δ 7.30 – 7.17 (m, 3H), 7.12 – 7.06 (m, 2H), 6.89 (dd, *J* = 2.4, 1.6 Hz, 1H), 6.86 (dt, *J* = 3.6, 1.9 Hz, 1H), 6.23 – 6.19 (m, 1H), 5.39 (s, 2H), 1.24 – 1.21 (m, 13H)

1-benzyl-3-(4,4,5,5-tetramethyl-1,3,2-dioxaborolan-2-yl)pyrrole (**10b'**): ^{1}H NMR (400 MHz, chloroform-*d*) δ 7.36 – 7.26 (m, 3H), 7.17 – 7.12 (m, 3H), 6.73 – 6.68 (m, 1H), 6.51 (dd, *J* = 2.6, 1.7 Hz, 1H), 5.06 (s, 2H), 1.31 (s, 12H);

Mixture: ^{13}C{^{1}H} NMR (126 MHz, chloroform-*d*) δ 139.8, 137.7, 130.4, 128.9, 128.5, 127.9, 127.7, 127.5, 127.2, 127.0, 122.4, 122.3, 114.6, 109.1, 83.3, 82.9, 53.5, 52.9, 25.0, 24.8; ^{11}B{^{1}H} NMR (160 MHz, chloroform-*d*): δ 27.8.

Borylation of 1-(triisopropylsilyl)pyrrole

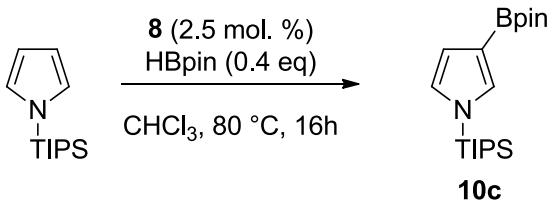

10c

Figure 7-23: Borylation of 1-(triisopropyl)pyrrole catalyzed by **8**.

The general procedure was followed with 1-(triisopropylsilyl)pyrrole (305 µL, 321 mg, 2.44 mmol) and HBpin (177 µL, 156 mg, 1.22 mmol). Complete conversion was observed by NMR and 342 mg (98 %) of 1-triisopropylsilyl-3-(4,4,5,5-tetramethyl-1,3,2-dioxaborolan-2-yl)pyrrole was obtained as a colorless solid after thorough evaporation of the volatile under vacuum. NMR characterization was conform to that of the reported product.[196] M^{+}: 349.3 (calc.: 349.26).

^{1}H NMR (500 MHz, chloroform-*d*) δ 7.23 (br. s, 1H), 6.81 (m, 1H), 6.62 (m, 1H), 1.46 (sept, J = 7.3 Hz, 3H), 1.32 (s, 12H), 1.09 (d, J = 7.3 Hz, 18H); ^{13}C{^{1}H} NMR δ (126 MHz, chloroform-*d*) δ 133.8, 125.1, 115.7, 82.9, 25.0, 18.0, 11.8; ^{11}B{^{1}H} NMR δ (160 MHz, chloroform-*d*): 30.0.

Borylation of 1-(trimethylsilyl)pyrrole

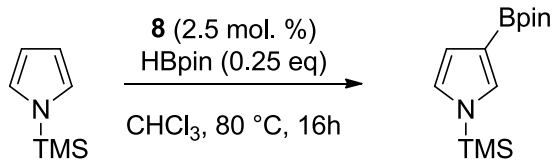

10d

Figure 7-24: Borylation of 1-(trimethyl)pyrrole catalyzed by **8**.

The general procedure was followed with 1-(trimethylsilyl)pyrrole (680 mg, 4.89 mmol) and HBpin (177 µL, 156 mg, 1.22 mmol). A conversion of 75 % was observed by NMR and 342 mg (98 %) of 1-trimethylsilyl-3-(4,4,5,5-tetramethyl-1,3,2-dioxaborolan-2-yl)pyrrole was obtained as a colorless solid after thorough evaporation of the volatile under vacuum. M^+: 265.1 (calc.: 265.17).

^{1}H NMR (400 MHz, chloroform-*d*) δ 7.28 (m, 1H), 6.83 (t, J = 2.2, 1H), 6.63 (m, 1H), 1.35 (s, 12H), 1.32 (s, 12H), 0.42 (9H); ^{13}C{^{1}H} NMR (126 MHz, chloroform-*d*) δ 132.9, 124.0, 116.3, 83.0, 77.2, 25.0, -0.2; ^{11}B{^{1}H} NMR (160 MHz, chloroform-*d*): δ 30.0.

Borylation of 1-methylindole

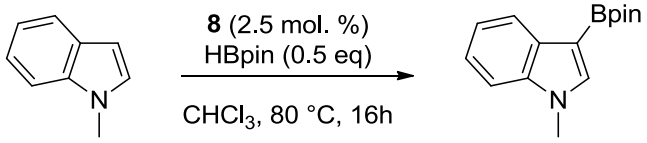

10e

Figure 7-25: Borylation of 1-methylindole catalyzed by **8**.

The general procedure was followed with 1-methylindole (305 µL, 321 mg, 2.44 mmol) and HBpin (177 µL, 156 mg, 1.22 mmol). Complete conversion was observed by NMR and 267 mg (85 %) of 1-methyl-3-(4,4,5,5-tetramethyl-1,3,2-dioxaborolan-2-yl)indole was obtained as pale yellow crystals. NMR characterization was conform to that of the reported product.[196] M^+: 257.2 (calc.: 257.16).

^{1}H NMR (400 MHz, chloroform-*d*) δ 8.04 (ddd, *J* = 7.7, 1.4, 0.8 Hz, 1H), 7.52 (s, 1H), 7.35 – 7.31 (m, 1H), 7.25 – 7.15 (m, 2H), 3.80 (s, 3H), 1.37 (s, 12H); ^{13}C{^{1}H} NMR (101 MHz,

chloroform-*d*): δ 138.6, 138.0, 132.6, 122.8, 121.9, 120.3, 109.3, 82.9, 33.1, 25.0; $^{11}B\{^{1}H\}$ NMR (160 MHz, chloroform-*d*): δ 29.7.

Monoborylation of 3,4-ethylenedioxythiophene

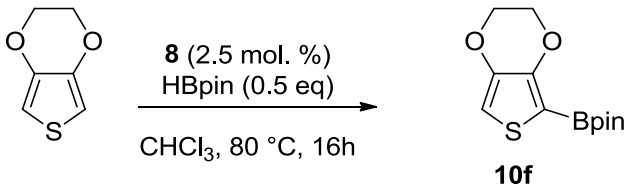

Figure 7-26: Monoborylation of 3,4-ethylenedioxythiophene catalyzed by **8**.

The general procedure was followed with 3,4-ethylenedioxythiophene (261 µL, 347 mg, 2.44 mmol) and HBpin (177 µL, 156 mg, 1.22 mmol). Complete conversion was observed by NMR and 285 mg (87 %) of 2-(4,4,5,5-tetramethyl-1,3,2-dioxaborolan-2-yl)-3,4-ethylenedioxythiophene was obtained as a white crystalline solid. NMR characterization was conform to that of the reported product.[371] M^+: 268.1 (calc.: 268.09).

^{1}H NMR (500 MHz, chloroform-*d*) δ 6.63 (s, 1H), 4.31 – 4.28 (m, 2H), 4.19 – 4.17 (m, 2H), 1.34 (s, 12H); $^{13}C\{^{1}H\}$ NMR (126 MHz, chloroform-*d*) δ 149.2, 142.5, 107.6, 84.0, 65.2, 64.4, 24.9; $^{11}B\{^{1}H\}$ NMR (160 MHz, chloroform-*d*): δ 28.2.

Diborylation of 3,4-ethylenedioxythiophene

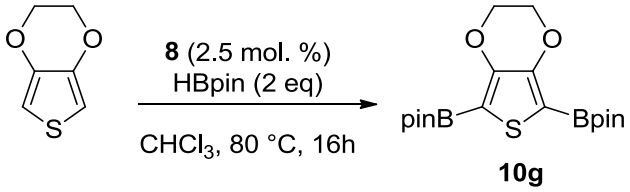

Figure 7-27: Diborylation of 3,4-ethylenedioxythiophene catalyzed by **8**.

The general procedure was followed with 3,4-ethylenedioxythiophene (65 µL, 87 mg, 0.611 mmol) and HBpin (177 µL, 156 mg, 1.22 mmol). Complete conversion was observed by NMR and 443 mg (92 %) of 2-(4,4,5,5-tetramethyl-1,3,2-dioxaborolan-2-yl)-3,4-ethylenedioxythiophene was obtained as pale yellow crystalline solid. NMR characterization was conform to that of the reported product.[372] M^+: 394.2 (calc.: 394.18).

^{1}H NMR (500 MHz, chloroform-*d*) δ 4.27 (s, 2H), 1.32 (s, 12H); ^{13}C{^{1}H} NMR (101 MHz, chloroform-*d*) δ 149.0, 84.0, 64.8, 24.9; ^{11}B{^{1}H} NMR (160 MHz, chloroform-*d*). δ 28.4.

Borylation of 2-methoxythiophene

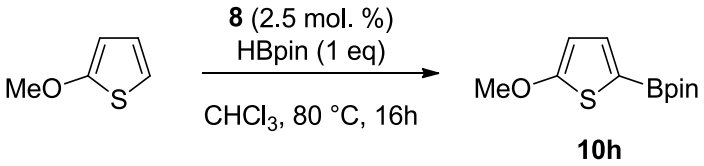

10h

Figure 7-28: Borylation of 2-methoxythiophene catalyzed by **8**.

The general procedure was followed with 2-methoxythiophene (123 µL, 140 mg, 1.22 mmol) and HBpin (177 µL, 156 mg, 1.22 mmol). Complete conversion was measured by NMR and 249 mg (85 %) of 2-(4,4,5,5-tetramethyl-1,3,2-dioxaborolan-2-yl)-5-methoxythiophene was obtained as pale yellow oil. M^{+}: 240.1 (calc.: 240.13).

^{1}H NMR (400 MHz, chloroform-*d*) δ 7.33 (d, *J* = 3.9, 1H), 6.30 (dd, *J* = 3.9, 1H), 3.92 (s, 3H), 1.32 (s, 12H); ^{13}C{^{1}H} NMR (126 MHz, chloroform-*d*) δ 173.0, 136.6, 106.3, 83.9, 60.5, 24.9; ^{11}B{^{1}H} NMR (160 MHz, chloroform-*d*): δ 28.7.

Borylation of furan

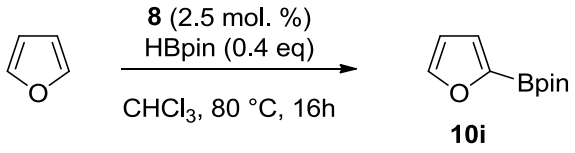

10i

Figure 7-29: Borylation of furan catalyzed by **8**.

The general procedure was followed with furan (222 µL, 208 mg, 3.06 mmol) and HBpin (177 µL, 156 mg, 1.22 mmol). A conversion of 79 % conversion was measured by NMR after 36 hours and 203 mg (80 %) of 2-(4,4,5,5-tetramethyl-1,3,2-dioxaborolan-2-yl)methylfuran was obtained as pale yellow oil. NMR characterization was conform to that of the reported product.[373] M^{+}: 194.1 (calc.: 194.11).

^{1}H NMR (400 MHz, chloroform-*d*) δ 7.65 (dd, J = 1.7, 0.6, 1H), 7.07 (dd, J = 3.4, 0.6, 1H), 6.62 (dd, J = 3.4, 1.7, 1H), 1.35 (s, 12H); ^{13}C{^{1}H} NMR (126 MHz, chloroform-*d*) δ 147.5, 123.4, 110.5, 84.4, 77.2, 24.9; ^{11}B{^{1}H} NMR (160 MHz, chloroform-*d*): δ 27.3.

Borylation of 2-methylfuran

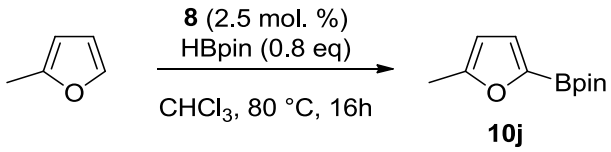

Figure 7-30: Borylation of 2-methylfuran catalyzed by **8**.

The general procedure was followed with 2-methylfuran (132 µL, 120 mg, 1.47 mmol) and HBpin (177 µL, 156 mg, 1.22 mmol). Complete conversion was measured by NMR and 203 mg (80 %) of 2-(4,4,5,5-tetramethyl-1,3,2-dioxaborolan-2-yl)-5-methylfuran was obtained as pale yellow oil. NMR characterization was conform to that of the reported product.[192] M^{+}: 208.1 (calc.: 208.13).

^{1}H NMR (500 MHz, chloroform-*d*) δ 6.99 (dd, *J* = 3.2, 0.6 Hz, 1H), 6.03 (dq, *J* = 3.2, 0.9 Hz, 1H), 2.36 – 2.35 (br. s, 3H), 1.34 (s, 12H); ^{13}C{^{1}H} NMR (101 MHz, chloroform-*d*) δ 157.9, 125.0, 107.0, 84.2, 24.9, 14.1; ^{11}B{^{1}H} NMR (160 MHz, chloroform-*d*): δ 27.1.

Borylation of 2-tertbutylfuran

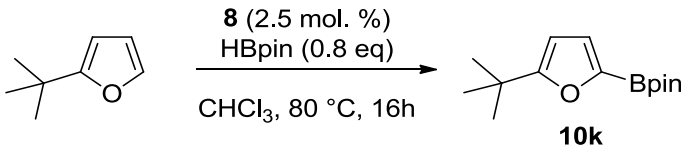

Figure 7-31: Borylation of 2-tertbutylfuran catalyzed by **8**.

The general procedure was followed with 2-*tert*butylfuran (209 µL, 182 mg, 1.47 mmol) and HBpin (177 µL, 156 mg, 1.22 mmol). Complete conversion was measured by NMR and 258 mg (86 %) of 2-(4,4,5,5-tetramethyl-1,3,2-dioxaborolan-2-yl)-5-*tert*Butylfuran was obtained as pale yellow oil. M^{+}: 250.2 (calc.: 250.17).

^{1}H NMR (400 MHz, chloroform-*d*) δ 6.98 (d, *J* = 3.3 Hz, 1H), 6.02 (d, *J* = 3.3 Hz, 1H), 1.33 (s, 12H), 1.31 (s, 9H); ^{13}C{^{1}H} NMR (101 MHz, chloroform-*d*) δ 169.9, 124.8, 103.3, 84.0, 77.2, 33.1, 29.3, 24.9; ^{11}B{^{1}H} NMR (160 MHz, chloroform-*d*): δ 27.4.

Borylation of 2-methoxyfuran

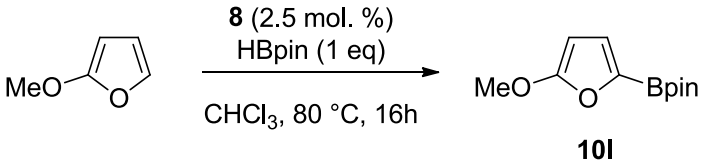

10l

Figure 7-32: Borylation of 2-methoxyfuran catalyzed by **8**.

The general procedure was followed with 2-methoxyfuran (113 µL, 120 mg, 1.22 mmol) and HBpin (177 µL, 156 mg, 1.22 mmol). After 16 hours, a 74 % conversion was measured by NMR and 170 mg (62 %) of 2-(4,4,5,5-tetramethyl-1,3,2-dioxaborolan-2-yl)-5-methoxyfuran was obtained as pale yellow oil. Although the product could be isolated and characterized, we found that it decomposed after a few hours at room temperature in chloroform-*d*. Its sensitivity presumably explains the lower yields obtained. The pure product can be kept for longer periods at low temperature in the dark. M^{+}: 224.1 (calc.: 224.12).

^{1}H NMR (400 MHz, chloroform-*d*) δ 7.00 (d, *J* = 3.4, 1H), 5.22 (d, *J* = 3.4, 1H), 3.87 (s, 3H), 1.32 (s, 12H); ^{13}C{^{1}H} NMR (126 MHz, chloroform-*d*) δ 126.5, 110.1, 84.0, 81.5, 58.0, 24.9; ^{11}B{^{1}H} NMR (160 MHz, chloroform-*d*): δ 26.9.

Borylation of 2-silyloxyfuran

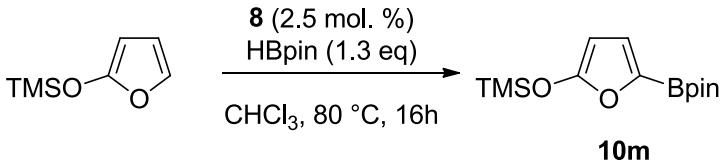

10m

Figure 7-33: Borylation of 2-silylfuran catalyzed by **8**.

The general procedure was followed on a smaller scale with 2-silyloxyfuran, (127.5 mg, 0.816 mmol) and HBpin (154 µL, 135 mg, 1.06 mmol) were added to 0.66 mL of the stock solution (0.0202 mmol of **8**). After 16 hours, a quantitative conversion was measured by NMR and 190 mg (84 %) of 2-(4,4,5,5-tetramethyl-1,3,2-dioxaborolan-2-yl)-5-silyloxyfuran was obtained as

a yellow oil. Although the product could be isolated and characterized, we found that it tended to decompose under ambient conditions. M^+: 282.2 (calc.: 282.15).

^{1}H NMR (400 MHz, chloroform-*d*) δ 6.96 (d, *J* = 3.3, 1H), 5.18 (d, *J* = 3.3, 1H), 1.31 (s, 12H), 0.30 (s, 9H); ^{13}C{^{1}H} NMR (101 MHz, chloroform-*d*) δ 126.4, 110.2, 85.5, 83.9, 24.9, -0.1; ^{11}B{^{1}H} NMR (160 MHz, chloroform-*d*): δ 26.7.

Borylation of 3-bromofuran

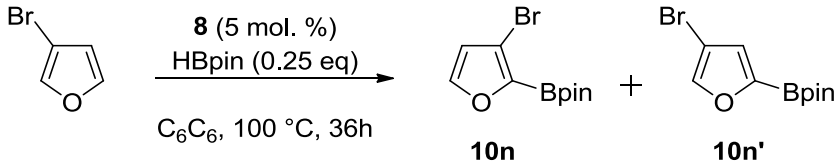

Figure 7-34: Borylation of 3-bromofuran catalyzed by **8**.

8 (2.1 mg, 0.045 mmol, 5 mol. %), 3-bromofuran (32.9 µL, 53.9 mg, 0.367 mmol), hexamethylbenzene (1.4 mg, 0.0086 mmol) and HBpin (12.8 µL, 11.7 mg, 0.0916) were dissolved in benzene-d_6 (0.4 mL) and placed in a J-Young tube. This mixture was heated to 100 °C for 36 hours before being analyzed by ^{1}H NMR to reveal a 90 % conversion to **3n** and **3n'**. The contents of the tube were then passed through a short pad of silica and the vaolatiles of the filtrate were evaporated *in vacuo*. 26.4 mg of a yellow oil were thus collected, which contained the starting hexamethylbenzene. By substracting the mass of starting hexamethylbenzene, we calculate a yield of 79 % (25.0 mg). M^+: 272.1 (calc.: 272.02).

2-(4,4,5,5-tetramethyl-1,3,2-dioxaborolan-2-yl)-3-bromofuran (**10n**): ^{1}H NMR (400 MHz, chloroform-*d*) δ 7.54 (m, 1H), 6.50 (m, 1H), 1.36 (s, 12H).

2-(4,4,5,5-tetramethyl-1,3,2-dioxaborolan-2-yl)-4-bromofuran (**10n'**): ^{1}H NMR (400 MHz, chloroform-*d*) δ 7.61 (m, 1H), 7.05 (m, 1H), 1.34 (s, 12H).

Mixture: ^{13}C{^{1}H} NMR (101 MHz, chloroform-*d*) δ 147.8, 145.7, 126.0, 115.1, 110.1, 84.7, 84.6, 24.9, 24.9; ^{11}B{^{1}H} NMR (160 MHz, chloroform-*d*): δ 26.7.

Unreactive substrates

While many heteroaromatic substrates could be successfully borylated, we found that some electron-poor five-membered heteroarenes were unreactive in our reaction condition. Both 1-

phenylpyrrole and tert-butyl 1-pyrrolecarboxylate (1-(BOC)pyrrole) are inert towards both C-H activation by **8** and catalytic borylation, presumably because of the electron-withdrawing properties of the substituting groups on pyrrole.

Similarly, no catalytic results were obtained with methyl-2-furylketone. The electron withdrawing properties of the ketone substituent result once again in loss of activity. In addition, a small amount of hydroboration products can be observed in the reaction mixture.

Unsubstituted thiophene also could not be borylated or activated. DFT calculations predict a higher activation barrier for it than for other heterarenes. These findings can be rationalized by considering the higher electron delocalisation in thiophene which diminishes the nucleophilicity of each position.

7.6.5 Isotopic Labelling Experiments

Competitive stoichiometric C-H activation of 1-methylpyrrole and 1-methylpyrrole-d_4

Figure 7-35: Competitive C-H activation of 1-methylpyrrole and 1-methylpyrrole-*d*$_4$ by **8**.

8 (26.3 mg, 0.057 mmol) and hexamethylbenzene (7.6 mg, 0.047 mmol) in *ca.* 0.5 mL chloroform-*d* were introduced in a J-Young NMR tube. 10.2 µL (9.3 mg, 0.11 mmol) of each 1-Methylpyrrole and 1-methylpyrrole-*d*$_4$ was added by pipet. Immediate ^{1}H NMR analysis showed that the actual H/D ratio in 1-Methylpyrrole at the start was 43:57. After heating the mixture to 80 °C for 16 hours, ^{1}H NMR showed a H/D ratio in 2a of 57:43. A KIE k_H/k_D = 1.8 can be calculated for this reaction considering the starting ratio of products.

Warning: long relaxation times (60 s) have to be allowed for correct quantitative analysis.

Competitive catalytic borylation of 1-methylpyrrole and 1-methylpyrrole-d_4

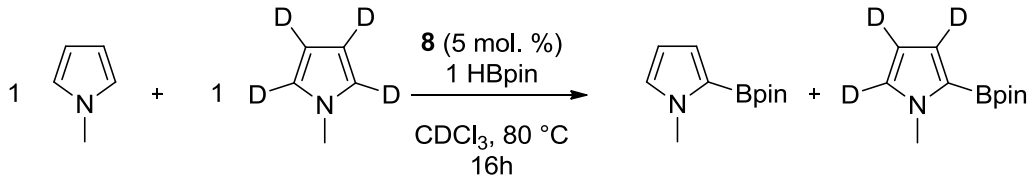

Figure 7-36: Competition experiment for the borylation of 1-methylpyrrole and 1-methylpyrrole-*d*$_4$ by **8**.

0.4 mL of the chloroform-*d* stock solution of catalyst (2.06 mg of **8**) was introduced in a J-Young NMR tube along with HBpin (26.1 µL, 23.0 mg, 0.180 mmol) and 15.9 µL (14.6 mg, 0.18 mmol) of each 1-methylpyrrole and 1-methylpyrrole-*d*$_4$. The resulting mixture was heated to 80 °C for 16 hours and analyzed by ^{1}H NMR (warning: long relaxation times have to be

allowed for correct quantitative analysis). A 65:35 H:D ratio was measured in the end product, while a ratio of 35:65 was found for the starting material, indicating that the catalytic borylation occurred with a KIE k_H/k_D = 1.9.

7.7 Computational Details

General Information: All the calculations were performed on the full structures of the reported compounds. Calculations were performed with the GAUSSIAN 09 suite of programs.(42) The ωB97XD functional[354] was qualified as promising by Grimme[353] and was used to accurately describe the mechanism of FLP mediated hydrogenation of alkynes which implies protodeborylation[62] and was thus used in combination with the 6-31G** basis set for all atoms.[321,322] The transition states were located and confirmed by frequency calculations (single imaginary frequency). The stationary points were characterized as minima by full vibration frequencies calculations (no imaginary frequency). All geometry optimizations were carried out without any symmetry constraints. The energies were then refined by single point calculations to include solvent effects using the SMD solvation model[325] with the experimental solvent, chloroform as well as benzene at the ωB97XD /6-31+G** level of theory.[324]

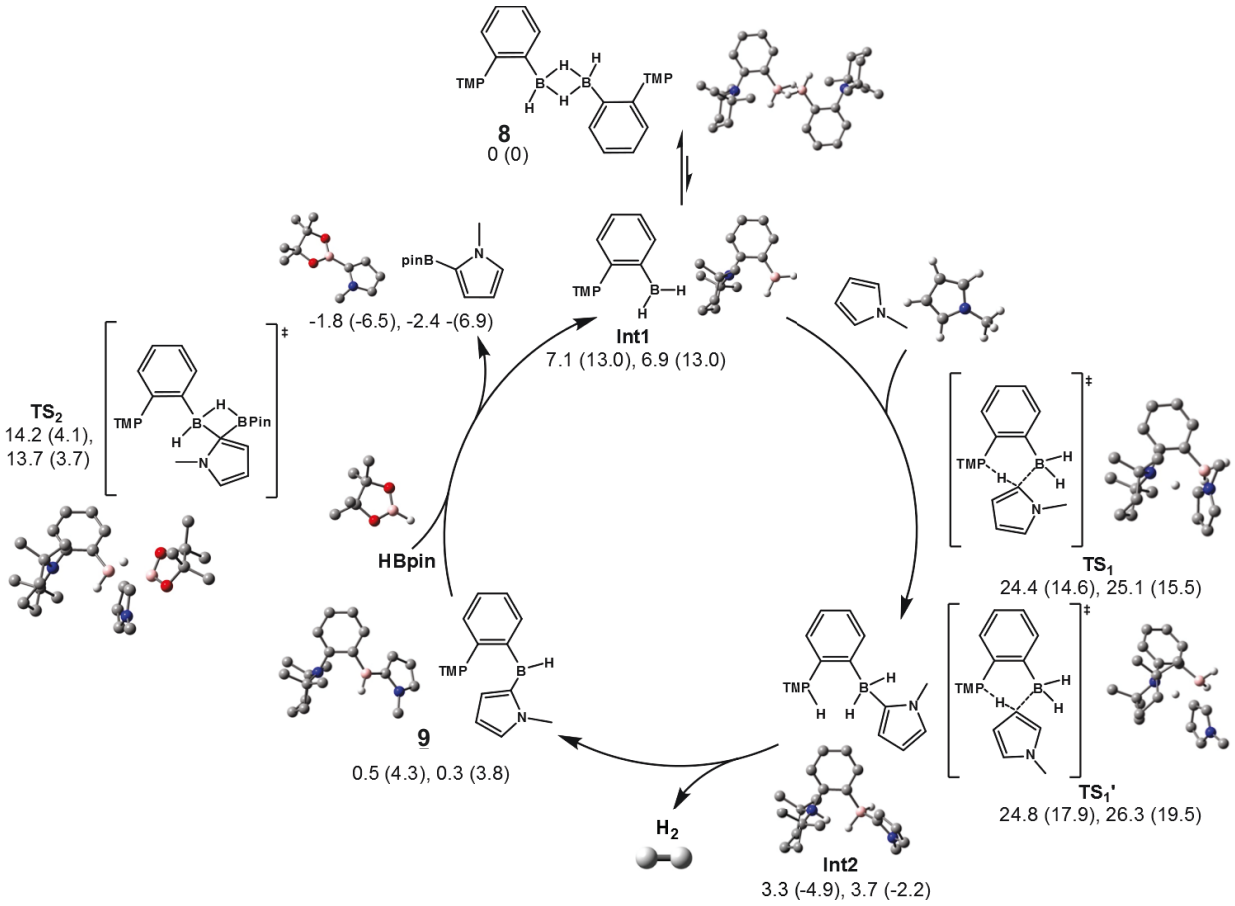

Figure 7-37: Calculated energies (ωb97xd-6-31+G**)(and enthalpies) for the catalytic cycle for the borylation of 1-methylpyrrole

ACKNOWLEDGEMENTS

We acknowledge the contribution of N. Bouchard and J. Légaré-Lavergne in the preparation of some compounds and discussions with S. A. Westcott and P. McBreen. We acknowledge D. Larivière and L. Whitty-Léveillé for the ICP-MS analyses and P. Audet for his technical help. The work was supported by the National Sciences and Engineering Research Council of Canada (NSERC) and the Centre in Green Chemistry and Catalysis (CGCC, Québec). Computational studies were made possible by Compute Canada. M.-A.L., M-A.C. and E. R. acknowledge NSERC and Fonds de Recherche Nature et Technologies (FRQNT) for scholarships.

Chapter 8 - Conclusion and Perspectives

In this dissertation, we have described and formulated processes by which Lewis bases modify and activate the reactivity of specially designed organoboron molecules. Amongst these processes, two mechanisms are outstanding: the electron transfer of the base to the organoboryl by coordination and the collaborative reactivity of unquenched acidic boranes and Lewis bases. In some cases, both mechanisms can be combined in order to mediate difficult reactions.

In our first case study, we have found that the reactivity of Lewis base adducts of borabenzene is dominated by a nucleophilic character. This character comes from the fact that the boron atom of borabenzene adduct is electronically saturated. Because of the low electronegativity of boron, the electron density of the base is delocalized into the aromatic cycle to make the ortho and para position of borabenzene particularly nucleophilic. For this reason, the aromatic cycle can be protonated, a process that is necessary for ligand exchange reactions to take place at boron. Furthermore, the electron richness of borabenzene is further highlighted in our study of its bonding with different bases that demonstrate its strong π-donor character.

We have also applied our work to the study of new catalysts for the reduction of carbon dioxide. We have reported phosphine-borane compounds as the most efficient homogeneous catalysts for the reduction of CO_2 to methanol derivatives. Our initial disclosure of these results took place in 2013 and the catalytic activity then reported has yet to be surpassed. The mechanism of action of the catalyst was found to rely on simultaneous activation of boranes by a phosphine moiety and of CO_2 by a boryl group. This reaction mode was successful in producing formaldehyde that, trapped by the catalyst, became an even more active catalyst. This mode of action highlights a double form of base-borane collaboration and makes our catalyst extremely active.

Similar catalytic efficiencies could not be reached using only Lewis bases instead of an ambiphilic catalyst. We found that bidentate bases – such as terpyridine or proton sponge - had the potential to activate borane-dimethylsulfide in an interesting way that involved the transfer of a hydride from one borane to another, effectively generating a boronium-borohydride ion pair. The borohydride anion thus formed is a strong reducing agent capable of converting carbon dioxide to formate. This mode of activation is in fact very interesting when

it is considered as a *remote* base-borane activation: the base activates not the boron to which it binds, but a second equivalent of borane.

Finally, we have found a completely new application for Frustrated Lewis Pairs in showing that they could cleave heteroaryl C-H bonds. Frustrated Lewis Pairs represent a pure expression of base-acid cooperation that had hitherto been mostly applied to hydrogen activation and catalytic hydrogenation. We reported, however, a catalyst for the borylation of heteroarenes, a reaction that is, as of today, almost exclusive to precious metal catalysts.

As a whole, our results show the power of the collaborative reactivity that is present in FLP chemistry. While we have presented examples of base enhancement of reactivity by coordination, our most impressive results were obtained with unquenched base-borane catalysts. With the goal of developing novel catalytic reactions that do not rely on metals, our results have shown the potential of main group elements to perform complex transformations when they are in suitable environments. Replacing traditional stoichiometric chemistry, as well as well-established precious metal catalysis with processes mediated only by non-toxic inexpensive main group elements, requires the development of new concepts and of new ways of thinking, as well as the subtle understanding of the behavior of these atoms. Frustrated Lewis Pair chemistry is one of such concept that, I believe, is called to play an important role in the future of green chemistry. While we did not invent this FLP concept, I hope that what we have learned in the study of ambiphilic molecules and may have contributed a little to the field. In the next paragraphs, I would like to succinctly expose what we have learned as a formulation of this doctoral thesis. While these ideas are not necessarily novel, they have developed new expressions in the course of research.

- Frustrated Lewis Pairs, or more fundamentally acid-base collaboration, use two (or more) atoms to perform many-electron processes that are otherwise impossible for main group elements.

Indeed, with their many d-orbitals that act together, precious metals possess a unique reactivity. One of the only ways for light elements of the main group to emulate their chemistry is by collaborative strategies. With, for example, an empty orbital from a boron atom and the lone pair of a nitrogen atom, an ambiphilic molecule can create a site in which the particular electronic environment is suitable to perform complex processes (**Figure 8-1**).

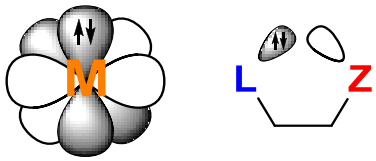

Figure 8-1: Analogy between the active orbitals of a transition-metal catalyst and that of an ambiphilic molecule.

Just like in transition metal complexes—or in enzymes—the modification of the steric or electronic properties of this active site will have tremendous effect on the substrates they can activate. Moving from the cleavage of molecular hydrogen to that of aryl C-H bonds is one of the most simple of such modifications. The future will surely see further development of FLP chemistry.

- The activity of an acid or a base is greater in a FLP system than the summed activity of the separate fragments.

This apparently trivial statement is still worth mentioning as it is the thermodynamic basis of FLP chemistry. It is possible to work on FLP reactivity without considering the underlying concept behind the reactivity. This concept is simple and can be formulated as above. For example, a Brønsted base, can deprotonate a substrate by stabilizing a proton more than the original molecule. In a FLP type reaction, on the other hand, the Lewis acid simultaneously stabilizes the deprotonated fragment. Thermodynamically, the latter case will be more favored, even using weaker bases and acids. Hence the catalytic possibilities coming from FLP chemistry: each fragment of the cleaved species is *individually* less strongly bound to the catalytic system and can be transferred to a substrate (**Figure 8-2**).

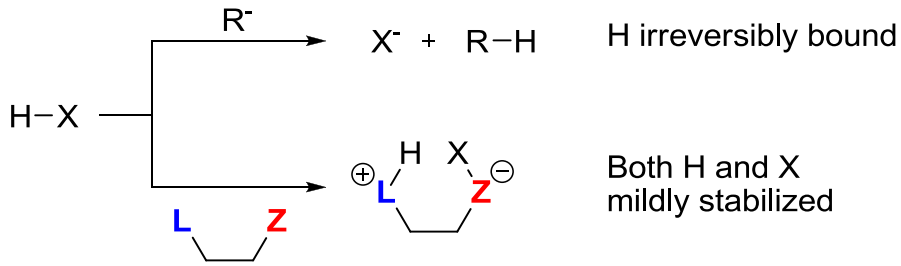

Figure 8-2: Comparison between the deprotonation of a substrate by a strong base and the use of FLPs to cleave the HX bond.

- All reaction steps in a catalytic cycle do not have to be thermodynamically downhill, but have to be kinetically accessible.

This concept is well recognized by chemists and is fundamental to reactivity as we know it. However, in the case of FLP chemistry, it surprisingly took time to be used. Indeed, many early reports on FLP systems looked for *observable* H_2 cleavage as a prerequisite to FLP-mediated reactions. The observability of an intermediate is, however, only an indication of it being downhill of the starting material. In many cases, the formation of H_2 activation intermediate can be endergonic, while still being important and relevant to a hydrogenation reaction, as was demonstrated in recent reports. This effect was also illustrated in the case of our endergonic C-H activation chemistry in which we never observed the C-H bond cleavage intermediate.

Finally, our main contribution to the advancement of chemical knowledge is the demonstration that main group elements can, in the form of Frustrated Lewis Pairs, activate and catalytically functionalize C-H bonds. We hope to continue to promote this reactivity as much research is still needed to fully appreciate the possibilities offered by FLP-mediated C-H activation.

8.1 Ongoing and Future Work

I propose that research focused on the topic of C-H activation should be conducted along three axes:

1. Expansion of the scope of substrates that can undergo C-H bond cleavage.
2. Development of new catalytic functionalization reactions based on FLP C-H bond cleavage.

3. Optimization of the FLP framework for convenient and efficient use by synthetic chemists.

8.1.1 Expansion of the Scope of Substrates That Can Undergo C-H Bond Cleavage

One limitation of our catalytic system in its current form is its need for electron-rich substrates. While this selectivity is interesting as a complement to transition metal systems that favor the activation of acidic C-H bonds, it remains lacking in generality. For this reason, we consider it to be of prime importance to increase the scope of the reaction through the modification of the catalyst. Work that we have already performed allows us to identify several prospective approaches to that end. In fact, we aim to diminish the energy barrier of the limiting C-H activation step. This would allow the system to not only perform the reaction at higher rate, but also to activate more inert substrates.

First, as we previously concluded computationally, the existence of our catalyst as a stable dimer in solution prevents us from activating certain substrates. Before the discovery of the catalytic system, we had predicted that **8**, as a monomeric unit possessing an intramolecular N-B bond should be suitable for the C-H activation of thiophene. Unfortunately, with the dimeric form being 7.1 $kcal.mol^{-1}$ more stable than our proposed active form, only more reactive substrates can undergo bond cleavage. Thus, it is rational to envision that inhibiting the formation of dimer would be a step towards the goal of activating new substrates.

Towards this first objective, an approach consisting of the inclusion of steric bulk around the boron atom would potentially prevent the formation of H-bridged dimers. In fact, we have already identified several possible conformations of ambiphilic amine-borane catalysts as dimers and monomers. Catalyst dimer has to favor the existence of monomeric forms in the reaction medium in order to maximize the scope of the reaction. With such a design a significant thermodynamic “sink” can be avoided by simply increasing the bulk at boron. As can be seen in **Figure 8-3**, a certain amount of bulk has to remain on the amine to avoid the formation of head-to-tail dimers.

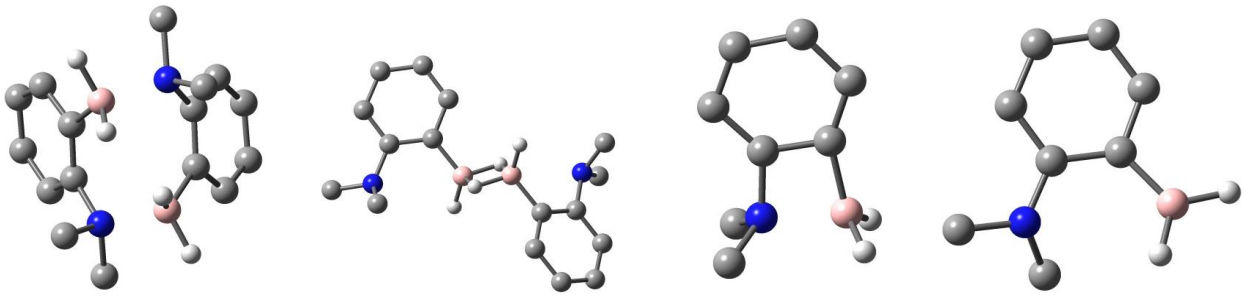

0 (0) **7.2 (12.5)** **12.5 (29.6)** **18.3 (37.0)**

Figure 8-3: Calculated free energies (enthalpies) (kcal.mol^{-1}) for different forms of phenylene-bridged NMe_2-BH_2, at the ωB97xd/ ωB97XD /6-31+G** level of theory, highlighting the thermodynamic sinks that can arise from the formation of dimers or closed forms.[351]

For the borylation reaction, a few key criteria have to be respected with regard to the design of the catalyst:

- A hydride has to remain as a group on boron as it has an active role in the catalytic cycle in the elimination of H_2.
- The steric bulk should not prevent the approach of the arene.
- The important groups at boron should not be susceptible to borylation themselves.

Since electron-rich aryl fragments are prone to migration, they should not be used as functional groups on the boron atom as they could be lost by borylation during the reaction. Alkyl groups are less susceptible to borylation.

Next, as our computational studies have shown, the electronic properties of the boron atom on the catalyst have the greatest impact on its potency. The C-H activation barrier is expected to be lower with increased Lewis acidity on the boron atom. As such special attention should be given to the design of the boryl moiety of the catalyst. For the borylation reaction, one electron withdrawing group should be present on the boron atom in addition to the hydride. Unfortunately, fluoroalkylboranes are known not to be stable because of β-F elimination and α-F exchange. Consequently, alternatives should be considered, with fluroaryl groups being candidates.

While the basicity of the base seems to be of lesser importance to C-H activation, the modification of the amine group still has to be considered. We suggest that using strongly basic phosphazene could have a positive effect on C-H activation, as well as providing a

catalyst framework in which the steric and electronic properties of the base would be easy to modulate.

Finally, work has to be performed on modification of the organic backbone. This part of the catalytically active molecule is to have a tremendous effect on its reactivity and its stability. Indeed, the nature of the linking backbone regulates the distance and the angle between the active Lewis base and boron atom on the catalyst. Modulating these features through various backbones will lead to improved knowledge of the optimal properties of the active site for efficient C-H bond cleavage of different molecules. Also, while aromatic backbones have proved very stable in classical FLP chemistry, they could be active in borylation chemistry, being structurally similar to the current substrates. As we have selected more nucleophilic arenes, we have not yet observed any backbone borylation. However, as we are trying to move to less reactive substrates, it could become a side-reaction. Consequently, we are beginning to investigate the potential of alkyl linker groups as a more stable and potentially more reactive alternative to aromatic backbones.

8.1.2 Development of New Catalytic Functionalization Reactions Based on FLP C-H Bond Cleavage

While we have demonstrated the ability of boron-based FLP systems to catalyze the borylation of aromatic molecules and have proposed modifications to further improve the scope and efficiency of the reaction, we believe that FLP C-H activation principles should be applied to the mediation of other reactions.

A first class of catalytic reaction that can be envisioned easily includes analogs of the borylation that may proceed through the same mechanism. The most simple of the proposed reactions is dehydrogenative alumination. Indeed, neutral aluminum hydrides, such as commercially available diisobutylaluminum hydride can putatively be involved in σ-bond metathesis in a manner analogous to hydroboranes. Arylaluminum compounds have a rich and interesting reactivity as they can undergo various coupling reactions without the use of a catalyst. Forming them in a transition metal-free C-H functionalization protocol would represent a green way to produce these useful reagents. In fact, we are looking to develop methods of one-pot alumination and coupling of arenes into various chemicals, including alcohol and biaryls.

We also propose to study the more challenging silylation reaction. While arylsilanes are of more limited synthetic use, silicium precursors are typically found as extremely cheap reagents. The direct metal-free silylation of arenes thus represents a potential large-scale entry into functionalized organic chemicals. Hydrosilanes are, however, typically less reactive than hydroboranes or aluminum hydrides. We consequently are working on silane activation protocols with the goal of performing the catalytic C-H silylation of aromatic molecules.

One last reaction of this kind that we propose to study is stannylation. Unfortunately, while very useful, organostannanes are both toxic and environmentally damaging. Their use is obviously incompatible with green processes. However, hydrostannane reactivity is predominantly based on radicals. It thus is a convenient platform on which to study the behavior of our FLP catalyst in the context of radical chemistry.

The next class of reactions that we propose to investigate is based on classical stoichiometric organoboron chemistry. In fact, after C-H activation of one electron-rich aromatic molecule and elimination of one H_2 molecule, our catalyst is formally an organoborane possessing a nucleophilic aryl group. The chemistry of such compounds has been investigated in depth during the XX^e century. Mechanisms based on the coordination of a substrate followed by 1,2-migration (as have been described in the introduction) have been described for many substrates and organoboranes. These reactions are stoichiometric in nature as the organoboranes that are used in them are preemptively prepared in stoichiometric reactions, usually from organometallic reagents. Our process, however, is a mild way to generate arylboranes directly from arenes. If the catalyst delivers its aryl group to a substrate, catalytic activity can potentially be achieved (**Figure 8-4**).

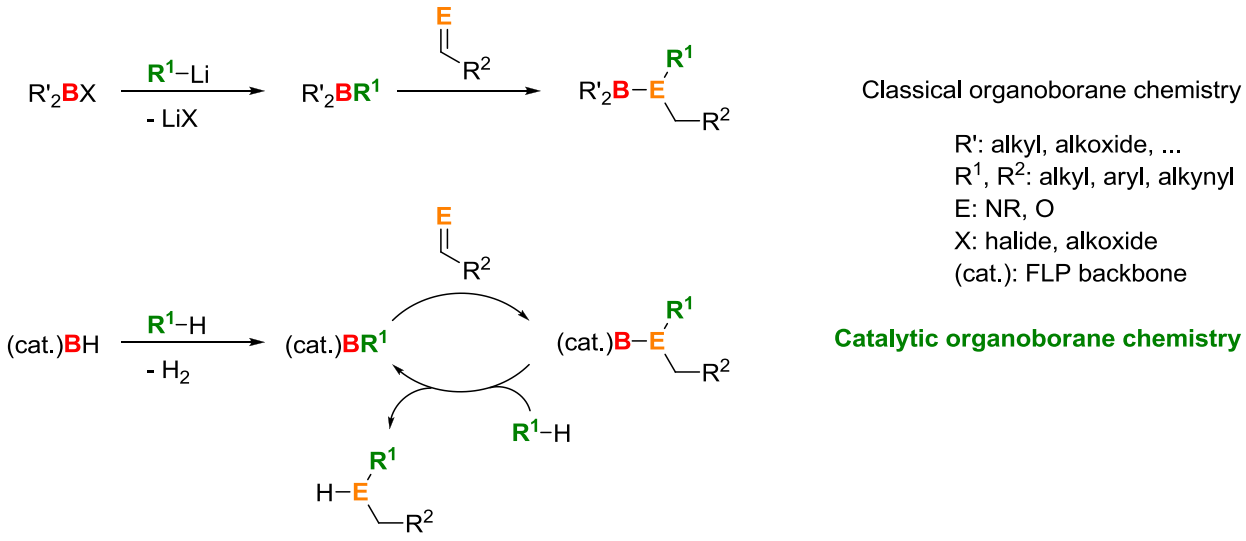

Figure 8-4: Possible parallel between classical organoboron chemistry and catalytic applications of boron-based FLPs.

However, with this kind of stoichiometric 1,2-migration mechanism, stable boron compounds are typically produced. B-O and B-N bonds that are typically formed are very stable. For this reason, we are working on the design of inexpensive and green “scrubbing” systems based on the use of silane to remove the end product from the boron atom of the catalyst.

In this class of reactions, we also propose the amination reaction. Hydroxylamines are very common building blocks for synthetic chemistry that provide access to electrophilic nitrogen groups. We propose that such compounds could react with FLP activated arenes to give arylamines, with a hydroxyl group left on boron. In combination with our scrubbing system, the reaction could be catalytic (**Figure 8-5**).

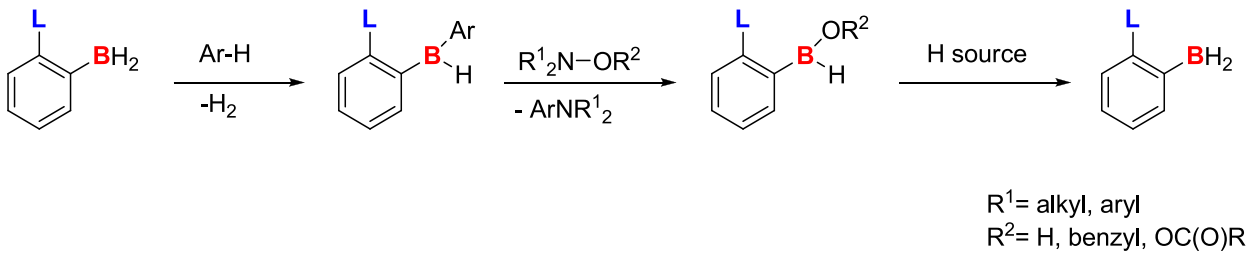

Figure 8-5: Proposed entry into amination reactions mediated by ambiphilic organoboron catalysts.

Organoboranes are also much more nucleophilic than their unsubstituted counterparts. Studies have shown that, as such, they could add to electron-deficient unsaturated bonds. This kind of reaction should also be investigated using amine-borane activated arenes as organoboranes.

The same studies have shown that anionic tetravalent arylborates were even stronger nucleophiles. Consequently, we also propose to design and study FLP systems that do not possess leaving groups—i.e. ambiphilic molecules that will not release H_2 upon C-H bond activation. If the C-H activation intermediate is accessible, it should constitute a highly activated aryl group that should be transferable in reactions of great interest like nucleophilic aromatic substitution or nucleophilic additions (**Figure 8-6**).

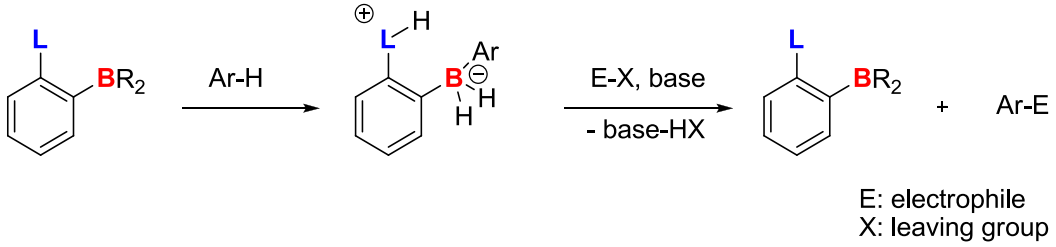

Figure 8-6: Schematic representation of the potential inclusion of tetravalent borate formed by C-H activation in catalytic reactions.

All in all, we believe that our demonstration of the possibility of C-H activation by FLP systems opens a wide range of possible reactions, some of which should be found in the near future. The end goal and most interesting process would be the ultimate development of metal-free catalytic C-C cross-coupling reactions (**Figure 8-7**).

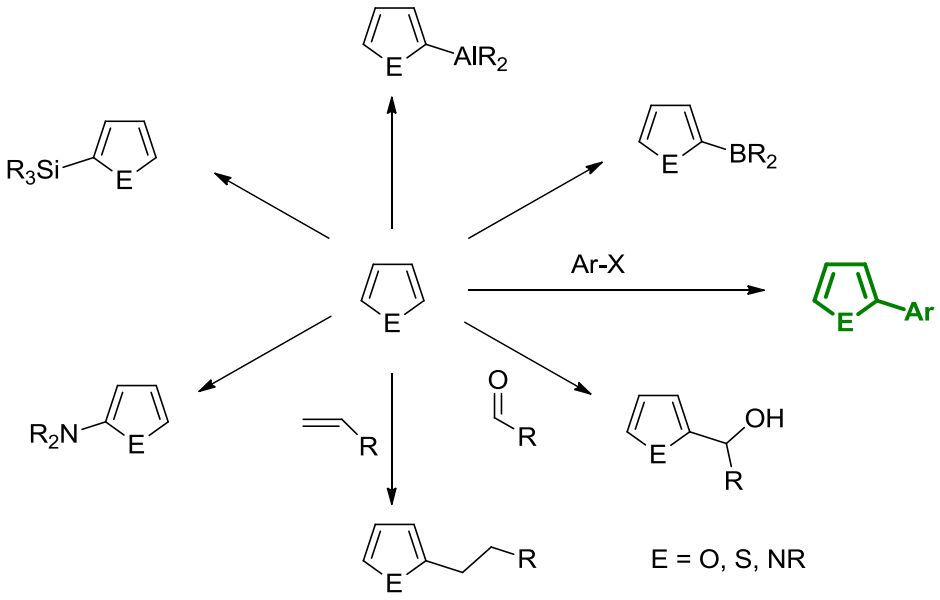

Figure 8-7: Partial overview of the reactions that will be investigated using ambiphilic organoboron compounds as mediators.

8.1.3 Optimization of the FLP Framework for Convenient and Efficient Use by Synthetic Chemists

Finally, while more stable than many organometallic catalysts, **8** still requires special considerations in handling, synthesis, and storage. We believe that the development of next-generation C-H functionalization catalysts should aim to optimize their air and moisture stability, as well as their convenience of handling and their efficiency. Catalysts should also be easy to prepare on the multi-gram scale.

Approaches to this end include the use of stable precatalysts than can be easily converted to active species in the reaction conditions. We have already found that methoxyboranes can slowly be converted to hydroboranes with reaction with pinacolborane. The reaction is faster when using $LiAlH_4$. Alkoxyboranes are more stable than hydroboranes and could represent a way to prepare convenient and commercializable precatalysts.

We are also looking at replacing the TMP group on the catalysts with amine residue that can be prepared more conveniently. Other anilines (such as diethylaniline, or N-[phenyl]morpholine) are inexpensive reagents. Ortho-metallation protocols could allow us to prepare catalysts on the multi-gram scale at extremely low costs. We are currently investigating whether catalysts based on these groups are suitable to the catalysis.

8.2 Final Words

In closing, we would like to reiterate the importance of chemical research focused on the improvement of the sustainability of chemical reactions. While traditional synthesis relies either on the substitution of leaving groups or on transition metal catalysis, the green, efficient, and selective C-H direct functionalization by environmentally benign and earth-abundant catalysts represents a challenge that will be increasingly present throughout the 21st century. In reporting the first catalyst for the metal-free C-H borylation of arenes, we hope to demonstrate that appropriate organic molecules can indeed mediate transformations that are commonly believed to be unique to transition metal complexes. With these results and this thesis, we hope to open a new dialog with the scientific community: one that challenges the hegemony of transition metals in catalysis. Frustrated Lewis Pairs are but one of the first of new concepts that will challenge the reign of precious metals. It is our hope that many more novel ideas will follow to pave the way to a chemical industry where earth-abundant catalysts are at the core of synthesis.

Chapter 9 - Bibliography

(1) *Applications of Transition Metal Catalysis in Drug Discovery and Development*; Crawley, M. L., Trost, B. M., Eds.; John Wiley & Sons, Inc.: Hoboken, NJ, USA, 2012.

(2) Lindström, B.; Pettersson, L. J. *CATTECH* **2003**, *7*, 130–138.

(3) IUPAC Gold Book - catalyst http://goldbook.iupac.org/C00876.html (accessed Jun 20, 2015).

(4) 12 Principles of Green Chemistry - American Chemical Society http://www.acs.org/content/acs/en/greenchemistry/what-is-green-chemistry/principles/12-principles-of-green-chemistry.html (accessed Jun 20, 2015).

(5) *Applied Industrial Catalysis*; Elsevier, 1983.

(6) All Nobel Prizes in Chemistry http://www.nobelprize.org/nobel_prizes/chemistry/laureates/ (accessed Jun 20, 2015).

(7) *Alkane C-H Activation by Single-Site Metal Catalysis*; Pérez, P. J., Ed.; Catalysis by Metal Complexes; Springer Netherlands: Dordrecht, 2012; Vol. 38.

(8) Wencel-Delord, J.; Glorius, F. *Nat. Chem.* **2013**, *5*, 369–375.

(9) International Conference on Harmonisation of Technical Requirements for Registration of Pharmaceuticals for Human Use - Q3D Elemental Impurities http://www.fda.gov/downloads/drugs/guidancecomplianceregulatoryinformation/guidances/ucm371025.pdf). (accessed Jun 20, 2015).

(10) Usluer, Ö.; Abbas, M.; Wantz, G.; Vignau, L.; Hirsch, L.; Grana, E.; Brochon, C.; Cloutet, E.; Hadziioannou, G. *ACS Macro Lett.* **2014**, *3*, 1134–1138.

(11) Brown, H. C.; Zweifel, G. *J. Am. Chem. Soc.* **1959**, *81*, 247–247.

(12) Kistler, R. B.; Helvaci, C. In *Industrial Minerals and Rocks (6th ed.)*; Society of Mining, Metallurgy and Exploration, Inc, 1994; pp 171–186.

(13) Kar, Y.; Şen, N.; Demirbaş, A. *Miner. Energy - Raw Mater. Rep.* **2006**, *20*, 2–10.

(14) Özbayoglu, G.; Poslu, K. *Miner. Procesing Extr. Metall. Rev.* **1992**, *9*, 245–254.

(15) Martin, D. R.. *Borax to Boranes*; Advances in Chemistry; American Chemical Society: Washington, D.C., 1961; Vol. 32.

(16) USGS Minerals Information: Boron http://minerals.usgs.gov/minerals/pubs/commodity/boron/ (accessed Jun 20, 2015).

(17) Shorrocks, V. M. *Plant Soil* **1997**, *193*, 121–148.

(18) Naghii, M. R.; Samman, S. *Prog. Food Nutr. Sci.* **1993**, *17*, 331–349.

(19) Toxicological Profile for Boron - U.S. Department Of Health And Human Services, http://www.atsdr.cdc.gov/toxprofiles/tp26.pdf.

(20) Klotz, J. H.; Moss, J. I.; Zhao, R.; Davis, L. R.; Patterson, R. S. *J. Econ. Entomol.* **1994**, *87*, 1534–1536.

(21) Nable, R. O.; Bañuelos, G. S.; Paull, J. G. *Plant Soil* **1997**, *193*, 181–198.

(22) Das, B. C.; Thapa, P.; Karki, R.; Schinke, C.; Das, S.; Kambhampati, S.; Banerjee, S. K.; Van Veldhuizen, P.; Verma, A.; Weiss, L. M.; Evans, T. *Future Med. Chem.* **2013**, *5*, 653–676.

(23) Thomas, S. E. *Organic Synthesis - The Role of Boron and Silicon*; Oxford University Primers, 1992.

(24) Hall, N. F. *J. Chem. Educ.* **1940**, *17*, 124.

(25) Arrhenius, S. A. *Philos. Mag. J. Sci.* **1896**, *41*, 237–276.

(26) Miessler, G. L.; Tarr, D. A. *Inorganic Chemistry*; Pearson Prentice Hall, 2011.

(27) Lewis, G. N. *Valence and the structure of atoms and molecules*; The Chemical Catalog Company, inc., 1923.

(28) *New Frontiers in Asymmetric Catalysis*; Mikami, K., Lautens, M., Eds.; John Wiley & Sons, 2007.

(29) Denmark, S. E.; Beutner, G. L. *Angew. Chem. Int. Ed. Engl.* **2008**, *47*, 1560–1638.

(30) Piers, W. E.; Chivers, T. *Chem. Soc. Rev.* **1997**, *26*, 345–354.

(31) Urch, C. J. In *Encyclopedia of Reagents for Organic Synthesis*; John Wiley & Sons, Ltd: Chichester, UK, 2001.

(32) Klare, H. F. T.; Oestreich, M. *Dalton Trans.* **2010**, *39*, 9176–9184.

(33) Rueping, M.; Nachtsheim, B. J. *Beilstein J. Org. Chem.* **2010**, *6*, 1–24.

(34) Price, C. C. In *Organic Reactions - Vol. 3*; John Wiley & Sons, Inc.: Hoboken, NJ, USA, 1946; pp 1–82.

(35) Friedel, C.; Crafts, J. M. *C. R. Hebd. Seances Acad. Sci.* **1877**, 1392.

(36) Smith, M. B.; March, J. *March's Advanced Organic Chemistry*; John Wiley & Sons, Inc.: Hoboken, NJ, USA, 2006.

(37) Brown, H. C.; Schlesinger, H. I.; Cardon, S. Z. *J. Am. Chem. Soc.* **1942**, *64*, 325–329.

(38) Wittig, G.; Benz, E. *Chem. Ber.* **1959**, *92*, 1999–2013.

(39) Tochtermann, W. *Angew. Chem. Int. Ed. English* **1966**, *5*, 351–371.

(40) Stephan, D. W.; Erker, G. *Angew. Chem. Int. Ed. Engl.* **2010**, *49*, 46–76.

(41) McCahill, J. S. J.; Welch, G. C.; Stephan, D. W. *Angew. Chem. Int. Ed. Engl.* **2007**, *46*, 4968–4971.

(42) Welch, G. C.; San Juan, R. R.; Masuda, J. D.; Stephan, D. W. *Science* **2006**, *314*, 1124–1126.

(43) Welch, G. C.; Stephan, D. W. *J. Am. Chem. Soc.* **2007**, *129*, 1880–1881.

(44) Stephan, D. W.; Erker, G. *Angew. Chem. Int. Ed.* **2015**, *54*, 6400–6441.

(45) *Frustrated Lewis Pairs I*; Erker, G., Stephan, D. W., Eds.; Topics in Current Chemistry; Springer: Berlin, Heidelberg, 2013; Vol. 332.

(46) Grimme, S.; Kruse, H.; Goerigk, L.; Erker, G. *Angew. Chem. Int. Ed. Engl.* **2010**, *49*, 1402–1405.

(47) Spies, P.; Erker, G.; Kehr, G.; Bergander, K.; Fröhlich, R.; Grimme, S.; Stephan, D. W. *Chem. Commun.* **2007**, 5072–5074.

(48) Fontaine, F.-G.; Boudreau, J.; Thibault, M.-H. *Eur. J. Inorg. Chem.* **2008**, *2008*, 5439–5454.

(49) Ekkert, O.; Kehr, G.; Fröhlich, R.; Erker, G. *Chem. Commun.* **2011**, *47*, 10482–10484.

(50) Chernichenko, K.; Nieger, M.; Leskelä, M.; Repo, T. *Dalton Trans.* **2012**, *41*, 9029–9032.

(51) Bertini, F.; Lyaskovskyy, V.; Timmer, B. J. J.; de Kanter, F. J. J.; Lutz, M.; Ehlers, A. W.; Slootweg, J. C.; Lammertsma, K. *J. Am. Chem. Soc.* **2012**, *134*, 201–204.

(52) Appelt, C.; Westenberg, H.; Bertini, F.; Ehlers, A. W.; Slootweg, J. C.; Lammertsma, K.; Uhl, W. *Angew. Chem. Int. Ed.* **2011**, *50*, 3925–3928.

(53) Kolychev, E. L.; Theuergarten, E.; Tamm, M. In *Frustrated Lewis Pairs I*; Stephan, D. W., Erker, G., Eds.; Springer: Berlin, Heidelberg, 2013; pp 121–155.

(54) Chase, P. A.; Welch, G. C.; Jurca, T.; Stephan, D. W. *Angew. Chem. Int. Ed. Engl.* **2007**, *46*, 8050–8053.

(55) Wang, H.; Fröhlich, R.; Kehr, G.; Erker, G. *Chem. Commun.* **2008**, 5966–5968.

(56) Spies, P.; Schwendemann, S.; Lange, S.; Kehr, G.; Fröhlich, R.; Erker, G. *Angew. Chem. Int. Ed. Engl.* **2008**, *47*, 7543–7546.

(57) Stephan, D. W.; Erker, G. In *Frustrated Lewis Pairs I*; Stephan, D. W., Erker, G., Eds.; Springer: Berlin, Heidelberg, 2013; Vol. 332, pp 85–110.

(58) Hounjet, L. J.; Bannwarth, C.; Garon, C. N.; Caputo, C. B.; Grimme, S.; Stephan, D. W. *Angew. Chem. Int. Ed. Engl.* **2013**, *52*, 7492–7495.

(59) Greb, L.; Oña-Burgos, P.; Schirmer, B.; Grimme, S.; Stephan, D. W.; Paradies, J. *Angew. Chem. Int. Ed. Engl.* **2012**, *51*, 10164–10168.

(60) Mahdi, T.; Stephan, D. W. *J. Am. Chem. Soc.* **2014**, *136*, 15809–15812.

(61) Scott, D. J.; Fuchter, M. J.; Ashley, A. E. *J. Am. Chem. Soc.* **2014**, *136*, 15813–15816.

(62) Chernichenko, K.; Madarász, A.; Pápai, I.; Nieger, M.; Leskelä, M.; Repo, T. *Nat. Chem.* **2013**, *5*, 718–723.

(63) Fontaine, F.-G.; Courtemanche, M.-A.; Légaré, M.-A. *Chemistry* **2014**, *20*, 2990–2996.

(64) Mömming, C. M.; Otten, E.; Kehr, G.; Fröhlich, R.; Grimme, S.; Stephan, D. W.; Erker, G. *Angew. Chem. Int. Ed. Engl.* **2009**, *48*, 6643–6646.

(65) *Frustrated Lewis Pairs II*; Erker, G., Stephan, D. W., Eds.; Topics in Current Chemistry; Springer: Berlin, Heidelberg, 2013; Vol. 334.

(66) Ashley, A. E.; O'Hare, D. In *Frustrated Lewis Pairs II*; Stephan, D. W., Erker, G., Eds.; Springer: Berlin, Heidelberg, 2015; pp 191–217.

(67) Lim, C.-H.; Holder, A. M.; Hynes, J. T.; Musgrave, C. B. *Inorg. Chem.* **2013**, *52*, 10062–10066.

(68) Roy, L.; Zimmerman, P. M.; Paul, A. *Chemistry* **2011**, *17*, 435–439.

(69) Ménard, G.; Stephan, D. W. *J. Am. Chem. Soc.* **2010**, *132*, 1796–1797.

(70) Ashley, A. E.; Thompson, A. L.; O'Hare, D. *Angew. Chem. Int. Ed. Engl.* **2009**, *48*, 9839–9843.

(71) Berkefeld, A.; Piers, W. E.; Parvez, M. *J. Am. Chem. Soc.* **2010**, *132*, 10660–10661.

(72) Jiang, C.; Blacque, O.; Berke, H. *Organometallics* **2010**, *29*, 125–133.

(73) Dureen, M. A.; Stephan, D. W. *J. Am. Chem. Soc.* **2009**, *131*, 8396–8397.

(74) Stephan, D. W. *Acc. Chem. Res.* **2015**, *48*, 306–316.

(75) *Handbook of Organopalladium Chemistry for Organic Synthesis*; Negishi, E.-I., Ed.; John Wiley & Sons: Weinheim, 2003.

(76) Zhao, X.; Liang, L.; Stephan, D. W. *Chem. Commun.* **2012**, *48*, 10189–10191.

(77) Housecroft, C. E.; Sharpe, A. G. *Inorganic Chemistry, Volume 1*; Pearson Prentice Hall, 2008.

(78) Brotherton, R. J.; Weber, C. J.; Guibert, C. R.; L., L. J. In *Ullmann's Encyclopedia of Industrial Chemistry, vol. 6*; Wiley-VCH Verlag GmbH & Co. KGaA: Weinheim, Germany, 2000; pp 237–258.

(79) De B. Darwent, B. *Bond Dissociation Energies in Simple Molecules - National Bureau of Standards*; 1970.

(80) Brown, W. G. *Org. React.* **1951**, *6*, 469–510.

(81) Mayer, I. *J. Mol. Struct. THEOCHEM* **1989**, *186*, 43–52.

(82) Brown, H. C.; Rao, B. C. S. *J. Am. Chem. Soc.* **1959**, *81*, 6428–6434.

(83) Brown, H. C. *Organic syntheses via boranes*; Wiley: Hoboken, NJ, USA, 1975.

(84) Brown, H. C. *Tetrahedron* **1961**, *12*, 117–138.

(85) Brown, H. C.; Rao, B. C. S. *J. Am. Chem. Soc.* **1956**, *78*, 2582–2588.

(86) Ilich, P.-P.; Rickertsen, L. S.; Becker, E. *J. Chem. Educ.* **2006**, *83*, 1681.

(87) Borane Reagents http://www.organic-chemistry.org/chemicals/reductions/boranes.shtm (accessed Jun 20, 2015).

(88) Soderquist, J. A.; Brown, H. C. *J. Org. Chem.* **1981**, *46*, 4599–4600.

(89) Clayden, J.; Greeves, N.; Warren, S. *Organic Chemistry*, Second Edi.; Oxford University Press: London, 2012.

(90) Ritmeyer, P.; Wietelmann, U. In *Ullmann's Encyclopedia of Industrial Chemistry*; Wiley-VCH Verlag GmbH & Co. KGaA: Weinheim, Germany, 2000; pp 103–132.

(91) Query, I. P.; Squier, P. A.; Larson, E. M.; Isley, N. A.; Clark, T. B. *J. Org. Chem.* **2011**, *76*, 6452–6456.

(92) Hirao, A.; Itsuno, S.; Nakahama, S.; Yamazaki, N. *J. Chem. Soc. Chem. Commun.* **1981**, 315–317.

(93) Corey, E. J.; Bakshi, R. K.; Shibata, S. *J. Am. Chem. Soc.* **1987**, *109*, 5551–5553.

(94) Corey, E. J.; Bakshi, R. K.; Shibata, S.; Chen, C. P.; Singh, V. K. *J. Am. Chem. Soc.* **1987**, *109*, 7925–7926.

(95) Breunig, J. M.; Lehmann, F.; Bolte, M.; Lerner, H.-W.; Wagner, M. *Organometallics* **2014**, *33*, 3163–3172.

(96) Onak, T. *Organoborane Chemistry*; Academic Press: New York, 1975.

(97) Batey, R. A.; Quach, T. D.; Shen, M.; Thadani, A. N.; Smil, D. V.; Li, S.-W.; MacKay, D. B. *Pure Appl. Chem.* **2002**, *74*, 43–55.

(98) Allred, A. L.; Rochow, E. G. *J. Inorg. Nucl. Chem.* **1958**, *5*, 264–268.

(99) Negishi, E. *J. Organomet. Chem.* **1976**, *108*, 281–324.

(100) Hall, D. G. *Boronic Acids*, 2nd Ed.; Wiley-VCH: Weinhein, 2011.

(101) Zweifel, G. In *Aspects of Mechanism and Organometallic Chemistry*; Brewster, J. H., Ed.; Springer US: Boston, MA, 1979; pp 229–249.

(102) Midland, M. M.; Brown, H. C. *J. Org. Chem.* **1975**, *40*, 2845–2846.

(103) Bonet, A.; Odachowski, M.; Leonori, D.; Essafi, S.; Aggarwal, V. K. *Nat. Chem.* **2014**, *6*, 584–589.

(104) Levy, A. B. *J. Org. Chem.* **1978**, *43*, 4684–4685.

(105) Ishikura, M.; Kato, H.; Ohnuki, N. *Chem. Commun.* **2002**, 220–221.

(106) Ishikura, M.; Kato, H. *Tetrahedron* **2002**, *58*, 9827–9838.

(107) Pelter, A.; Williamson, H.; Davies, G. M. *Tetrahedron Lett.* **1984**, *25*, 453–456.

(108) Marinelli, E. R.; Levy, A. B. *Tetrahedron Lett.* **1979**, *20*, 2313–2316.

(109) Davies, G. M.; Davies, P. S.; Paget, W. E.; Wardleworth, J. M. *Tetrahedron Lett.* **1976**, *17*, 795–798.

(110) Levy, A. B. *Tetrahedron Lett.* **1979**, *20*, 4021–4024.

(111) Negishi, E.-I.; Idacavage, M. J. In *Organic Reactions*; John Wiley & Sons, Inc.: Hoboken, NJ, USA, 2004; pp 1–246.

(112) Amatore, C.; Jutand, A.; Le Duc, G. *Chemistry* **2011**, *17*, 2492–2503.

(113) Matos, K.; Soderquist, J. A. *J. Org. Chem.* **1998**, *63*, 461–470.

(114) Han, F.-S. *Chem. Soc. Rev.* **2013**, *42*, 5270–5298.

(115) Raabe, G.; Heyne, E.; Schleker, W.; Fleischhauer, J. *Z. Naturforsch. A* **1984**, *39*, 678–681.

(116) Raabe, G.; Schleker, W.; Heyne, E.; Fleischhauer, J. *Z. Naturforsch. A* **1987**, *42*, 352–360.

(117) Karadakov, P. B.; Ellis, M.; Gerratt, J.; Cooper, D. L.; Raimondi, M. *Int. J. Quantum Chem.* **1997**, *63*, 441–449.

(118) Maier, G.; Reisenauer, H. P.; Henkelmann, J.; Kliche, C. *Angew. Chem. Int. Ed. Engl.* **1988**, *27*, 295–296.

(119) Herberich, G. E.; Greiss, G.; Heil, H. F. *Angew. Chem. Int. Ed.* **1970**, *9*, 805–806.

(120) Cade, I. A.; Hill, A. F.; Wagler, J. *Organometallics* **2008**, *27*, 4844–4846.

(121) Languérand, A.; Barnes, S. S.; Bélanger-Chabot, G.; Maron, L.; Berrouard, P.; Audet, P.; Fontaine, F.-G. *Angew. Chem. Int. Ed.* **2009**, *48*, 6695–6698.

(122) Herberich, G. E.; Ohst, H. *Adv. Organomet. Chem.* **1986**, *25*, 199–236.

(123) Hoic, D. A.; Wolf, J. R.; Davis, W. M.; Fu, G. C. *Organometallics* **1996**, *15*, 1315–1318.

(124) Zheng, X.; Wang, B.; Herberich, G. E. *Organometallics* **2002**, *21*, 1949–1954.

(125) Zheng, X.; Herberich, G. E. *Eur. J. Inorg. Chem.* **2003**, *30*, 2175–2182.

(126) Fu, G. C. *Adv. Organomet. Chem.* **2001**, *47*, 101–119.

(127) Herberich, H. E.; Englert, U.; Schmidt, M. U.; Standt, R. *Organometallics* **1996**, *15*, 2707–2712.

(128) Barnes, S. S.; Légaré, M. A.; Maron, L.; Fontaine, F.-G. *Dalton Trans.* **2011**, *40*, 12439–12442.

(129) Zheng, X.; Herberich, G. E. *Organometallics* **2000**, *19*, 3751–3753.

(130) Macha, B. B.; Boudreau, J.; Maron, L.; Maris, T.; Fontaine, F.-G. *Organometallics* **2012**, *31*, 6428–6437.

(131) Auvray, N.; Baul, T. S. B.; Braunstein, P.; Croizat, P.; Englert, U.; Herberich, G. E.; Welter, R. *Dalton Trans.* **2006**, *35*, 2950–2958.

(132) Cade, I. A.; Hill, A. F. *Dalton Trans.* **2011**, *40*, 10563–10567.

(133) Hagenau, U.; Heck, J.; Hendrickx, E.; Persoons, A.; Schuld, T.; Wong, H. *Inorg. Chem.* **1996**, *35*, 7863–7866.

(134) Ashe, A. J.; Shu, P. *J. Am. Chem. Soc.* **1971**, *93*, 1804–1805.

(135) Emslie, D. J. H.; Piers, W. E.; Parvez, M. *Angew. Chem. Int. Ed.* **2003**, *42*, 1252–1255.

(136) Bosdet, M. J. D.; Piers, W. E.; Sorensen, T. S.; Parvez, M. *Angew. Chem. Int. Ed. Engl.* **2007**, *46*, 4940–4943.

(137) Jaska, C. A.; Emslie, D. J. H.; Bosdet, M. J. D.; Piers, W. E.; Sorensen, T. S.; Parvez, M. *J. Am. Chem. Soc.* **2006**, *128*, 10885–10896.

(138) Jaska, C. A.; Piers, W. E.; McDonald, R.; Parvez, M. *J. Org. Chem.* **2007**, *72*, 5234–5243.

(139) Qiao, S.; Hoic, D. A.; Fu, G. C. *J. Am. Chem. Soc.* **1996**, *118*, 6329–6330.

(140) Ghesner, I.; Piers, W. E.; Parvez, M.; McDonald, R. *Chem. Commun.* **2005**, 2480–2482.

(141) *Activation and Functionalization of C—H Bonds*; Goldman, A. S., Goldberg, K. I., Eds.; American Chemical Society: Washington D. C., 2004.

(142) Chatt, J.; Davidson, J. M. *J. Chem. Soc.* **1965**, 843.

(143) Gol'dshleger, N. F.; Tyabin, M. B.; Shilov, A. E.; Shteinman, A. A. *Zhurnal Fiz. Khimii* **1969**, *43*, 2174.

(144) Periana, R.; Taube, D.; Gamble, S.; Taube, H.; Satoh, T.; Fujii, H. *Science* **1998**, *280*, 560–564.

(145) Janowicz, A. H.; Bergman, R. G. *J. Am. Chem. Soc.* **1982**, *104*, 352–354.

(146) Hoyano, J. K.; Graham, W. A. G. *J. Am. Chem. Soc.* **1982**, *104*, 3723–3725.

(147) Saillard, J. Y.; Hoffmann, R. *J. Am. Chem. Soc.* **1984**, *106*, 2006–2026.

(148) Jones, W. D.; Feher, F. J. *J. Am. Chem. Soc.* **1982**, *104*, 4240–4242.

(149) Jones, W. D.; Feher, F. J. *Acc. Chem. Res.* **1989**, *22*, 91–100.

(150) Belt, S. T.; Dong, L.; Duckett, S. B.; Jones, W. D.; Partridge, M. G.; Perutz, R. N. *J. Chem. Soc. Chem. Commun.* **1991**, 266–269.

(151) Periana, R. A.; Bergman, R. G. *J. Am. Chem. Soc.* **1986**, *108*, 7332–7346.

(152) Westaway, K. C. *Advances in Physical Organic Chemistry Volume 41*; Advances in Physical Organic Chemistry; Elsevier, 2006; Vol. 41.

(153) Burger, P.; Bergman, R. G. *J. Am. Chem. Soc.* **1993**, *115*, 10462–10463.

(154) Niu, S.; Hall, M. B. *J. Am. Chem. Soc.* **1998**, *120*, 6169–6170.

(155) Klei, S. R.; Tilley, T. D.; Bergman, R. G. *J. Am. Chem. Soc.* **2000**, *122*, 1816–1817.

(156) Mleczko, L.; Buchholz, S.; Münnich, C. In *Handbook of C–H Transformations*; Dyker, G., Ed.; Wiley-VCH Verlag GmbH: Weinheim, Germany, 2005; pp 11–27.

(157) Fisher, B. J.; Eisenberg, R. *Organometallics* **1983**, *2*, 764–767.

(158) Kunin, A. J.; Eisenberg, R. *J. Am. Chem. Soc.* **1986**, *108*, 535–536.

(159) Sakakura, T.; Tanaka, M. *Chem. Lett.* **1987**, 249–252.

(160) Jones, W. D.; Foster, G. P.; Putinas, J. M. *J. Am. Chem. Soc.* **1987**, *109*, 5047–5048.

(161) Kakiuchi, F.; Murai, S. *Acc. Chem. Res.* **2002**, *35*, 826–834.

(162) Ritleng, V.; Sirlin, C.; Pfeffer, M. *Chem. Rev.* **2002**, *102*, 1731–1770.

(163) Kakiuchi, F.; Yamamoto, Y.; Chatani, N.; Murai, S. *Chem. Lett.* **1995**, 681–682.

(164) Ball, L. T.; Lloyd-Jones, G. C.; Russell, C. A. *Science* **2012**, *337*, 1644–1648.

(165) McGlacken, G. P.; Bateman, L. M. *Chem. Soc. Rev.* **2009**, *38*, 2447–2464.

(166) Rousseaux, S.; Liégault, B.; Fagnou, K. In *Modern Tools for the Synthesis of Complex Bioactive Molecules*; Cossy, J., Arseniyadis, S., Eds.; John Wiley & Sons, Inc.: Hoboken, NJ, USA, 2012; pp 1–32.

(167) Lafrance, M.; Fagnou, K. *J. Am. Chem. Soc.* **2006**, *128*, 16496–16497.

(168) Ackermann, L. *Chem. Rev.* **2011**, *111*, 1315–1345.

(169) Gorelsky, S. I. *Organometallics* **2012**, *31*, 4631–4634.

(170) Gorelsky, S. I. *Coord. Chem. Rev.* **2013**, *257*, 153–164.

(171) Berrouard, P.; Najari, A.; Pron, A.; Gendron, D.; Morin, P.-O.; Pouliot, J.-R.; Veilleux, J.; Leclerc, M. *Angew. Chem. Int. Ed. Engl.* **2012**, *51*, 2068–2071.

(172) Morin, P.-O.; Bura, T.; Sun, B.; Gorelsky, S. I.; Li, Y.; Leclerc, M. *ACS Macro Lett.* **2015**, *4*, 21–24.

(173) Lam, K. C.; Marder, T. B.; Lin, Z. *Organometallics* **2010**, *29*, 1849–1857.

(174) Dombray, T.; Werncke, C. G.; Jiang, S.; Grellier, M.; Vendier, L.; Bontemps, S.; Sortais, J.-B.; Sabo-Etienne, S.; Darcel, C. *J. Am. Chem. Soc.* **2015**, *137*, 4062–4065.

(175) Hartwig, J. F.; Huber, S. *J. Am. Chem. Soc.* **1993**, *115*, 4908–4909.

(176) Waltz, K. M. *Science (80-.).* **1997**, *277*, 211–213.

(177) Marder, T. B.; Norman, N. C.; Rice, C. R.; Robins, E. G. *Chem. Commun.* **1997**, 53–54.

(178) Dai, C.; Stringer, G.; Marder, T. B.; Scott, A. J.; Clegg, W.; Norman, N. C. *Inorg. Chem.* **1997**, *36*, 272–273.

(179) Hartwig, J. F.; He, X. *Angew. Chem. Int. Ed. English* **1996**, *35*, 315–317.

(180) Ishiyama, T.; Matsuda, N.; Murata, M.; Ozawa, F.; Suzuki, A.; Miyaura, N. *Organometallics* **1996**, *15*, 713–720.

(181) Iverson, C. N.; Smith, M. R. *Organometallics* **1996**, *15*, 5155–5165.

(182) Chen, H.; Hartwig, J. *Angew. Chem. Int. Ed. Engl.* **1999**, *38*, 3391–3393.

(183) Chen, H.; Schlecht, S.; Semple, T. C.; Hartwig, J. F. *Science*, **2000**, *287*, 1995–1997.

(184) Shimada, S.; Batsanov, A. S.; Howard, J. A. K.; Marder, T. B. *Angew. Chem. Int. Ed. Engl.* **2001**, *40*, 2168–2171.

(185) Ishiyama, T.; Takagi, J.; Ishida, K.; Miyaura, N.; Anastasi, N. R.; Hartwig, J. F. *J. Am. Chem. Soc.* **2002**, *124*, 390–391.

(186) Ishiyama, T.; Takagi, J.; Hartwig, J. F.; Miyaura, N. *Angew. Chem. Int. Ed. Engl.* **2002**, *41*, 3056–3058.

(187) Takagi, J.; Sato, K.; Hartwig, J. F.; Ishiyama, T.; Miyaura, N. *Tetrahedron Lett.* **2002**, *43*, 5649–5651.

(188) Ishiyama, T.; Nobuta, Y.; Hartwig, J. F.; Miyaura, N. *Chem. Commun.* **2003**, 2924.

(189) Larsen, M. A.; Hartwig, J. F. *J. Am. Chem. Soc.* **2014**, *136*, 4287–4299.

(190) Furukawa, T.; Tobisu, M.; Chatani, N. *Chem. Commun.* **2015**, *51*, 6508–6511.

(191) Boller, T. M.; Murphy, J. M.; Hapke, M.; Ishiyama, T.; Miyaura, N.; Hartwig, J. F. *J. Am. Chem. Soc.* **2005**, *127*, 14263–14278.

(192) Hatanaka, T.; Ohki, Y.; Tatsumi, K. *Chem. Asian J.* **2010**, *5*, 1657–1666.

(193) Mazzacano, T. J.; Mankad, N. P. *J. Am. Chem. Soc.* **2013**, *135*, 17258–17261.

(194) Obligacion, J. V; Semproni, S. P.; Chirik, P. J. *J. Am. Chem. Soc.* **2014**, *136*, 4133–4136.

(195) Del Grosso, A.; Pritchard, R. G.; Muryn, C. A.; Ingleson, M. J. *Organometallics* **2010**, *29*, 241–249.

(196) Del Grosso, A.; Singleton, P. J.; Muryn, C. A.; Ingleson, M. J. *Angew. Chem. Int. Ed. Engl.* **2011**, *50*, 2102–2106.

(197) Bagutski, V.; Del Grosso, A.; Carrillo, J. A.; Cade, I. A.; Helm, M. D.; Lawson, J. R.; Singleton, P. J.; Solomon, S. A.; Marcelli, T.; Ingleson, M. J. *J. Am. Chem. Soc.* **2013**, *135*, 474–487.

(198) Prokofjevs, A.; Kampf, J. W.; Vedejs, E. *Angew. Chem. (International Ed.)* **2011**, *50*, 2098–2101.

(199) NMR Frequency Table http://web.mit.edu/speclab/www/Facility/nmrfreq.html (accessed Jun 25, 2015).

(200) Declercq, R.; Bouhadir, G.; Bourissou, D.; Légaré, M.-A.; Courtemanche, M.-A.; Nahi, K. S.; Bouchard, N.; Fontaine, F.-G.; Maron, L. *ACS Catal.* **2015**, *5*, 2513–2520.

(201) Koch, W.; Holthausen, M. C. *A Chemist's Guide to Density Functional Theory*, Second Edi.; Wiley-VCH Verlag GmbH: Weinheim, 2001.

(202) Hohenberg, P. *Phys. Rev.* **1964**, *136*, B864–B871.

(203) Kohn, W.; Sham, L. J. *Phys. Rev.* **1965**, *140*, A1133–A1138.

(204) Tolman, C. A. *Chem. Rev.* **1977**, *77*, 313–348.

(205) Oliveri, I. P.; Maccarrone, G.; Di Bella, S. *J. Org. Chem.* **2011**, *76*, 8879–8884.

(206) Laurence, C.; Gal, J.-F. *Lewis Basicity and Affinity Scales: Data and Measurements*; Wiley: Chichester, U.K., 2010.

(207) Courtemanche, M.-A.; Légaré, M.-A.; Maron, L.; Fontaine, F.-G. *J. Am. Chem. Soc.* **2013**, *135*, 9326–9329.

(208) Boudreau, J.; Courtemanche, M.-A.; Fontaine, F.-G. *Chem. Commun.* **2011**, *47*, 11131–11133.

(209) Kuzu, I.; Krummenacher, I.; Meyer, J.; Armbruster, F.; Breher, F. *Dalton Trans.* **2008**, *43*, 5836–5865.

(210) Bouhadir, G.; Amgoune, A.; Bourissou, D. *Adv. Organomet. Chem.* **2010**, *58*, 1–107.

(211) Amgoune, A.; Bourissou, D. *Chem. Commun.* **2011**, *47*, 859–871.

(212) Grimmett, D. L.; Labinger, J. A.; Bonfiglio, J. N.; Masuo, S. T.; Shearin, E.; Miller, J. S. *J. Am. Chem. Soc.* **1982**, *104*, 6858–6859.

(213) Hill, A. F.; Owen, G. R.; White, A. J. P.; Williams, D. J. *Angew. Chem. Int. Ed.* **1999**, *38*, 2759–2761.

(214) Fontaine, F.-G.; Zargarian, D. *J. Am. Chem. Soc.* **2004**, *126*, 8786–8794.

(215) Parkin, G. *Organometallics* **2006**, *25*, 4744–4747.

(216) Hill, A. F. *Organometallics* **2006**, *25*, 4741–4743.

(217) Boudreau, J.; Fontaine, F.-G. *Organometallics* **2011**, *30*, 511–519.

(218) Miller, A. J. M.; Labinger, J. A.; Bercaw, J. E. *J. Am. Chem. Soc.* **2010**, *132*, 3301–3303.

(219) Cowie, B. E.; Emslie, D. J. H.; Jenkins, H. A.; Britten, J. F. *Inorg. Chem.* **2010**, *49*, 4060–4072.

(220) Anderson, J. S.; Moret, M. E.; Peters, J. C. *J. Am. Chem. Soc.* **2013**, *135*, 534–537.

(221) Sircoglou, M.; Mercy, M.; Saffon, M.; Coppel, Y.; Bouhadir, B.; Maron, L.; Bourissou, D. *Angew. Chem. Int. Ed.* **2009**, *48*, 3454–3457.

(222) James, T. D.; Sandanayake, K. R. A. S.; Shinkai, S. *Angew. Chem. Int. Ed. Engl.* **1996**, *35*, 1910–1922.

(223) Zhu, L.; Zhong, Z.; Anslyn, E. V. *J. Am. Chem. Soc.* **2005**, *127*, 4260–4269.

(224) Hudnall, T. W.; Kim, Y.-M.; Bebbington, M. W. P.; Bourissou, D.; Gabbaï, F. P. *J. Am. Chem. Soc.* **2008**, *130*, 10890–10891.

(225) Hudson, Z. M.; Wang, S. *Acc. Chem. Res.* **2009**, *42*, 1584–1596.

(226) Braunschweig, H.; Chiu, C.-W.; Radacki, K.; Kupfer, T. *Angew. Chem. Int. Ed.* **2010**, *49*, 2041–2044.

(227) Wood, T. K.; Piers, W. E.; Keay, B. A.; Parvez, M. *Chem. Eur. J.* **2010**, *16*, 12199–12206.

(228) Wood, T. K.; Piers, W. E.; Keay, B. A.; Parvez, M. *Angew. Chem. Int. Ed.* **2009**, *48*, 4009–4012.

(229) Kinjo, R.; Donnadieu, B.; Celik, M. A.; Frenking, G.; Bertrand, G. *Science*, **2011**, *333*, 610–613.

(230) Raabe, G.; Baldofski, M. *Aust. J. Chem.* **2011**, *64*, 957–964.

(231) Semenov, S. G.; Sigolaev, Y. F. *Russ. J. Gen. Chem.* **2006**, *76*, 580–582.

(232) Boese, R.; Finke, N.; Henkelmann, J.; Maier, G.; Paetzold, P.; Reisenauer, H. P.; Schmid, G. *Chem. Ber.* **1985**, *118*, 1644–1654.

(233) Woodmansee, D. H.; Bu, X.; Bazan, G. C. *Chem. Commun.* **2001**, *37*, 619–620.

(234) Komon, Z. J. A.; Rogers, J. S.; Bazan, G. C. *Organometallics* **2002**, *21*, 3189–3195.

(235) Loginov, D. A.; Starivoka, Z. A.; Petrovskaya, E. A.; Kudinov, A. R. *J. Organomet. Chem.* **2009**, *694*, 157–160.

(236) Cui, P.; Chen, Y.; Zeng, X.; Sun, J.; Li, G.; Xia, W. *Organometallics* **2007**, *26*, 6519–6521.

(237) Yuan, Y.; Chen, Y.; Li, G.; Xia, W. *Organometallics* **2010**, *29*, 3722–3728.

(238) Bélanger-Chabot, G.; Rioux, P.; Maron, L.; Fontaine, F.-G. *Chem. Commun.* **2010**, *46*, 6816–6818.

(239) Yuan, Y.; Wang, X.; Li, Y.; Fan, L.; Xu, X.; Chen, Y.; Li, G.; Xia, W. *Organometallics* **2011**, *30*, 4330–4341.

(240) Cui, P.; Chen, Y.; Li, G.; Xia, W. *Organometallics* **2011**, *30*, 2012–2017.

(241) Lu, E.; Yuan, Y.; Chen, Y.; Xia, W. *ACS Catal.* **2013**, *3*, 521–524.

(242) Boese, R.; Finke, N.; Keil, T.; Paetzold, P.; Schmid, G. *Z. Naturforsch. B* **1985**, *40*, 1327–1132.

(243) Amendola, M. C.; Stockman, K. E.; Hoic, D. A.; Davis, W. M.; Fu, G. C. *Angew. Chem. Int. Ed.* **1997**, *36*, 267–269.

(244) Tweddell, J.; Hoic, D. A.; Fu, G. C. *J. Org. Chem.* **1997**, *62*, 8626–8627.

(245) Cui, P.; Chen, Y.; Li, G.; Xia, W. *Angew. Chem. Int. Ed.* **2008**, *47*, 9944–9947.

(246) Neue, B.; Araneda, J. F.; Piers, W. E.; Parvez, M. *Angew. Chem. Int. Ed.* **2013**, *52*, 9966–9969.

(247) Wood, T. K.; Piers, W. E.; Keay, B. A.; Parvez, M. *Org. Lett.* **2006**, *8*, 2875–2878.

(248) Mushtaq, A.; Bi, W.; Légaré, M.-A.; Fontaine, F.-G. *Organometallics* **2014**, *33*, 3173–3181.

(249) Potter, R. G.; Camaioni, D. M.; Vasiliu, M.; Dixon, D. A. *Inorg. Chem.* **2010**, *49*, 10512–10521.

(250) Semenov, S. G.; Sigolaev, Y. F. *Russ. J. Gen. Chem.* **2006**, *76*, 1925–1929.

(251) Tolman, C. A. *J. Am. Chem. Soc.* **1970**, *92*, 2956–2965.

(252) Grant, D. J.; Dixon, D. A. *J. Phys. Chem. A* **2006**, *110*, 12955.

(253) Cioslowski, J.; Hay, P. J. *J. Am. Chem. Soc.* **1990**, *112*, 1707–1710.

(254) Becke, A. D. *J. Chem. Phys.* **1993**, *98*, 5648–5652.

(255) Miehlich, B.; Savin, A.; Stoll, H.; Preuss, H. *Chem. Phys. Lett.* **1989**, *157*, 200–206.

(256) Lee, C.; Yang, W.; Parr, R. G. *Phys. Rev. B* **1988**, *37*, 785–789.

(257) Vosko, S. H.; Wilk, L.; Nusair, M. *Can. J. Phys.* **1980**, *58*, 1200–1211.

(258) Schäfer, A.; Huber, C.; Ahlrichs, R. *J. Chem. Phys.* **1994**, *100*, 5829–5835.

(259) Csaszar, P.; Pulay, P. *J. Mol. Struct.* **1984**, *114*, 31–34.

(260) Farkas, Ö.; Schlegel, H. B. *J. Chem. Phys.* **1999**, *111*, 10806–10814.

(261) Gonzalez, C.; Schlegel, H. B. *J. Chem. Phys.* **1989**, *90*, 2154–2161.

(262) Gonzalez, C.; Schlegel, H. B. *J. Phys. Chem.* **1990**, *94*, 5523–5527.

(263) Tans, P. (NOAA/ESRL); Keeling, R. (Scripps I. of O. Global Greenhouse Gas Reference Network www.esrl.noaa.gov/gmd/ccgg/trends/ (accessed May 25, 2015).

(264) Greenhouse gas benchmark reached http://research.noaa.gov/News/NewsArchive/LatestNews/TabId/684/ArtMID/1768/ArticleID/11153/Greenhouse-gas-benchmark-reached-.aspx (accessed May 25, 2015).

(265) Aresta, M.; Dibenedetto, A. *Dalton Trans.* **2007**, 2975–2992.

(266) Olah, G. A.; Goeppert, A.; Prakash, G. K. S.; Alain Goeppert, G. K.; Prakash, S. *Beyond Oil and Gas: The Methanol Economy*; Wiley, 2006.

(267) Behrens, M. *J. Catal.* **2009**, *267*, 24–29.

(268) *Handbook of Heterogeneous Catalysis*; Ertl, G., Knozinger, H., Schuth, F., Weitkamp, J., Eds.; Wiley-VCH Verlag GmbH & Co. KGaA: Weinheim, Germany, 2008.

(269) (Carbon Recycling International). World's Largest CO2 Methanol Plant http://cri.is/index.php?option=com_content&view=article&id=14&Itemid=8&lang=en (accessed May 25, 2015).

(270) Kasatkin, I.; Kurr, P.; Kniep, B.; Trunschke, A.; Schlögl, R. *Angew. Chem. Int. Ed. Engl.* **2007**, *46*, 7324–7327.

(271) Studt, F.; Sharafutdinov, I.; Abild-Pedersen, F.; Elkjær, C. F.; Hummelshøj, J. S.; Dahl, S.; Chorkendorff, I.; Nørskov, J. K. *Nat. Chem.* **2014**, *6*, 320–324.

(272) Wang, W.; Wang, S.; Ma, X.; Gong, J. *Chem. Soc. Rev.* **2011**, *40*, 3703–3727.

(273) Chakraborty, S.; Zhang, J.; Krause, J. A.; Guan, H. *J. Am. Chem. Soc.* **2010**, *132*, 8872–8873.

(274) Bontemps, S.; Vendier, L.; Sabo-Etienne, S. *Angew. Chem. Int. Ed.* **2012**, *51*, 1671–1674.

(275) Balaraman, E.; Gunanathan, C.; Zhang, J.; Shimon, L. J. W.; Milstein, D. *Nat. Chem.* **2011**, *3*, 609–614.

(276) Wesselbaum, S.; Vom Stein, T.; Klankermayer, J.; Leitner, W. *Angew. Chem. Int. Ed. Engl.* **2012**, *51*, 7499–7502.

(277) Mitton, S. J.; Turculet, L. *Chem. - Eur. J.* **2012**, *18*, 15258–15262.

(278) Lalrempuia, R.; Iglesias, M.; Polo, V.; Sanz Miguel, P. J.; Fernández-Alvarez, F. J.; Pérez-Torrente, J. J.; Oro, L. A. *Angew. Chem. Int. Ed. Engl.* **2012**, *51*, 12824–12827.

(279) Tominaga, K.; Sasaki, Y.; Kawai, M.; Watanabe, T.; Saito, M. *J. Chem. Soc. Chem. Commun.* **1993**, 629–631.

(280) Matsuo, T.; Kawaguchi, H. *J. Am. Chem. Soc.* **2006**, *128*, 12362–12363.

(281) Schmeier, T. J.; Dobereiner, G. E.; Crabtree, R. H.; Hazari, N. *J. Am. Chem. Soc.* **2011**, *133*, 9274–9277.

(282) Huff, C. A.; Sanford, M. S. *J. Am. Chem. Soc.* **2011**, *133*, 18122–18125.

(283) Zhang, L.; Cheng, J.; Hou, Z. *Chem. Commun.* **2013**, *49*, 4782–4784.

(284) Kleeberg, C.; Cheung, M. S.; Lin, Z.; Marder, T. B. *J. Am. Chem. Soc.* **2011**, *133*, 19060–19063.

(285) Berkefeld, A.; Piers, W. E.; Parvez, M.; Castro, L.; Maron, L.; Eisenstein, O. *Chem. Sci.* **2013**, *4*, 2152–2162.

(286) Park, S.; Bézier, D.; Brookhart, M. *J. Am. Chem. Soc.* **2012**, *134*, 11404–11407.

(287) Khandelwal, M.; Wehmschulte, R. J. *Angew. Chem. Int. Ed. Engl.* **2012**, *51*, 7323–7326.

(288) Schäfer, A.; Saak, W.; Haase, D.; Müller, T. *Angew. Chem. Int. Ed. Engl.* **2012**, *51*, 2981–2984.

(289) Riduan, S. N.; Zhang, Y.; Ying, J. Y. *Angew. Chem. Int. Ed. Engl.* **2009**, *48*, 3322–3325.

(290) Huang, F.; Lu, G.; Zhao, L.; Li, H.; Wang, Z.-X. *J. Am. Chem. Soc.* **2010**, *132*, 12388–12396.

(291) Courtemanche, M.-A.; Larouche, J.; Légaré, M.-A.; Bi, W.; Maron, L.; Fontaine, F.-G. *Organometallics* **2013**, *32*, 6804–6811.

(292) *Carbon Dioxide Capture and Storage*, Intergover.; Metz, B., Davidson, O., de Conninck, H., Loos, M., Meyer, L., Eds.; Cambridge University Press: New york, 2005.

(293) Olah, G. A.; Goeppert, A.; Prakash, G. K. S. *J. Org. Chem.* **2009**, *74*, 487–498.

(294) Olah, G. A. *Angew. Chem. Int. Ed. Engl.* **2005**, *44*, 2636–2639.

(295) Federsel, C.; Boddien, A.; Jackstell, R.; Jennerjahn, R.; Dyson, P. J.; Scopelliti, R.; Laurenczy, G.; Beller, M. *Angew. Chem. Int. Ed.* **2010**, *49*, 9777–9780.

(296) Schaub, T.; Paciello, R. A. *Angew. Chem. Int. Ed.* **2011**, *50*, 7278–7282.

(297) Tanaka, R.; Yamashita, M.; Nozaki, K. *J. Am. Chem. Soc.* **2009**, *131*, 14168–14169.

(298) D., M.; Langer, R.; Diskin-Posner, Y.; Leitus, G. W.; Shimon, L. J.; Ben-David, Y.; Milstein, D. *Angew. Chem. Int. Ed.* **2011**, *50*, 9948–9952.

(299) Jeletic, M. S.; Mock, M. T.; Appel, A. M.; Linehan, J. C. *J. Am. Chem. Soc.* **2013**, *135*, 11533-11536.

(300) Bontemps, S.; Sabo-Etienne, S. *Angew. Chem. Int. Ed.* **2013**, *52*, 10253-10255.

(301) Bontemps, S.; Vendier, L.; Sabo-Etienne, S. *J. Am. Chem. Soc.* **2014**, *136*, 4419-4425.

(302) Metsänen, T. T.; Oestreich, M. *Organometallics* **2015**, *34*, 543-546.

(303) LeBlanc, F. A.; Piers, W. E.; Parvez, M. *Angew. Chem.* **2014**, *126*, 808–811.

(304) Laitar, D. S.; Müller, P.; Sadighi, J. P. *J. Am. Chem. Soc.* **2005**, *127*, 17196–17197.

(305) Wehmschulte, R. J.; Saleh, M.; Powell, D. R. *Organometallics* **2013**, *32*, 6812–6819.

(306) Boudreau, J.; Courtemanche, M.-A.; Marx, V. M.; Jean Burnell, D.; Fontaine, F.-G. *Chem. Commun.* **2012**, *48*, 11250–11252.

(307) Ménard, G.; Stephan, D. W. *Dalton Trans.* **2013**, *42*, 5447–5453.

(308) Ménard, G.; Gilbert, T. M.; Hatnean, J. A.; Kraft, A.; Krossing, I.; Stephan, D. W. *Organometallics* **2013**, *32*, 4416–4422.

(309) Wen, M.; Huang, F.; Lu, G.; Wang, Z.-X. *Inorg. Chem.* **2013**, *52*, 12098–12107.

(310) Wang, T.; Stephan, D. W. *Chemistry* **2014**, *20*, 3036–3039.

(311) Das Neves Gomes, C.; Jacquet, O.; Villiers, C.; Thuéry, P.; Ephritikhine, M.; Cantat, T. *Angew. Chem. Int. Ed.* **2012**, *51*, 187–190.

(312) Das Neves Gomes, C.; Blondiaux, E.; Thuéry, P.; Cantat, T. *Chemistry* **2014**, *20*, 7098–7106.

(313) Légaré, M.-A.; Courtemanche, M.-A.; Fontaine, F.-G. *Chem. Commun.* **2014**, *50*, 11362–11365.

(314) Ho, S. Y.-F.; So, C.-W.; Saffon-Merceron, N.; Mézailles, N. *Chem. Commun.* **2015**, *51*, 2107–2110.

(315) Fujiwara, K.; Yasuda, S.; Mizuta, T. *Organometallics* **2014**, *33*, 6692–6695.

(316) Blondiaux, E.; Pouessel, J.; Cantat, T. *Angew. Chem. Int. Ed.* **2014**, *53*, 12186–12190.

(317) Courtemanche, M.-A.; Légaré, M.-A.; Maron, L.; Fontaine, F.-G. *J. Am. Chem. Soc.* **2014**, *136*, 10708–10717.

(318) Porcel, S.; Bouhadir, G.; Saffon, N.; Maron, L.; Bourissou, D. *Angew. Chem. Int. Ed. Engl.* **2010**, *49*, 6186–6189.

(319) Tamm, M.; Dreßel, B.; Baum, K.; Lügger, T.; Pape, T. *J. Organomet. Chem.* **2003**, *677*, 1–9.

(320) Burke, K.; Perdew, J. P.; Wang, Y. In *Electronic Density Functional Theory*; Dobson, J. F., Vignale, G., Das, M. P., Eds.; Springer US: Boston, MA, 1998; pp 81–111.

(321) Francl, M. M.; Pietro, W. J.; Hehre, W. J.; Binkley, J. S.; Gordon, M. S.; Defrees, D. J.; Pople, J. A. *J. Chem. Phys.* **1982**, *77*, 3654–3665.

(322) Hehre, W. J.; Ditchfield, R.; Pople, J. A. *J. Chem. Phys.* **1972**, *56*, 2257–2261.

(323) Andrae, D.; Häussermann, U.; Dolg, M.; Stoll, H.; Preuss, H. *Theor. Chim. Acta* **1990**, *77*, 123–141.

(324) Grimme, S. *J. Comput. Chem.* **2006**, *27*, 1787–1799.

(325) Marenich, A. V; Cramer, C. J.; Truhlar, D. G. *J. Phys. Chem. B* **2009**, *113*, 6378–6396.

(326) Wang, T.; Stephan, D. W. *Chem. Commun.* **2014**, *50*, 7007–7010.

(327) D'Alessandro, D. M.; Smit, B.; Long, J. R. *Angew. Chem. Int. Ed. Engl.* **2010**, *49*, 6058–6082.

(328) Huang, K.; Sun, C.-L.; Shi, Z.-J. *Chem. Soc. Rev.* **2011**, *40*, 2435–2452.

(329) Sakakura, T.; Choi, J.-C.; Yasuda, H. *Chem. Rev.* **2007**, *107*, 2365–2387.

(330) Mincione, E. *J. Org. Chem.* **1978**, *43*, 1829–1830.

(331) Wartik, T.; Pearson, R. K. *J. Inorg. Nucl. Chem.* **1958**, *7*, 404–411.

(332) Burr, J. G.; Brown, W. G.; Heller, H. E. *J. Am. Chem. Soc.* **1950**, *72*, 2560–2562.

(333) Shintani, R.; Nozaki, K. *Organometallics* **2013**, *32*, 2459–2462.

(334) Schmidbaur, H.; Wimmer, T.; Reber, G.; Müller, G. *Angew. Chem. Int. Ed. English* **1988**, *27*, 1071–1074.

(335) Ashby, E. C.; Dobbs, F. R. J.; Hopkins, H. P. *J. Am. Chem. Soc.* **2002**, *97*, 3158–3162.

(336) *Encyclopedia of Reagents for Organic Synthesis*; John Wiley & Sons, Ltd: Chichester, UK, 2001.

(337) Axtell, D. D.; Cambell, A. C.; Keller, P. C.; Rund, J. V. *J. Coord. Chem.* **1976**, *5*, 129–134.

(338) Onak, T.; Rosendo, H.; Siwapinyoyos, G.; Kubo, R.; Liauw, L. *Inorg. Chem.* **1979**, *18*, 2943–2945.

(339) Keller, P. C.; Rund, J. V. *Inorg. Chem.* **1979**, *18*, 3197–3199.

(340) Schultz, D. R.; Parry, R. W. *J. Am. Chem. Soc.* **1958**, *80*, 4–8.

(341) Bowden, M.; Heldebrant, D. J.; Karkamkar, A.; Proffen, T.; Schenter, G. K.; Autrey, T. *Chem. Commun.* **2010**, *46*, 8564–8566.

(342) Hamilton, C. W.; Baker, R. T.; Staubitz, A.; Manners, I. *Chem. Soc. Rev.* **2009**, *38*, 279–293.

(343) Londesborough, M. G. S.; Bould, J.; Base, T.; Hnyk, D.; Bakardjiev, M.; Holub, J.; Císarová, I.; Kennedy, J. D. *Inorg. Chem.* **2010**, *49*, 4092–4098.

(344) Collman, J. P.; Zhong, M.; Zhang, C.; Costanzo, S. *J. Org. Chem.* **2001**, *66*, 7892–7897.

(345) Yamasaki, T.; Ozaki, N.; Saika, Y.; Ohta, K.; Goboh, K.; Nakamura, F.; Hashimoto, M.; Okeya, S. *Chem. Lett.* **2004**, *33*, 928–929.

(346) Kögel, J. F.; Xie, X.; Baal, E.; Gesevičius, D.; Oelkers, B.; Kovačević, B.; Sundermeyer, J. *Chemistry* **2014**, *20*, 7670–7685.

(347) Geis, V.; Guttsche, K.; Knapp, C.; Scherer, H.; Uzun, R. *Dalton Trans.* **2009**, 2687–2694.

(348) *Inorganic Experiments*, 3rd Revise.; Woollins, J. D., Ed.; Wiley-VCH: Weinheim, 2010.

(349) Ciobanu, O.; Kaifer, E.; Enders, M.; Himmel, H.-J. *Angew. Chem. Int. Ed. Engl.* **2009**, *48*, 5538–5541.

(350) Courtemanche, M.-A.; Légaré, M.-A.; Rochette, É.; Fontaine, F.-G. *Chem. Commun.* **2015**, *51*, 6858–6861.

(351) Courtemanche, M.-A.; Pulis, A. P.; Rochette, É.; Légaré, M.-A.; Stephan, D. W.; Fontaine, F.-G. F.-G. *Chem. Commun.* **2015**, *51*, 9797–9800.

(352) Stephan, D. W. *Org. Biomol. Chem.* **2012**, *10*, 5740–5746.

(353) Goerigk, L.; Grimme, S. *Phys. Chem. Chem. Phys.* **2011**, *13*, 6670–6688.

(354) Chai, J.-D.; Head-Gordon, M. *Phys. Chem. Chem. Phys.* **2008**, *10*, 6615–6620.

(355) Baslé, O.; Porcel, S.; Ladeira, S.; Bouhadir, G.; Bourissou, D. *Chem. Commun.* **2012**, *48*, 4495–4497.

(356) Chernichenko, K.; Kótai, B.; Pápai, I.; Zhivonitko, V.; Nieger, M.; Leskelä, M.; Repo, T. *Angew. Chem. Int. Ed. Engl.* **2015**, *54*, 1749–1753.

(357) Truhlar, D. G.; Garrett, B. C.; Klippenstein, S. J. *J. Phys. Chem.* **1996**, *100*, 12771–12800.

(358) Gorelsky, S. I.; Lapointe, D.; Fagnou, K. *J. Org. Chem.* **2012**, *77*, 658–668.

(359) Gorelsky, S. I.; Lapointe, D.; Fagnou, K. *J. Am. Chem. Soc.* **2008**, *130*, 10848–10849.

(360) Mkhalid, I. A. I.; Barnard, J. H.; Marder, T. B.; Murphy, J. M.; Hartwig, J. F. *Chem. Rev.* **2010**, *110*, 890–931.

(361) Cho, J.-Y.; Tse, M. K.; Holmes, D.; Maleczka, R. E.; Smith, M. R. *Science* **2002**, *295*, 305–308.

(362) Miyaura, N.; Suzuki, A. *Chem. Rev.* **1995**, *95*, 2457–2483.

(363) Nielsen, F. H. *Plant Soil* **1997**, *193*, 199–208.

(364) Gómez-Gallego, M.; Sierra, M. A. *Chem. Rev.* **2011**, *111*, 4857–4963.

(365) Tajuddin, H.; Harrisson, P.; Bitterlich, B.; Collings, J. C.; Sim, N.; Batsanov, A. S.; Cheung, M. S.; Kawamorita, S.; Maxwell, A. C.; Shukla, L.; Morris, J.; Lin, Z.; Marder, T. B.; Steel, P. G. *Chem. Sci.* **2012**, *3*, 3505–3515.

(366) Vanchura, B. A.; Preshlock, S. M.; Roosen, P. C.; Kallepalli, V. A.; Staples, R. J.; Maleczka, R. E.; Singleton, D. A.; Smith, M. R. *Chem. Commun.* **2010**, *46*, 7724–7726.

(367) Smith, C. J.; Tsang, M. W. S.; Holmes, A. B.; Danheiser, R. L.; Tester, J. W. *Org. Biomol. Chem.* **2005**, *3*, 3767–3781.

(368) Villarreal, C.; Martínez, R. *Synthesis (Stuttg).* **2010**, *2010*, 3346–3352.

(369) Toutov, A. A.; Liu, W.-B.; Betz, K. N.; Fedorov, A.; Stoltz, B. M.; Grubbs, R. H. *Nature* **2015**, *518*, 80–84.

(370) Billingsley, K.; Buchwald, S. L. *J. Am. Chem. Soc.* **2007**, *129*, 3358–3366.

(371) Zulauf, A.; Mellah, M.; Guillot, R.; Schulz, E. *European J. Org. Chem.* **2008**, *2008*, 2118–2129.

(372) Ji, L.; Edkins, R. M.; Sewell, L. J.; Beeby, A.; Batsanov, A. S.; Fucke, K.; Drafz, M.; Howard, J. A. K.; Moutounet, O.; Ibersiene, F.; Boucekkine, A.; Furet, E.; Liu, Z.; Halet, J.-F.; Katan, C.; Marder, T. B. *Chemistry* **2014**, *20*, 13618–13635.

(373) Melaimi, M.; Mathey, F.; Le Floch, P. *J. Organomet. Chem.* **2001**, *640*, 197–199.

(374) Frisch, M. J.; Trucks, G. W.; Schlegel, H. B.; Scuseria, G. E.; Robb, M. A.; Montgomery, J. A., Jr.; Vreven, T.; Kudin, K. N.; Burant, J. C.; Millam, J. M.; Iyengar, S. S.; Tomasi, J.; Barone, V.; Mennucci, B.; Cossi, M.; Scalmani, G.; Rega, N.; Petersson, G. A.; Nakatsuji, H.; Hada, M.; Ehara, M.; Toyota, K.; Fukuda, R.; Hasegawa, J.; Ishida, M.; Nakajima, T.; Honda, Y.; Kitao, O.; Nakai, H.; Klene, M.; Li, X.; Knox, J. E.; Hratchian, H. P.; Cross, J. B.; Bakken, V.; Adamo, C.; Jaramillo, J.; Gomperts, R.; Stratmann, R. E.; Yazyev, O.; Austin, A. J.; Cammi, R.; Pomelli, C.; Ochterski, J. W.; Ayala, P. Y.; Morokuma, K.; Voth, G. A.; Salvador, P.;

Dannenberg, J. J.; Zakrzewski, V. G.; Dapprich, S.; Daniels, A. D.; Strain, M. C.; Farkas, O.; Malick, D. K.; Rabuck, A. D.; Raghavachari, K.; Foresman, J. B.; Ortiz, J. V.; Cui, Q.; Baboul, A. G.; Clifford, S.; Cioslowski, J.; Stefanov, B. B.; Liu, A. L. G.; Piskorz, P.; Komaromi, I.; Martin, R. L.; Fox, D. J.; Keith, T.; Al-Laham, M. A.; Peng, C.; Nanayakkara, A.; Challacombe, M.; Gill, P. M. W.; Johnson, B.; Chen, W.; Wong, M.; Gonzalez, C.; Pople, J. A. Gaussian 03, revision D.01; Gaussian, Inc.: Wallingford, CT, **2004**.

(375) Frisch, M. J.; Trucks, G. W.; Schlegel, H. B.; Scuseria, G. E.; Robb, M. A.; Cheeseman, J. R.; Scalmani, G.; Barone, V.; Mennucci, B.; Petersson, G. A.; Nakatsuji, H.; Caricato, M.; Li, X.; Hratchian, H. P.; Izmaylov, A. F.; Bloino, J.; Zheng, G.; Sonnenberg, J. L.; Hada, M.; Ehara, M.; Toyota, K.; Fukuda, R.; Hasegawa, J.; Ishida, M.; Nakajima, T.; Honda, Y.; Kitao, O.; Nakai, H.; Vreven, T.; Montgomery, J. A., Jr.; Peralta, J. E.; Ogliaro, F.; Bearpark, M.; Heyd, J. J.; Brothers, E.; Kudin, K. N.; Staroverov, V. N.; Kobayashi, R.; Normand, J.; Raghavachari, K.; Rendell, A.; Burant, J. C.; Iyengar, S. S.; Tomasi, J.; Cossi, M.; Rega, N.; Millam, J. M.; Klene, M.; Knox, J. E.; Cross, J. B.; Bakken, V.; Adamo, C.; Jaramillo, J.; Gomperts, R.; Stratmann, R. E.; Yazyev, O.; Austin, A. J.; Cammi, R.; Pomelli, C.; Ochterski, J. W.; Martin, R. L.; Morokuma, K.; Zakrzewski, V. G.; Voth, G. A.; Salvador, P.; Dannenberg, J. J.; Dapprich, S.; Daniels, A. D.; Farkas, Ö.; Foresman, J. B.; Ortiz, J. V.; Cioslowski, J.; Fox, D. J. Gaussian 09, revision C.01; Gaussian, Inc.: Wallingford, CT, **2009**.